



HAL
open science

Identification and characterization of the RIG-I helicase partners involved in the balance proliferation / cell differentiation. Characterization of G-quadruplex resolving by the helicase Pif1 in Bacteroides sp 3_1_23.

Cel Areny Naves

► **To cite this version:**

Cel Areny Naves. Identification and characterization of the RIG-I helicase partners involved in the balance proliferation / cell differentiation. Characterization of G-quadruplex resolving by the helicase Pif1 in Bacteroides sp 3_1_23.. Cellular Biology. Université Paris Saclay (COmUE), 2018. English. NNT : 2018SACLN002 . tel-01783170

HAL Id: tel-01783170

<https://theses.hal.science/tel-01783170>

Submitted on 2 May 2018

HAL is a multi-disciplinary open access archive for the deposit and dissemination of scientific research documents, whether they are published or not. The documents may come from teaching and research institutions in France or abroad, or from public or private research centers.

L'archive ouverte pluridisciplinaire **HAL**, est destinée au dépôt et à la diffusion de documents scientifiques de niveau recherche, publiés ou non, émanant des établissements d'enseignement et de recherche français ou étrangers, des laboratoires publics ou privés.

Identification and characterization of the RIG-I helicase partners involved in the balance proliferation / cell differentiation

Characterization of G-quadruplex resolving by the helicase Pif1 in Bacteroides sp 3_1_23

Thèse de doctorat de l'Université Paris-Saclay
préparée à l'École normale supérieure de Cachan
(École normale supérieure Paris-Saclay)

École doctorale n°577 Structure et Dynamique des Systèmes Vivants
(SDSV)
Spécialité de doctorat: Sciences de la vie et de la santé

Thèse présentée et soutenue à Cachan, le 2 mars 2018, par

Cel Areny Navés

Composition du Jury :

Françoise PORTEU
Directrice de recherche, Gustave Roussy Cancer Campus (UMR 1170) Présidente

Emmanuelle DELAGOUTTE
Chargée de recherche, MNHN (UMR 7196) Rapportrice

Stéphane RETY
Chargé de recherche, ENS Lyon (UMR 5239) Rapporteur

Olivier KOSMIDER
Maître de conférences-PH, Université Paris V (U1016/ UMR 8104) Examineur

Xu-Guang XI
Directeur de recherche, ENS Paris-Saclay (UMR 8113) Directeur de thèse

Elisabeth BUGNARD
Maître de conférences, Université Paris-Sud (UMR 8113) Co-Directrice de thèse

Acknowledgments

This work, carried out at the ENS Paris Saclay, would not have been possible without the support of the "Structures et interaction des acides nucléiques" team and the Dr. Malcom Buckle director of Laboratoire de Biologie et Pharmacologie Appliquée (LBPA) UMR 8113.

I would like to express my gratitude to my two co-supervisors, Dr. Elisabeth BUGNARD for her courage and great learning giving me the love of science and Dr. Xu-Guang XI.

My great appreciation also goes to my thesis committee members: Dr. Emmanuelle DELAGOUTTE, Dr. Stéphane RETY, Dr. Françoise PORTEU and Dr. Olivier KOSMIDER, to have accepted to evaluate my theses work.

I am tempted to individually thank all the team members, students and permanents, Romain RETUREAU, Ahmad ELBAHNSI, Akli BEN, Ouerdia MASKRI, Anissa BELFETMI Olivier MAUFFRET, Philippe FOSSÉ Brigitte RÉNE, Brigitte HARTMANN, Loussine ZARGARIAN and Brahim HEDDI.

Last but not least, I want to thank my family, Ramon NAVÉS SIMÓ el meu padrí, Rosa Maria NAVÉS SOLDEVILA per escoltar-me totes les nits, Jaume ARENY NAVARRO and Lluç ARENY NAVÉS per les abraçades i petons, gràcies per ajudar-me a arribar on he arribat. Romain BERRIER pour tout l'amour donné and his family, my french family: Daniel BERRIER, Fabienne BERRIER, Rémy BERRIER and Estelle WECKERLE. Also the religious sisters of Sagrada Família de Urgell per haver-me acollit i permés treballar en les millors condicions. Finally my dear friends que sou nombrosos però que heu fet possible cadascun a la vostra manera l'arribada d'aquest final d'etapa.

Résumé

Les hélicases sont des protéines qui utilisent l'énergie fournie par l'hydrolyse de l'ATP ou du GTP pour catalyser le déroulement des doubles hélices d'ADN ou d'ARN. Cette activité confère à ces enzymes un rôle essentiel dans le métabolisme des acides nucléiques, le maintien de la stabilité du génome et les processus de signalisation cellulaire. Par conséquent, ces enzymes sont impliqués dans des processus aussi divers que le vieillissement, l'apparition de cancers, l'immunité innée. Cette thèse porte sur la compréhension de la fonction et des mécanismes moléculaires de deux hélicases différentes et le manuscrit est donc divisé en deux parties.

La première partie est dédiée à l'hélicase RIG-I (Retinoic acid-Induced Gene I) spécifique de l'ARN. RIG-I est une protéine hautement conservée chez les vertébrés qui appartient à la famille des RLR (RIG-I Like Receptors) qui sont des hélicases à DExD/H-box de la superfamille des hélicases SF2. RIG-I possède comme toutes ces protéines un domaine hélicase central dont le fonctionnement dépend de l'hydrolyse de l'ATP suivi d'un domaine C-terminal régulateur interagissant avec des ARN de petite taille. Mais RIG-I possède également deux domaines CARD (Caspase Activation and Recruitment Domain) en tandem à l'extrémité N-terminale. Ce domaine est essentiel pour l'activation de la production d'INF- β , par interactions homotypiques essentiellement. L'induction du son gène de RIG-I (Ddx58) a été initialement observée lors du traitement à l'acide rétinoïque de la lignée cellulaire NB4, dérivée de la moëlle osseuse d'une patiente atteinte de Leucémie Promyélocytaire Aiguë (APL). Lors de ce traitement, les myeloblastes NB4 cessent de proliférer en promyélocytes pour se différencier en granulocytes (Yu M et al., 1997; Liu TX et al., 2000). Par ailleurs, RIG-I est également associé à l'infection virale en raison de la découverte de son induction par le virus du Syndrome Dysgénésique et Respiratoire du Porc (SDRP) (Zhang X et al., 2000) et son rôle indispensable dans la reconnaissance de l'ARN double brin des virus ainsi que l'initiation de la protection des cellules contre la réplication des génomes viraux. Dès lors, RIG-I a suscité un intérêt croissant puisqu'il s'est avéré jouer un rôle crucial dans l'immunité innée et dans la détection de différents acides nucléiques viraux, des ARN simple brin (ARNsb) porteurs de 5'triphosphate (5'ppp) ou des ARN double brin (ARNdb) (Yoneyama M et al., 2004; Hornung V et al., 2006; C et al., 2010; Pichlmair A et al., 2006; Wang Y et al.,

2010; Baum A et al., 2010), avec une préférence pour les ARN de taille courte (10-25 nucléotides de long) (Kato H et al., 2008).

RIG-I est donc impliqué dans deux aspects cruciaux de la vie cellulaire qui sont la réponse immunitaire et la différenciation cellulaire. Le mécanisme d'action de RIG-I est bien décrit dans le contexte de l'infection virale. Mais dans le cas de la différenciation des cellules myéloïdes, son intervention et son rôle dans la balance prolifération / différenciation restent partiellement compris. Les interactions de RIG-I notamment avec des ligands cellulaires ne sont pas totalement élucidées. La première partie de ce travail a donc consisté à tenter d'isoler et de caractériser les partenaires de RIG-I lors de la différenciation des cellules leucémiques NB4. Le but a d'abord été d'identifier des ligands spécifiques de l'hélicase au cours du traitement par l'ATRA qui déclenche la différenciation et le blocage de la prolifération. Cette identification se réalisant par co-immunoprécipitation et séquençage haut débit ou analyse protéomique. Après identification, la deuxième étape du travail concerne la caractérisation biochimique de l'interaction puis sa vérification dans la cellule suivie de l'effet sur la différenciation et la prolifération des cellules. La possibilité d'une étude structurale a même été envisagée.

Ce travail est basé sur deux points: 1) la structure en domaines de RIG-I lui permettant de lier les ARN et les protéines, 2) plusieurs travaux montrant que la spécificité des hélicases à leurs ligands est due à plusieurs facteurs tels que la localisation subcellulaire ou le profil d'expression de la protéine en plus de la séquence nucléotidique. Ainsi, certaines hélicases peuvent avoir de nouvelles fonctions participant aux processus de signalisation cellulaire.

Cette première partie de ma thèse est donc divisée en deux parties: RIG-I étant une hélicase à ARN, ce travail débute par la recherche de partenaire(s) ARN endogène(s). Dans la littérature, non seulement des ARN viraux, mais plusieurs types d'ARN différents sont connus pour se lier à RIG-I. Dans le cas des lymphocytes B murins, RIG-I marqué par His se lie à de multiples ARNm endogènes tels que l'ARNm 3'UTR de NF-kb1 (Zhang HX et al., 2013). Les ARNsn U1 et U2 dans les cellules de carcinome colorectal peuvent également lier RIG-I conduisant à l'activation de la voie IFN (Ranoa DR et al., 2016). Parmi les partenaires ARN possibles, les miARN sont également de bons candidats. Plusieurs travaux ont montré que les miARN affectent la progression tumorale et la différenciation cellulaire. Dans le cas de la différenciation hématopoïétique, ils peuvent tous deux avoir un rôle de suppresseur de tumeur ou des activités oncogènes (Schotte D et al., 2012). Plus tard, l'orientation du travail a été réajustée à la recherche de partenaire(s) protéique(s) reposant sur la présence de deux domaines CARD dans l'hélicase. Dans le cas de la différenciation myéloïde, seule la protéine

Src est actuellement connue pour interagir avec RIG-I (Li XY et al., 2014) Cette interaction a lieu au niveau des domaines CARD et le linker entre les domaines CARD et Helicase de RIG-I. Ces travaux sont intéressants mais l'étude a été réalisée dans la lignée cellulaire macrophagique (U937). Bien qu'il s'agisse d'une lignée myéloïde, elle diffère de notre lignée cellulaire APL NB4 qui elle correspond à une situation pathologique réelle. Par ailleurs, les auteurs affirment que cette interaction se produit d'une manière indépendante de l'ARN, puisque la transfection de petits ARN synthétiques PolyI:C ou 5'-pppARNsb inhibe partiellement l'interaction. Mais ils ne prennent pas en compte le fait que ces ARN ne sont pas des ARN endogènes, qui peuvent se comporter différemment. De plus, ils proposent un modèle d'interaction entre RIG-I et Src, qui libère complètement les domaines hélicase et ATPase. La conformation de RIG-I ainsi modifiée rend ces deux domaines totalement accessibles soit aux ARN, soit à d'autres protéines. Néanmoins, ces travaux révélant l'identification de l'interaction entre Src et RIG-I, ont contribué à la compréhension de la position de RIG-I dans la cascade de signalisation du contrôle de la prolifération. En effet, ils ont montré que l'hélicase interagit avec le processus de prolifération par un programme de mort via une inhibition AKT-mTOR indépendante de l'apoptose et une activation autophagique. En terme de recherche de ligands de RIG-I, un autre groupe a observé la possibilité d'interactions de multiples protéines. Zhang HX et al., ont démontré par immunoprécipitation et iTRAQ-MS que RIG-I interagit à la fois avec le 3'UTR de l'ARNm de Nf- κ b1 / p105 et Rpl13, qui est un composant de la grande sous-unité 60S du ribosome. Dans cette étude, il est également important de noter que d'autres protéines ont également été identifiées par iTRAQ-MS. Seuls quelques-unes présentaient un intervalle de confiance total du score ionique supérieur à 95%. Le groupe n'a pas davantage travaillé sur ces candidats. Parmi ces protéines trois d'entre elles (IGFBP5, protéine apparentée à Hip1, et VLA-4) auraient pu être étudiées en raison de leur rôle intéressant dans la prolifération, différenciation et adhésion cellulaire (Zhang HX et al., 2013).

Dans le cas de la recherche des partenaires de type ARN, grâce à des expériences de CLIP (cross-linking et immunoprécipitation) suivies de migration sur gel, un signal plus fort a été observé chaque fois dans le cas du traitement à l'ATRA qu'avec le DMSO (le solvant de l'ATRA) révélant la présence de complexes RIG-I-acide nucléique. Les échantillons étant préalablement traités avec de la DNase et l'observation de la diminution du signal après traitement à la RNase, ont permis de considérer que des ARN ou des protéines endogènes en plus de RIG-I sont présents dans les complexes. Le signal obtenu avec un traitement au DMSO (le solvant de l'ATRA) pourrait être lié comme déjà mentionné par d'autres équipes

(Khanna-Gupta A et al., 1994; Qiu H et al., 2011) à l'initiation du processus de différenciation. Aussi en l'absence d'ATRA et de DMSO, un fort signal a pu être observé. Dans cette situation expérimentale les cellules sont en état de prolifération et ce signal peut correspondre à la présence des ARNr ou des ARNt connus pour être abondants et "collants", "contaminant" les échantillons. Nous savons en effet que la capacité de croissance et de prolifération des cellules est couplée à la transcription de l'ARNr qui est alors abondant. Au cours de la différenciation, l'expression de la protéine proto-oncogène c-Myc est diminuée en réponse à la transition de l'état proliférant à l'état non proliférant. Cette régulation négative de c-Myc diminue l'expression des facteurs de transcription liés à Pol I conduisant à la régulation négative de la transcription de l'ARNr (Hayashi Y et al., 2014). Par conséquent, cette différence de niveau d'ARNr entre l'état de prolifération et de différenciation peut expliquer le signal fort en absence de traitement, mais il peut aussi masquer la présence d'autres candidats ARN intéressants. Finalement l'observation d'un signal compacte nous amène à envisager de gros complexes RIG-I-ARN-protéines. Dans un deuxième temps, le travail a consisté à démasquer les partenaires protéiques de RIG-I selon la même approche de co-immunoprécipitation sans crosslinking cellulaire. Avant d'effectuer une approche protéomique une migration SDS page et une coloration à l'argent ont été réalisés. Comme on pouvait l'attendre, le signal RIG-I a été obtenu de manière satisfaisante en présence d'ATRA. En gel 1D il a été très difficile de voir des différences de migration et d'intensité de bande entre les différentes conditions de traitement. Seule une migration en gel 2D aurait pu permettre de visualiser des différences et de poursuivre le projet.

La seconde partie de la thèse a été consacrée à l'étude du mécanisme moléculaire sous-jacent au déroulement des G-quadruplexes par l'hélicase BsPif1. Les hélicases sont des enzymes qui se déplacent à travers des acides nucléiques appariés sous forme bicaténaire pour catalyser la séparation des brins et permettre la réplication ou la transcription de la molécule d'ADN. Cette translocation se produit initialement grâce à la liaison entre les acides nucléiques et l'hélicase permettant un changement conformationnel de l'hélicase conduisant à l'hydrolyse de l'ATP. L'hydrolyse de l'ATP déclenche un état d'oscillation entre un état d'affinité maximale et un état d'affinité faible dans le site de liaison à l'ADN, ce qui entraîne la translocation à travers l'ADN. Dans le cas des structures d'ADN non canoniques formées par l'empilement de plusieurs G-quartets appelés G-quadruplex (G4), le mécanisme moléculaire sous-jacent à leur déroulement est plus complexe à cause de la présence de plusieurs quartets G générant une conformation spécifique caractérisée par des propriétés électrophysiques particulières,

maintenues par l'appariement Hoogsteen et des cations monovalents. Les G-quadruplexes sont présents dans les télomères, les origines de réplication de l'ADN, les régions régulatrices de la transcription des gènes, les promoteurs de certains oncogènes et également les régions de commutation des immunoglobulines. Leur formation peut influencer les processus biologiques tels que la réplication de l'ADN, la traduction et le maintien de l'intégrité des télomères. Pour contrer la formation de G4, certaines hélicases spécifiques ont la capacité de les résoudre, telles que (Pif1 et DNA2 dans la famille SF1, FANCI, DDX11, RTEL1, BLM, WRN et DHX9 dans la famille SF2, SV40T-ag dans la famille SF3, Twinkle dans la famille SF4 et RHAU pour la famille SF5) (Mendoza O et al., 2016), mais le mécanisme moléculaire n'est pas encore complètement compris. Parmi les questions qui se posent, il n'est pas clairement établie: 1) si les hélicases résolvant les G4 possèdent un site spécifique de liaison de ces structures qui soit différent du site de liaison classique des ADN simple et double brin, 2) si le déroulement des G-quadruplexes dépend de l'ATP et 3) comment l'hélicase utilise l'énergie dérivée de l'hydrolyse de l'ATP pour effectuer le dépliement des G-quadruplexes. Afin de répondre à ces questions un homologue de Pif1p de *S cerevisiae*, BsPif1 (de *Bacteroides sp. 3_1_23*) a été utilisé.

La première étape de mon travail a consisté à analyser quantitativement et comparer la stimulation des activités ATPase de BsPif1 par différentes structures d'ADN : G-quadruplexes, ADN double brin et ADN simple brin. Les résultats ont montré que seul l'ADNsb déclenche efficacement l'hydrolyse de l'ATP, mais cette activité est proportionnelle à la longueur de brin. Un résultat similaire a été observé avec Pif1 humain, qui nécessite un minimum de 10 bases pour une liaison efficace de l'enzyme (Gu Y et al., 2013). Lorsque la structure de l'ADN est plus complexe et en particulier dans le cas de l'appariement brin / base, cette activité est fortement diminuée comme observé avec l'ADNdb. Dans le cas du G-quadruplex, sa structure et sa conformation déterminent l'activité ATPase. Par dichroïsme circulaire j'ai pu observer une différence de stabilité entre deux G-quadruplexes utilisés: un G4 monomère avec une conformation parallèle et une structure très stable, un G-quadruplex antiparallèle de type télomérique plus instable. Le G4 stable conduit à une hydrolyse négligeable de l'ATP, alors que le G4 de type télomérique et moins stable permet une récupération partielle de l'activité ATPase de BsPif1. D'autre part, lorsqu'un ADNsb est présent à l'extrémité 5' des G-quadruplex l'activité spécifique de l'ATPase est restaurée, et comparable à celle de l'ADNsb. La nécessité d'une queue à l'extrémité 5' du G-quadruplex pour l'activité ATPase a également été rapportée avec Pif1 humain (Sanders CM, 2010). Ces résultats montrent que le G-quadruplex ne stimule pas l'activité ATPase de BsPif1 de manière

efficace. En combinant l'activité ATPase et des tests de liaison de BsPif1 à l'ADN, et par des expériences de compétition entre ADNsb et G-quadruplex, on observe que l'ADNsb et l'ADN G4 se lient à des sites distincts avec une affinité de liaison similaire (nM). La réalisation d'une carte de potentiel électrostatique de surface de la structure de BsPif1 a permis de déterminer deux régions chargées positivement et adaptées pour héberger le G-quadruplex. Mais une étude plus approfondie doit être effectuée afin de discriminer les deux sites de liaison possibles. Après avoir clarifié la relation entre la liaison du G-quadruplex à l'enzyme et l'activité ATPase, le lien entre le déroulement de l'ADN et l'hydrolyse de l'ATP a été étudié. En présence du G-quadruplex stable aucune de ces deux activités n'a été observée. En revanche, le même G-quadruplex avec une queue d'ADNsb à l'extrémité 5' stimule l'activité ATPase et peut être déroulée par BsPif1. Le motif G4 stable est donc un obstacle physique et plus d'énergie est nécessaire pour résoudre la structure G4. Dans le cas du G4 moins stable l'activité d'ATPase est modérée avec une activité de déroulement qui augmente quand une queue simple brin en 5' est ajoutée. L'ensemble des résultats démontrent que BsPif1 nécessite une queue simple brin en 5' pour résoudre les G4 et cette activité de déroulement est déterminée par la stabilité du G4.

Summary

| | |
|--|----|
| <u>General Objectives</u> | 1 |
| <u>Introduction</u> | 2 |
| 1. Helicases | 2 |
| 1.1. Discovery and definition | 2 |
| 1.2. Helicases classifications and families | 2 |
| 1.3. General Mechanisms of Helicases | 5 |
| 1.3.1. NTP binding and hydrolysis of NTP | 6 |
| 1.3.2. Interaction with nucleic acid substrates | 6 |
| 1.3.3. Translocation mechanism | 7 |
| 1.3.4. Base pair separation or unwinding mechanism | 9 |
| 1.3.5. Annealing | 11 |
| 1.3.6. Regulatory domains and specificity | 12 |
| 1.4 Biological functions of helicases | 12 |
| 1.4.1. Biological functions of DNA helicases | 15 |
| 1.4.1.1. DNA replication | 15 |
| 1.4.1.2. DNA transcription | 15 |
| 1.4.1.3. DNA repair | 16 |
| 1.4.1.4. Chromosome recombination | 18 |
| 1.4.1.5 Telomeres maintenance and G-quadruplexes metabolism | 20 |
| 1.4.1.6. DNA sensing | 21 |
| 1.4.2. Biological functions of RNA helicases | 23 |
| 1.4.2.1. RNA splicing | 24 |
| 1.4.2.2. Nuclear mRNA export | 25 |
| 1.4.2.3. mi-RNA-induced gene silencing | 26 |
| 1.4.2.4. Ribosome biogenesis | 27 |
| 1.4.2.5. Translation initiation and regulation | 27 |
| 1.4.2.6. RNA decay | 28 |
| 1.4.2.7. Cytoplasmic transport and storage | 30 |
| 1.4.2.8. RNA sensing | 30 |

Chapter I: Identification and characterization of the RIG-I helicase partners involved in the balance proliferation / cell differentiation in the acute promyelocytic leukemia

| | |
|--|----|
| <u>Objectif</u> | 32 |
| <u>Introduction</u> | 34 |
| 1. RIG-I Like Receptors (RLR) | 34 |
| 1.1. RLR structure | 34 |
| 1.2. RLR localization | 36 |
| 1.3. RLR ligands | 37 |
| 1.4. Signal transduction in the RLR pathway | 38 |
| 1.5. RLR regulation by host viruses | 41 |
| 2.The RIG-I helicase | 41 |
| 2.1. Molecular structure | 41 |
| 2.2. RIG-I helicase activity | 42 |
| 2.3. RIG-I activation mechanisms | 44 |
| 2.4. Additional cellular factors regulate RIG-I | 46 |
| 2.5. RIG-I partners | 48 |
| 2.6. RIG-I recognizes various endogenous RNAs | 50 |
| 2.7. RIG-I has multiple roles in cell development and cancer: case of the myeloid differentiation | 50 |
| 3. Hematopoiesis and Leukemia | 52 |
| 3.1. Normal hematopoiesis | 52 |
| 3.1.1. Hematopoietic hierarchy | 52 |
| 3.1.2. Hematopoietic cells and their biological functions | 55 |
| 3.2. Leukaemia | 56 |
| 3.2.1. Leukaemia classification | 56 |
| 3.2.2. Acute Promyelocytic Leukaemia | 58 |
| 3.2.2.1. APL molecular pathology | 59 |
| 3.2.2.1.1. Role of PML | 60 |
| 3.2.2.1.2. RARα and granulopoiesis | 61 |
| 3.2.2.1.3. PML-RARα induced APL | 63 |

| | |
|---|-----------|
| 3.2.2.2. APL cellular model: NB4 cells..... | 64 |
| 3.2.2.3. APL Treatment strategies and side effects..... | 65 |
| 3.2.2.3.1. ATRA / Chemotherapy strategy..... | 65 |
| 3.2.2.3.2. Arsenic Trioxyde (ATO) strategy..... | 67 |
| 3.2.2.3.3. Other reported secondary effects..... | 69 |
| <u>Materials and Methods</u> | 71 |
| 1. Cell culture..... | 71 |
| 2. Cell coloration..... | 71 |
| 3. UV Cross-Linking Immunoprecipitation (CLIP) of RIG-I/RNA complexes..... | 71 |
| 3.1. UV cross-linking..... | 72 |
| 3.2. Preparation of antibodies-conjugated beads..... | 72 |
| 3.3. Cell lysates preparation..... | 73 |
| 3.4. Immunoprecipitation..... | 73 |
| 3.5. Radiolabelling and elution of the crosslinked RNA-RIG-I complexes..... | 73 |
| 3.6. Enzymatic treatment of immunoprecipitated complexes..... | 73 |
| 3.7. Gel migration and revelation..... | 74 |
| 3.8. Western Blot..... | 74 |
| 4. RIG-I/partner proteins complexes immunoprecipitation..... | 75 |
| 4.1. Cell lysates preparation..... | 75 |
| 4.2. Preparation of antibodies-conjugated beads..... | 75 |
| 4.3. Cross-linking antibodies to sepharose beads..... | 75 |
| 4.4. Immunoprecipitation..... | 75 |
| 4.5. Elution and TCA precipitation..... | 76 |
| 4.6. Western Blot..... | 76 |
| 4.7. Silver staining..... | 76 |
| <u>Results</u> | 78 |
| 1. Effect of ATRA on NB4/NB4R cells differentiation..... | 78 |
| 2. Effect of ATRA on NB4 and NB4R proliferation..... | 82 |
| Identification of RNA partmers of RIG-I involved in the proliferation/cell differentiation balance in the case of Acute Promyelocytic leukemia (APL) | 83 |
| 3. Expression of RIG-I in NB4 cells..... | 83 |

| | |
|--|-----------|
| 4. Detection of RIG-I/RNA complexes in NB4 cells..... | 85 |
| Identification of protein partners of RIG-I involved in the proliferation/cell differentiation balance in the case of Acute Promyelocytic leukemia (APL)..... | 89 |
| 5. Isolation of RIG-I from NB4 cells..... | 89 |
| <u>Discussion-Conclusion</u>..... | 93 |

Chapter II: Characterization of G-quadruplex resolving by the helicase Pif1 in Bacteroides

| | |
|---|-----|
| <u>Objectif</u> | 98 |
| <u>Introduction</u> | 100 |
| 1. Pif1 | 100 |
| 1.1. Discovery and definition | 100 |
| 1.2. Pif1 isoforms and cell localization | 101 |
| 1.3. Pif1 structure | 102 |
| 1.4. Functions of Pif1 | 105 |
| 1.4.1. Synthesis of Okazaki fragments | 105 |
| 1.4.2. Unfolding G-quadruplexes | 107 |
| 1.4.3. Telomerase regulation | 108 |
| 1.4.3.1. Processivity of telomerase limitation by Pif1 | 109 |
| 1.4.3.2. Pif1 inhibits the recruitment of telomerase to DNA double-strand breaks | 110 |
| 1.5. Pif1 regulation | 110 |
| 2. Bacteroides spp | 111 |
| 2.1. Biochemical characterization of BsPif1 | 112 |
| 2.2. BsPif1 mechanism of unwinding | 113 |
| 3. DNA structures | 114 |
| 4. G-quadruplexes | 115 |
| 4.1. Structural polymorphism of G4 | 116 |
| 4.1.1. Strands number | 116 |
| 4.1.2. Glycosidic torsion angle | 116 |
| 4.1.3. Strand orientation | 117 |
| 4.1.4. Loop conformation | 117 |
| 4.1.5. Cation nature | 118 |
| 4.1.6. Bulges in G-quadruplexes | 119 |
| 4.2. Regulation of G-quadruplex formation | 119 |
| 4.3. G-quadruplexes in vivo | 121 |

| | |
|--|------------|
| 4.4. G-quadruplexes localization..... | 122 |
| 4.5. Fonctions of G-quadruplexes..... | 123 |
| 4.5.1. Role of G-quadruplexes in promoter region..... | 123 |
| 4.5.2. Role of G-quadruplexes in DNA replication..... | 124 |
| 4.5.3. Role of G-quadruplexes in telomeres..... | 126 |
| 4.6. Characterization of telomeric G-quadruplex motif and (GGGT) ₄ motif..... | 127 |
| <u>Materials and Methods</u> | 131 |
| 1. Protein expression and purification..... | 131 |
| 2. DNA sequences..... | 132 |
| 3. DNA substrates preparation..... | 134 |
| 4. ATPase activity assay..... | 134 |
| 5. DNA labelling..... | 135 |
| 6. DNA strand annealing..... | 135 |
| 7. Helicase assays..... | 136 |
| 8. Annealing assays..... | 136 |
| 9. DNA-binding assay..... | 136 |
| 10. Circular dichroism (CD) | 137 |
| 11. Electrostatic potential surface map..... | 137 |
| <u>Results</u> | 138 |
| 1. Verification of G-quadruplex structure..... | 138 |
| 2. ATP hydrolysis stimulation..... | 139 |
| 3. Determination of distinct binding sites for ssDNA and G4 motif..... | 143 |
| 4. Potential G4 bindings sites..... | 147 |
| 5. ATP hydrolysis is required for G4 unfolding..... | 149 |
| 6. BsPif1 does not catalize dsDNA annealing..... | 152 |
| <u>Discussion-Conclusion</u> | 154 |
| <u>References</u> | 158 |

General Objectives

Helicases are proteins that utilize the energy provided by the hydrolysis of ATP or GTP to catalyse the disjunction of double DNA or RNA helices. This double strand unwinding activity gives them an essential role in the metabolism of nucleic acids, the maintenance of the genome stability and cell signalling processes. As a result, they are involved in processes as diverse as aging, the appearance of cancers, innate immunity. This thesis is focused on the understanding of the function and the molecular mechanisms of two different helicases and the manuscript is therefore divided in two parts. The first one is dedicated to the RIG-I helicase, an RNA helicase, expressed when leukemic cells stop proliferate and are induced to differentiate in granulocytes, which are essential in the recognition of double-stranded RNA of viruses, initiating the protection of the cells against the replication of the viral genomes. The mechanism of action of RIG-I is well described in the context of viral infection. But in the case of the differentiation of myeloid cells, the intervention of RIG-I and its influence on the equilibrium proliferation / differentiation remains incomplete. Indeed, RIG-I interactions in particular with cellular ligands are not fully understood. The first part of my work consisted in an attempt to isolate and characterize RIG-I partners during differentiation of NB4 leukemic cells. The second one is devoted to the study of mechanisms underlying G-quadruplexes resolving by helicases. Several questions remain about the interactions between the particular structure of G-quadruplexes and these enzymes. A *Bacteroides sp 3_1_23* helicase, BsPif1, was chosen to compare and characterize the interaction between G-quadruplexes and canonical Watson-Crick DNA. In the two parts of the work, the interactions were investigated by biochemical techniques using either a cell line or purified protein and synthetic nucleic acids.

Introduction

1. Helicases

1.1. Discovery and definition

Helicases are enzymes discovered in *E. coli* in the late 1970s, firstly described as DNA-stimulated ATPases (Denhardt et al., 1967; Abdel-Monem M et al., 1976). In the presence of DNA, RNA hybrid duplexes and DNA-DNA partial duplexes, the enzyme purified by Abdel-Monem M was found to denature the duplexes in an ATP-dependent reaction without any degradation of the duplexes (Abdel-Monem M et al., 1976). The authors assumed that after binding to the DNA molecule, the enzyme unwinds the double-strand DNA in a processive fashion, thanks to ATP hydrolysis. Three years later, Takahashi demonstrated that the enzyme discovered earlier in 1967 by Denhardt, had helicase properties (Takahashi S et al., 1979). Later, it was established that helicases function as molecular motors that transfer the chemical energy derived from binding and hydrolysis of ATP into mechanical force to drive directional translocation along nucleic acid duplex and separate it into individual single strands (Lohman TM and Bjornson KP, 1996; Caruthers JM and McKay DB, 2002; Tanner NK and Linder P, 2001; von Hippel PH and Delagoutte E, 2001).

1.2. Helicases classifications and families

In 1988, Gorbalyena and Koonin performed sequence analysis of several helicases allowing a classification based on conserved motifs (Figure 1). They identified 3 superfamilies (SFs) and 2 smaller families (Fs), called SF1 to SF5 (Gorbalenya AE et al., 1988; Hodgman TC, 1988; Gorbalenya AE et al., 1989; Gorbalenya AE et al., 1990; Gorbalenya AE and Koonin EV, 1993). All the superfamilies possess the Walker A and Walker B motifs (motifs I and II). These motifs are involved in the binding and hydrolysis of NTP (Walker JE et al., 1982). They are common to the large family of translocases which couple NTP hydrolysis to nucleic acid translocation. Therefore helicases constitutes a subset of translocases. A sixth superfamily has been identified and consists of helicases containing the AAA+ conserved module (ATPases Associated with diverse cellular Activities). This last helicase family is also characterized by the presence of the Walker A and Walker B motifs (Erzberger JP and Berger JM, 2006). All the superfamilies also possess an “arginine finger” (R), which helps to couple the NTP hydrolysis to conformational change (Rittinger K et al., 1997; Scheffzek K et al., 1997; Nadanaciva S et al., 1999).

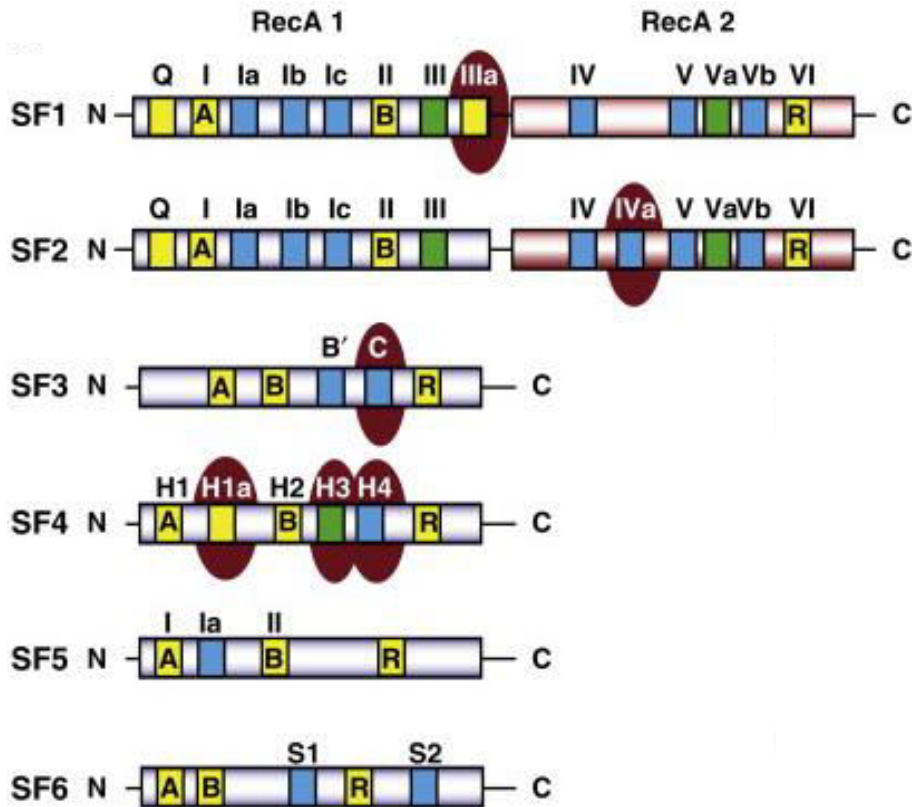


Figure 1. Helicase classification. The “core domains” and the positions of the signature motifs are shown for each class of helicase. The N-terminal RecA domain (RecA1) is represented by a blue cylinder and the C-terminal RecA domain (RecA2) is shown as a red cylinder. The conserved amino acid motifs are colored according to their helicase function. The motif involved in NTP binding/hydrolysis is shown in yellow, the motif associated with translocation appears in green and the nucleic acid interacting motif is colored in blue. The motifs that are unique to specific superfamilies are highlighted with a red oval. The Walker A ("A"), Walker B ("B") and arginine finger ("R") motifs are conserved across all helicase superfamilies. In the family SF6 de RecA represented by a blue cylinder is named AAA+. Adapted from Jackson RN et al., 2014.

Other classifications of helicases are also used and they are based on their substrate specificity (RNA, DNA or DNA-RNA hybrids), their polarity (5'-3' or 3'-5'), or their oligomerization. Structurally, helicases are classified in two categories: hexameric proteins forming a ring which are members of SF3 to 6 (Figure 2B) and non toroidal proteins belonging to SF1 and 2 (Figure 2A). These different tridimensional structures share a common module called “RecA-like” referring to the RecA protein present in bacteria which was the first enzyme with ATPase activity and whose tridimensional structure was determined (Story RM and Steitz

TA, 1992). The RecA-like module consists of a beta-sheet sandwiched by alpha helices (Singleton MR et al., 2007). Two RecA-like domains can be linked in tandem by a flexible linker of varying length (SF1 and SF2 helicases) (Figure 2A) or can be present in different subunits arranged in an hexameric ring (SF3 to 6) (Figure 2B).

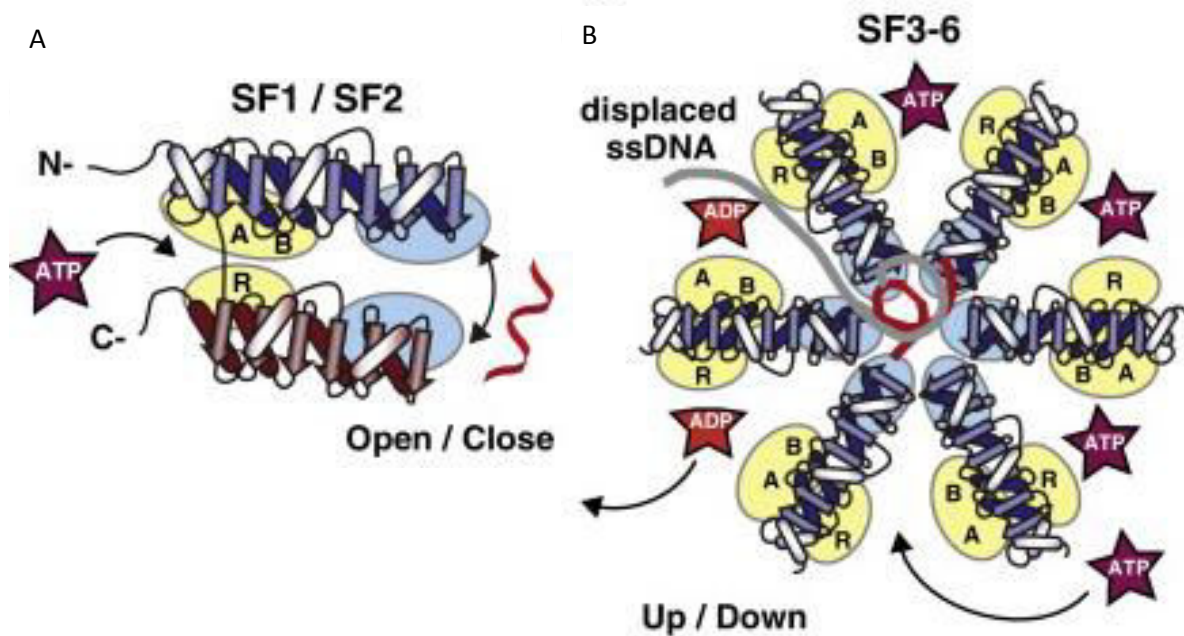


Figure 2. Representative core structures. (A) Secondary structure of the tandem RecA-like (RecA1 colored in blue and the RecA2 in red) folds observed in SF1 and SF2 helicases. The RecA-like domains form a cleft that contains an NTP binding pocket in yellow and a nucleic acid binding site in blue. The NTP binding and hydrolysis causes the cleft to cycle between the closed and open states. (B) SF3, SF4, SF5 and SF6 secondary structure consists in six individual RecA- or AAA+-like domains (RecA1 colored in blue) arranged into toroidal hexamers that radially array the bipartite NTP binding sites in yellow and a nucleic acid binding site in blue in the center. Adapted from Jackson RN et al., 2014.

During my PhD, I was interested in DNA/RNA helicases, which are members of SF1 and 2. Therefore I will mainly introduce these two families.

SF1 and SF2 helicases are the most characterized superfamilies and can translocate along DNA or RNA. They are either monomers or dimers and their core domains share twelve motifs out of thirteen (Q, I, Ia, Ib, Ic, II, III, IV, V, Va, Vb, VI), which fold RecA-like domains, named RecA1 and RecA2 (Figure 1). The domains RecA1 and RecA2 are separated

by a deep cleft. The site for ATP binding is localized in this cleft, between the motifs Q, I, II and VI, which are localized in the interface of the two RecA-like domains (Korolev S et al., 1997). Motifs III and Va, which are important for the coordination between NTP and the binding site of the substrate to determine the translocation, are less conserved within the two families. Finally the domains Ia, Ib, Ic, IV, V and Vb are involved in nucleic acid binding (Fairman-Williams ME et al., 2010).

Superfamily 1 members carry out different biochemical functions. They can be subdivided in two groups according to the polarity of translocation along the DNA or RNA: SF1A helicases (3' to 5') such as Rep, PcrA, UvrD and SF1B (5' to 3') helicases including RecD, Dda of T4 bacteriophage, Rrm3, Pif-1-like, Upf1 (Subramanya HS et al., 1996; Korolev S et al., 1997; Velankar SS et al., 1999; Tomko EJ et al., 2007; Saikrishnan K et al., 2008; Zhang DH et al., 2006; Saikrishnan K et al., 2009).

Superfamily 2 is the largest helicase family, with members involved in various cell processes. They present a specific motif IVa involved the interaction with the nucleic acid (Korolev S et al., 1997). The SF2 family includes RNA helicases box DEXD/H as RIG-I-like (Cordin O et al., 2006), RecQ helicase (Bachrati CZ and Hickson ID, 2003), Swi/Snf2-like helicases (Flaus A et al., 2006; Flaus A and Owen-Hughes T, 2004). The members of this family are able to move over nucleic acids, single or double strands. Some of them are even able to move in both directions of migration (Cordin O et al., 2006).

SF3 share four conserved motifs: Walker A and B, B' and C, the latter being SF3 specific (Singleton MR et al., 2007). SF3 helicases translocate in the 3' to 5' direction (Thomsen ND and Berger JM, 2009). SF4 is characterized by five conserved motifs: H1, H1a, H2, H3 and H4 (H1 and H2 correspond to Walker A and B) (Ilyina TV et al., 1992). SF5 is the smallest family and an important member is the transcription terminator Rho, which is related to SF4 but it has been included in a separate family on the basis of the sequence (Singleton MR et al., 2007). They translocate in 5' to 3' direction (Thomsen ND and Berger JM, 2009). Finally, SF6 includes the helicases containing the core AAA+ fold that do not fall into superfamily 3.

1.3. General mechanisms of helicases

Mechanisms of helicases have been widely discussed in the literature (Lohman TM and Bjornson KP, 1996; Patel SS and Picha, KM 2000; Cordin O et al., 2006). The enzymes can also be classified on the basis of their biochemical properties. But they have several common properties namely the NTP binding and hydrolysis, the interaction with the nucleic acid

substrates, the translocation mechanism, the base pair separation, the coupling of NTPase to translocation and unwinding, and the annealing, regulatory modules.

1.3.1. NTP binding and hydrolysis of NTP

NTP binding and hydrolysis drive the helicase activity leading the enzyme to go through defined ligation state, triggering changes in the affinity of the enzyme for the nucleic acid and bringing about power stroke for translocation and strand separation. The NTP binding at the interface between two RecA domains is a common feature and the presence of a divalent cation, normally Mg^{2+} , is required (Bennett RJ et al., 1999; Bae SH et al., 2001). Most helicases preferentially hydrolyse ATP than the three other nucleotides (TTP, GTP and CTP). Generally, the NTPase activity of helicases is stimulated by the binding of nucleic acid (DNA or RNA). However several helicases display ATPase activity even in the absence of nucleic acids like DnaB protein (Roychowdhury A et al., 2009). However, it is known that helicases do not display specification sequence for ATPase activity, except of Dbpa. The binding of NTP at the interface of 2 domains serves several purposes. After binding, changes occurring in the pocket assume different ligation states and trigger the subunit movements thanks to the contact between the NTP and the subunit. Crystal structures reveal highly conserved arginine residues (arginine finger) in the helicase core domain which is involved in ATP hydrolysis (Matson SW et al., 1994; Ren H et al., 2007). This conserved arginine residue senses the change in the NTP binding state and transmits the change to cause subunit movement (Singleton MR et al., 2000; Sawaya MR et al., 1999).

1.3.2. Interaction with nucleic acid substrates

Helicase binding to nucleic acids is an important step towards nucleic acids separations. The mechanism of binding can be different according to the helicase families. However most of them need a single-stranded nucleic acid region to bind. Once loaded on the strand, they translocate either 5' to 3' or 3' to 5'. The crystal structures of helicases bound to DNA or RNA revealed that helicases bind to nucleic acids through their phosphate backbones or nucleotide bases in the conserved motifs in the helicase core domain (Velankar SS et al., 1999; Lee JY and Yang W, 2006; Saikrishnan K et al., 2008; He X et al., 2012; Chen WF et al., 2016). As mentioned earlier, the NTP binding state causing a subunit movement, the nucleic acid affinity changes. Moreover, there is a special domain named the zinc-binding motif, which has also been found in some helicases to contribute to nucleic acid binding (Alberts IL et al., 1998; Guo RB et al., 2005). The consequence is a significant conformational change in the

helicase domain. This change is absolutely necessary for ATPase and DNA/RNA unwinding. For example, when the DEAD box helicase YxiN binds to RNA, it will induce the closer conformational change of two helicase subdomains for RNA unwinding (Karow AR and Klostermeier D, 2009). Similar structure changes also have been indicated in PcrA and Rep helicases (Velankar SS et al., 1999; Korolev S et al., 1997). In addition, some helicases are sensitive to chemical modifications of the nucleic acid substrate such as breaks (discontinuities in sugar phosphate backbone; substituted with ethylene glycol), abasic sites, or electrostatic disruptions (Eoff RL et al., 2005).

1.3.3. Translocation mechanism

Helicases are defined as enzymes that translocate through double-stranded nucleic acid to catalyse the separation or unwinding of the complementary nucleic acid strands. Therefore they need to unwind nucleic acids much longer than their binding sites. The unwinding occurs in a stepwise manner. The helicase stays on the nucleic acid track and catalyzes repeated cycles of base pair separation steps coupled to unidirectional translocation. But several helicases can translocate along nucleic acids uncoupled from base pair separation (Soulтанas P et al., 2000). Therefore, translocation and base pair separation mechanisms can be distinguished. Many different mechanisms have been proposed for translocation and base pair separation. The diverse biochemical properties (the helicase oligomeric state, its binding mode of the nucleic acid, the effect of the NTP binding state on nucleic acid binding properties) are reflected in the proposed mechanisms. The translocation is characterized by the polarity and the step-size.

Polarity is defined as the direction of helicase translocation along the double-stranded nucleic acid (5' to 3' or 3' to 5') and unwinding. For example FANCI, XPD and RecD unwinds in direction 5' to 3', RecQ helicase family displays 3' to 5' polarity. However, some helicases like RecBDC, PcrA they can show bipolar unwinding activity (Dillingham MS et al., 2003; Naqvi A et al., 2003).

Step-size is defined as the number of steps resulting in the unwinding of a certain number of base pairs during each reaction cycle, which is defined as sequence of chemical and conformational states, such as ATP binding, hydrolysis, and product release. To date, the reported step-size value of helicases varies largely; it is as small as 1 base pair for PcrA helicase and large as 23 base pairs for RecBC (Wigley DB, 2000).

Actually, three models have been accepted to explain the mechanism by which helicases translocate. These three models are named as 'rolling model', 'inchworm model' and

'Brownian model'. These models are illustrated by Figure 3. The inchworm and the rolling models are stepping mechanisms in which two nucleic acid binding sites independently bind and release nucleic acid in response to the signals received from the NTPase site (Wong I and Lohman TM, 1992; Yarranton GT and Gefter ML, 1979; Velankar SS et al., 1999). In these models, the helicase is always bound to the nucleic acid via one nucleic acid binding site.

The Inchworm model (Figure 3A) works with a monomer or oligomer state, and both subdomains bind single strands. One helicase domain is bound tightly to the nucleic acid and the second helicase domain is bound weakly to the nucleic acid. ATP binding and hydrolysis cause that the protein goes through a series of conformational states that move the domains 1 and 2 closer or further apart relative to each other. The weak site dissociates from the nucleic acid and in a power stroke motion moves away from the tight site to bind at a position ahead. After the weak site has moved and made tight interactions ahead, the original tight site becomes weak. The latter dissociates from the nucleic acid and in a power stroke motion it moves forward to get close in distance to the site ahead. One cycle in an inchworm stepping mechanism is completed in six conformational changes. This model has been proposed by the observations of PcrA (Kim JL et al., 1998; Velankar SS et al., 1999).

The Rolling model (Figure 3B) requires a dimerized helicase and each monomer presents different conformational state. One state has a high affinity for single strand RNA/DNA and the other has higher affinity for double strand RNA/DNA. The conformational states vary by NTP binding and hydrolysis. During the hydrolysis of ATP and the ADP ejection, the two monomers change their conformation to adopt "that of the other" allowing their migration. This model had been proposed from the observation of the Rep helicase whose crystals revealed two different conformations (Korolev S et al., 1997).

The Brownian model (Figure 3C) is more recent than the others and comes from a study of NS3 (Levin MK et al., 2005). It is based on two conformational states of the helicase resulting from the different NTP binding states. In the absence of ATP, the helicase binds tightly to DNA in its lowest energy state, unable to translocate. The binding of ATP weakens the affinity of the helicase to DNA and the binding free energy is constant along the nucleic acid length. The consequence is a random Brownian movement of the helicase, which can slide along the length of the nucleic acid in either directions. This movement can lead to the dissociation of the helicase from the DNA. The weak binding mode is characterized by a short life time, since ATP hydrolysis takes place and the enzyme can rebind the DNA tightly. The translocation of the helicase and unwinding of the DNA result from the combination of power stroke and Brownian motion: if the helicase is in the forward position when ATP is

hydrolyzed and released, the helicase will end up one step forwards from its original position upon tight binding to the nucleic acid; whereas, no net unidirectional translocation of the helicase will occur if the helicase is in the backward position when ATP is hydrolyzed. This model is applicable to helicases that function as monomers or oligomers. This mechanism is very similar to the inchworm model but it does not explain the polarity.

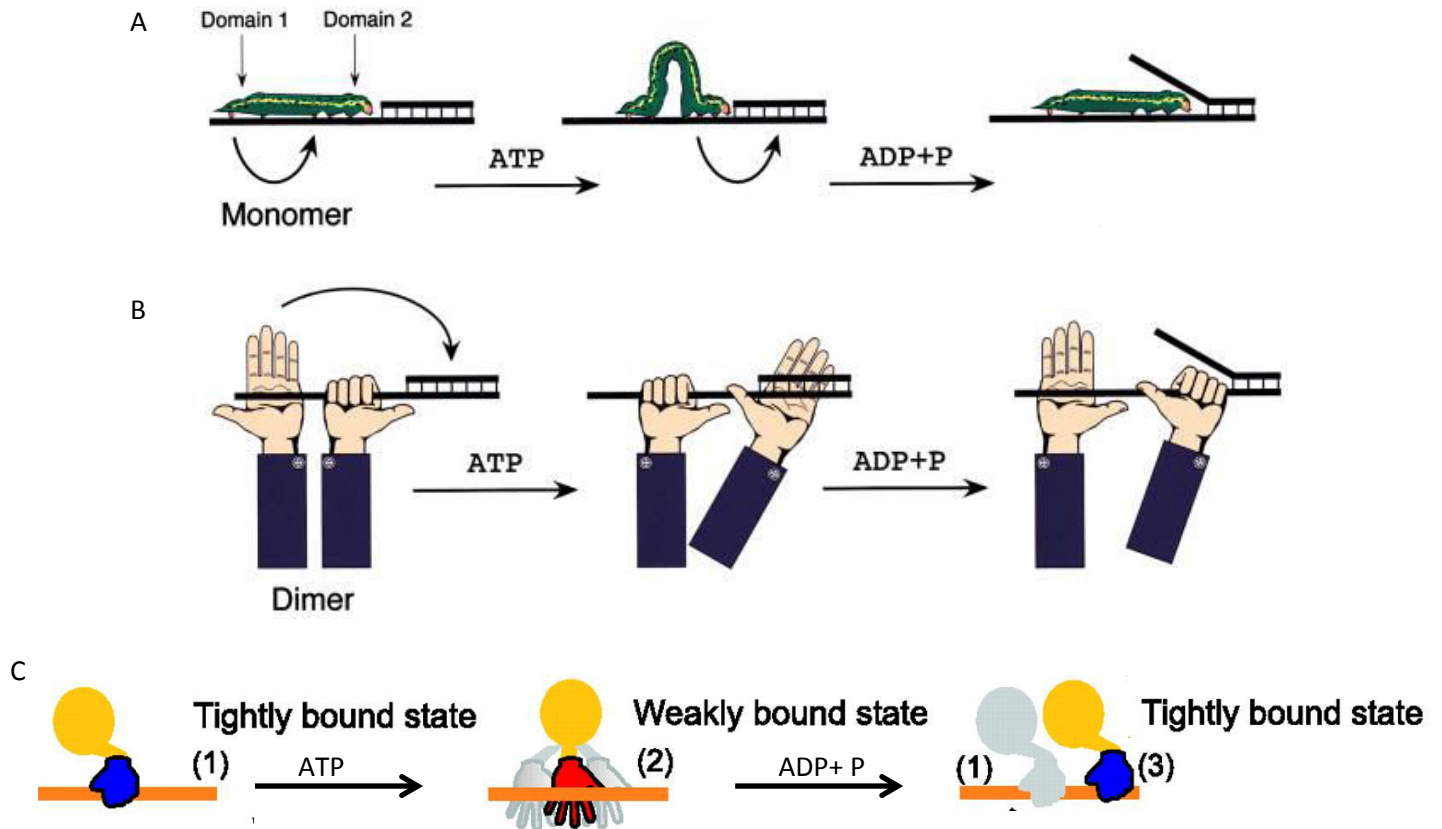


Figure 3. Models of Helicase Activity. (A) Inchworm model: the distance between domains 1 and 2 varies with NTP binding and hydrolysis. Adapted from Tanner NK and Linder P, 2001 (B) Rolling model: each monomer of the helicase has a different conformational state and affinity for single-stranded and double-stranded nucleic acids. Adapted from Tanner NK and Linder P, 2001 (C) Brownian model: the helicase undergo nucleic acid by affinity changes (tight to weak). Adapted from Patel SS and Donmez I, 2006.

1.3.4. Base pair separation or unwinding mechanism

Unwinding activity is characterized by the processivity, which is defined as the number of unwound base pairs before the helicase dissociates from the substrate. It is shown that some helicases exhibit a high processivity. It is normally the case of helicases involved in genome replication. Others can only separate just few bases and are involved in some DNA repair or in helping to prevent the breakdown of DNA replication. But it is important to note that many

helicases interact physically with other proteins in the cell, and this could regulate the processivity (Lohman TM and Bjornson KP, 1996; Bennett RJ et al., 1999; Bianco PR et al., 2001).

Base pair separation occurs at the junction of single-stranded and duplex regions. Long stretches of duplex nucleic acids are unwound by coupling base pair separation to translocation. Two base pair separation mechanisms are possible: an active or a passive mechanism (von Hippel PH and Delagoutte E, 2001; Betterton MD and Julicher F; Lohman TM, 1992) (Figure 4). In the case of the passive mechanism (Figure 4A), thermal fluctuation allows spontaneous base pair opening before the helicase moves and binds to the newly opened base. The opening of several base pairs at the same time is very unlikely near the junction. In this case, to move and bind more than one base at a time, an active mechanism is necessary (Figure 4B). Helicase translocate one strand while excluding the complementary strand (Jezewska MJ et al., 1998; Kaplan DL 2000; Kaplan DL et al., 2003; Tackett AJ et al., 2001; Kawaoka J et al., 2004; Ahnert P and Patel SS 1997; McGeoch AT et al., 2005). This mechanism prevents re-annealing of the unwound strands. Duplex DNA can be destabilized by other ways. For example helicases can interact and distort the duplex region near the unwinding junction before separating the strands (Wong I and Lohman TM 1992; Velankar SS et al., 1999).

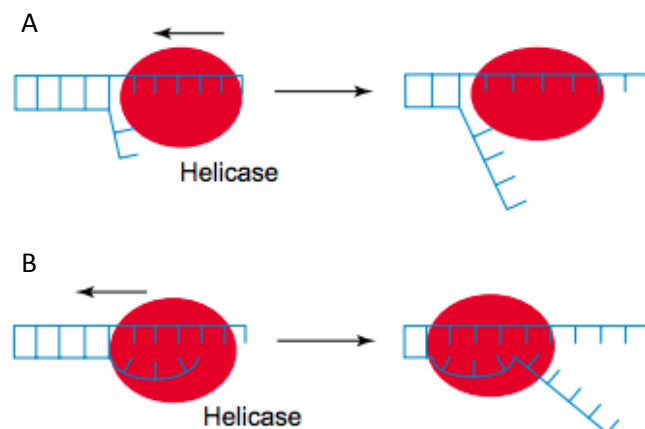


Figure 4. Passive and active mechanisms for helicase unwinding. (A) In the passive mechanism, the helicase does not contact directly with the duplex. Instead, it operates by trapping ssDNA at a thermally fraying ss–dsDNA junction. (B) In the active mechanism the helicase interacts directly destabilizing the dsDNA by actively unwinding the strands. Adapted from Soutanas P and Wigley DB, 2001.

1.3.5. Annealing

Although helicase can separate nucleic acid duplexes, they also possess strand-annealing activity. Several lines of evidence have shown that annealing activity is a result of oligomeric state of helicases. Some laboratories found the C-terminal region of helicase is required for the annealing ability (Muftuoglu M et al., 2008). The human RecQ5 (Ren H et al., 2008), RECQ4 (Macris MA et al., 2006), the Bloom Syndrome helicase (BLM) (Cheok CF et al., 2005), the Werner Syndrome helicase (WRN) (Brosh RM Jr et al., 2006) are examples of helicases with significant strand annealing activity. The consequence can be the processing of Okazaki fragments (Bartos JD et al., 2006), RNA secondary structure formation (Muller UF et al., 2001), the redox-regulated (Chamot D et al., 2005). Some RNA helicases, are able to carry out the unwinding function in the presence of ATP, and the annealing activity independent of ATP (Chamot D et al., 2005). Structure and length of substrate influence the annealing ability of helicase (Muller UF et al., 2001). It increases with the length of the strands in the cases of BLM and WRN (Machwe A et al., 2006). The unwinding activities are significantly stronger than annealing for several helicases, as the redox-regulated cyanobacterial RNA helicase (CrhR) (Chamot D et al., 2005). Other proteins regulate the balance between annealing and unwinding (Machwe A et al., 2006). Some studies have revealed that some proteins present domains responsible of annealing activity, as the RecQ5 β helicase in the C-terminus (Garcia PL et al., 2004), Pif1 in the N-terminal domain (Gu Y et al., 2008). Also the N-terminal region of RECQ1 (Lucic B et al., 2011) and the C-terminal region of the WRN helicase are required for annealing activity (Muftuoglu M et al., 2008). Demonstrating that it is not a single conserved domain responsible for the annealing activity. The oligomeric state of the helicase is also involved in the annealing activity. The tetrameric state of the human RECQ1 helicase promotes annealing whereas monomeric or dimeric states have unwinding activity (Muzzolini L et al., 2007; Lucic B et al., 2011). Also the ATP permits the unwinding activity and inhibits the annealing. This has been seen with BLM (Cheok CF et al., 2005), Pif1 (Gu Y et al., 2008) and the RNA helicase Ddx42p (Uhlmann-Schiffler H et al., 2006). Moreover some proteins can regulate the annealing activity. For example RPA stimulates the unwinding activity of many helicases *in vitro* such as WRN (Brosh RM Jr et al., 1999; Shen JC et al., 1998), BLM (Brosh RM Jr et al., 2000), RECQ1 (Cui S et al., 2004), and FANCD1 (Gupta R et al., 2007) by inhibiting unwinding and annealing activity of RECQ1 (Sharma S et al., 2005), PIF1 (Gu Y et al., 2008), and CSB (Muftuoglu M et al., 2006). Also other proteins as U2AF permits annealing of RNA helicase A (Lee CG et al., 1993) and XPG permitting annealing activity of the WRN helicase (Trego KS

et al., 2011).

1.3.6. Regulatory domains and specificity

Helicases are also characterized by the presence of accessory domains. They can be localized in the N terminal region, inside the RecA domain, or in the C terminal region. The length, the topology and the activities of these domains are variable. These domains are responsible of the specificity and the regulation of the enzymatic activity. UvrD/Rep and Pif1-like have accessory domains (motif Ia and III) located on top of the nucleic acid binding site, on the helicase core determining the definition of the translocation polarity (Saikrishnan K et al., 2009). Accessory domains modulate the enzymatic activity by targeting the protein at a specific substrate such as RecQ-like, that contain DNA-binding accessory domain called HRDC domain involved in targeting a variety of substrates. Also DbpA has accessory domains, which target different RNA structures (Bennett RJ and Keck JL, 2004; Diges CM and Uhlenbeck OC, 2001). In the case of Mss116p's two sub-regions in the C-terminal domain modulate and support the activities of the helicase core, the translation and RNA splicing (Mohr G et al., 2008). The accessory regions can constitute dimerization sites in the case of helicase Hera, which presents a dimerization motif in the C-terminal domain connected with RecA domain by a hinge region that confers flexibility onto the helicase, allowing for different juxtapositions of the RecA-domains in the dimer (Klostermeier D and Rudolph MG, 2009). The accessory domains interact also with proteic partners: among the DExD/H box ATPases, Prp2, Prp16, Prp22 and Prp43 allows the assembly of the spliceosome, the catalysis of the splicing reaction and the dissociation of the intron-lariat spliceosome. For exemple see the case of Prp43, which interacts with the G-patch motif of Ntr1 and Prp2 with Spp2 (Company M et al., 1991; Arenas JE and Abelson JN, 1997; Edwalds-Gilbert G et al., 2004; Silverman EJ et al., 2004; Christian H et al., 2014).

1.4 Biological functions of helicases

Helicases being conserved enzymes from bacteria to human and having interactions with nucleic acids, it confers them a key role in genomic metabolism and stability, involving them in various cellular processes. Mutations in helicases lead to a number of human diseases such as cancer, premature aging, Bone Marrow failure, neurodegenerative diseases, telomere shortening and autoimmune diseases. The tables 1 and 2 below summarizes the helicase functions related to human diseases:

| DNA Helicase | Disease(s) | Genome metabolic pathway | Reference |
|---------------------|--|---|---|
| WRN | Werner syndrome | Repair | Bernstein KA et al., 2010; van Brabant AJ et al., 2000; Suhasini AN and Brosh RM, Jr, 2013 |
| BLM | Bloom syndrome | Repair | Bernstein KA et al., 2010; van Brabant AJ et al., 2000; Suhasini AN and Brosh RM, Jr, 2013 |
| RECQ4 | Rothmund-Thomson syndrome, Baller-Gerold syndrome, & Rapadilino syndrome | Replication and Mitochondrial DNA metabolism | Bernstein KA et al., 2010; van Brabant AJ et al., 2000; Suhasini AN and Brosh RM, Jr, 2013; Liu Y, 2010 |
| FANCI | Fanconi anemia | Repair | Kim H and D'Andrea AD, 2012; Wu Y et al., 2008 |
| XPD and XPB | Xeroderma pigmentosum, Cockayne syndrome, and trichothiodystrophy | Reparation and Transcription | Fuss JO and Tainer JA, 2011; Egly JM and Coin F, 2011; |
| RTEL1 | Dyskeratosis congenital and Hoyeraal-Hreidarsson syndrome | Telomere maintenance and Homologous recombination | Walne AJ et al., 2013; Le Guen T et al., 2013 |
| PIF1 | Cancer | Replication, Transcription, Telomere maintenance and Mitochondrial DNA metabolism | Chisholm KM et al., 2012 |

Adapted from Bochman ML, 2014 and Brosh RM Jr, 2013.

| RNA Helicase | Disease(s) | Genome metabolic pathway | Reference |
|---------------------|--|---|---|
| RIG-I like | Viral infection | RNA sensor | Bruns AM and Horvath CM, 2011 |
| DDX1 | Viral infection and Cancer | Transcription, mRNA processing, Translation | Fang J et al., 2005; Robertson-Anderson RM et al., 2011; Ishaq M et al., 2009; Tanaka K et al., 2009; Bléoo S et al., 2001; Kanai Y et al., 2004 |
| DHX36 | Viral infection, Aging and Cancer | Telomere maintenance, mRNA processing | Naji S et al., 2011; Sexton AN and Collins K, 2011; Lattmann S et al., 2010; Tran H et al., 2004 |
| DHX9 | Viral infection and Systemic lupus erythematoses | RNA sensor, Transcription, Translation | Zhang Z et al., 2011; Jeang KT and Yedavalli V, 2006; Roy BB et al., 2006; Nakajima T et al., 1997; Fujii R et al., 2001; Aratani S et al., 2001; Hartman TR et al., 2006 |
| DDX39 | Cancer | Telomere maintenance | Yoo HH and Chung IK, 2011 |
| DDX19 | Lethal congenital contracture syndrome | RNA transport | Hurt JA and Silver PA, 2008 |
| DDX25 | Azoospermia and Oligospermia | RNA transport | Sheng Y et al., 2006 |
| Gu | Gastric antral vascular ectasia | mRNA processing, Translation | Schmid SR and Linder P, 1992 |

Adapted from Steimer L and Klostermeier D, 2012.

Defining the cellular roles of these helicases and determining the exact steps in which they are involved in the metabolic pathway will allow to link the defect in a particular helicase to the human disease. Helicases being classified on the basis of their substrate, they can be distinguished as DNA helicases and RNA helicases.

1.4.1. Biological functions of DNA helicases

DNA helicases are required for the maintenance of genome integrity including DNA replication, repair, chromosome recombination and transcription. These proteins are also involved in functions in which their helicase activity is not required. Indeed they can interact with nucleic acids and other protein partners in the cell, playing the role of molecular sensor and participating to signal transductions. The breakdown of genome integrity and cellular signaling cascades are a characteristic of many diseases and places them at the forefront of biomedical research into genetic disorders, ageing and cancer biology.

1.4.1.1. DNA replication

DNA replication consists in the production of two identical replicas of DNA from one original DNA molecule. Numerous studies were performed to understand the mechanisms of the replication initiation. For instance, in *E. coli*, the replication origine (Ori C) is recognized by the dnaA protein, which allows the fixation of dnaB, which is characterized by a helicase activity. Associated with an enhancer of this activity dnaC, dnaB can unwind DNA (Baker TA et al., 1987). Therefore helicase acts as a roadblock remover permitting the formation of the replication fork. They function as a checkpoint and a surveillance mechanism to remove structural roadblock in S-phase of DNA replication. Some DNA replication intermediates such as DNA hairpins, D-loop, triple junctions, Holliday junctions can be solved by helicases (Hickson ID, 2003).

1.4.1.2. DNA Transcription

Transcription is a very elaborated process consisting in copying the information of a DNA strand into a molecule of messenger RNA (mRNA). It requires several transcription factors and helicases play a major role in the initiation of the transcription. Among the transcription factors, TFIIH is a large complex of nine subunits with helicase and kinase activities (Eisen A and Lucchesi JC, 1998; Frit P et al., 1999). The 3'-5' helicase XPB is one of them and is essential for both DNA repair and transcription initiation (Coin F et al., 1999). The TFIIH complex enables the formation of the RNA polymerase II pre-initiation complex by

phosphorylation of the C-terminal domain. The active RNA polymerase allows the opening of the double-stranded DNA and template transcription. Several other helicases have been identified in the initiation of the transcription such as MOT1 in yeast (Davis JL et al., 1992), Brahma in *Drosophila* (Tamkun JW et al., 1992), hBrm in human (Muchardt C et al., 1993). In yeast, the helicase domain of SNF2 is necessary for the transcription activity (Laurent BC et al., 1993) and the N- and C-terminal domains of the protein interact with other members of the SWI/SNF family which are DNA binding activators and specific for some general transcription factors. The ATPase activity contributes to the unwinding at the initiation site (Laurent BC et al., 1993). Other helicases such as Senataxin and Rho are involved in the transcription termination at RNA polymerase pause sites (Alzu A et al., 2012; Richardson JP, 2002).

1.4.1.3. DNA repair

Genetic information during metabolic activities is permanently submitted to different stresses such as UV irradiations, chemicals leading to DNA damages, mismatches, DNA modifications. Fatal damages are DNA Double-Strand Breaks (DSBs) or interstrand DNA crosslinks and small DNA lesions such as oxidized or reduced bases, fragmented or non-bulky adducts. These lesions can block DNA replication and transcription. Therefore DNA sequences must be quickly repaired otherwise mutations, cancerogenesis, loss of genetic information can occur and lead to cell death. Cells repair these fatal damages by different cell pathways: Homologous Recombination (HR), Non-Homologous End-Joining (NHEJ), Base Excision Repair (BER) Nucleotide-excision repair (NER) and Interstrand CrossLink (ICL) repair. Homologous Recombination (HR) is a type of genetic recombination in which nucleotide sequences are exchanged between two similar or identical molecules of DNA and it is normally used to repair damage. RTEL1 suppresses homologous recombination (HR) by unwinding displacement loop (D-loop) (Uringa EJ et al., 2012) and BLM helicase (BLM) interacts with DNA2 helicase/nuclease, EXO1, the MRN complex and Replication Protein A (RPA) allowing DSB resection during HR-mediated repair (Nimonkar AV et al., 2011) (Figure 5A). Like homologous recombination (HR), Non-Homologous End-Joining (NHEJ) allows to repair the double-strand breaks (DSB). It is known that WNR interacts with the Ku protein complex (Cooper MP et al., 2000) and DNA ligase IV (Kusumoto R et al., 2008), which are both implicated in NHEJ. The resulting single-strand break can be processed by short-patch BER through a single nucleotide replacement or long-patch BER through which 2-10 new nucleotides (Figure 5B). The Werner syndrome helicase

(WRN) participates in long-patch BER by unwinding 5'-flaps and interacting with BER proteins (Rossi ML et al., 2010), by interacting with poly (ADP-ribose) polymerase 1 (PARP1), which is a sensor of DNA breaks (Lebel M et al., 2003) and other proteins, notably DNA polymerase- β , apurinic/apyrimidinic endonuclease 1 (APE1), and flap endonuclease 1 (FEN1) (Rossi ML et al., 2010).

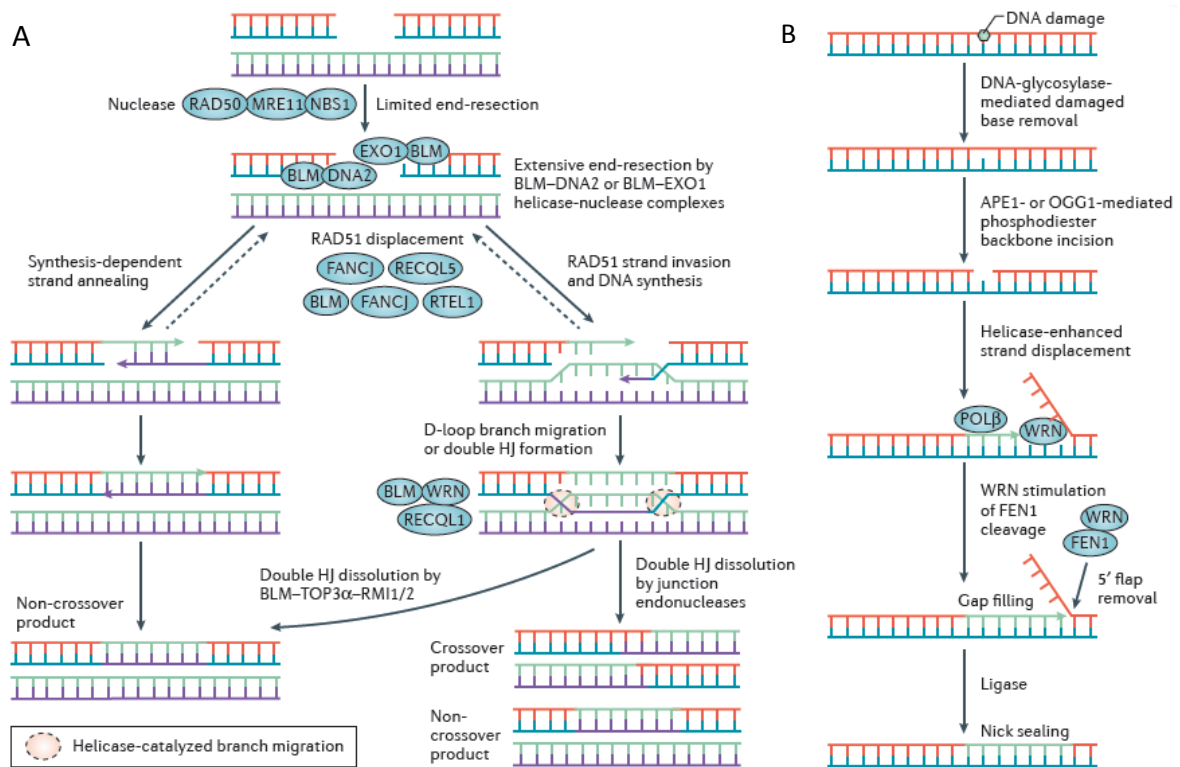


Figure 5. Helicases in Homologous Recombination (HR) and Base Excision DNA Repair (BER). (A) The Homologous Recombination (HR) allows the disruption of displacement loops (D-loops) and decreases double Holliday Junction (HJ) formation. (B) The Base Excision DNA Repair (BER) by WNR action in the long-patch allows the strand displacement. Adapted from Brosh RM Jr, 2013.

The bulky distortions in the DNA can be recognized by Nucleotide-excision repair (NER) leading to the removal of a short single-stranded DNA segment, which includes the lesion and creates a single-strand gap in the DNA, which is filled by a DNA polymerase (Figure 6A). In this case the TFIIH complex is activated. This complex is composed of two DNA helicases XPD (5' to 3') and XPB (3' to 5'), which open the DNA duplex around the lesion. Then the Replication Protein A (RPA) enables nucleases recruitment (the XPF-ERCC1 complex and XPG) which can then remove the damaged strand (Egly JM and Coin F, 2011). Also HR and NER involve the FA pathway of ICL mechanism through a variety of proteins (Figure 6B). FA core complex contains FANCM which participates to the ICL detection, FANCD1 which

operates downstream of FANCD2 and FANCI mono-ubiquitylation to facilitate recombinational repair (Peng M et al., 2007). Moreover BLM participates in this FA complex by stabilizing the stalled replication fork (Meetei AR et al., 2003).

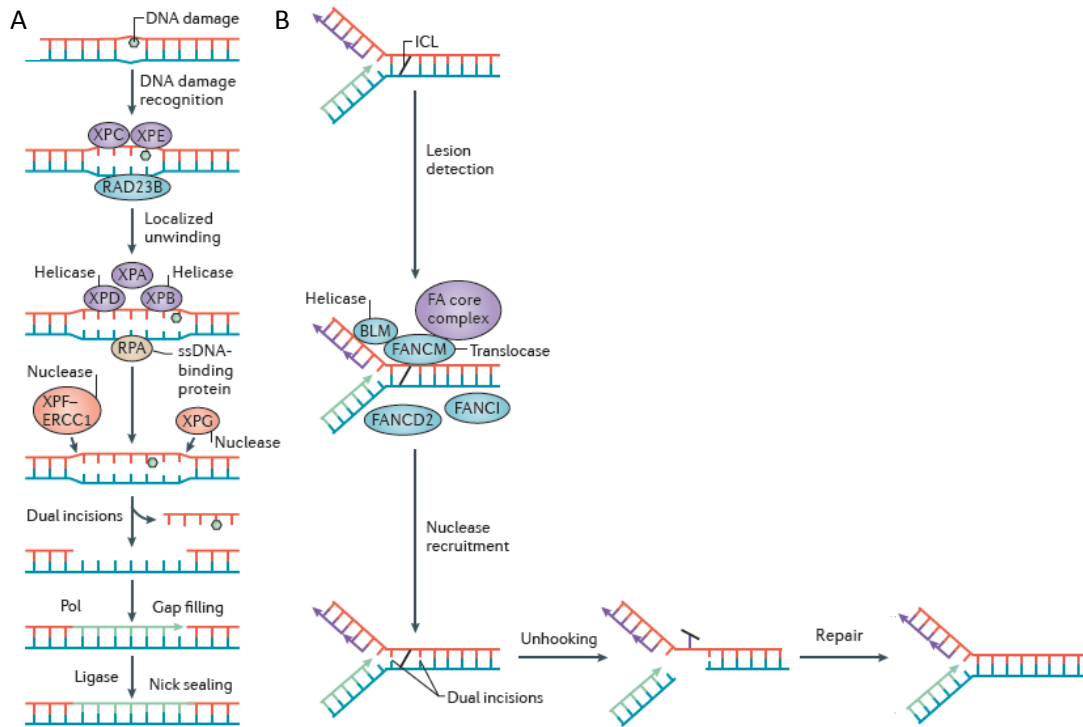


Figure 6. Helicases in Nucleotide Excision (NER) and Interstrand Crosslink (ICL) DNA Repair. (A) The Nucleotide Excision Repair (NER) by the action of XPB and XPD leads to the dsDNA opening. (B) The Interstrand Crosslink (ICL) DNA Repair by the participation of various helicases such as FANCI and BLM allows the action of nucleases which cause the removal of one strand, leaving a gap that will be resolved by parallel repair pathways. Adapted from Brosh RM Jr, 2013.

1.4.1.4. Chromosome recombination

DNA recombination is involved in several biological functions. It is firstly involved in meiosis leading to new combinations of DNA sequences, to make gamete cells, sperm and egg cells in animals. This results in a genetic variation, which allows adaptation during evolution. Also it is used to accurately repair harmful breaks that occur on both strands of DNA (DBSs), named in the previous paragraph. In the case of homologous recombination in meiosis some helicases are required.

In normal cells, the sister chromatid exchanges (SCEs) is low (Chaganti RS et al., 1974) due to the molecular mechanism which allows mitotic recombination intermediates separation

(Bizard AH and Hickson ID, 2014). The uncoupling of single and double Holliday junctions (HJs) proceeds through two mechanisms: dissolution, in which a double HJ (dHJ) is dissolved by a DNA helicase or motor protein and unlinking by a type IA topoisomerase (ex. BLM–TOPIII α –RMI1–RMI2 (BTRR) in humans), or resolution, in which an HJ or precursor is cut by one or several endonucleases (ex. MUS81–EME1, SLX1–SLX4, or GEN1 in humans). The dissolution pathway exclusively produces noncrossover products, but the resolution pathway may produce either crossover or noncrossover products (Bizard AH and Hickson ID, 2014; Wyatt HD and West SC, 2014).

In the case of Double-Strand Breaks (DSBs), in bacteria (*E. coli*) two helicases of the RecBDC pathway are active: RecB which is a 3' to 5' helicase and RecD which is a 5' to 3' helicase (Dillingham MS and Kowalczykowski SC, 2008), they move both in the same direction and cause a faster unwinding (Singleton MR et al., 2004; Liu B et al., 2013) (Figure 7A). In eukaryotes a heterotrimeric complex Mre11–Rad50–Xrs1–Sae2 (MRX) binds to a DSB (Figure 7B). In vitro, MRX presents a 3' to 5' exonuclease activity (Cannavo E and Cejka P, 2014). MRX (MRN in humans) produces an important intermediate that commits a DSB to HR versus nonhomologous end joining (NHEJ), producing a long ssDNA region upon which a Rad51 filament forms (Symington LS, 2014). This long-range resection proceeds through two alternative routes: the Sgs1–Dna2–RPA pathway and the Exo1 pathway (Symington LS, 2014). The Sgs1–Dna2–RPA pathway permits the resolution by the Sgs1 5' to 3' unwinding activity and the Dna2 5' to 3' nuclease activity stimulated by RPA (Cejka P and Kowalczykowski SC 2010; Cejka P et al., 2010; Niu H et al., 2010).

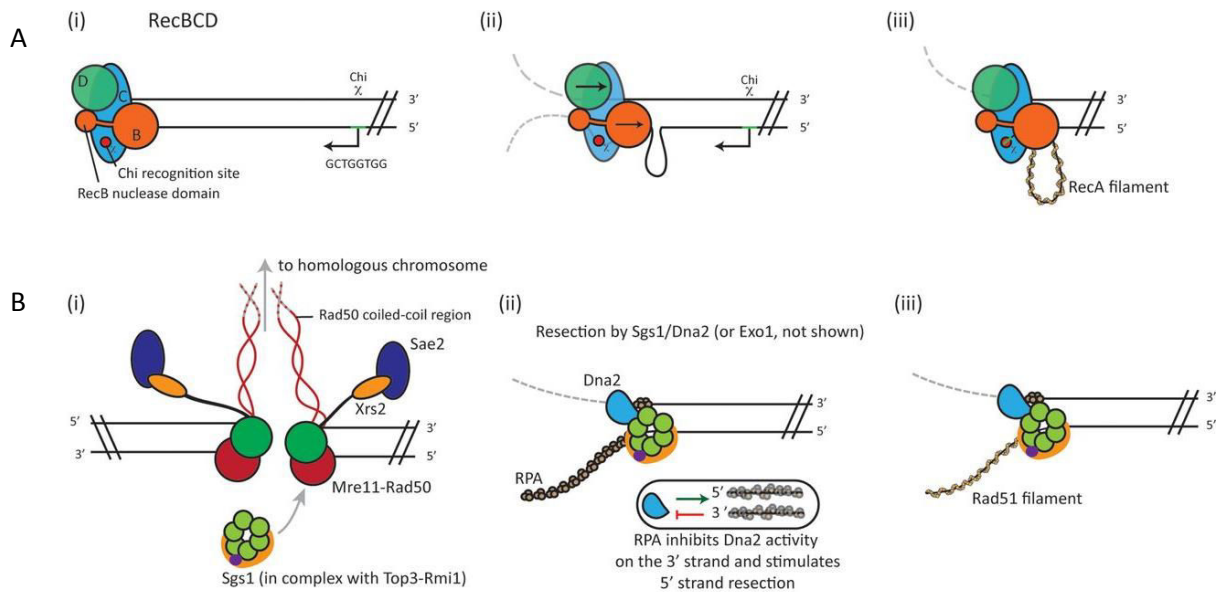


Figure 7. Chromosome recombination in the case of Double-Strand Breaks (DSBs). (A) The bacterial RecBCD pathway (*E. coli*). (i) RecBCD helicase-nuclease complex recognises the DNA end. (ii) The two helicases translocate each strand: RecD in green (5' to 3') and RecB in orange (3' to 5'). The nuclease domain is located at the C-terminus of RecB. Before encountering a Chi (crossover hotspot initiator) site, the 3' strand is more cleaved than the 5' strand and a loop of single-stranded DNA accumulates ahead of RecB. (iii) Chi recognition by RecC subunit in blue leads to the stimulation of the nucleases activity complex on the 5' strand only. Finally RecA loads on the resulting 3' single-stranded DNA tail, which allows Homologous Recombination (HR). (B) The eukaryotic MRX complex pathway (*S. cerevisiae*). (i) The MRX complex (Mre11 in green; Rad50 in red; Xrs1 in orange; Sae2 in purple) recognises DNA ends. (ii) MRX recruits Sgs1 helicase in light green to the DSB end. The extensive end-resection is performed by DNA2 (in blue) associated with Sgs1 or in an alternative way by Exo1. RPA is bound to the unwound single-strands and stimulates Dna2 nuclease activity on the 5' strand only. (iii) RPA is replaced by Rad51 recombinase on the 3' tail initiating Homologous Recombination (HR). Adapted from Blackwood JK et al., 2013.

1.4.1.5. Telomeres maintenance and G-quadruplexes metabolism

In vivo observations have shown that several helicases having different functions at telomeres, are directly involved in telomere maintenance. The helicase Pif1p from yeast inhibits telomerase-mediated telomere lengthening by removing the telomerase from telomeric DNA (Zhou J et al., 2000; Boule JB et al., 2005). Helicases such as RTEL1 (Regulator of Telomere Elongation heLicase 1) and WRN (WNR syndrome helicase) resolve

T-loops to enable telomere replication or repair (Vannier JB et al., 2012; Opresko PL et al., 2004). Also in human, the DNA helicase DDX11 determines telomere length (Vasa-Nicotera M. et al., 2005)

G-quadruplexes are non typical DNA structures composed of planar stacks of four guanines interacting by Hoogsteen hydrogen bonds. They are present in promoters and telomers. Certain DNA helicases such as WRN, BLM, FANCD1 and PIF1 have the ability to unwind G4 DNA substrates *in vitro* (Wu Y and Brosh RM Jr, 2010)

In the second part of this manuscript dealing with the interaction between the Pif1 helicase and the G-quadruplex, more informations will be given on these aspects.

1.4.1.6. DNA sensing

In the case of a microbe infection, the innate immune system comprises the cells of the first defense mechanism of host (Wu J and Chen ZJ, 2014). The pattern-recognition receptors (PRRs) allow to recognize in microbes different pathogen-associated molecular patterns (PAMPs), such as peptidoglycans (Schwandner R et al., 1999), lipopolysaccharides (LPS) (Brightbill HD et al., 1999; Zhang FX et al., 1999) and flagellin (Mizel SB et al., 2003). Also PRRs can detect damage associated molecular pattern molecules (DAMPs) that are derived from the host itself under stresses, including heatshock proteins (Wick G et al., 2014), HMGB1 (Bangert A et al., 2016), ATP (Kouzaki H et al., 2011), uric acid (Andrews NW, 2005), heparin sulfate (Tsunekawa N et al., 2016) and DNA (Chan YK and Gack MU, 2016). The most studied PRRs are the Toll-like receptor (TLR) family that is expressed on innate immune cells such as dendritic cells (DCs), macrophages and neutrophils (Yin Q et al., 2015). Most TLRs detect extracellular PAMPs (Gay NJ et al., 2014). For exemple TLR1 and TLR2 recognize triacylated lipoproteins from bacteria and GPI anchored proteins from parasites (Kirschning CJ et al., 1998). But also microbes can deliver PAMPs to the cytosol of the host cells, and these cytosolic PAMPs are recognized by intracellular PRRs (Beachboard DC and Horner SM, 2016). For instance, intracellular LPS can be recognized by inflammatory caspases (Shi J et al., 2014) and also Engulfed CpG rich DNAs are sensed by TLR9 in the endosomal compartment (Hemmi H et al., 2000).

In general, all the pathogens contain DNA or RNA for their basic life activities such as protein encoding, movement and proliferation. These nucleic acids are potential PAMPs but their detection must be tightly regulated because improper recognition of host self nucleic acids will cause autoimmune diseases (Burdette DL and Vance RE, 2013). In the case of DNA it is more complicated, however eukaryotic genomic DNAs is in the cell nucleus

separated from the cytosol. In fact a DNA sensing activity has been described for three helicases only: DDX41, DHX9 and DHX36, which are members of the DExD/H-box helicases (DDX) protein family. DDX41 (Figure 8A) detects and binds double stranded DNAs (dsDNAs) through its DEAD domain (Asp-Glu-Ala-Asp). This interaction enables the protein to interact with STING and activate the STING-TBK1-IRF3 pathway in myeloid dendritic cells (mDCs) (Zhang Z et al., 2011) allowing finally the subsequent type I interferon production (Tanaka Y and Chen ZJ, 2012). It has also been reported that DDX41, directly binds cyclic dinucleotides (CDNs), such as cyclic di-GMP (c-di-GMP) inducing IFN (Parvatiyar K et al., 2012). In the case of DHX9 and DHX36, these two helicases bind CpG DNA (Figure 8B). DHX36 binds CpG-A using the DEAH domain leading to IRF7 activation, whereas DHX9 binds CpG-B using the DUF domain (Domain of Unknown Function) leading to NF κ B activation, both through MyD88 in plasmacytoid dendritic cells (pDCs) (Kim T et al., 2010). Moreover DHX9 has the capacity to bind viral RNA of influenza A and reovirus inducing the MAVS-dependent IFN and cytokine expression in myeloid DCs (Zhang Z et al., 2011). It is important to notice that these three helicases possess other cellular activities such as mRNA splicing and translation initiation for DDX41 (Polprasert C et al., 2015; Ilagan JO et al., 2013), telomere maintenance and mRNA processing for DHX36 (Sexton AN and Collins K, 2011; Lattmann S et al., 2010; Tran H et al., 2004) and transcription and translation for DHX9 (Jeang KT and Yedavalli V, 2006; Roy BB et al., 2006; Nakajima T et al., 1997; Fujii R et al., 2001; Aratani S et al., 2001; Hartman TR et al., 2006). In the situation of the DNA sensing activity by these enzymes, the helicase activity in the literature.

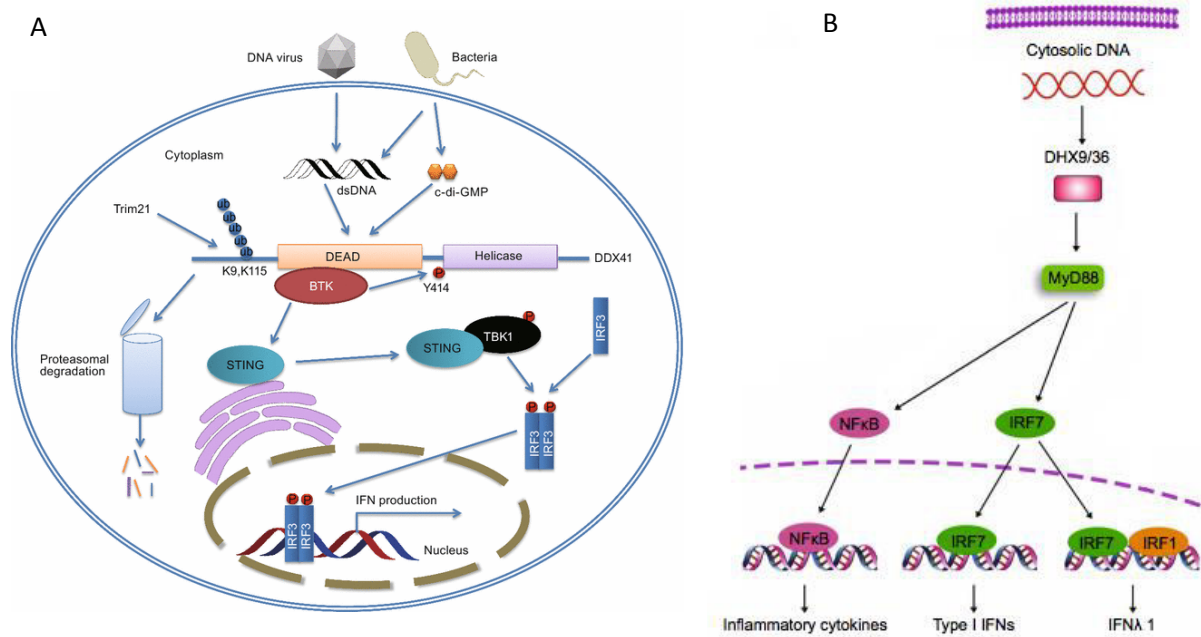


Figure 8. Signalling pathways of helicase DNA sensors in innate immunity. (A) The signalling pathway of DDX41. After infection, virus and bacteria release dsDNA or c-di-GMP. DDX41 is then phosphorylated by BTK kinase and gets active. This activation allows DEAD domain interaction with foreign PAMPs and activation of STING. STING translocates from the endoplasmic reticulum (ER) to Golgi apparatus and interacts with TBK1 leading to TBK1 activation and subsequent phosphorylation resulting in nuclear translocation of IRF3 and IFN type 1 expression. After immune response, DDX41 is ubiquitinated by TRIM21 leading to its degradation in the proteasome. Adapted from Jiang Y et al., 2017. (B) The signalling pathway of DHX9/36. After cell infection DHX9/36 interacts with infectious dsDNA and activates NFκB and IRF7 through MyD88, producing inflammatory cytokines and INF type I. Adapted from Xia P et al., 2016.

1.4.2. Biological functions of RNA helicases

RNA helicases are thought to be mainly involved in RNA unwinding. However, they can exhibit a large range of activities (Putnam AA and Jankowsky E, 2013). Being engaged in several steps of the mRNA metabolism, RNA helicases control the gene expression process and the flow of the genetic information by driving and guiding the synthesized molecules towards dedicated molecular factories. Several RNA helicases (DDX1, DDX5, DDX17, DDX20, DDX21 and DHX9) have a role in transcription regulation and they function as transcription co-activators or co-repressors (Fuller-Pace FV, 2006). This category of helicases does not interact with mRNAs only, but also with rRNAs, miRNA, and RNPs. Below we

focus on the roles of RNA helicases in translation regulation, ribosome biogenesis, nuclear mRNA export, RNA decay, splicing, gene silencing, cytoplasmic transport and storage (Lüking A et al., 1998). RNA helicases are also involved in viral RNAs sensing triggering innate immune response (Yoneyama M et al., 2004). Moreover, deregulation of certain RNA helicases have been linked to neuro-degenerative disorders (Fogel BL and Perlman S, 2006), cancers (Abdelhaleem M, 2005) and several research works reveal helicase contribution during the differentiation process (Abdelhaleem M, 2005).

1.4.2.1. RNA splicing

Splicing of mRNA is an essential cellular process to produce mature mRNAs and to translate them into proteins. This process consists in removing additional sequences called introns and joining the exons. This process requires more than hundred proteins. Among them, the RNA-binding proteins (RBPs), and five small nuclear RNA (snRNA), which form RNP complex (splicing complex). These complexes take place in 5' and 3' of the intron and also around the connection point of the intron. The recognition of splicing sites by the spliceosome is modulated by the binding of RBPs on the nascent mRNA and regulates alternative splicing (Fu XD and Ares M Jr, 2014; Witten JT and Ule J, 2011; Irimia M and Blencowe BJ, 2012). Several RNA helicases have been purified from different splicing complexes (Ilagan JO et al., 2013; Will CL et al., 2002). They function in various species (Burckin T et al., 2005). In human, DDX5 and DDX17 control the splicing of a large number of exons (Dardenne E et al., 2014). DDX41 interacts with a large number of spliceosome components, and the gene mutation of this RNA helicase affects alternative splicing (Polprasert C et al., 2015; Ilagan JO et al., 2013). Additionally, some RNA helicases have a role in the splicing fidelity by rejecting suboptimal splicing substrates (Koodathingal P and Staley JP 2013). Core spliceosome helicases may therefore contribute to alternative splicing site selection. It is the case for the Prp16 and Prp22 RNA helicases in budding yeast (Semlow DR et al., 2016). Seven RNA helicases DExD/H family and one of Ski2-like are necessary for splicing (de la Cruz J et al., 1999). The role of these helicases is required to control the correct RNA base pairing during spliceosomal assembly and also to unfold the secondary structures during the splicing reaction.

1.4.2.2. Nuclear mRNA export

In eukaryotic cells, mRNAs reach the cytoplasm to be translated. This implies it must get the nuclear membrane through the nuclear pores. Several factors are required for this passage (Figure 9). mRNA competent for nuclear export are made thanks to the recruitment to the mRNP of adaptor proteins such as Aly/REF export factor (ALYREF or Yra1 in budding yeast), the subcomplex THO, which are recruited by the helicase DDX39B (UAP56 or Sub2 in budding yeast) (Luo ML et al. 2001) giving the TREX complex. This helicase recruits nuclear RNA export factor 1 (NXF1; also known as TAP or MEX67 in budding yeast) (Gatfield D et al., 2001; Jensen TH et al., 2001; Luo ML et al., 2001; Strasser K and Hurt E, 2001). Two other RNA helicases have also been shown to play a part in co-transcriptional mRNP assembly and mRNA export: DDX5 in humans and its budding yeast homologue Dbp2. Then, once mRNPs have transited through the nuclear pore complex, they are remodeled by DDX19B (DBP5 in budding yeast) in the cytoplasm, and the nuclear RBPs is released from mRNPs in an ATPase-dependent manner (Lund MK and Guthrie C, 2005; Tran EJ et al., 2007; Tieg B and Krebber H, 2013).

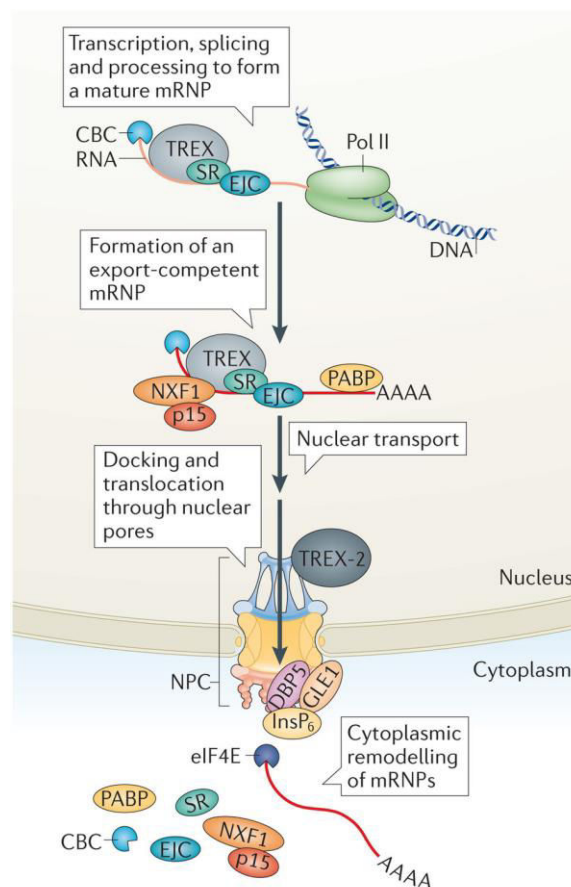


Figure 9. mRNA export from nucleus to the cytoplasm. The nascent messenger ribonucleoprotein particle (mRNP) is recruited for the transcription-export complex TREX.

After mRNP maturation, the nuclear RNA export factor 1 (NXF1) is recruited to the mRNP through direct interactions with several TREX components (such DDX39B). Both TREX and TREX-2 cooperate to export the same transcripts with NXF1 and its cofactor p15. This triggers the transit through the nuclear pore by interacting directly with the nucleoporins. After mRNPs have transited through NPCs and arrived in the cytoplasm, the different receptors of cargo mRNAs are removed by the action of RNA helicase DBP5 (also known as DDX19B). The ATPase activity of DBP5 catalyses the release of RNA-binding proteins (RBPs) from mRNAs. This process is regulated by three DBP5-interaction partners: the mRNA export factor nucleoporin GLE1 and the small signaling molecule inositol hexakisphosphate (InsP6). Adapted from Wickramasinghe VO and Laskey RA, 2015.

An increasing number of RNA helicases have been shown to have a role in selective mRNA export: for example, selected mRNAs involved in spermatogenesis are exported thanks to the participation of DDX25 (Sheng Y et al., 2006). In *Xenopus laevis* oocytes, Xp54 or DDX6 in humans binds to and exports a set of transcripts that are stored in the cytoplasm and not translated (Smillie DA and Sommerville J, 2002). Finally, DDX1, DDX3X, DDX56, DDX21, DHX9 and MOV10 participate in the nuclear export of viral RNAs (Yedavalli VS et al., 2004; Huang, F. et al., 2015; Yasuda-Inoue M et al., 2013; Reddy TR et al., 2000).

1.4.2.3. mi-RNA-induced gene silencing

miRNAs are small non-coding RNAs that assemble with Argonaute proteins into miRNA-induced silencing complexes (miRISCs). They mediate post-transcriptional silencing by interacting with complementary mRNAs (Jonas S and Izaurralde E, 2015; Ha M and Kim VN, 2014). Several RNA helicases participate in miRNA biogenesis and miRISC assembly (Ha M and Kim VN, 2014). Some of them promote the maturation of specific pri-miRNAs, as DDX5, DDX17 (Motino O et al., 2015; Moy RH et al., 2014). DHX9 (Kawai S and Amano A, 2012), DDX1 (Han C et al., 2014; Gregory RI et al., 2004), DDX23 (Yin J et al., 2015) and DDX3X inhibits Drosha-mediated processing of a subset of pri-miRNAs (Krol J et al., 2015). Some helicase such as DHX36 can inhibit miRNA maturation by competing with Dicer for binding to the terminal loop of pre-miR-134 (Bicker S et al., 2013), whereas other (DDX5) unwinds a miRNA precursor duplex to facilitate its loading on to miRISCs (Salzman DW et al., 2007).

1.4.2.4. Ribosome biogenesis

Ribosome biogenesis is a complex and multistep process. The first step consists in the transcription of ribosomal RNA, several cleavage steps permit the rRNA maturation and finally the ribosome formation. Three to four rRNAs (in prokaryotes or eukaryotes), several snoRNAs (small nucleolar RNAs) behaving as transactivator factors are involved with many ribosomal proteins (Kressler, D et al. 1999). More than 20 RNA helicases have a role in rRNA processing without having a role in mRNA metabolism. Only DDX5 and DDX17 have been found to participate in both processes. Therefore, it seems that RNA helicases have evolved to acquire specialized functions (Bourgeois CF et al., 2016). The depletion of some helicases had permitted the determination of their involvement in pre-rRNA folding, RNA structural rearrangements, unwinding of snoRNA-pre-rRNA base pairing, and remodelling of protein-RNA interactions (Eichler DC and Craig N, 1994; Ripmaster TL et al., 1992). Almost all members of the DExD/H family in yeast and higher eukaryotes participate in ribosome biogenesis (Bleichert F and Baserga SJ, 2007). For instance, they unwind short duplexes of snoRNA-rRNA, rRNA-rRNA, or they are required for the dissociation of RNA-protein complexes (Rocak S and Linder P, 2004). Consequently, a considerable number of DEAD-box proteins are associated with ribosomal RNA maturation (de la Cruz J et al., 1999; Kressler D et al., 1999).

1.4.2.5. Translation initiation and regulation

The translation permits the production of specific amino acid chains, which fold into an active protein and perform their functions in the cell from a messenger RNA (mRNA) obtained by a ribosome. mRNAs are exported to the cytoplasm, they are associated to the cap-binding complex (CBC). But the CBC-dependent translation depends on the unwinding of the 5' untranslated regions (5' UTRs) by DDX48 helicase. This enzyme interacts directly with CTIF (CBC-dependent translation initiation factor) (Choe J et al., 2014). DDX2A and 2B, eukaryotic translation initiation factors known as eIF4A1 and eIF4A2 unwind secondary structures in the 5' UTR after activation by various factors associated with the eIF4F complex otherwise the binding and movement of the 40S ribosome is prevented (Pestova, TV and Kolupaeva VG, 2002; Svitkin, YV et al., 2001). These two helicases are also extremely important for oncogenes and epigenetic regulators translation with G/C-rich 5' UTRs and/or 3' UTRs with miRNA target sites (Modelska A et al., 2015; Wolfe AL et al. 2014). Furthermore, the translation inhibitor DDX3X, stimulates the translation of mRNAs with long and structured 5' UTRs, such as those encoding cyclin E1 or RAC1 (Lai MC et al., 2008; Sen,

ND et al., 2015; Lai MC et al., 2010). RNA helicases, such as DHX29, can also bind directly to the 40S subunit leading to enhancement of the processivity and the correct positioning of mRNAs at the ribosome entry channel (Dhote, V et al., 2012; Pisareva VP et al., 2008) Others RNA helicases like DHX9, are recruited to specific internal secondary structures. Thus, they can regulate translation in different ways: by facilitating 40S scanning, by stimulating ribosome recycling or mRNA circularization (Halaby MJ et al., 2015; Peng S et al., 2011). At later stages of translation RNA helicases can also operate. For instance, the assembly of elongation-competent 80S ribosome is promoted by DHX33 (Zhang Y et al., 2015). Moreover, recognition of stop codons requires DDX19B which also allows the recruitment of eukaryotic polypeptide chain release factor eRF3 to translation termination complexes (Wang Y et al., 2015).

1.4.2.6. RNA decay

The mRNA turnover plays a key role in gene expression and is a important in the physiology of the cell. mRNA degradation occurs in the 5'-to-3' or 3'-to-5' direction (Siwaszek A et al., 2014). In the 5'-to-3' direction, the DDX6 helicase enhances the mRNA decapping, facilitating the access to the nucleic acid by the 5'-to-3' exoribonuclease XRN1 (Siwaszek A et al., 2014; Fischer N and Weis, K 2002; Collier JM et al., 2001). Modulation by DDX6 of the mRNAs coding for proteins involved in autophagy has also been observed (Hu G et al., 2015). mRNA decay in the 3'-to-5' direction starts with deadenylation producing a shortened poly(A) tail (Siwaszek A et al., 2014) which is then degraded via the exosome complex assisted by the RNA helicase SKI2. DHX36 (RHAU) helicase is also recruited and interacts with the deadenylation complex to enhance the mRNA decay (Johnson SJ and Jackson RN, 2013; Tran H et al., 2004). Cells present a surveillance mechanism named Nonsense Mediated Decay (NMD), which is a crucial mechanism detecting mRNA transcripts bearing translation termination codons positioned in abnormal contexts (Lykke-Andersen S and Jensen TH, 2015) (Figure 10). It is dedicated to the clearance of these mRNAs and involves several RNA helicases. The helicase eIF4AIII binds the mRNA and plays the role of a scaffold protein for the Exon Junction Complex (EJC). The UPF1 RNA helicase is recruited and translocates over the nucleic acid, scans the transcript, remodels the mRNP, removes mRNA-associated proteins, and signals the RNA for degradation (Fiorini F et al., 2015). NMD is also facilitated by the interaction between UPF1 and another helicase, MOV10 by resolving structures and displacing proteins from 3' UTRs (Gregersen LH et al., 2014). Other RNA helicases, DHX34,

DHX5, also operate by allowing the assembly of the decay-inducing complex. (Hug N and Cáceres JF 2014; Geissler V et al., 2013; Bond AT et al., 2001).

In bacteria, the degradation complex (degradosome) is constituted by the RNase E, responsible of the RNA decay, PNPase, a 3'-5' exoribonuclease polynucleotide phosphorylase, and the RNA helicase RhlB (Py B et al., 1996; Coburn GA et al., 1999). In *E. coli* the helicases RhlB and CsdA are part of the RNA (Prud'homme-Genereux A et al., 2004).

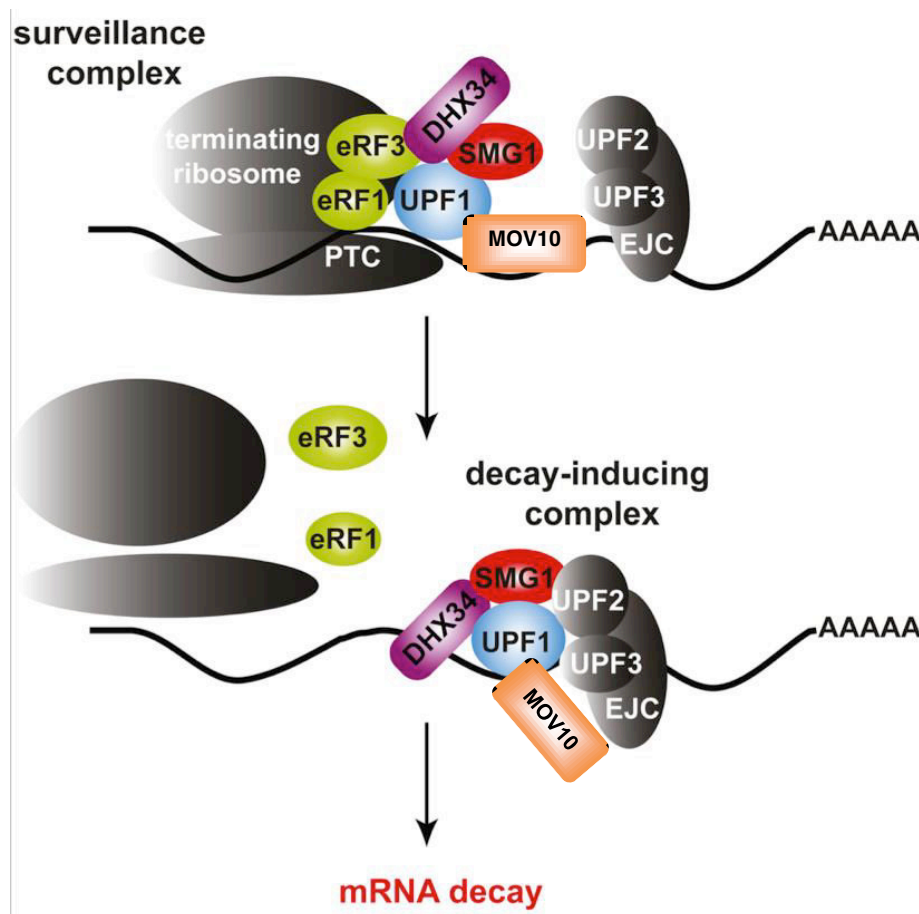


Figure 10. Normal and nonsense-mediated mRNA decay (NMD). The translation is terminated when the termination codon (TC) is in physical proximity to the 3' poly(A) tail (AAAAAAAAA) and/or the 5' 7-methylguanosine (m7 G) leading the recruitment of UPF1 and SMG1 by the eukaryotic translation release factors eRF1 and eRF3, forming the surveillance complex (SURF). Also the two helicases DHX34 and MOV10 are recruited. The recruitment of UPF2 and UPF3 is assisted by EJC bound to the 3' untranslated region (UTR). Then the assembly of the decay-inducing complex (DECID), the interaction of UPF1 with UPF2 induces UPF1 conformational change and activation by SMG1 kinase giving the displacement of the ribosome and the eRFs from the RNP complexes enhanced by DHX34 and MOV10 in an ATP hydrolysis-dependent manner. Endonucleolytic cleavage, decapping and

deadenylation are followed by complete mRNA degradation. Adapted from Hug N and Cáceres JF 2014.

1.4.2.7. Cytoplasmic transport and storage

mRNAs have an alternative fate to translation and decay: transportation and storage in cytoplasmic RNA granules protecting them from degradation (Hooper C and Hilliker A, 2013; Hilliker A, 2012; Pimentel J and Boccaccio GL, 2014; Kanai, Y et al., 2004) allowing localized translation, which occurs in many (Buxbaum AR et al., 2015). In some cases it occurs as a response to cellular stresses or during germ cell differentiation (Hooper C and Hilliker A, 2013; Hilliker A, 2012; Pimentel J and Boccaccio GL, 2014; Kanai, Y et al., 2004). RNA helicases have a major role in RNA granule dynamics. For instance, the formation of RNA granules is influenced in an ATP-independent manner by DDX6, DDX3X and DDX4, as well as their disassembly upon ATP turnover (Hooper C and Hilliker A, 2013; Hilliker A, 2012). DDX25 has a dual function: the storage of mRNP-containing mRNAs coding for spermatogenesis factors, and the promotion of their translation (Tsai-Morris CH et al., 2010; Sheng Y et al., 2006).

1.4.2.8. RNA sensing

A collection of cytosolic receptors has been identified for their ability to recognize multiple forms of nucleic acids. During the last decade, in addition to studies on DNA sensors as exposed above (in the section dealing with the biological functions of DNA helicases), numerous works have focused on receptors related to RNA helicases such as DICERs and the RIG-I Like Receptors (RLRs) because of their critical role in cell signaling and the initiation of innate responses against viruses. DICERs bind dsRNAs derived from the viral genome, replication intermediates or subgenomic products and cleave them into small RNAs, which will be targeted in order to degrade it. DICERS are sensors of RNA interference (Cerutti H and Casas-Mollano JA, 2006; Bernstein E et al., 2001). The RLR (RIG-I Like Receptors) helicases are cytosolic proteins and expressed by most cells of the human organism. RLRs belong to the family of aspartate-glutamate-any amino acid-aspartate/histidine (DEXD/H)-box helicases. Upon RNA-binding, the RLRs activate a signaling cascade leading to the transcription of type I and type III IFN genes (Goubau D et al., 2013).

The first part of the thesis dealing with an attempt of partners identification of RIG-I, an RLR helicase, in the signalling and cellular proliferation/differentiation balance in the APL, more extensive informations will be given on this aspect in the next chapter.

While the term “helicase” implicitly suggests a duplex unwinding activity, some helicases and more exactly members of the SF2 family (Rig-I-like, Swi/Snf2, RecG) do not share this activity. They stably associate with the duplex and they use the energy of ATP-hydrolysis to translocate on duplex DNA by a mechanism independent strand-separation (Saha A et al., 2002; Ristic D et al., 2001; Durr H et al., 2005; Whitehouse I., 2003; Lia G et al., 2006).

Chapter I: Identification and characterization of the RIG-I helicase partners involved in the balance proliferation / cell differentiation in the acute promyelocytic leukemia

Objectif

RIG-I was initially identified as a gene that was induced in retinoic acid-treated Acute Promyelocytic Leukemia (APL) NB4 cells and its expression was associated with the differentiation of the cells (Yu M et al., 1997; Liu TX et al., 2000). RIG-I, a human homolog gene of RNA helicase, is induced by retinoic acid during the differentiation of acute promyelocytic leukemia cell (Yu M et al., 1997) and also associated with viral infection when a porcine homolog was displayed to be induced by porcine reproductive and respiratory syndrome virus (Zhang X et al., 2000). RIG-I has then generated growing interest since it has been found to play a crucial role in innate immunity and in the detection of different viral nucleic acids particularly dsRNA (Yoneyama M et al., 2004). Indeed, to respond to a broad spectrum of pathogens the immune system operates via different and sophisticated mechanisms depending on the nature of pathogen antigen. But the key to establish a specific immune response consists in discriminating between “self” and “non self” components. Pattern Recognition Receptors (PRRs) were identified to respond to conserve Pathogen Associated Molecular Patterns (PAMPs) present on invading pathogens (Hemmi H et al., 2000; Hoffmann JA et al., 1999; Medzhitov R et al., 1997; Poltorak A et al., 1998). PRR are now well characterized and include membrane-associated Toll-Like Receptors (TLRs), C-type Lectin Receptors (CLRs), cytosolic receptors such as NOD-Like Receptors (NLRs), RIG-I Like Receptors (RLRs) and AIM2-Like Receptors (ALRs) (Kawai T and Akira S, 2011).

Therefore RIG-I is involved in two crucial aspects of the cell life that are the immune response and the cell differentiation. The first one has been subjected to numerous studies whereas the second one is not well described in terms of interactions with partners. The present work is focused on the role of the RIG-I helicase during the differentiation of NB4 APL cells. The goal was firstly to identify specific ligand(s) of the helicase during ATRA treatment triggering the differentiation and the proliferation block, by coimmunoprecipitation and High Throughput Sequencing or proteomic analysis. Depending on the obtained ligand(s),

the second step of the work was to characterize the interaction at the biochemical level and then to verify the interaction in the cell and the effect on the differentiation and proliferation by RNAi or truncated proteins. The possibility of a structural study was even considered. This work is based on two points: 1) the domain structure of RIG-I which makes it able to bind both RNAs and proteins, 2) several works show that the specificity of the RNA helicases to their ligands is due to several factors such as the subcellular localization or the expression pattern of the protein in addition to the nucleotide sequence. As a result, certain helicases can have new functions taking part to cell signalling processes. This chapter of the thesis is therefore divided in two parts: RIG-I being an RNA helicase, I started my work searching for RNA partner(s). Later on, the orientation of the work has been readjusted to the search for protein partner(s) relying on the presence of two CARD domains in the helicase. The present work being focused on a member of the RLR, the RIG-I helicase, the following paragraphs will introduce this receptor family, describe the RIG-I helicase accompanied by the downstream signaling pathway and its involvement in APL.

Introduction

1. RIG-I Like Receptors (RLR)

1.1. RLR structure

RLRs have emerged as one of the most important PRR families in immunity to viruses. The RLR family includes the Retinoic acid-Inducible Gene I (RIG-I) encoded by the gene Ddx58, Melanoma Differentiation-Associated antigen 5 (MDA5) encoded by the gene Ifih1, and Laboratory of Genetics and Physiology 2 (LGP2) encoded by Dhx58 (Yoneyama M et al., 2004; Kato H et al., 2011; Loo YM and Gale M Jr, 2011). RLRs are DExD/H-box helicase-like proteins of the SF2 family. RIG-I and MDA5 presents three functional domains, whereas LGP2 has only two functional domains. The Figure 11 illustrates the RLR structure.

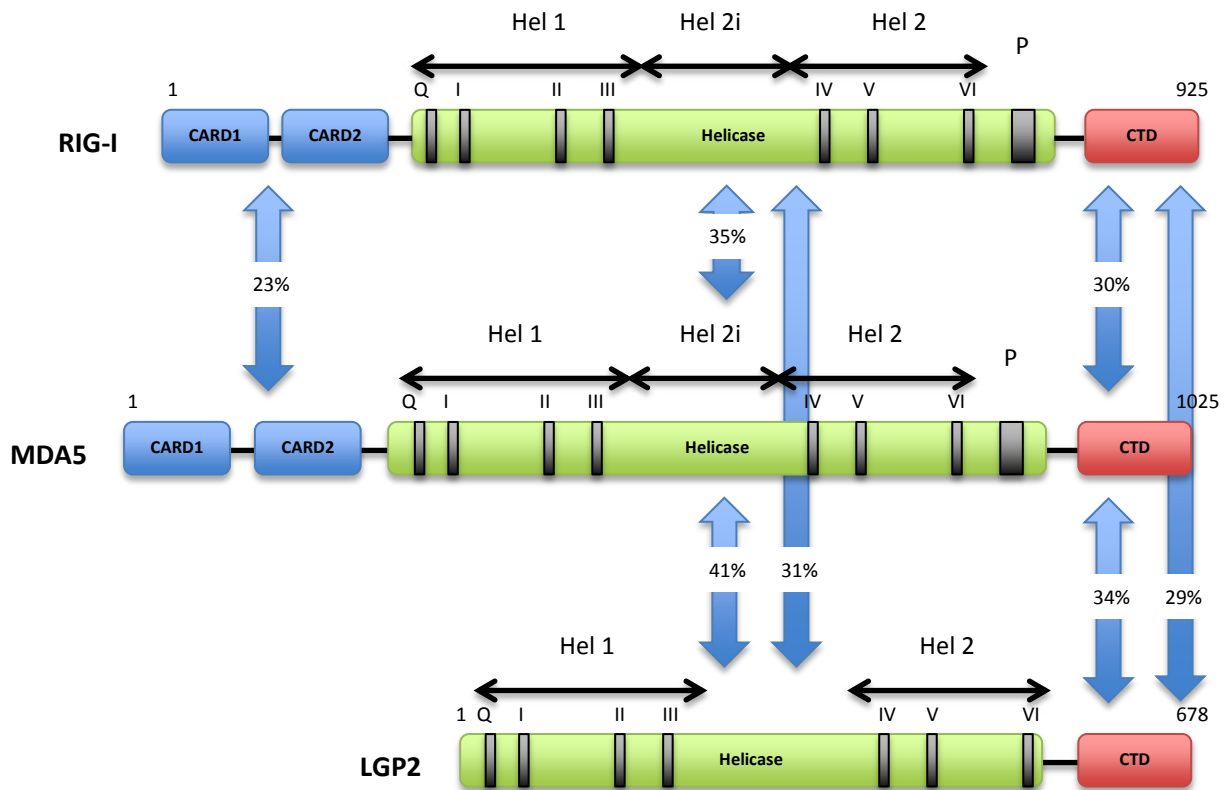


Figure 11. RLR structure. The RLR family includes the Retinoic acid-Inducible Gene I (RIG-I), Melanoma Differentiation-Associated antigen 5 (MDA5) and Laboratory of Genetics and Physiology 2 (LGP2). These SF2 type helicase proteins are composed of DExD/H-box helicase domain that contains the conserved domains Hel1 (motifs Q, I, II and III) and Hel2 (motifs IV, V, VI). Between the two helicases domains lies the domain Hel2i, only present in RIG-I and MDA5 and the bridging helices (Br) or Pincer (P) within the boarder helicase domain. DExD/H-box helicase domain is involved in the typical helicase functions: RNA

binding and ATPase activity. All RLRs also contain the C-Terminal Domain (CTD) leading to RNA recognition. Finally RIG-I and MDA5 present two N-terminal Caspase Activation and Recruitment Domain (CARDs) essential for interaction with MAVS and initiation of downstream antiviral signaling. Adapted from Bruns AM and Horvath CM, 2015.

They all share a central ATP dependent DExD/H-box helicase domain. The DExD/H-box helicase-like domain is conserved in the three RLR with a 31% of similarity between RIG-I and LGP2, 35% between RIG-I and MDA5 and 41% between MDA5 and LGP2 (Takahasi K et al., 2009). The helicase presents two RecA-like domains (Hel1 and Hel2): the domain 1 presents six motifs (Q, I (WalkerA), Ia-Ic, II (Walker B), IIa and III) and the domain 2 has four motifs (IV, V, Va and VI). These two fundamental helicase domains are interrupted by an intervening insertion, Hel2i, and bridging helices (Br) or Pincer (P) within the boarder helicase domain structure, only present in RIG-I and MDA5. Hel2i allows the autorepression and inhibition of CARDs domains in RIG-I but in MDA5 this region is shorter and missing a key phenylalanine residue. This suggests that MDA5 does not interact with CARDs in absence of RNA (Berke IC and Modis Y, 2012). The Motif II is also known at the Walker B site and contains the amino acids DExH/D (DECH in the case of RLRs), which gives its name to this helicase family. Both RecA domains are involved in the typical helicase functions: RNA binding and ATPase activity. The ATPase activity is essential for the immune response signal. A mutation of Lys270 of the ATPase site inhibits enzyme activity and makes impossibility of signal transduction (Plumet S et al., 2007; Saito T et al., 2007). In the case of LGP2 ATPase activity is essential to increase both, its ability to recognize and to bind ARNs. It also seems to be important for MDA5 activation (Bruns AM et al., 2013).

RIG-I and MDA5 present two tandem Caspase Activation and Recruitment Domain (CARDs) at the N-terminus, whose amino acid sequences are 23% similar. This domain is essential for the activation of the production of IFN- β , since CARD domains deletion prevent antiviral response and sole CARDs domain expression allows the INF production (Saito T et al., 2007; Yoneyama M et al., 2004; Fujita T et al., 2007; Wang Y et al., 2010). The CARD motif belongs to the family of death fold protein motifs with a characteristic six helical bundle (Monie TP et al., 2009). These domains function in the regulation of apoptosis and inflammatory responses by mediating homotypic interactions between proteins. They are often highly multimeric complexes and the signaling is achieved by receptor clustering (Martinon F and Tschopp J, 2004; Bouchier-Hayes L and Martin SJ, 2003). LGP2 differs from the two other RLRs because it lacks the two CARDs domains. Single CARDs structures

but no exact stoichiometry of the various CARD-CARD complexes are available. The structure of the N-terminal single CARD domain of the mitochondrial adapter of RIG-I, MAVS (Mitochondrial antiviral-signaling protein), has been solved by X-ray crystallography (Potter JA et al., 2008).

Additionally RLRs possess a C-terminal regulatory domain (CTD) also called regulatory domain (RD). This domain presents a similarity of sequence of 30% between MDA5 and RIG-I, 34% between MDA5 and LGP2, and 29% between RIG-I and LGP2 (Takahasi K et al., 2009). It is responsible for initial RNA binding (Takahasi K et al., 2009; Lu C et al., 2010; Cui S et al., 2008). Mutagenesis studies have led to identify a conserved lysine at the bottom of a positively charged groove, which allowed the recognition of 5'-triphosphate RNA. This lysine and other features of the recognition groove are different in LGP2 and MDA5 suggesting the specificity of RD in determination of the different viral ligands (Cui S et al., 2008; Takahasi K et al., 2009). Crystallographic and NMR high-resolution structures are available for all RLR CTD domains. CTD domain forms a globular structure. It is made of twisted anti-parallel main β -sheet and a smaller second anti-parallel β -sheet. Loop regions and short helices stabilize the sheets by surrounding them. One Zn^{2+} ion is coordinated close to the smaller β sheet. The RNA binding site has been localized to a large positively charged patch on the surface of the main β -sheet of all three molecules (Takahasi K et al., 2009). RIG-I and LGP2 CTDs were both co-crystallized in a complex with dsRNA. One protein molecule is bound to each 5' end of the dsRNA to form a 2:1 protein: dsRNA complex (Wang Y et al., 2010; Lu C et al., 2010; Li X et al., 2009). In RIG-I, electrostatic interactions allow the positively charged residues of the RNA to interact with the 5'-PPP. All kinds of interactions permit the rest of the RNA to interact with other parts of the CTD (Cui S et al., 2008; Lu C et al., 2010; Takahasi K et al., 2009; Wang Y et al., 2010).

1.2. RLR localization

It has been shown that RIG-I localizes to the membrane ruffles, in the motile cell surface, associated with F-actin, depending on Rac GTPase activity. The inhibition of Rac induces RIG-I relocation to the cell periphery. This association of RIG-I with the actin depends on CARDs domains and induces cellular migration. MDA5 localizes in the cytoplasm, but co-localization experiments don't show F-actin co-localization, (Mukherjee A et al., 2009). RIG-I localization on the actin network is not surprising because the cytoskeleton is a major player in the first line of host defence against pathogens. Indeed other components of the inflammatory pathway have been shown to interact directly or indirectly with the actin

cytoskeleton, such as caspase-11 (Li J et al., 2007), p65 subunit of nuclear factor NF-kappaB (Are AF et al., 2000) and Nucleotide Oligomerization Domain 2 (NOD2), which also is associated with RIG-I (Legrand-Poels S et al., 2007; Morosky SA et al., 2011). Finally other PRR as toll-like receptors (TLRs), which are transmembrane proteins also allow the recognition of the pathogen-associated molecular patterns (PAMPs).

1.3. RLR ligands

Several studies have investigated how RLR distinguish viral RNAs from host RNAs. Initially, both RIG-I and MDA5 were thought to detect poly I:C (a synthetic RNA double strand analog) but these two sensors are not redundant (Kato H et al., 2006). The key signature for RIG-I recognition is short blunt-ended dsRNA (20 bases) with a 5' triphosphate (5'ppp), a modification that is not found on normal capped or processed cellular RNA (Hornung V et al., 2006; Cui S et al., 2008; Schlee M et al., 2009; Pichlmair A et al., 2006; Baum A et al., 2010; Marq JB et al., 2010; Schmidt A et al., 2009) whereas MDA5 is activated upon binding to longer dsRNA (Pichlmair A et al., 2009). Several viruses are differentially recognized based upon the length of viral dsRNA produced following infection. RIG-I interacts with dsRNA of Reoviridae family (such as Orthoreovirus) (Broquet AH et al., 2011). It also recognizes many single-stranded RNA viruses. These include negative-stranded viruses of the Orthomyxovirus (such as influenza A or B virus) (Kato H et al., 2006; Loo YM et al., 2008), Paramyxovirus (such as measles, and Sendai virus) (Plumet S et al., 2007; Kato H et al., 2005; Yoneyama M et al., 2005), Rhabdoviridae (such as vesicular stomatitis virus) (Kato H et al., 2005; Yoneyama M et al., 2005) and Filoviridae (such as ebola virus) (Habjan M et al., 2008), and positive-stranded viruses like Flaviviridae (such as hepatitis C and Japanese encephalitis viruses) (Sumpter R Jr et al., 2005; Saito T et al., 2007). Additionally, DNA viruses activate RIG-I via RNA intermediates, such as herpes virus (Paludan SR et al., 2011). RNA polymerase III is involved in a DNA sensing pathways in the innate immune system and transcribes microbial DNA templates into dsRNA containing 5'-PPPs, which in turn activate RIG-I (Hornung V et al., 2009; Takaoka A et al., 2007). Modified secondary structures also influence RIG-I recognition as incorporation of modified bases such as pseudouridine (often found in cellular RNAs) (Hornung V et al., 2006) and phosphorothioated single-stranded DNA oligonucleotides (containing a sulfur-substituted internucleotide bond) (Ranjith-Kumar CT et al., 2009). Furthermore, products of host RNA cleavage by ribonuclease (RNase L) (Malathi K et al., 2007). Finally surprisingly, some RNAs without 5'PPPs have also been reported to trigger RIG-I (Kato H et al., 2008).

MDA5 is not studied as well as RIG-I but it is known that MDA5 interacts with dsRNA of Reoviridae family (such as Orthoreovirus) like RIG-I (Kato H et al., 2008; Loo YM et al., 2008), positive-stranded viruses of Picornaviridae (such as Theiler's Murine Encephalomyelitis Virus (TMEV), Encephalomyocarditis virus (EMCV) and Enterovirus) (Kato H et al., 2006), Calciviridae (Norovirus) (McCartney SA et al., 2008) and finally Flaviviridae (such as hepatitis C and Japanese encephalitis viruses) like RIG-I (Kato H et al., 2006; Loo YM et al., 2008; Fredericksen BL et al., 2008).

LGP2 is also able to recognize different types of RNA, but preferentially dsRNA and the presence of 5'ppp favours the interaction. LGP2 detects the genome of hepatitis C virus (Saito T et al., 2007). Having no CARD domain, LGP2 acts as a regulator of RIG-I and MDA5. LGP2 overexpression permits the inhibition of INF induction (Yoneyama M et al., 2005), it has an inhibitory role. It is also able to interact with RIG-I and inhibit its necessary homodimerization to translate the signal (Yoneyama M and Fujita T, 2009). In low concentration, LGP2 participates in the activation of MDA5 while a high concentration inhibits MDA5 activation (Bruns AM et al., 2013). Therefore LGP2 is a negative regulator of RIG-I and ambivalent regulator for the MDA5 activation.

1.4. Signal transduction in the RLR pathway

In most cells types, upon viral RNA recognition, the RLRs are the main sensors that induce IFN (Gitlin L at al., 2006; Yoneyama M et al., 2004). Moreover RIG-I knockout mice demonstrated that epithelial cells, conventional dendritic cells, and fibroblasts are dependent on the RLR pathway to stimulate IFN production (Kato H et al., 2005). The components of the RLR signaling cascade have been well defined and their interactions are shown by the Figure 12.

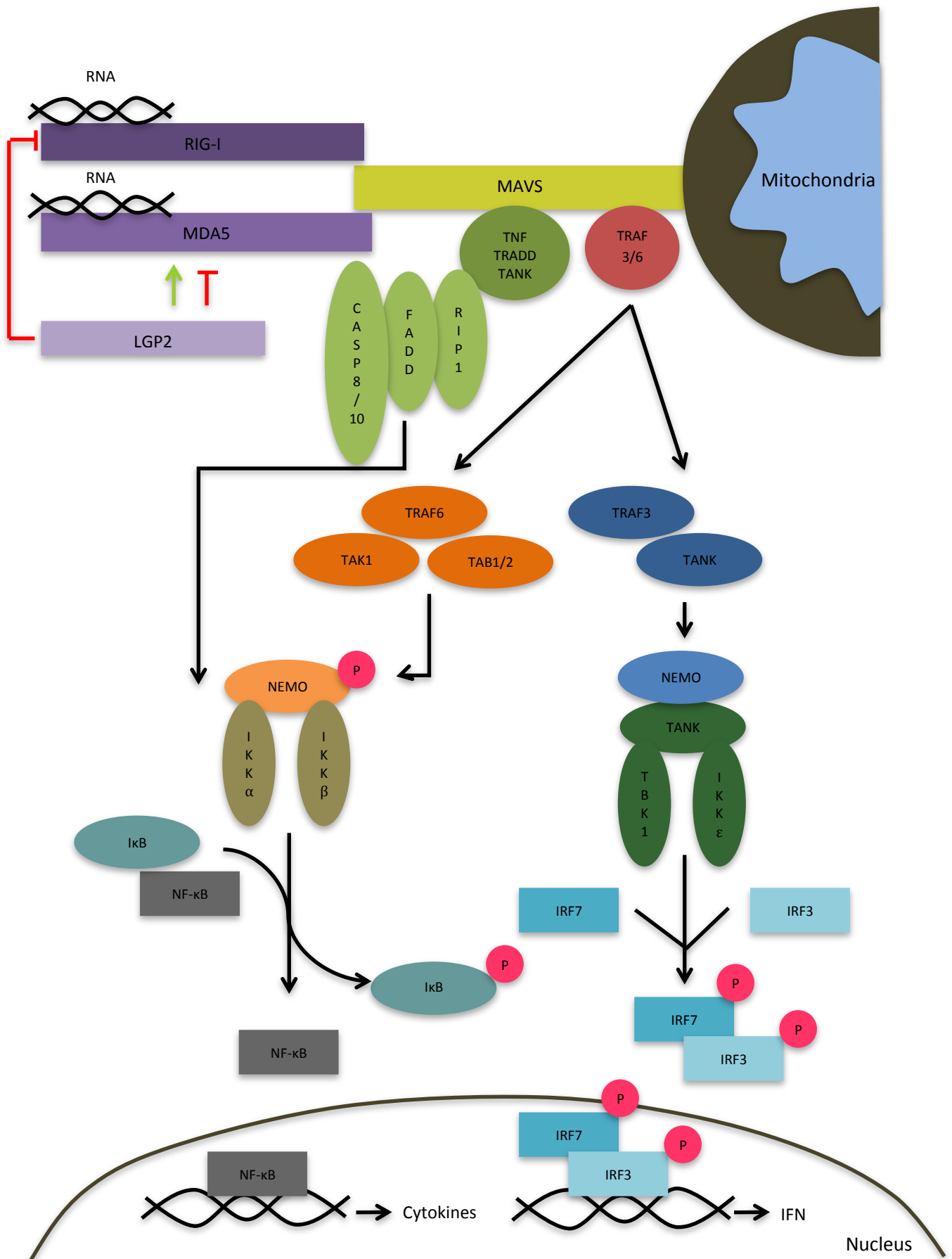


Figure 12. Activation of the IFN response under RLR regulation. Detection of RNA, by RIG-I and MDA5 triggers their binding to MAVS through CARD domains. MAVS then recruits a panel of several proteins (as TRAFF, TRADD, FADD...), which will allow the activation of the transcription factors NF-κB, IRF3 and IRF7 inducing INF expression.

Upon binding of viral RNA to the helicase domain, the molecule undergoes a conformational change that exposes the CARD domains (the activation mechanism is detailed further in the paragraph dedicated to RIG-I) and promotes RLR dimerization. This conformational change is dependent on the ATPase activity of the helicase domain. As a dimer, the RLR binds to MAVS (Mitochondrial AntiViral Signaling protein) also known as IPS-1 (IFN β -Promoter Stimulator 1) VISA (Virus Induced Signaling Adaptor) or Cardif (CARD adaptor inducing IFN β) (Kawai T et al., 2005; Seth RB et al., 2005; Xu L G et al., 2005; Meylan, E et al., 2005) through shared CARD-domain. MAVS contains an N-terminal CARD domain, a proline rich region and a C-terminal transmembrane (TM) domain anchoring the protein in the mitochondrial membrane, the mitochondrial-associated ER membrane or the peroxisomes associated with the mitochondrial-associated ER (Seth RB et al., 2005; Horner SM et al., 2011; Dixit E et al., 2010). Upon interaction with an activated RIG-I or MDA5, MAVS oligomerizes and acts as a scaffold for a multiprotein complex called the ‘MAVS signalosome’. This complex includes tumor necrosis factor (TNF) (Baril M et al., 2009), receptor-associated death domain (TRADD), TRAF family member-associated NF- κ B activator (TANK), and the E3 ubiquitin ligases TNF receptor associated factor (TRAF) 6 and 3 for NF- κ B and IRF activation, respectively (Yoshida R et al., 2008; Konno H et al., 2009). In the case of NF- κ B activation, the TAK1/TAB1/2 complex is recruited by TRAF6 leading to the phosphorylation of the NF- κ B essential modulator (NEMO, also called IKK γ). Once NEMO is activated it can serve as a scaffold for IKK α and IKK β . The IKK complex can recruit I κ B (inhibitor of NF- κ B) and NF- κ B subunits, canonically the p65 and p50 subunits. IKK β phosphorylates I κ B leading to its dissociation from p65/p50, and NF- κ B translocation to the nucleus to promote transcription of NF- κ B target genes. In the case of IRF 3/7, MAVS recruits the E3 ligase TRAF3 (Oganesyan G et al., 2006; Saha SK et al., 2006) which activates NEMO. NEMO then forms a signaling complex with TANK, IKK ϵ , and TBK1. After formation of this complex, TBK1 is activated to directly phosphorylate IRF3/7. Once phosphorylated, IRF3 and IRF7 dimerize and translocate to the nucleus to induce target genes including type-I IFNs and proinflammatory cytokines leading to the inhibition of infected cells proliferation (Seth RB et al., 2006). STING (also known as MITA, ERIS and MPYS) is also involved in RNA sensing downstream of RIG-I only, whereas MAVS is involved in both RIG-I and MDA5 signaling (Ishikawa H and Barber GN, 2008). STING predominantly resides in the endoplasmatic reticulum (ER), but is also found in the mitochondrial membrane and even the plasma membrane (Jin L et al., 2008).

Other proteins also are involved in the MAVS signalling pathway as: caspase8/10, TRADD (TNF receptor 1-associated death domain), TANK, FADD (Fas-associated death domain, RIP (receptor interacting protein 1) (Yoneyama M and Fujita T, 2009).

When present in small amounts, LGP2 acts as a positive regulator of MDA5, and as an inhibitor of RIG-I and MDA5 at high concentration (Rothenfusser S et al., 2005; Satoh T et al., 2010; Yoneyama M and Fujita T, 2009). Moreover, LGP2 seems to interact with MAVS and block recruitment of IKK ϵ , thus preventing signal induction (Komuro A and Horvath CM, 2006).

1.5. RLR regulation by host viruses

To evade detection by RLR, viruses have different strategies. For instance, V proteins of paramyxoviridae including NDV and SeV interact with MDA5 interfering with its activity to transmit a signal. The Influenza A non-structural protein 1 (NS1) interacts and inhibits RIG-I to prevent its ubiquitination (Guo Z et al., 2007; Gack MU et al., 2009). It may also bind RNA, sequestering it from RLR recognition. NS3/4a of HCV cleaves MAVS and disrupt its mitochondrial activation leading to inhibition of RIG-I mediated IRF3 (Yoneyama M and Fujita T, 2009). Ebola virus VP35 protein serves as a competitor for dsRNA. It disrupts RIG-I mediated Type-I IFN production, while SeV V protein selectively binds MDA5 and inhibits dsRNA induced activation of Type-I IFNs (Wang Y et al., 2011).

2.The RIG-I helicase

2.1. Molecular structure

RIG-I, also known as DDX58, is a highly conserved protein within vertebrates. Its gene was cloned from leukaemia cells in 1997 as mentioned earlier and codes for a 106 KDa protein of 925 residues. The protein harbours the three classical regions: the DExD/H box helicase core domain between the amino acids 239 and 793, the RNA binding domain known as C-terminal domains (CTD) or repressor domain (RD) between the amino acids 804 to 925, and a tandem caspase activation and recruitment domain (CARDs) at the N-terminus between amino acids 1 to 92 and 101 to 186 (Louber J and Gerlier D, 2010). Teams working on the RIG-I protein of duck, human and mouse resolved the three-dimensional structure of entire RIG-I protein and truncated forms, interacting or not with dsRNA. Civril F et al., have reported the crystal structure of the helicase domain of RIG-I in mouse by in-drop proteolysis approach with a resolution of 2.2Å (Civril F et al., 2011). Jiang F et al., worked on the helicase-RD domain in human with a 14 base pair dsRNA to 2.9 Å resolution (Jiang F et al., 2011) and Luo D et al.,

determined the deleted CARD domains RIG-I structure in human and in the presence of a 10 base pair dsRNA to 2.5 Å resolution (Luo D et al., 2011). Finally Kowalinski E et al., describe the full-length RIG-I structure in duck in the presence of 5ppp-dsRNA (Kowalinski E et al., 2011). The study of RIG-I in presence and absence of different types of DNA has allowed to determine the conformation changes and the amino acids interacting with the RNA. The CARD1 and CARD2 domains contain 7 and 6 α -helices respectively and they are connected rigidly forming a single functional unit (Saito T et al., 2007). The helicase domain contains three structural subdomains. The helicase core consists of four major subdomains: two RecA helicase domains (Hel1 and Hel2), each composed of one β -sheet and some α -helix, a unique insertion domain (Hel2i) (Helicase 2 insertion domain) made of 5 α -helices, and a bridging domain (Br) or pincer domain located between Hel2 and CTD and composed of two α -helix in V-shaped (Jiang F et al., 2011; Kowalinski E et al., 2011; Luo D et al., 2011). The pincer coordinates the functions of Hel1, Hel2 and CTD. It also couples RNA binding with ATP hydrolysis (Civril F et al., 2011; Jiang F et al., 2011; Kowalinski E et al., 2011; Luo D et al., 2011). Finally, the CTD domain is structurally organized in two four-stranded antiparallel β sheets connected by small helical turns (Cui S et al., 2008).

2.2. RIG-I helicase activity

RIG-I being a helicase, the enzymatic activities of ATPase, RNA unwinding and translocation are expected. These activities have not been studied a lot. However the different works have mainly been performed to understand the synergy between the helicase and the RNA recognition.

First studies have shown that mutation of K270A in the ATPase site of RIG-I causes an inactive antiviral signalling (Yoneyama M et al., 2004) without affecting the RNA binding ability (Plumet S et al., 2007). In 2008, Cui S et al. observed that ATPase activity and the oligomerization of the protein are stimulated by 5'-triphosphate dsRNA. Moreover when both CARDS are deleted, the ATPase activity is stimulated in the absence of a 5'-triphosphate RNA (Cui S et al., 2008). In 2009, Myong S et al. have shown by single-molecule fluorescence assays that RIG-I can translocate on dsRNA in an ATP-dependent manner affirming that RIG-I catalyses translocation in successive repetitions on the same RNA molecule without unwinding. This translocation is made possible only on the RNA strand, which bears a 5'-triphosphate. However, CARDS deleted RIG-I is able to translocate in the absence of a 5'-triphosphate. In fact, RIG-I translocation is regulated by its N-terminal (CARDS) and C-terminal (RD or CTD) domains (Myong S et al., 2009). Recently in 2015, Anchisy S et al.

have shown that ATPase activity is independent of 5'ppp and that only a base pair end is required. This emphasizes the role of the CTD, which interacts with the blunt end of the dsRNA (independently of the 5'ppp). Tests with ssRNA in the presence of 5'ppp do not trigger ATPase activity even if 5' overhangs cause a low ATPase activity, assuming the requirement of dsRNA in 5'. In the case of RNA/DNA hybrids that trigger very poor ATPase activity despite normal binding to RIG-I, the presence of a minimal number of 5 ribonucleotides on the bottom strand is required to induce a normal ATPase activity. These studies with hybrids containing increasing numbers of desoxyribonucleotides in the RNA bottom strand showed that residues at positions 2 and 5 are key residues for the recovery of normal ATPase activity. Their role appeared crucial because they bind to HEL1 and HEL2 respectively. Moreover, the increase in the number of ribonucleotides on the bottom strand from 6 to 10, which corresponds to the total coverage of one RIG-I molecule, causes an enhancement of the relative ATPase activity to that promoted by pure dsRNA. This increase is determined by the contact with the HEL2i domain and the duplex instability due to mismatches by facilitating the discharge of ADP and P_i from the active site. But this type of substrates is unable to induce IFN determining that this ATPase activity functions in RIG-I recycling (Anchisy S et al., 2015). In 2011, Jiang F et al., observed that ATP hydrolysis is necessary for RIG-I activation and RNA recognition without unwinding (Jiang F et al., 2011). Regarding the role of the ATPase and translocation activities, it has been suggested that they allow repetitive shuttling at specific dsRNA regions of the viral genome providing a structural conformation in RIG-I with exposed CARDS to attract the next players in the signalling cascade (Myong S et al., 2009). Also the translocation can interfere with viral proteins by preventing them from binding to the viral RNA, by blocking their progression on the viral genome and sometimes going as far as moving them away. All this results in interfering with viral replication (Myong S et al., 2009). Finally the ATPase activity is involved in RIG-I recycling activity and leads to competition between recycling, RIG-I oligomerization and translocation, and it is important for self-RNA discrimination. This RIG-I recycling activity promotes dissociation of RIG-I from inappropriate ligands, as well as from those with a dsRNA less than 13bp in length (Anchisy S et al., 2015). Also other studies with RIG-I mutants allowing ATP binding and preventing hydrolysis (such as “multi-system disorder Singleton-Merten Syndrome SMS mutations phenocopy”), showed that this mutant of RIG-I is bound to a 60S ribosomal expansion segment as a dominant self-RNA. But the wild type RIG-I displaces this self-RNA (60S ribosomal expansion segment) restoring ATP hydrolysis (Lässig C et al., 2015).

To conclude, ATP binding and hydrolysis plays a key role in the identification of viral targets and the activation of signalling (Rawling DC et al., 2015). ATP binding is required for RIG-I signalling on viral RNA and ATP hydrolysis provides an important function by recycling RIG-I and promoting its dissociation from non-pathogenic RNA by translocation.

2.3. RIG-I activation mechanisms

In the absence of activators, RIG-I exists in the cytoplasm in an inactive conformation, preventing effector access to the N-terminal CARDs and the helicase domain (Leung DW et al., 2012). Different studies of RIG-I functionality have demonstrated the conformation change mechanism for RIG-I activation (Myong S et al., 2009; Yoneyama M and Fujita T, 2009). The CARD tandem is a constitutive activator of IFN production, while in absence of RNA agonist the whole protein is inactive (Saito T et al., 2007; Yoneyama M et al., 2004). The transition from the inactive conformation to an active conformation allows CARD-CARD interaction between RIG-I and MAVS (Leung DW et al., 2012).

A multistep mechanism for the complete activation of RIG-I has been raised with the structure of this protein. The comparison of RIG-I structure in the absence of ligand and presence of dsRNA and non-hydrolysable ATP reveals the conformation changes (Kowalinski E et al., 2011). In the absence of RNA stimulation RIG-I is kept inactive in the cytoplasm in a self-repressed form through the phosphorylation of multiple residues (Figure 13A). T770, S854, and S855 in the CTD are phosphorylated by Casein Kinase II (CK2), which promotes interactions necessary for auto-repression (Sun Z et al., 2011). In the CARD domains, phosphorylation of S8 and T170 by Protein Kinase C- α and β (PKC α/β) is also required to maintain RIG-I auto-repression in the absence of viral infection (Gack MU et al., 2010; Maharaj NP et al., 2012; Nistal-Villán E et al., 2010). In the self-repressed conformation, part of CARD domains is hidden by CARD2 and Hel2i interaction, thereby preventing the recruitment of protein partners required for signalling. The CTD domain is flexibly linked to the helicase, without strong interaction with the rest of the protein. It is therefore able to detect and bind with dsRNA 5'ppp with high affinity. The recognition of the 5'ppp by CTD leads to a competition between dsRNA and CARD2 for the binding of the helicase domain in presence of ATP. This double bound causes a conformational change in the areas Hel1 and Hel2 fold on each other according to a twist movement causing a reposition of CTD and the release of CARDs domains (Figure 13B). The 3' dsRNA binds to the helicase domain in the Ia, Ib and Ic of Hel1 and IIa motif, which interacts with the 5' strand of dsRNA. The Q motif, Ia II, Va and VI of Hel1 and Hel2 binds the ATP (Kowalinski E et al., 2011; Luo D et al.,

2011). Also Hel2i binds the 5' and 3' strands of dsRNA. The Hel1, Hel2, Hel2i and CTD domains enclose the dsRNA in an almost circular channel whose stability is ensured by the binding of ATP. The release of the CARDs domains leads the recruitment of the signalling cascade, producing the IFN and cytokines secretion. To ensure the recruitment of MAVS, additional factors facilitate a series of changes in post-translational modifications leading to the fully active form of RIG-I. The E3 ubiquitin ligase Riplet is a regulator of RIG-I through activating K63-linked ubiquitination (Oshiumi H et al., 2009; Gao D et al., 2009). Ubiquitination of K788 increases the ability of RIG-I to bind to its viral RNA ligand promoting the transition to the open conformation for further post-translational modifications and interaction with signaling partners (Oshiumi H et al., 2009; Oshiumi H et al., 2013). The CARD domains of RIG-I become accessible thanks to RIG-I dephosphorylation by the phosphatases PP1 α / PP1 γ (Wies E et al., 2013). The RIG-I dephosphorylated form is required for the recruitment of the E3 ubiquitin ligase TRIM25 (TRIPartite Motif containing 25). TRIM25 transfers short unanchored poly-ubiquitin chains to the two CARD domains allowing the aggregation of the MAVS protein, and thus the induction of IFN (Jiang X et al., 2012). In addition to the changes in RIG-I post-translational modifications, the protein must be relocated for signal activation. In the uninfected cell, RIG-I is dispersed in the cytosol to survey the intracellular space for invading pathogens. A third partner is involved as a result of the interaction between RIG-I and TRIM25, the chaperone protein 14-3-3 ϵ . This complex promotes ubiquitination of RIG-I and allows its translocation to the cytoplasm to interact with MAVS (Liu HM et al., 2012). From 2007-2008, two studies suggested that RIG-I oligomerization is a required step to transduce the signal (Saito T et al., 2007; Cui S et al., 2008). The deacetylation of CTD domain is also crucial for the activation of RIG-I, preventing the interaction of the CTD with the 5'ppp-dsRNA. This deacetylation by HDAC6 promotes RIG-I sensing of viral RNAs and facilitates RIG-I oligomerization (Choi SJ et al., 2016; Liu HM et al., 2016). More recently, other teams observed the oligomerization of the RIG-I (Beckham SA et al., 2013; Jiang X et al, 2012; Weber M et al., 2013). According to Beckham et al. RIG-I oligomerization is dependent on the length of the RNA ligand. When RIG-I is associated with short RNAs, 10-19 base pairs (bp), it is a monomer form, while RIG-I binds a 39pb RNA it takes a dimer form (Beckham SA et al., 2013). But the oligomerization of RIG-I seems to result more of protein accumulation on the RNA than a protein-protein interaction. The oligomerization model proposed currently says that a RIG-I molecule is capable of binding a RNA ligand by its 5'ppp end and move along the RNA by translocation produced for the ATP hydrolysis. The 5'ppp end again free permits that another RIG-I

molecule can associate with the RNA and get oligomer form. The RIG-I oligomerization promotes activation of MAVS (Patel JR et al., 2013).

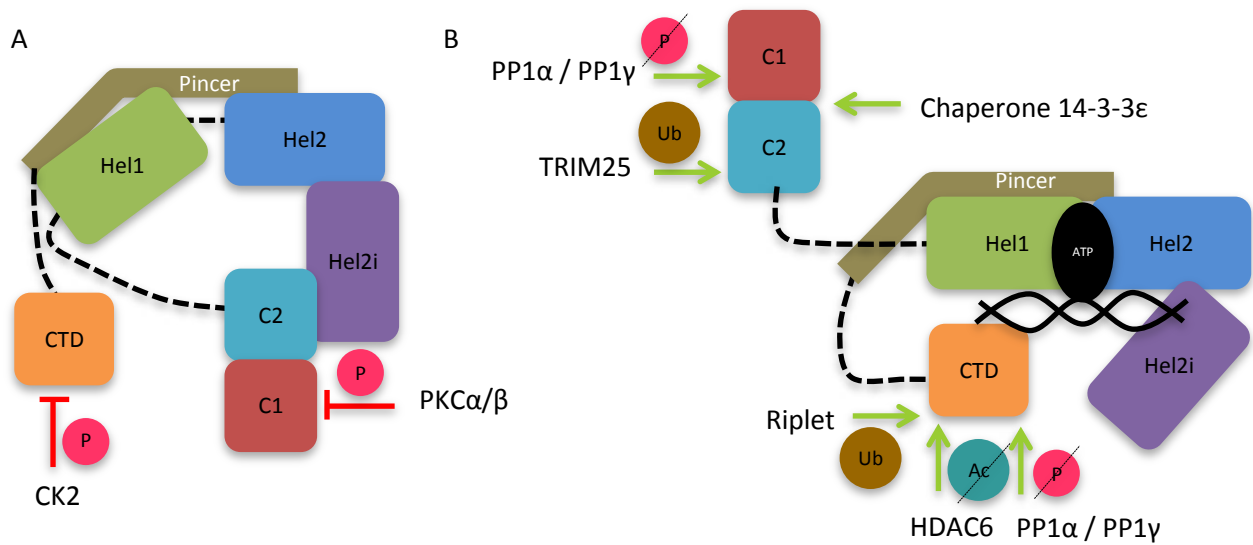


Figure 13. Structure-based model for RIG-I activation by dsRNA. RIG-I domains are coloured in different colours, the flexible linkers are represented by dotted lines and dsRNA is represented by a black helix. The inactivation of RIG-I by different partners is represented in red and activation in green. (A) Autorepressed state is potentiated by Casein Kinase II (CK2) and Protein Kinase C- α and β (PKC α/β). (B) Activated state by ATP and dsRNA binding leads to a conformational switch allowing the release of CARDs domains and their interaction with MAVS. Also some proteins permits post-translational modifications of RIG-I such as PP1 α / PP1 γ , Riplet, TRIM25, Chaperone protein 14-3-3 ϵ and HDAC6 deacetylation.

2.4. Additional cellular factors regulate RIG-I

Prolonged or excessive activation will have deleterious effects on the host tissues. Therefore, a wide range of regulators allows keeping control of the IFN induction. Among these regulations we find modifications by protein-protein interactions and post-translational modifications, such as ubiquitination, phosphorylation and SUMOylation (Maelfait J and Beyaert R, 2012; Zhao C et al., 2005; Mi Z et al., 2010). In the case of post-translational modifications, several factors regulate RIG-I either by removing the activating K63-linked ubiquitination or by affecting RIG-I protein stability through K48-linked ubiquitination and proteasome dependent degradation. K63-linked ubiquitination of RIG-I is crucial for its signaling activity. Four different deubiquitinases (DUBs) counteract this modification and inhibit RIG-I signaling: Cyldromatosis (CYLD) (Friedman CS et al., 2008) which prevents any basal activation levels, USP21 (Ubiquitin-Specific Protease 21)(Fan Y et al., 2014), USP3

(Ubiquitin-Specific Protease 3)(Cui J et al., 2014) and USP15 (Ubiquitin-Specific Protease 15) act as a negative regulator of RIG-I signalling to attenuate the establishment of an antiviral state by removing ubiquitin chains from CARD domains and interact directly with RIG-I to reduce MAVS–RIG-I binding (Zhang H et al., 2015). Following K48-linked ubiquitination, RIG-I is also subject to proteasomal degradation: the E3 ligase RNF125 and c-Cbl binds to and ubiquitinates RIG-I with K48-linked chains, leading to RIG-I degradation (Arimoto K et al., 2007; Chen W et al., 2013). Also, LUBAC (the Linear UBiquitin Assembly Complex), composed of two E3 ligases, HOIL-1L and HOIP, which regulate negatively RIG-I signaling by two mechanisms (Inn KS et al., 2011). First, LUBAC induces TRIM25 ubiquitination with K48-linked chains leading to proteasomal degradation, and the second mechanism depends on the NZF (Npl4 zinc finger) domain of HOIL-1L, which competes with TRIM25 for RIG-I binding. As a result, TRIM25-mediated ubiquitination and activation of RIG-I are impaired. PKC- α / β (Conventional Protein Kinase) is also a negative regulator, which cause the phosphorylation of the N-terminal CARD domains, preventing TRIM25 interaction (Maharaj NP et al., 2012). Finally it has been reported that, RIG-I is modified by small ubiquitin-like modifier-1 (SUMO-1). SUMOylation enhances IFN-1 production, the increase of RIG-I ubiquitylation and the intermolecular interaction between RIG-I and MAVS (Mi Z et al., 2010). Figure 14 summarizes the different cellular regulators of RIG-I leading to degradation by proteasome.

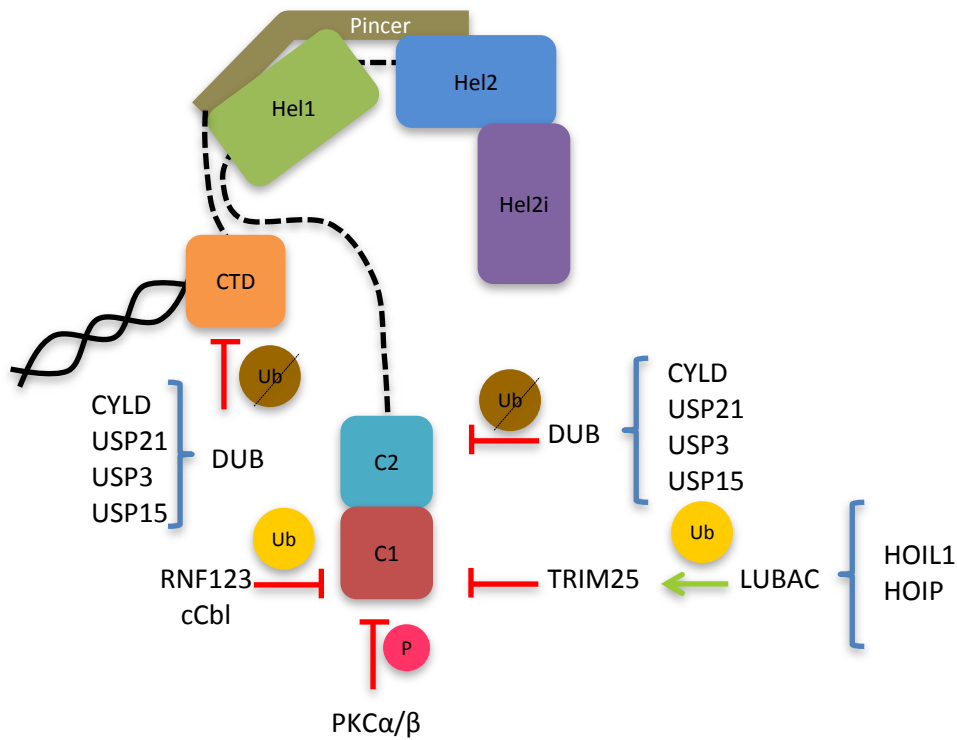


Figure 14. Structure-based model for RIG-I inactivation and degradation by proteasome. RIG-I domains are coloured in different colours, the flexible linkers are represented by dotted lines and dsRNA is represented by a black helix. The inactivation of RIG-I by different partners is represented in red and activation in green. The RIG-I inactivation and degradation is regulated by the removing of K63-linked ubiquitination and the addition of K48-linked ubiquitination regulated by DUB, LUBAC and RNF123 and cCbl.

2.5. RIG-I partners

In the case of innate immunity and activation of IFN pathway, RIG-I has two types of partners: those causing RIG-I post-translational modifications, such as ubiquitination, phosphorylation and SUMOylation (developed in the previous paragraph) and those acting on molecular pathways by protein-protein interaction. The chaperone HSP90 (Heat Shock Protein 90) has a major role on RIG-I degradation. It interacts directly with RIG-I without involving the participation of the CARD domains. The inhibition of HSP90 activity leads to the dissociation with RIG-I, followed by ubiquitination and proteasomal degradation of the helicase. This interaction stabilizes RIG-I but may be compromised in the case of infection (Matsumiya T et al., 2009). ARL16 (ARF (ADP-Ribosylation Factor)-like Protein 16), which is member of the Ras superfamily of GTPases, interacts with the C-terminal domain of RIG-I to suppress the association between RIG-I and RNA. In absence of viral infection, ARL16 is in its GTP-disassociated and inactive state. Upon virus stimulation, ARL16 binds to GTP and sequesters the CTD of RIG-I, preventing overactivation of RIG-I (Yang YK et al., 2011).

Atg5 and Atg12 are key regulators of the autophagy process. The Atg5-Atg12 conjugated inhibits the type I IFN production pathway by intercalation between the CARDS of RIG-I and IPS-1 during virus infection (Jounai N et al., 2007). Furthermore PACT physically binds to the C-terminal domain of RIG-I leading to the stimulation of its ATPase activity. It can also bind to RNA ligands of RIG-I leading to an amplified activation signal in innate immunity. This interaction between PACT and RIG-I preferentially activates IRF3 pathway (Kok KH et al., 2011). It has also been shown that RIG-I interacts with the apoptotic pathway, particularly with Caspase 9, which interacts with the CARD domain of RIG-I inducing apoptosis. In the case of HNSCC (head and neck squamous cell carcinoma) cells, RIG-I activation presents a dual role in the regulation of the Akt activation. In the presence of low-dose of viral dsRNA promotes NF- κ B- and Akt-dependent cell proliferation, whereas in the case of high level of viral dsRNA it leads to apoptosis accompanied by decreased activation of Akt (Hu J et al., 2013). Moreover, RIG-I can form a tri-molecular complex with MAVS and Lyn, which belongs to the Src-family-tyrosine kinases. Upon induction by short poly I:C, the complex plays a positive regulatory role leading to IRF3 activation and INF- β expression (Lim YJ et al., 2015). It also has been reported that some viral proteins can interact physically with RIG-I such as US11 protein of HSV-1 (Herpes Simplex Virus 1), which causes inhibition of RIG-I pathway, preventing the production of IFN (Xing J et al., 2012) and RNA polymerase subunits (PB2, PB1 and PA) of Influenza A virus (Li W et al., 2014).

Finally in the case of myeloid differentiation, RIG-I regulates the proliferation and survival of granulocytes by down-regulating the expression level of IFN consensus sequence binding protein (ICSBP), a major transcription factor regulating myeloid cell differentiation (Zhang NN et al., 2008). Also RIG-I allows the expression of other IFN stimulatory genes (ISGs) by promoting STAT1 activation in a MAVS-independent manner (Jiang LJ et al., 2011). RIG-I may competitively bind the SH2-TA domain of STAT1 so as to disrupt the binding of STAT1 with its negative regulator SHP1 being a crucial event in the downstream signal transduction IFN pathway (Hou J et al., 2014) since it leads to the transcription of numerous ISG resulting in antiviral innate immunity (Levy DE and Darnell JE Jr, 2002) and the cell cycle arrest (Altucci L et al., 2001). In macrophages, RIG-I has the capacity to bind directly Src through a PxxP motif located between the CARD tandem and the helicase domain of RIG-I. This interaction leads to the inhibition of AKT-mTOR signalling pathway (Li XY et al., 2014).

2.6. RIG-I recognizes various endogenous RNAs

Recognition of RNAs by RIG-I is the most explored aspect of RIG-I studies (Loo YM and Gale M Jr, 2011). In addition to viral RNAs, RIG-I is able to recognize cellular RNAs in different situations. It is involved in the modulation of the metabolism of some endogenous RNAs by forming a complex with protein partners or RNAs. In murine B lymphocytes, His-tagged RIG-I binds to multiple endogenous mRNAs. For instance, it interacts with Nf- κ b1 3' UTR mRNA, regulating positively its expression. The authors show that RIG-I can recognize three tandem motifs in Nf- κ b1 3' UTR mRNA. Moreover RIG-I regulates the protein translation by interaction with ribosomal components (Zhang HX et al., 2013). After ionizing radiations, the two key components of spliceosomes snRNA U1 and U2 in colorectal carcinoma cells translocate to the cytoplasm of the cell and bind RIG-I leading to the IFN pathway activation (Ranoa DR et al., 2016). Several miRNAs are able to bind RIG-I. For instance, during H5N1 infection of human lung epithelial cells, upregulated miR-136 interacts with RIG-I, inducing IFN- β and IL-6 expression (Zhao L et al., 2015). Karlsen TA et al., have observed that the off-target immune responses of mesenchymal stem cells is triggered by upregulating IFN stimulatory genes (ISGs) following the delivery of miR-145 by liposome and interaction with RIG-I (Karlsen TA and Brinchmann JE, 2013). Furthermore, RIG-I can bind to short interspersed elements (SINES) when they are transcribed by polymerase III during stresses (Mu X et al., 2016).

2.7. RIG-I has multiple roles in cell development and cancer: case of the myeloid differentiation

The observations reported above suggest that RIG-I functions far beyond being a PRR. It plays more diverse roles in the cellular life and its biological functions are more complicated than expected. Recent studies have shown that the RNA helicase is also involved in the regulation of basic cellular processes such as hematopoietic proliferation and differentiation, maintenance of leukemic stemness, and tumorigenesis of hepatocellular carcinoma.

In melanoma cells RIG-I activation by RNA ligands triggers apoptosis and induces proapoptotic proteins (Puma and Noxa), which depends on IPS-1 activation and TNF α without type I IFN induction or p53 pathway (Poeck H et al., 2008). In human head and neck squamous cell carcinoma, foreign RNA primed RIG-I associates with caspase 9, a potent initiator of apoptosis, through hemophilic CARD (Hu J et al., 2013). Therefore these studies suggest that foreign RNA primed RIG-I might be exploited to kill tumor cells by activation of the MAVS pathway. Based on the fact that apoptotic tumor cells secrete type I IFNs together

with other types of immunostimulatory cytokines if RIG-I is activated by foreign RNA, some groups have tried to develop active cellular vaccine (Loo YM and Gale M Jr, 2011). Poeck et al., delivered 50-ppp siRNA against the antiapoptotic protein Bcl-2 into melanoma cells in vitro and in vivo. As a result, they obtained Bcl-2 silencing, stimulation of the RIG-I/MAVS pathway leading to the tumor cells apoptosis and created a microenvironment full of type I IFNs leading to an immunosupportive state (Poeck H et al., 2008). A similar study on tumor immunosurveillance was performed by targeting a synthetic 50-ppp siRNA against TGF- β 1, which plays a critical role in the growth, invasion, and metastasis of pancreatic cancer. This siRNA showed significant therapeutic efficacy in a murine model of pancreatic cancer, inducing apoptosis of tumor cells, induction of type I IFN (Ellermeier J et al., 2013; Schnurr M and Duewell P, 2013). Moreover, the delivery of replication-incompetent virus (such as HVJ-E) or ordinary RIG-I ligands (such as Poly I:C or 50-ppp RNA) drove potent induction of apoptosis in multiple types of human tumor cells including prostate cancer, mammary carcinoma, lung cancer, and glioblastoma cells (Poeck H et al., 2008; Hu J et al., 2013; Ellermeier J et al., 2013; Schnurr M and Duewell P, 2013; Glas M et al., 2013; Kaneda Y, 2013; Kubler K et al., 2010; Petrocca F and Lieberman J, 2008; Qu J et al., 2013; Rehwinkel J and Reis e Sousa C, 2013; van den Boorn JG and Hartmann G, 2013; Wolf D et al., 2014; Zitvogel L and Kroemer G, 2009).

In addition to its involvement in apoptosis, as already mentioned above, RIG-I plays a regulatory role in the differentiation of granulocytes from Acute Promyelocytic Leukemia in NB4 cells. During ATRA induced differentiation of these cells, RIG-I mRNA is highly upregulated (Liu TX et al., 2000). Moreover, disruption of RIG-I gene in mice impairs granulopoiesis resulting in a progressive myeloproliferative disorder (Zhang NN et al., 2008). It has also been observed in U937 AML cell line, that RIG-I regulates the proliferation and the granulocytes survival by down-regulating the expression level of ICSBP (IFN cConsensus Sequence Binding Protein) which is the major transcription factor regulating myeloid cell differentiation. RIG-I has been therefore taken as a tumor suppressor in the case of terminal granulocytic differentiation. Also, the expression of other numerous ISG (IFN Stimulatory Genes) is enhanced by RIG-I, which promotes STAT1 activation in a MAVS-independent manner. The result is the amplification of IFN- α /RA-induced differentiation and proliferation restriction of leukemia cell (Jiang LJ et al., 2011). Following these observations, two independent mechanisms have been documented. First in HepatoCellular Carcinoma (HCC), RIG-I level predicts cell survival and the response to IFN α (Hou J et al., 2014). In this case, IFN α signaling induces association of RIG-I to STAT1 via tethering the CARD domains of

RIG-I with SH2-transactivation (SH2-TA) domain of STAT1. This prevents the dephosphorylation and inactivation of STAT1 by the phosphatase SHP1. The activation of STAT1 being enhanced, downstream and apoptotic ISGs such as TRAIL, PML, XAF1, and OAS1 are then induced and control HCC carcinogenesis and progression (Liu Z et al., 2016), have shown that miR-545 down regulates RIG-I and the HCC development is promoted by activated PI3K/Akt signaling. On the other hand in pancreatic ductal adenocarcinoma (PDAC), miR545 can down-regulate RIG-I. Tumor cell growth is promoted by the low miR-545 expression level and the high RIG-I protein level (Song B et al., 2014). The effect is therefore totally opposite. Another mechanism has been proposed in U397 cells. When RIG-I is upregulated following doxycycline treatment, the AKT-mTOR signaling pathway is inhibited. RIG-I inhibits AKT phosphorylation and activation by preventing AKT-Src interaction in a STAT1 independent manner. A classic conserved PxxP motif in RIG-I between the CARDS and the helicase core interacts with Src (Li XY et al., 2014). CARDS and PxxP motif cooperation leads to the disruption of the association between AKT and Src. Initially physical association established by tethering RIG-I CARDS with the SH1 domain of active Src, is followed by the interaction between the RIG-I PxxP motif and the SH3 domain of Src thereby preventing the association of Src SH3 with AKT PxxP. The AKT/Src interaction is impaired and as a result the proliferation of myeloid is restricted. Therefore all these datas suggest an anti leukemia activity of RIG-I via partner associations. However, how RIG-I is integrated in the regulatory program governing the myeloid differentiation and proliferation is not totally elucidated.

3. Hematopoiesis and Leukemia

3.1. Normal hematopoiesis

3.1.1. Hematopoietic hierarchy

Hematopoiesis is the process allowing the regulated renewal of blood cells. A healthy adult produces 10^{11} - 10^{12} blood cells per day. Hematopoiesis takes place in different tissues all along the development. During fetal life, it occurs in yolk sac until the 2nd month of gestation. Thereafter, it takes place from the second month in the liver, the spleen until the 6th months and from the fourth month in the spinal cord. In adults, haematopoiesis takes place exclusively in the bone marrow and lymphoid organs. Until the age of five years all the bones are involved beyond this age it is only in the flat bones. Hematopoiesis is initiated from Hematopoietic Stem Cells (HSCs) and give rise to lineage-committed progenitors and end-stage mature cells. Hematopoiesis starts with the Long-Term reconstituting HSCs (LT-HSCs),

which have two properties: multipotency and self-renewal. HSC multipotency consists in the ability to differentiate into multiple types of blood. HSC self-renewal consists in the ability to give rise to identical daughter cells with the same multipotent properties as the parent cell. Under steady-state conditions, HSCs numbers is regulated and are maintained in a quiescent state (Jude CD et al., 2008). Then appear the Short-Term reconstituting HSCs (ST-HSCs), which derive from from LT-HSCs and, although they maintain multipotency, they exhibit more-limited self-renewal potential. Upon differentiation, HSCs give rise to MultiPotent Progenitors (MPP), which then differentiate into lineage committed progenitors. Then all the differentiated blood cells will be produced. MPPs are developmentally more restricted than HSCs in their lineage commitment, giving rise to mature blood cells losing the ability to proliferate and self-renew. Progenitors compartment is constituted by a heterogenous cell population. Two main categories are distinguished: immature progenitors which conserve a quite high ability to proliferate and generate several lineages, and mature progenitors showing a more reduced proliferation potential with a restricted ability to differentiate in one lineage. Progenitors are designated by their ability to form colonies in semi solid medium growth (CFU: Colony Forming Unit), which are characterized by their morphology and a limited mobility (Bradley TR and Metcalf D, 1966). MPP differentiation leads to hematopoietic myeloid or lymphoid progenitors which are pluripotent and able to differentiate as blasts (Orkin SH and Zon LI, 2008) which finally give rise to ten HSC-derived blood cell lineages as shown by the Figure 15: myeloid cells by the Common Myeloid Progenitor (CMP) (mast cells, dendritic cells (DCs) and GMP), granulocytes and monocytes by the granulocyte-monocyte progenitor (GMP) (neutrophils, basophils, eosinophils, macrophages), erythroid cells by the Megakaryocyte Erythrocyte Progenitor (MEP) (megakaryocytes and erythrocytes) and lymphoid cells by the common lymphoid progenitor (CLP) (B and T lymphocytes, and natural killer cells). Finally mature cells pass into the bloodstream.

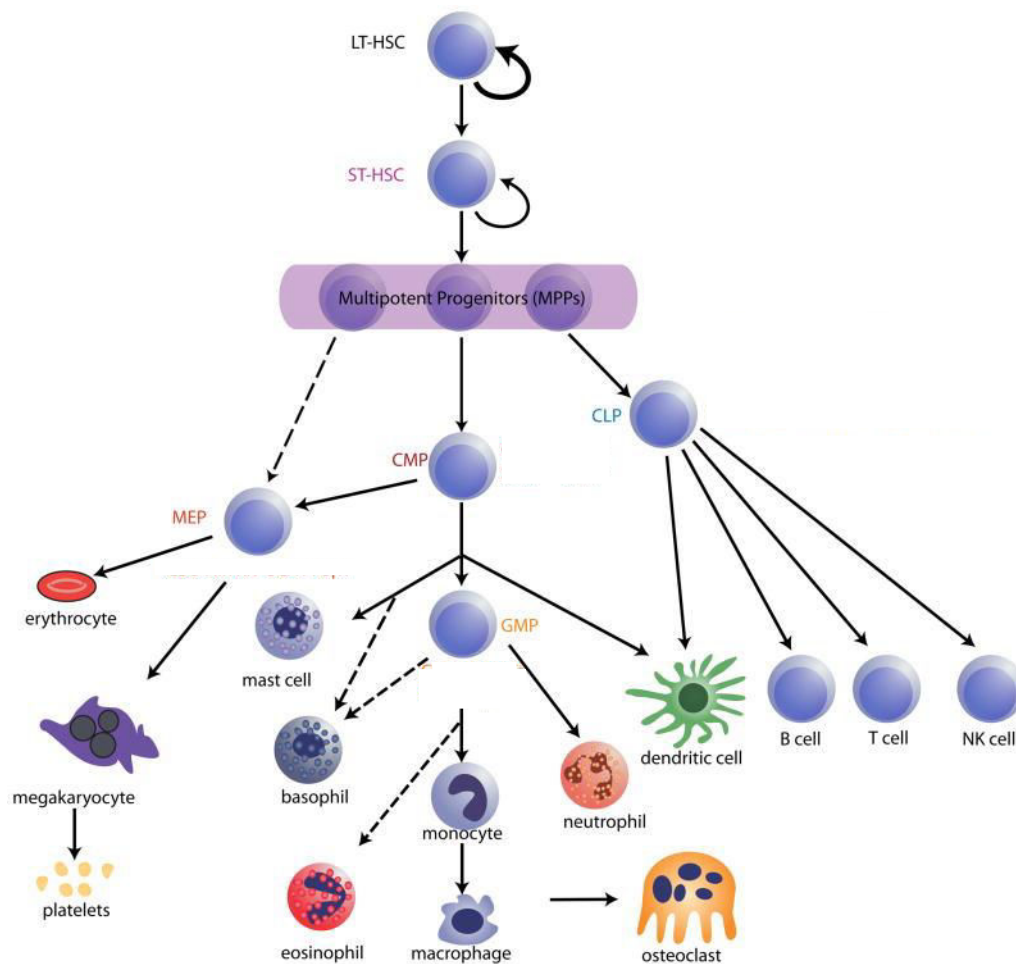


Figure 15. Schematic representation of hematopoiesis. The hierarchical organization comprises the Hematopoietic Stem Cells (HSC), which are the origin of the myeloid and lymphoid lineages, then the more or less differentiated progenitors and finally the mature cells which pass into the blood. Adapted from Wang LD and Wagers AJ, 2011.

The haematopoiesis and HSCs are regulated by the bone marrow microenvironment (niche), which release many factors (growth factors, cytokines, hormones and transcription factors). In the hematopoietic niche a variety of cells types is present including osteoblasts, osteoclasts, mesenchyme stem cells, adipocytes, endothelial cells, perivascular reticular cells, sympathetic neurons, macrophages and the extracellular matrix (Krause DS et al., 2014).

The stromal cells of hematopoietic niche are essential for the survival of the hematopoietic precursors, permitting their proliferation and differentiation into different lineages. They produce several growth factors involved either in the positive or the negative regulation of haematopoiesis. The different positive growth factors are IL-6, Il-1, SCF (Stem Cell Factor), LIF (Leukemic Inhibitory Factor) that increase the number of stem cells in the cell cycle and sensitize multipotent stem cells. The CSF (Colony Stimulating Factor) regulates the proliferation of the progenitors and also acts on the survival and action of myeloid and

lymphoid cells, some being specific to a single cell line as G-CSF (granulocyte-CSF) and M-CSF (macrophage-CSF). There are also growth factors that negatively regulate haematopoiesis such as TGF (Transforming Growth Factor β) and TNF (Tumour Necrosis Factor).

Several transcription factors are involved in the regulation of haematopoiesis. The primitive haematopoiesis is regulated by SCL (Stem Cell Leukemia hematopoietic transcription factor), GATA2 (GATA binding protein 2), LMO2 (LIM Domain Protein 2 Only) and AML-1. HSCs self-renewal is induced by Ikaros, HOXB4 (Homeobox protein 4) and GATA2 while differentiation is under control of PU-1 factor. In addition, for each cell lineage there are specific transcription factors such as RAR α that allows differentiation of promyelocytes into neutrophils.

3.1.2. Hematopoietic cells and their biological functions

Three kinds of blood cells differentiate from the HSCs: erythrocytes, thrombocytes and leucocytes. They represent 45% of the blood tissue circulating in the plasma, which represents 55% of the tissue.

Erythrocytes (red blood cells) carry oxygen and collect carbon dioxide thanks to the haemoglobin.

Thrombocytes (platelets) come from fragments of megakaryocytes. They release a multitude of growth factors including Platelet-Derived Growth Factor (PDGF), a potent chemotactic agent, TGF beta which stimulates the deposition of extracellular matrix and other basic fibroblast growth factor, insulin-like growth factor 1, platelet-derived epidermal growth factor, and vascular endothelial growth factor. Thrombocytes have a fundamental role in coagulation.

Basophil granulocytes are involved in the immune response and allergic reactions. Cytoplasmic granules contain histamin and heparin preventing coagulation but allowing diapedesis. After recognition of allergens and parasites, basophils release histamine that activates inflammatory response.

Eosinophil granulocytes are involved in the immune response and allergic inflammation. They play a crucial role in the destruction of parasites thanks to bactericidal proteins contained in their granules. Eosinophils also have the ability to participate in phagocytosis permitting the regulation of T cells and B cells by antigen-presentation.

Neutrophil granulocytes are involved in the immune response. To attack microorganisms, intracellular granules have protein-destroying and bactericidal properties

leading to phagocytosis of the pathogen. They can also stimulate macrophages by the release of Macrophage Inflammatory Protein-1 α (MIP-1 α), MIP-1 β and IFN- γ leading to the activation and maturation of macrophages.

Monocytes are leucocyte that differentiate into macrophages (which have the capacity to phagocyte the pathogen and it is involved in adaptive immunity and innate immunity) or dendritic cells (involved in antigen presentation and in triggering the adaptive immune response).

Lymphocytes B are responsible of the adaptive immune system by the production of antibodies or immunoglobulin after antigen presentation by antigen presenting cells (macrophages, follicular cells, dendritic cells). In the secondary lymphoid organs takes place the antibodies production and the transformation of lymphocytes into plasma cells.

Lymphocytes T are involved in the adaptive immune system by stimulating or inhibiting antibody production by B-lymphocytes and in cell-mediated immunity by the secretion of cytokines or lymphokines. They mature in the thymus (primary lymphoid organ). They are classified into different categories according to their membrane receptor expression: CD4+ or T helpers, CD8+ or T suppressors or cytotoxic.

3.2. Leukaemia

Leukaemia is a malignant haematological disorder characterized by the uncontrolled proliferation of white blood cells in the bone marrow. Malignant cells are characterized by the inhibition of their differentiation during the hematopoietic process. The transformation of leukemic cells is frequently associated with the accumulation of mutations, chromosomal translocations and epigenetic changes (Sachs L, 1985).

3.2.1. Leukaemia classification

Leukaemia is classified in four major types according to the rate of disease change (acute or chronic) and the cell lineage (lymphoblastic or myelogenous). Chronic leukaemia is characterized by a long clinical course (several years) by proliferation or accumulation of cells in the bone marrow at advanced stage of their proliferation. If the cell proliferation concerns lymphocyte cells, leukemia is called chronic lymphocytic and if it involves myeloid cells it will be referred to as chronic myelogenous. Acute leukaemia is characterized by a rapid clinical progression and proliferation first in the bone marrow then in the blood; cells are blocked at an early stage of their differentiation. As chronic leukaemia, depending on the origin of the blast, acute leukaemia (AL) is divided in acute myeloid leukaemia (AML) and

acute lymphoblastic leukaemia (ALL). ALL are more frequent in children (80% of AL) whereas AML occur mainly in adults around 60s.

Leukaemias were historically classified based on the French, American and British (FAB) classification system, in the 70's. This classification is based on cytological criteria. A new classification was proposed by the WHO (World Health Organisation) in 1999, taking into account morphological, cytological, cytochemical and cytogenetic data. The following table (Table 3) summarizes this classification:

| | | | |
|--------------------------|--|--|---|
| Chronic Leukaemia | Chronic myeloid leukaemia (CML) | | Proliferation of mature granulocytes (neutrophils, eosinophils and basophils). Characteristic chromosomal translocation called the Philadelphia chromosome (where a portion of chromosome 22 binds to chromosome 9). Appears more commonly in the elderly with a median age at diagnosis of 65 years. |
| | Chronic lymphoid leukaemia (CLL) | | B cell lymphocytes affection by its high presence. More present in adults older than 60 years |
| Acute leukaemia | Acute myeloid leukaemia (AML) (with recurrent genetic abnormalities) the most frequent | AML with t(8; 21)(q22; q22) (M2) | Formation of a fusion protein, AML1-ETO or RUNX1-RUNX1T1. Affects the adult population principally. |
| | | AML with inv(16)(p13q22) or t(16;16)(p13;q22) (M4Eo) | Presence of myelomonocytic blasts and atypical eosinophils by gene fusion CBF-beta/MYH11. Present in adults and children. |
| | | AML with t(9;11)(p22;q23) (M5) | High presence of monocytic cells by the gene fusion MLLT3-MLL. This AML type is sub-divided based on morphology into M5a (predominantly monoblasts) and M5b (mixture of monoblasts and promonocytes) |
| | | APL t(15; 17) (q22;q12) (M3) | Accumulation of immature granulocytes called promyelocytes with gene fusion PML-RARA. Affects the median |

| | | | |
|--|-------------------------------------|--|--|
| | | | age, approximately 30–40 years. |
| | | AML with t(6;9)(p23;q34) (M2) | In FAB classification this leukaemia type is associated with M2, but in this case the chromosome translocation is different and give different gene fusion, DEK-NUP214 but has a poor prognosis compared to the t(8;21). |
| | | AML with inv(3)(q21q26.2) or t(3;3)(q21;q26.2) | They present the gene fusion RPN1-EVI1, which cause hyperplasia with dysplasia of megakaryocytes with a poor prognosis. |
| | | AML with t(1;22)(p13;q13) (M7) | It is a form of leukaemia where a majority of the blasts are megakaryoblastic. Determinated by the gen fusion RBM15-MKL1. Its presence is increased in individuals with Down Syndrome. |
| | Acute lymphoblastic leukaemia (ALL) | B-cell lymphoblastic leukaemia | It is characteristic for the presence of many B-cells lymphoblasts found in the blood and bone marrow. It is classified in different types, depending in chromosome translocation: t(9;22)-BCR/ ABL; t(v;11q23)-MLL rearrangement; t(1;19)-E2A/PBX1; t(12;21)-ETV/ CBF α ; t(17;19)-E2A/HLF. It is principally present in childrens from 1-5 years. |
| | | T-lymphoblastic leukaemia | Consists in a high presence of T-cells lymphoblasts. It is principally present in children in oldest ages. |

My PhD work was focused on acute promyelocytic leukaemia.

3.2.2. Acute Promyelocytic Leukaemia (APL)

Acute Promyelocytic Leukaemia (APL) is a subtype of AML M3 (Acute Myelogenous Leukaemia) according to FAB classification. APL represents 10% of AML (Douer D, 2003). This leukaemia was first described by Hillestad (Hillestad LK, 1957) as a fatal disease with an aggressive course and short duration. It is characterized by the occurrence of sudden

haemorrhages mainly caused by coagulation disorders due to thrombocytopenia, which comes from an excessive consumption of platelets and bone marrow failure. There is diminished platelet count and abnormal accumulation of immature undifferentiated granulocytes called promyelocytes. APL reached all ages with equal incidence in men and woman. In France, about hundreds of new cases for year are counted. If no therapy is administered quickly, this illness leads to death, associated with severe coagulopathy leading to a stroke.

3.2.2.1. APL molecular pathology

In 1977, Rowley et al identified the reciprocal $t(15;17)$ translocation as the Hallmark of the pathology (Rowley JD et al., 1977). Later, de Thé et al discovered the fusion of the unknown promyelocytic leukaemia (PML) gene on chromosome 15 to the Retinoic Acid (RA) Receptor α (RAR α) gene on chromosome 17, resulting in the chimeric gene encoding PML-RAR α fusion protein (de Thé H et al., 1990) (Figure 16).

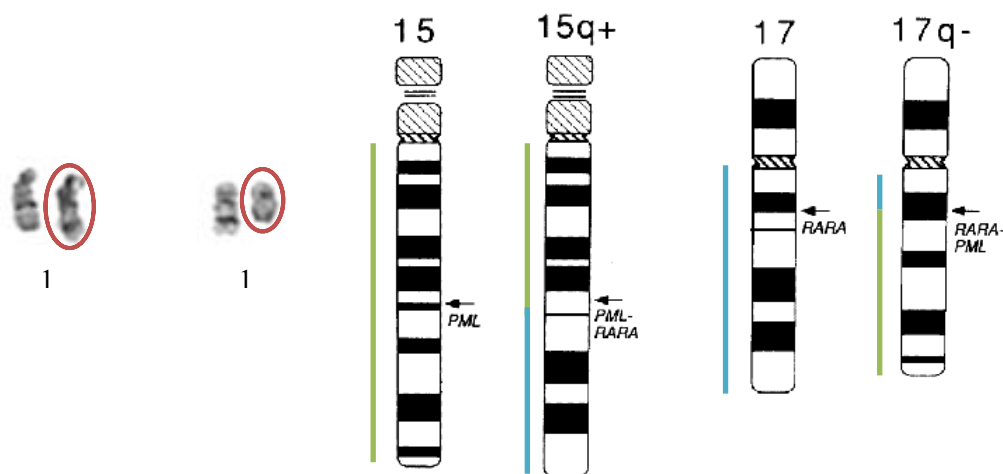


Figure 16. Representation of the reciprocal translocation $t(15;17)(q24;q21)$ specific to the APLs bringing the PML and RAR genes in contact. Adapted from Chauffaille ML et al., 2001 and Legües ME et al., 2002.

Since then, other translocations have been identified, representing 2% of the APL cases. They all involve RAR α gene in APL patients and one of the following genes: Zinc Finger and BTB domain containing 16 (ZBTB16) (Najfeld V et al., 1989; Sainty D et al., 2000); NucleoPhosMin (NPM) (Corey SJ et al., 1994); NUclear Mitotic Apparatus protein 1 (NUMA1)(Wells RA et al., 1996); Signal Transducer and Activator of Transcription 5B (STAT5B) (Jonveaux P et al., 1996); BCL6 CORepressor (BCOR) (Yamamoto Y et al., 2010); PRotein Kinase, cAMP-dependent PRotein Kinase type I-alpha regulatory subunit

(PRKAR1A) (Catalano A et al., 2007); Factor Interacting with PAPOLA and CPSF1 (FIP1L1) (Buijs A and Bruin M, 2007; Kondo T et al., 2008); Nucleic acid-binding protein 1 (NABP1) (Won D et al., 2013) (Figure 17).

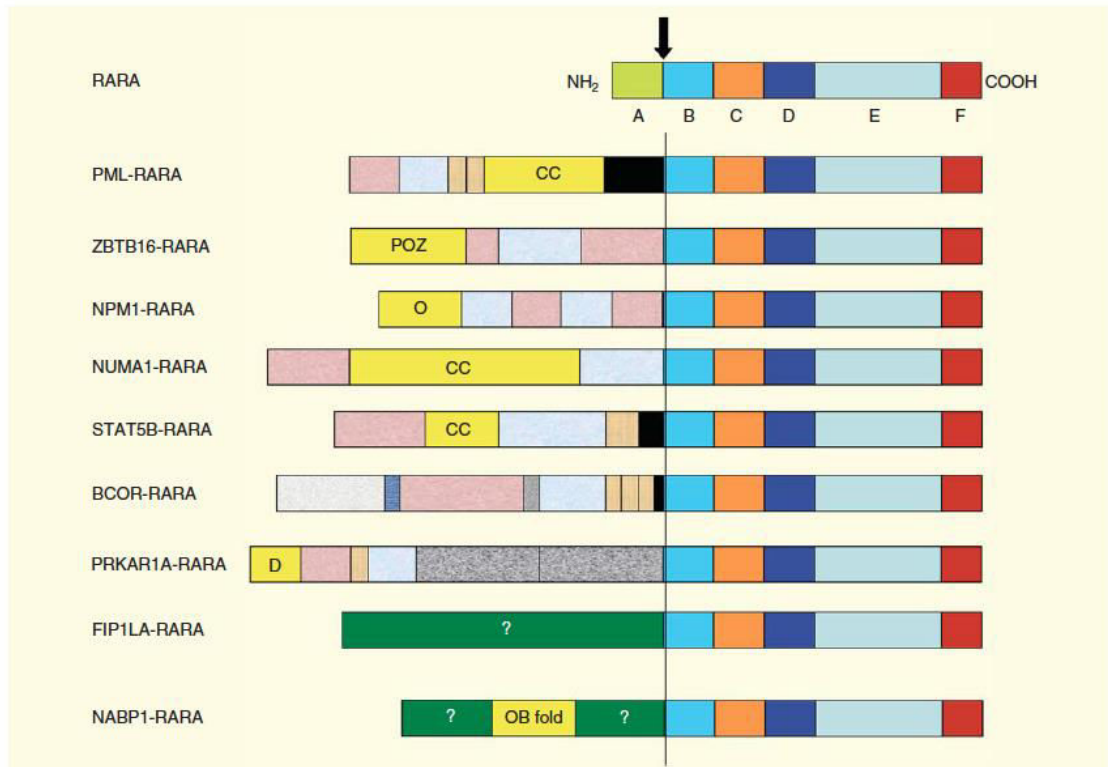


Figure 17. Schematic representation of the various partner genes of RARA in the APL. PML: Promyelocytic leukemia; ZBTB16: Zinc finger and BTB domain containing 16; NPM: Nucleophosmin; NUMA1: Nuclear mitotic apparatus protein 1; STAT5B: Signal transducer and activator of transcription 5B; BCOR: BCL6 corepressor; PRKAR1A: cAMP-dependent PRotein Kinase type I-alpha regulatory subunit; FIP1L1: Factor interacting with PAPOLA and CPSF1; NABP1: Nucleic acid-binding protein 1. cc: Coiled-coil domain; D: Dimerization domain; O: Oligomerization domain; OB-fold: OB-fold–nucleic acid binding domain; POZ: BTB/POZ domain. Adapted from De Braekeleer E et al., 2014.

3.2.2.1.1. Role of PML

The PML gene (Promyelocytic Leukaemia) is located on chromosome 15 and is expressed ubiquitously. It codes for the PML protein mainly localized in nuclear bodies called PML – nuclear bodies (NB), nuclear domain 10 (ND10), or PML oncogenic domains (PODs) (Zhong S et al., 2000). Alternative splicing of PML gene leads to seven isoforms of PML that is a

member of the TRIM family (TRIPartite Motif). PLM expression is controlled by STAT3 (Signals Transducers and Activators of Transcription 3) and IRF3 (IFN Regulatory Factor 3). (Bernardi R and Pandolfi PP, 2007) and is essential to NBs genesis (Ishov AM et al., 1999). The PML protein has been described as a tumour suppressor and is involved in several processes such as apoptosis, senescence, DNA repair, transcriptional regulation, differentiation and immunity in the case of viral infections (Strudwick S and Borden KL, 2002). PML overexpression leads to the cell growth arrest and knock out cell lines show a dramatic increase in their proliferation (Ruggero D et al., 2000). Some of PML roles depend in the accumulation of the protein in PODs or PML NBs and the recruitment of specific proteins. For example, the recruitment of hMre11/Rad50/NBS1 repair complex involved in DNA repair (Zhou W and Bao S, 2013).

3.2.2.1.2. RAR α and granulopoiesis

Retinoid signalling plays an important role in the development and the differentiation of several tissues such as the musculoskeletal and central nervous systems, the heart and respiratory systems, the eye and the hematopoiesis (Mark M et al., 1999; Ross SA et al., 2000). In different cell lines, it has been shown that retinoids are involved in the terminal differentiation of neutrophils (Mehta K et al., 1996; Shiohara M et al., 1999; Nagy L et al., 1995; Idres N et al., 2001; Benoit G et al., 1999; Ricote et al., 2006; Taschner S et al., 2007). Retinoid Acid (RA) is a vitamin A metabolite, which is present in the serum with physiological concentrations varying from 1 to 10 nM. It binds to specific nuclear receptors, retinoid (RAR) and rexinoid (RXR) which are encoded by three genes giving rise to related isoforms α , β and γ having a more or less similar expression pattern (Mangelsdorf DJ and Evans RM 1995). Both RAR and RXR are activated upon binding with ATRA (All-trans retinoic acid) and 9-cis-retinoic acid with a different affinity (Heyman RA et al., 1992). RAR and RXR bind together to form an heterodimer (Melnick A et al., 1999). RXR has been identified as co-regulators and are required for an efficient binding of RAR to their target (Hallenbeck PL et al., 1992; Leid M et al., 1992; Yu VC et al., 1991). Like other nuclear receptors, RARs contain different evolutionary conserved domains. Among them, the DNA binding domain that binds to Retinoic Acid Response Element (RARE) located in the promoter elements of retinoid target genes (Chambon P, 1996), the ATRA binding domain, the Retinoid X Receptor Alpha (RXRA) dimerization site and the nuclear co-repressor and co-activator binding sites (Nagpal S et al., 1993).

In the absence of RA ligand (Figure 18A), the RAR/RXR heterodimer recruits co-repressors such as Nuclear receptor CO-Repressor1 (NCOR1) and Silencing Mediator of Retinoid and Thyroid receptor (SMRT also named NCOR2) allowing the interaction with the Histone DeAcetylases (HDAC)-containing Sin3A complex (Hörlein AJ et al., 1995) and Polycomb Repressive Complex 2 (PRC2) (Gillespie RF and Gudas LJ, 2007). Histone deacetylation causes chromatin condensation and transcription repression (Pazin MJ and Kadonaga JT, 1997). Binding of ATRA to RAR α (Figure 18B) induces a conformational change in the heterodimer causing co-repressor disruption and the sequential recruitment of coactivators complexes such as Nuclear receptor CO-Activator 1 (NCOA1; also known as SRC1), NCOA2 (also known as SRC2) or NCOA3 (also known as SRC3). These co-activators recruit Histone AcetylaseTransferase (HAT) complexes and Trithorax proteins, which cause histone acetylation leading to chromatin relaxation and allowing transcription activation of target genes implicated in myeloid differentiation (McInerney EM et al., 1998; Kashyap V and Gudas LJ, 2010).

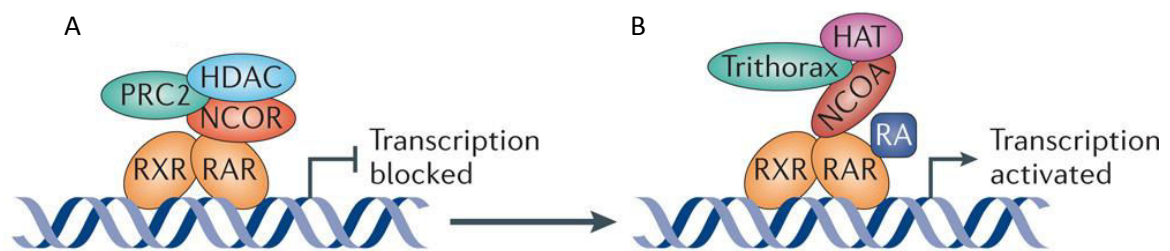


Figure 18. RA signalling mechanism. Retinoic acid (RA) binds to RA Receptor (RAR) which form a heterodimer complex with Retinoid X Receptor (RXR) and binds to RA Reponse Elements (RAREs) near target genes. (A) The absence of RA allows co-repressors as Nuclear receptor CO-Repressor (NCOR) family to bind to RAR and recruit repressive factors such Polycomb Repressive Complex 2 (PRC2) and Histone DeAcetylases (HDAC), (B) whereas the presence of RA releases co-repressors and permits co-activators recruitment of the Nuclear receptor CO-Activator (NCOA) family to bind to RAR and recruit activating factors such as Trithorax and histone acetylase (HAT). Adapted from Cunningham TJ and Duester G, 2015.

It is important to notice that activation of RARs in the absence of RA ligand has been reported during different stages of myelopoiesis (Collins SJ, 2002). In these cases, RAR interact with transcription factors such as STAT proteins, the PKA receptor. Moreover some hematopoietic

cytokines (IL-3, GM-CSF, IL-1) enhance the transcriptional activity of RA receptors through the JAK//STAT pathway (Nakamaki T et al., 1994).

3.2.2.1.3. PML-RAR α induced APL

The chromosomal translocation t(15;17) leads to the expression of a fusion protein containing a N-terminal portion of the protein PML and a C-terminal portion corresponding RAR α (de Thé H et al., 1990). There are three variants of the fusion protein PML-RAR α according to three different points of break in the PML gene. There is a short form (PML- RAR α S), a middle form (PML-RAR α M) and a long form (PML-RAR α L). These forms are present in respectively 70 %, 20% and 10% of patients with APL (Pandolfi PP et al., 1992). Show in the Figure 19, PML-RAR α has the same affinity as RAR α for ATRA and conserves both the DNA binding and the heterodimerization properties of each original protein. However, the APL fusion protein has altered DNA binding properties and can bind RAREs as homodimer (Perez A et al 1993). Moreover, it has dramatic increased ability to bind to co-repressors NCOR1 and SMRT rendering ATRA physiological doses (10^{-9} - 10^{-8} M) inefficient to dissociate the complexes, leading to apply pharmacological ATRA doses. The fusion protein behaves as an aberrant transcriptional repressor on RA target genes. In addition PML-RAR α can bind multiple NCOR/SMRT complexes (Lin RJ and Evans RM, 2000; Minucci S et al., 2000) leading to an increased concentration of HDAC complex on the target gene, enforcing DNA deacetylation, and enhanced transcription repression in the presence of physiological concentration of RA (Di Croce L et al., 2002). Addition of pharmacological concentrations of ATRA greater than 10^{-6} M does not only release the co-repressors and stimulates the genes of myeloid differentiation (Licht JD, 2006), it also degradate the PML-RAR α fusion protein and allows the restoration of the retinoid signaling.

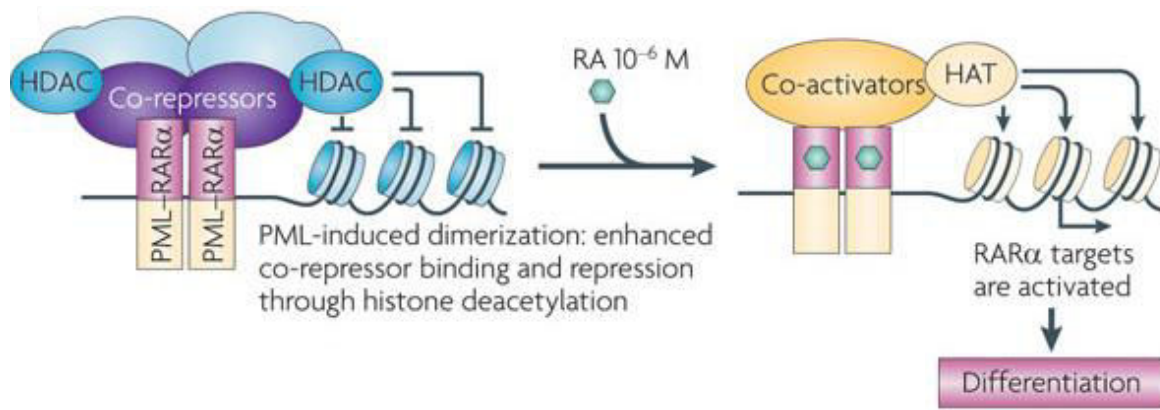


Figure 19. Promyelocytic leukaemia (PML) and retinoic acid receptor- α (RAR α) protein fusion. PML-RAR α binds and repress RAR α target genes by recruitment of co-repressors and the HDAC (Histone Deacetylase), which causes histone deacetylation and transcription repression. Pharmacological Retinoic acid (RA) converts PML-RAR α into an activator and restores differentiation by the recruitment of Co-activators and HAT (histone acetyltransferase). Adapted from de Thé H and Chen Z, 2010.

Additional investigations suggest that the origin of APL is multifactorial. The PML-RAR α protein is not only involved in the repression of RAR α target genes. It has been observed that the expression of PML-RAR α in myeloid cells in transgenic mice promotes only 15 to 20% of the development of APL after a long period of latency (6 to 13 month) (He LZ et al., 1997). It has been shown that secondary events like affection on FLT3 or RAS are required for the full development of APL phenotype (Sohal J et al., 2003; Chan IT et al., 2006). Martens et al., showed that PML-RAR α can bind 3000 sites on DNA corresponding to genes that encode proteins involved in the regulation of the cell cycle, differentiation, apoptosis, metabolism and protein synthesis (Martens JH et al., 2010). In some cases PML-RAR α binding to DNA sites is more or less affected by interactions with Polycomb Repressor Complex (PRC1 and PRC2) proteins. These complexes induce chromatin remodelling, transcription repression. PRC2 is involved in the maintenance of stem cells by repressing the transcription of genes involved in the differentiation (Villa R et al., 2007). And finally PML-RAR α inhibits various functions of PML described previously as its role in apoptosis and senescence, by the inhibition of POD formation and modifying the activity of p53 and AKT (Koken MH et al., 1994; Trotman LC et al., 2006).

3.2.2.2. APL cellular model: NB4 cells

The NB4 cell line is a permanent cell line first described by Lanotte in 1991, derived from the marrow of a 20-years-old woman with APL in the second relapse. The cells are hypergranular promyelocytes in G0/G1 phase and the karyotype complexity is characterized by the t(15;17)

chromosomal translocation with the expression the variant L of PML-RAR α , hypotetraploidy with loss of several chromosomes, rearrangement of chromosome 19 and simultaneous expression of myeloid and T cell markers (Lanotte M et al., 1991). It has been reported that NB4 cells in presence of 5 μ mol/l of ATRA during three days can be differentiated in myelocytes (Khanna-Gupta A et al., 1994).

Therefore this cell line has been chosen for my PhD work because 1) It is the cell line of choice, the closest to APL by comparison to other cell lines (HL60 and PL21) (Drexler HG et al., 1995), 2) The treatment with 1 μ M ATRA allows its differentiation like in vivo. 3) After 4 to 6 days of treatment the cells are totally differentiated being similar to neutrophils and conserving the active functions of neutrophils (Grégoire C et al., 1998).

3.2.2.3. APL Treatment strategies and side effects

3.2.2.3.1. ATRA / Chemotherapy strategy

In the early 70s monochemotherapy (daunorubicin) was the only treatment practiced with a 65% remission and only 35-45 % of 5 years event-free survival was obtained (Bernard J et al., 1973; Tallman MS et al., 2002). But patients developed coagulopathies causing patients death. A combination of chemotherapeutic agents (anthracycline, daunorubicin, idarubicin and cytarabine) was tested and showed similar patients outcomes. The complete response rate was 55-73% and the survival after treatment did not exceed 2 to 5 years for the majority of patients.

In the mid-1980s, since ATRA was reported to induce in vitro differentiation of the terminal APL cells, its introduction as a cancer differentiation inducer and therefore a therapeutic agent improved the outcome of de novo patients. To induce differentiation, ATRA acts at different levels (Figure 20): 1) it converts PML-RAR α into a transcriptional activator permitting differentiation (de Thé et al., 2012), 2) few minutes after ATRA treatment, there is an increase of cAMP level upregulating cAMP-dependent protein kinase (PKA). PKA permits the RAR α phosphorylation and triggers its activation or degradation (Zhao Q et al., 2004; Nasr R et al., 2008), 3) the degradation of PML-RAR α by the proteasome after ubiquitination (Zhu J et al., 1999) and autophagy (Isakson P et al., 2010). The degradation of the PML-RAR α allows the reformation of nuclear bodies and restores various functions of PML, such as apoptosis.

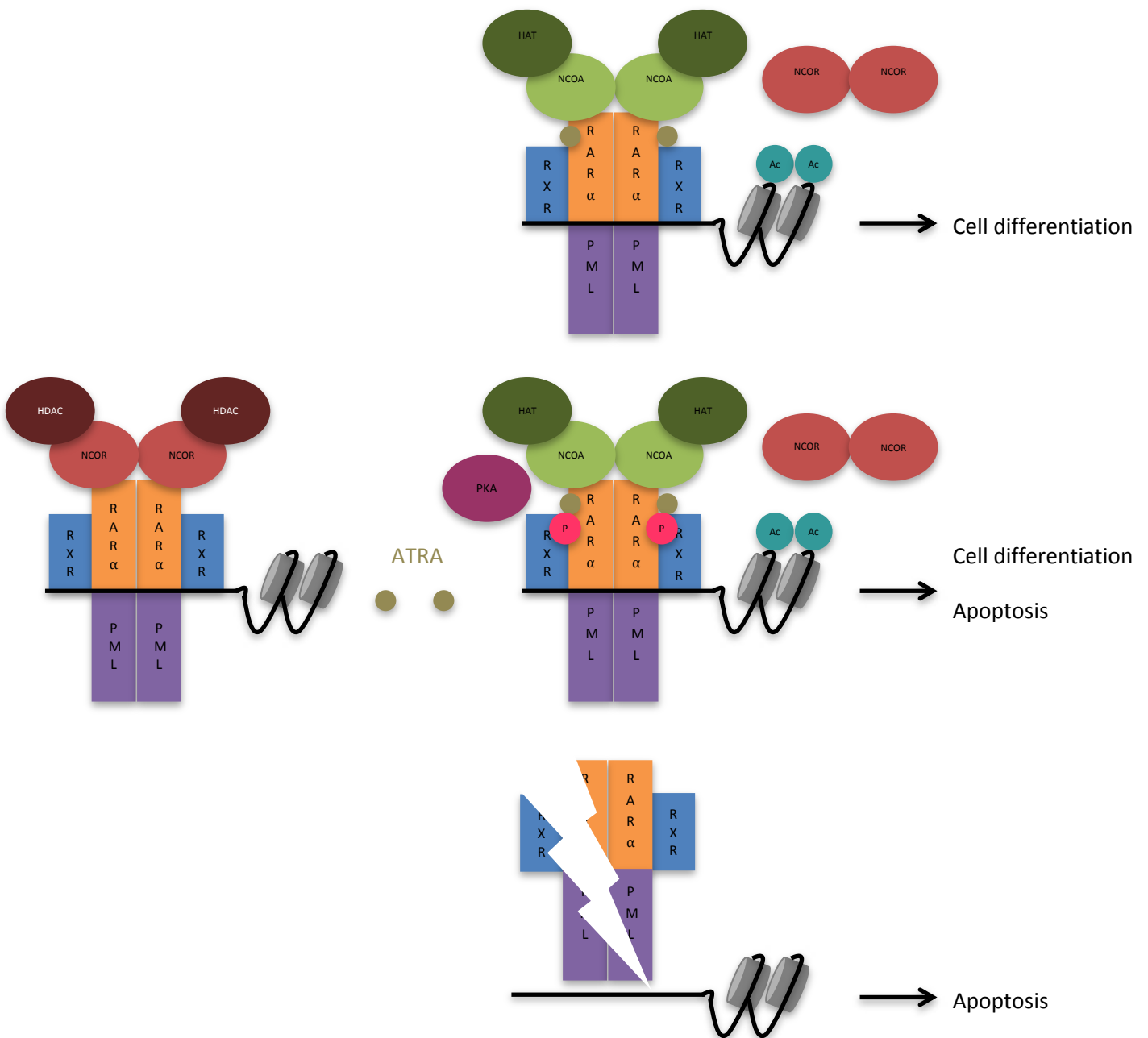


Figure 20. Effects of ATRA on APL cells. ATRA induces differentiation by conversion of PML-RAR α into a transcriptional activator thanks to Nuclear receptor CO-Activator (NCOA) recruitment and regulation of cAMP-PKA signaling pathway. Besides ATRA could degrade PML-RAR α oncoprotein as well.

But only 77% of patients had a complete remission and the remission durations were short. Moreover this treatment induces side effects. During this induction approximately 25% of the patients could develop the Retinoic Acid Syndrome (RAS) also known as differentiation syndrome. It is the main complication for APL patients treated with ATRA. During the treatment a massive accumulation of differentiated cells in the blood cause various side effects. The characteristic symptoms of this disease are respiratory distress, the appearance of fever, weight gain, pulmonary infiltrates and vascular leak syndrome causing renal failure and

pleural and pericardial effusion. 2% of the RAS affected patients died. In the case of RAS, patients are treated with glucocorticoids such as dexamethasone until the complete disappearance of symptoms. Subsequently, treatment with ATRA was associated with chemotherapy for 95% of complete remission in patients with survival without disease for 5 years in 50-75% of cases (Tallman MS et al., 2002; Coombs CC et al., 2015). It is known that the use of chemotherapy with ATRA reduces RAS incidence, to 9-2% of patients (De Botton S et al., 2003). But chemotherapy obviously adds associated complications. The causes of RAS are not currently fully understood. However, the APL cells treated with ATRA release inflammatory cytokines, such as interleukin IL-1 β , IL-6, IL-8 and Tumor Necrosis Factor alpha (TNF- α) (Dubois C et al., 1994). Moreover these mature cells also release cathepsin G, a serine protease that is involved in endothelium damage (Seale J et al., 1996). It has also been suggested that ATRA would induce changes in the adhesive properties of APL cells promoting the aggregation of promyelocytes, mediated by interaction of adhesion molecules such as InterCellular Adhesion Molecule 2 (ICAM2) and Lymphocyte Function-associated Antigen 1 (LFA1) (Larson RS et al., 1997).

Moreover, after ATRA treatment, relapse cases have been described suggesting the resistance to ATRA. It has been shown that continuous ATRA treatment was associated with a marked decrease in plasma drug concentration due to mutations in retinoic acid receptors or alterations in the expression of CRABP (act to sequester ATRA) or the development of enzymes responsible for catabolic drug conversion. (Muindi J et al., 1992). Some mutations have been reported in the ATRA binding domain of PML-RAR α (Duprez E et al., 2000). ATRA resistance could also be linked to the alteration of signaling pathways necessary for the granulocytic differentiation. It has been shown that in resistant APL cells, retinoid can associate with agonists of protein kinase cAMP (PKA) (Ruchaud S et al., 1994). Consequently a defect in cAMP/PKA pathways in APL cells could involve cell resistance to ATRA treatment.

3.2.2.3.2. Arsenic Trioxide (ATO) strategy

In 1990, the trioxide arsenic (ATO) was introduced with a high Complete Remission rate (73-85%) and a relatively long-term remission. But the use of ATO in relapsed patients after treatment with ATRA induces complete remission in 95% of cases (Niu C et al., 1999). These results indicate that ATO could be efficient to treat APL patients with relapses after treatment with ATRA. In vitro, ATO treatment induces two different effects depending on the dose (Figure 21). At high doses (0.5 to 2 micromol/L), it induces apoptosis whereas in lower

concentrations (0.1 to 0.5 micromol/L) it induces cell differentiation (Chen GQ et al., 1997). In the patients, the treatment with ATO induces incomplete differentiation and high cell apoptosis. At the molecular level, treating the cells by ATO causes cell death by apoptosis, by the downregulation of bcl-2 gene expression at both mRNA and protein levels, and modulation of the PML staining pattern (Chen GQ et al., 1996). More recently, it has been demonstrated that ATO causes a decrease of the mitochondrial transmembrane potential ($\Delta\psi_m$) and the opening of mitochondrial permeability transition pore (PTP) by targetting the voltage-dependant anion channel (VDAC), a component of the protein complex regulating PTP, and releasing cytochrome c with other apoptosis-inducing proteins (Zheng Y et al., 2004). Also the apoptosis by ATO is caused by the accumulation of reactive oxygen species, c-Jun N-terminal Kinase (JNK) activation and the inhibition of Nuclear Factor-KappaB (NF- κ B) (Chou WC et al., 2004; Davison K et al., 2004; Mathieu J and Besançon F, 2006). Finally the ATO causes the degradation of PML-RAR α by UBC9 (SUMO-ligase) triggering the degradation of PML-RAR α by RNF4 polyubiquitination and final proteasome degradation (Lallemand-Breitenbach V et al., 2008) and also by autophagy (Isakson, P et al., 2010). Currently, the standard treatment is the combination of ATRA with chemotherapy (anthracyclines) for a complete remission of 90% of patients. And the use of ATO in relapse cases.

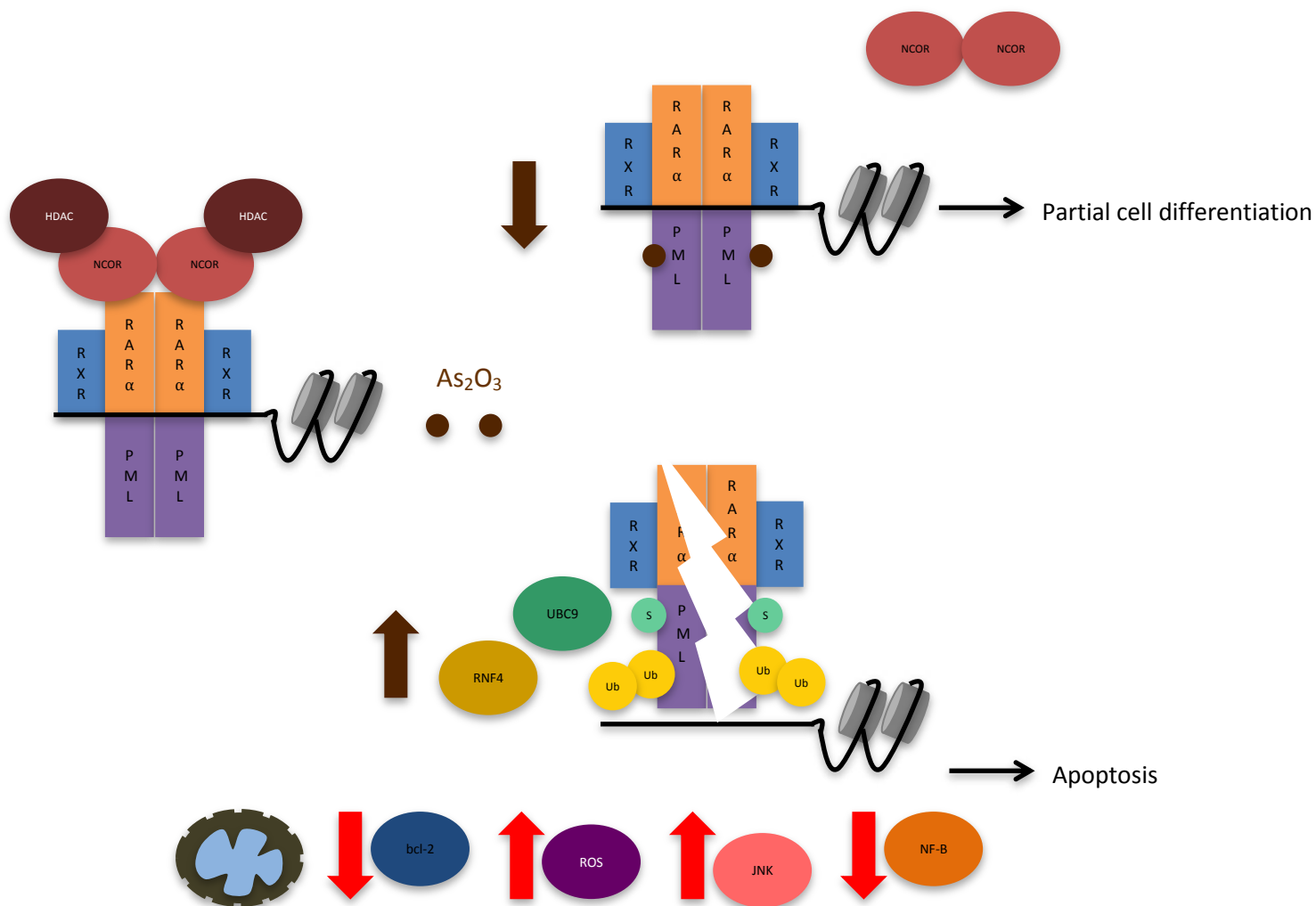


Figure 21. Effects of As_2O_3 on APL cells. As_2O_3 action depends on its dose. Low dose ($<0.5 \mu M$) of As_2O_3 mediates differentiation of APL cells by degradation of PML-RAR α oncoprotein by sumoylation. On the other hand, a high dose of As_2O_3 initiates apoptosis by opening mitochondrial permeability transition pore (PTP) and releasing cytochrome c and other pre-apoptotic factors. Also the downregulation of bcl-2 and accumulation of reactive oxygen species, c-Jun N-terminal Kinase (JNK) activation and the inhibition of Nuclear Factor-KappaB (NF- κ B) give cell apoptosis. Adapted from Shen ZX et al., 2004.

3.2.2.3.3. Other reported secondary effects

Some cases of PseudoTumor Cerebri (PTC) have been reported in early phase of ATRA treatment, mostly in children. The exact reason for this complication is not known. One of them could be the existence of retinoid receptors and related cytoplasmic binding proteins in the nervous system (Ruberte E et al., 1993). Also it has been postulated that in children there is a reduction of RAR expression and also a change in RAR response to retinoid stimulation in central nervous system (Visani G et al., 1996).

Treatment with ATRA / ATO and chemotherapy causes new medical problems as HTN, cardiac disease, renal insufficiency, DM, haematological disorders, pulmonary disorders and neurological disorders. And finally second malignancies as breast cancer (Eghtedar A et al., 2015). Furthermore, cells having a chromosomal translocation PLZF-RAR are not very sensitive to ATRA compared to those expressing PML-RAR translocation. This difference can be explained by the fact that PLZF-RAR, compared to PML-RAR, binds stably with PRC1 preventing its release during ATRA treatment blocking the transcription of genes involved in the granulocytic differentiation (Boukarabila H et al., 2009).

Materials and Methods

1. Cell culture

The NB4 APL cell line was a gift from Pr. H. de Thé (Hôpital St Louis, Paris, France). NB4 cell suspensions were grown at 37°C and 5% CO² in RPMI with 1% L-Glutamine (Gibco), 1% Penicillin/Streptomycin (Gibco) supplemented with 10% decompeted FBS for 30 min at 56°C (Sigma). Cell differentiation was induced by the addition of 10µM ATRA (Sigma) or 10µM DMSO (Sigma) to the culture medium during different periods of time (0, 24, 48, 72, 96, 120 and 140 h) in a confluent max value of 10⁷cells/ml. Cell adhesion to the bottom of the flask indicated that NB4 cells were definitively in the differentiation process.

2. Cell coloration

Firstly the cell suspensions were concentrated at 0,3x10⁶ cells/ml in 150µl of medium then placed in a cytospin chamber. The cells were spun down at 440 rpm for 10 min on glass slides, air-dried during 30 seconds and processed for May-Grünwald Giemsa R (RAL diagnostics) staining as follow: during 3 min samples were stained with pure May-Grünwald, then with 50% May-Grünwald during 3 more min and finally with Giemsa R during 10 min. At the end of the staining, the slides were then washed in distilled water during 30 seconds and air-dried. Pictures of the cells were taken with a Trybun microscopy setup at x40 magnification.

3. UV Cross-Linking Immunoprecipitation (CLIP) of RIG-I/RNA complexes

The UV cross-linking method, originally described by Ule et al., is able to define sites of direct contact between RNA and protein (Ule J et al., 2003). This method is based on the intrinsic photoreactivity of nucleic acids bases such as pyrimidines, and some amino acids such as cysteine, lysine, phenylalanine, Tryptophane, or tyrosine at 254 nm (Brimacombe R et al., 1988; Hockensmith JW et al., 1986; Shetlar MD et al., 1984). UV cross-linking does not cross-link proteins to proteins in contrast to formaldehyde that induces multi molecular chemical bridges. UV CLIP is therefore specific for nucleic acids-protein interactions (Greenberg JR, 1979). Moreover, this method has several advantages over other methods. It is performed on live and intact cells, reflecting unperturbed in vivo environment. The UV cross-linking results in an irreversible covalent bound allowing to remove unspecific co-immunoprecipitated partners during further steps, and to partially digest the interacting RNA

into shorter nucleic acid to facilitate identification. The major drawback of the method is the low amount of purified RNA at the end of the multi-step protocol. Several successful CLIP studies have been undertaken and to identify the nature of the co-immunoprecipitated RNA, next-generation high throughput sequencing method is generally applied to CLIP, termed HITS-CLIP.

3.1. UV cross-linking

The UV cross-linking was performed at each time of treatment with/without ATRA or DMSO (a control was performed without UV cross-linking). Cells were harvested either by recovering the cell suspension or by trypsination of adhesive cultures, followed by ice cold PBS washes. Then 2×10^7 cells for each culture condition were set up in 15 cm tissue culture dishes lid off, on ice and cross-linked with UVC (254 nm) at 400 mJ/cm^2 , in a UV crosslinker 1800 Stratagene in 10ml of ice cold 1X DPBS (no Ca^{2+} , no Mg^{2+}). The irradiated cells were transferred into 15ml tube, centrifuged at 2000rpm for 10 min, pelleted in eppendorf tube in a final concentration of 10^8 cells/eppendorf. The pelleted cross-linked cells were frozen in liquid nitrogen and stored at -80°C until further use, if not processed the same day for lysis and immunoprecipitation.

3.2. Preparation of antibodies-conjugated beads

Protein A sepharose beads (50 μl , GE Healthcare) were washed 3 times with lysis buffer (10mM Tris-HCl pH 7.4, 2.5 mM MgCl_2 , 150 mM NaCl, 0.5% NP40, 2 mM DTT 2 mM, EDTA 0.5 mM), at 4°C and incubated with 5 μg of rabbit polyclonal anti RIG-I antibody (Millipore), during 4h at 4°C under rotation. Then, to remove unbound antibodies, the antibodies-conjugated beads were washed 3 times with 500 μl of lysis buffer and by 10 min centrifugation at 13000 rpm at 4°C .

Just before immunoprecipitation, to avoid co-elution of antibodies with protein-RNA complexes, antibodies were cross-linked to the beads according to Lamond lab protocol (<http://www.lamondlab.com/newwebsite/Protocols%20for%20Website/Covalently%20Conjugate%20Antibody%20to%20Beads.pdf>). Antibodies-conjugated beads were washed twice with sodium borate 0,1M (pH 9) and centrifuged 10 min a 13000rpm at 4°C . Then incubated two times with 20mM DMP (Cross-linking reagent: Dimethyl pimelimidate) and sodium borate 0,1M for 30min at room temperature under rotation. Finally the antibodies-conjugated beads were washed twice with 50mM glycine (pH 2,5), centrifuged 10 min a 13000 rpm at 4°C and three times with lysis buffer.

3.3. Cell lysates preparation

The cell pellet was resuspended and disrupted in 500µl ice-cold lysis buffer (10mM Tris-HCl pH 7.4, 2.5 mM MgCl₂, 150 mM NaCl, 0.5% NP40, 2 mM DTT 2 mM, EDTA 0.5 mM, proteases inhibitor cocktail 1X (Millipore), RNasin 1:100 (Promega), RQ1 DNase 1:50 (Promega)). Cell lysis was performed during 40 min, vortexing every 2-3 minutes. The cell extract was centrifuged at 13000 rpm, at 4°C for 25 min to spin down the cell debris. Bradford assay was performed on the soluble fraction and 1 mg of total proteins was processed for immunoprecipitation and 50µg in Western Blot.

3.4. Immunoprecipitation

The 1mg cell lysate prepared as above was pre-cleared by incubation with 50µl Protein A Sepharose beads for 10min at room temperature vortexing every 2-3 minutes, then added to the 50µl antibodies-conjugated beads in a final volume of 500 µl and incubated overnight on a rotating wheel at 4°C to immunoprecipitate the RNA-RIG-I complexes. The following day, the immunoprecipitated RNA-RIG-I beads complexes were washed 3 times with lysis buffer and centrifuged each time 10 min at 13000 rpm at 4°C. For each time point and drug treatments controls were performed without antibody. At this step of the protocol a western blot was performed with 50µg of immunoprecipitated proteins to check the presence of the protein.

3.5. Radiolabelling and elution of the crosslinked RNA-RIG-I complexes

The immunoprecipitated RNA-RIG-I-beads complexes were washed with T4 PNK buffer (70 mM Tris-HCl pH 7.6, MgCl₂ 10 mM, DTT 5 mM), resuspended in 20µl of T4 PNK buffer (Biolabs), treated with T4 PNK enzyme (10 U, Biolabs) and 0.5µl γP³²ATP (10 mCi/ml, 3000 Ci/mmol, Perkin Elmer) at 37°C for 20 min. The beads were then washed 3 times with 500µl of PNK buffer. Elution of the radiolabeled complexes was performed by incubation in lysis buffer with SDS (1%) at 37°C for 10 min.

3.6. Enzymatic treatment of immunoprecipitated complexes

To demonstrate the presence of RNA or protein in the complexes after elution, immunoprecipitated complexes were treated either by 0,01mg RNase A (Macherey Nagel) during 20min at 37°C or 2mg/ml Proteinase K (Euromedex) during 45min at 55°C.

3.7. Gel migration and revelation

To denature secondary RNA structures, samples were loaded on 8% polyacrylamide/urea gels (Polyacrylamide/Urea 25% (19:1 for sequencing nucleic acids or 37.5:1 for protein electrophoresis, 8M Urea, 10X TBE, 10% APS and 1% TEMED) and run in TBE buffer at 200V either at 4°C or 20°C, during 4 to 7 hours. Migrations were also performed with 8% SDS page gel, to denature proteins (resolving gel: Running buffer pH 8.8 (1.5M Tris and 0.4% SDS), 40% Acrylamide 37:1, 10% APS and 1% TEMED; stacking gel: Stacking buffer pH 6.8 (0.5M Tris and 0.4% SDS), 40% Acrylamide 37:1, 10% APS and 1% TEMED) These gels were run in 10X Electrode Running buffer (30g/L Trisbase, 144g/L Glycine and 10g/L SDS) at 150V and room temperature for 1 hour. Finally the samples were also run in a 8%Nupage gels, which denatures the proteins but have a neutral pH environment that minimizes protein modifications (1M BisTris pH:6.5, 40% Acrylamide 37:1, 10% APS and TEMED) In this case, gels were run in 5X High-MW running buffer (250mM MOPS, 250mM TrisBase, 5mM EDTA, 0.5% SDS) and 200X Running buffer reducing agent (1M Sodium bisulfite) at 150V at RT for 1 hour. After migration, the gels were directly exposed overnight on an X- ray film (Fujifilm) at -80°C, and the following day the film was processed for development to see the RNA-RIG-I complexes.

3.8. Western Blot

The western blots were performed just after cell extract preparation or immunoprecipitation. The samples were denatured in 6x blue loading buffer (Tris pH 6.8 0.375M, SDS 12%, glycerol 60%, DTT 0.6M, bromophenol blue 0.06%) for 8min at 90°C, then loaded on 10% SDS page-gel (Running buffer pH 8.8 (1.5M Tris and 0.4% SDS), 40% Acrylamide 37:1, 10% APS and TEMED) (Stacking buffer pH 6.8 (0.5M Tris and 0.4% SDS), 40% Acrylamide 37:1, 10% APS and TEMED) run in 10X Electrode Running buffer (30g/L Trisbase, 144g/L Glycine and 10g/L SDS) at 150V during 1h 30min at room temperature. The semi-dry transfer was performed at 15V during 30min, on nitrocellulose membrane 0.2µm Amersham (GE Healthcare Life Sciences). Membranes were blotted with a polyclonal anti RIG-I antibody (at 1/1500 for 2.30hours, Millipore) and an anti rabbit IgG HRP linked antibody (at 1/2000 for 1.30hours, Cell Signaling). The result was visualized by exposing the membrane to ECL and autoradiographic film (GE Healthcare), then analysed with ChemiDoc XRS (BioRad). Quantifications were performed with ImageLab (BioRad) software.

4. RIG-I/partner proteins complexes immunoprecipitation

4.1. Cell lysates preparation

Cells were harvested either by recovering the cell suspension or by trypsination of adhesive cultures, followed by ice cold PBS washes. Then 2×10^7 cells for each culture condition resuspended and disrupted in 500 μ l ice-cold co-IP buffer (Tris-HCl pH 7.5 20mM, NaCl 137 mM, NP40 1%, EDTA 1 mM, proteases inhibitor cocktail 1X (Millipore)) during 30 min vortexing every 5 minutes at 4°C. The cell extract was centrifuged at 1200g, 4°C for 25 min to spin down the cell debris. BCA assay was performed on the soluble fraction and 2 mg of total proteins was processed for immunoprecipitation.

4.2. Preparation of antibodies-conjugated beads

Protein A sepharose beads (20 μ l, GE Healthcare) were washed 1 time with 1x PBS at 4°C and incubated with 15 μ g of rabbit polyclonal anti RIG-I antibody (Millipore) in co-IP incubation buffer (Tris-HCl pH 7.5 20mM, NaCl 137 mM, EDTA 1 mM), during 4h at 4°C under rotation. Then, the antibodies-conjugated beads were washed 3 times with PBS 1X to remove unbound antibodies by centrifuging 10 min at 10000 rpm and 4°C.

4.3. Cross-linking antibodies to sepharose beads

Just before immunoprecipitation, to avoid co-elution of antibodies with protein-protein complexes, antibodies were cross-linked to the beads according to Mayeux lab protocol (https://www.institutcochin.fr/les-plateformes/proteomique/prestations/prestations/HP_Fixation_AC_DMP.doc). Antibodies-conjugated beads were washed once with Bicarbonate pH 8 0.2M with 0.5M NaCl and centrifuged 10 min at 13000rpm at 4°C. Then incubated two times in 50 μ l of ethanolamine 0,1M in Bicarbonate pH 8 0.2M for 1h at 4°C under rotation. Finally the antibodies-conjugated beads were washed twice with 1x PBS then once with 50mM glycine pH 2.8, then twice with co-IP buffer and finally once with co-IP with proteases inhibitor cocktail 1X (Millipore), centrifuged 10 min at 13000 rpm at 4°C each time.

4.4. Immunoprecipitation

2mg of cell lysate prepared as above was pre-cleared by incubation with 75 μ l of Protein A Sepharose beads for 10min at 4°C, then the entire pre-cleared lysate was added to the antibodies-conjugated beads and incubated overnight on a rotating wheel at 4°C to immunoprecipitate the protein-RIG-I complexes. The following day, the immunoprecipitated

protein-RIG-I complexes beads were washed 3 times with 1x PBS and centrifuged each time 10 min at 13000 rpm at 4°C. Controls were performed without antibody.

4.5. Elution and TCA precipitation

Three consecutive elutions of the protein complexes were performed by incubation in 40µl of 0.1M glycine for 10 min at room temperature followed by the addition of 5µl of Tris-HCl pH 9.5 1M. Then the protein complexes were precipitated overnight at -20°C in 10% TCA and centrifugated at 14000rpm and 4°C during 15min. Incubation with acetone was performed for 1h at -20°C vortexing every 20min. The precipitated protein complexes were centrifuged at 14000rpm and 4°C during 15min and the pellet was air dried at room temperature during 30min. The pelleted proteins were solubilized in solubilization buffer (Urea 6M, Thiourea 1.5M, CHAPS 3%, DTT 0.06M) during 2h at 4°C vortexing every 20min.

4.6. Western Blot

Western blots were performed just after cell extract preparation or immunoprecipitation. The samples were denatured in 6x blue loading buffer (Tris pH 6.8 0.375M, SDS 12%, glycerol 60%, DTT 0.6M, bromophenol blue 0.06%) for 8min at 90°C, then loaded on 10% SDS-page gel and run at 150V during 1h 30min at room temperature. The liquid transfer was performed at 40V during 16h with 15% ethanol (0.75A during 1.2h), on nitrocellulose membrane 0.2µm Amersham (GE Healthcare Life Sciences). Membranes were blotted with a polyclonal anti RIG-I antibody (at 1/1500 for 2,30 hours, Millipore) and an anti rabbit IgG HRP linked antibody (at 1/2000 for 1,30 hours, Cell Signaling). The result was visualized by exposing the membrane to ECL and autoradiographic film (GE Healthcare), then analysed with ChemiDoc XRS (BioRad). Quantifications were performed with ImageLab (BioRad) software.

4.7. Silver staining

After migration, the gel fixation was performed overnight in 50% Methanol and 12% acetic acid. After being washed three times during 20min with 50% Ethanol, the gel was sensitized for 1min with a solution of Na₂SO₃x5H₂O 0.2g/L and three washes of 20 seconds in H₂O. The gel was then stained during 50 minutes maximum in staining solution (AgNO₃ 2g/L, Formaldehyde 37% 0.7mL/L) and washed three times for 20 seconds in H₂O. The gel was incubated in the development solution (Na₂CO₃ 30g/L, Formaldehyde 37% 0.25mL/L, Na₂SO₃x5H₂O 10mg/L) for 20-30min. To stop the reaction the gel was incubated during

30min in Trizma base 50g/L and 2.5% acetic acid. Finally, it was washed twice for 10 minutes in H₂O and stored in water with 10% glycerol.

Results

1. Effect of ATRA on NB4/NB4R cells differentiation

Granulopoiesis is the process leading the myeloblast, unipotent stem cell of the bone marrow, to differentiate into granulocyte. During this process the myeloblast gives successively rise to 5 different cell stages according to the following sequence: Myeloblast (Mb), ProMyelocyte (PM), Myelocyte (Mc), MetaMyelocyte (MM), Polynuclear (PN) (Figure 22).

Identification of the different cell stages is allowed by staining with May-Grünwald-Giemsa. Once the cells are transferred onto coverslips, the staining can be performed. May-Grünwald-Giemsa staining is based on two neutral dyes: the May-Grünwald, which contains eosin (an acidic stain) and methylene blue (a basic dye) and the Giemsa also containing eosin and related azures (also basic dyes). The basic dyes carry net positive charges that consequently stain nuclei (because of the negative charges of phosphate groups of DNA and RNA molecules), granules of basophil granulocytes, and RNA molecules of the cytoplasm of white blood cells. The eosin carries net negative charge and stains red blood cells and granules of eosinophil granulocytes.

As a first step of my study, the effect of ATRA, which is known to induce differentiation, was followed on the evolution of the NB4 cell differentiation by visualizing the cell aspect at different times of treatment with the drug. As shown in Figure 22 and as expected, I could observe all the differentiation stages after different times of treatment with the drug. In the presence of ATRA the cells are supposed to show an extended morphology with a condensed nucleus, characteristic of the PN morphology. After 72 hours of treatment, I could observe the beginning of the cell adhesion. The morphological observation of the cells revealed that they correctly differentiated.

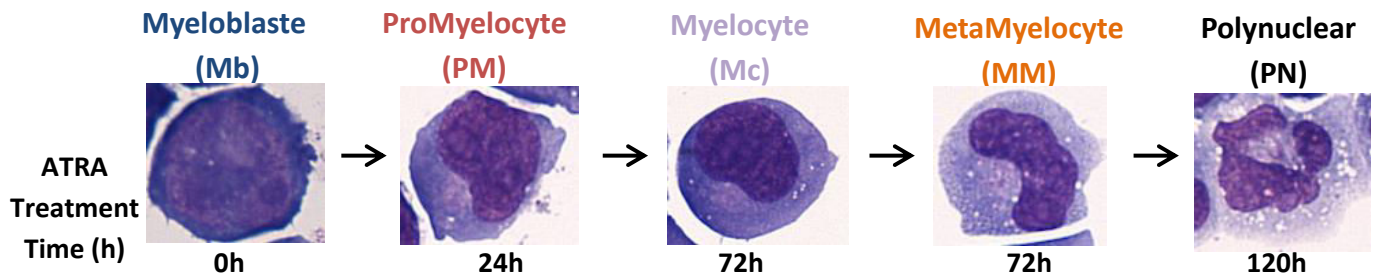


Figure 22. The different stages of differentiation in NB4 cells. NB4 cells were grown in the presence of 10 μ M ATRA during different times, then stained with May-Grünwald-Giemsa and observed with phase contrast microscope at 40X magnification.

To better characterize the evolution of the cell population during the drug treatment, and monitor the effect of ATRA on NB4 cell line, I counted each maturing cell type for each time of treatment. Comparison was made with DMSO application during the same treatment time and is presented in Figure 23.

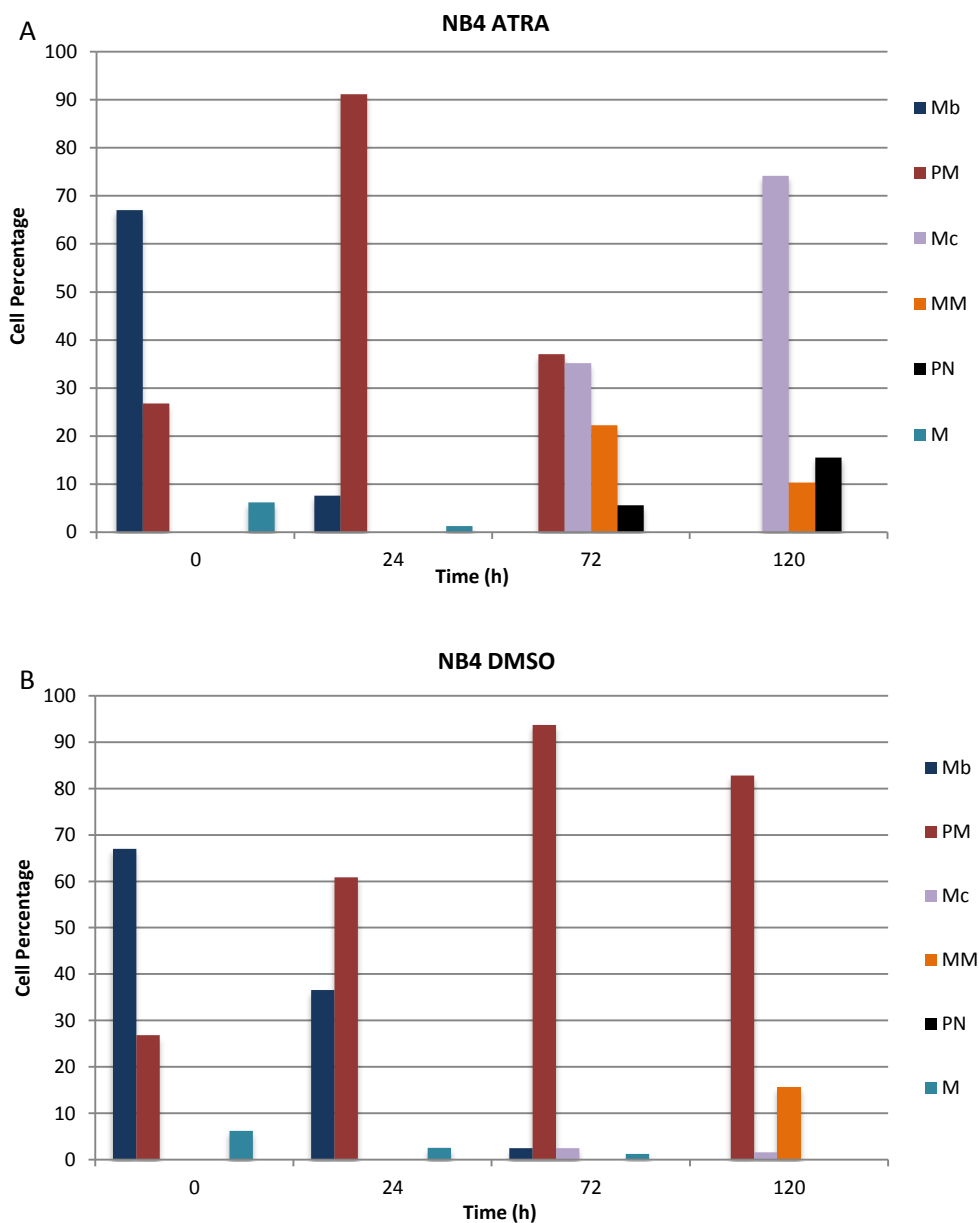


Figure 23. Differentiation of NB4 cells treated with. (A) ATRA and (B) DMSO. The graphs present the percentage of the different cell stages at different time points of treatment (0h (before treatment application) 24h, 72h and 120h). In dark blue the percentage of Myeloblast (Mb), in red the ProMyelocyte (PM), in light purple the Myelocyte (Mc), in orange the MetaMyelocyte (MM), in black the Polynuclear (PN) and in light blue the mitotic cells (M).

As shown by the Figure 23A, a 24h treatment with ATRA induced a dramatic change in the cell population where PM represented more than 90% of the culture and the number of proliferative Mb is clearly diminished indicating that the differentiation process has started. After 72h, whereas the proportion of PM decreases, three other cellular stages appear in the culture Mc, MM and PN. At this time point of treatment cells are adherent. At this time of treatment, it is confirmed that the differentiation process is therefore undoubtedly engaged and some fully differentiated cells (PN) are present. However and as expected, they are far to be predominant and the two previous stages of hematopoïesis (Mc and MM) are majority. After 120h (or 5 days), PM cannot be observed anymore being replaced by Mc. Also MM decrease to the benefit of PN, which increase. In the presence of DMSO (Figure 23B), starting from 24h PM are majority in the culture throughout DMSO treatment until 120h and I could never observe the presence of PN. Cell adhesion could be observed for a very small proportion of cells which were mainly MM. Therefore I could verify that in our culture conditions 10 μ M ATRA has released the differentiation block as soon as 72h allowing then to obtain fully differentiated cells, PN. In the presence of DMSO, the solvent of the drug may have triggered an incompleted and inefficient differentiation process. Treatment with ethanol as an other drug solvent led to the same observations.

The NB4R cell line is a distinct type of maturation deficient subline, which was derived from the ATRA sensitive NB4 line (Ruchaud S et al., 1994). The NB4R1 like the NB4 cells express the PML-RAR α protein but their terminal differentiation is triggered by the addition of cAMP to ATRA treated cultures (Duprez E et al., 1996). We hypothesized that NB4R1 cells are an interesting tool as a control cell line in which some terminal differentiation markers and RIG-I partners are not expected.

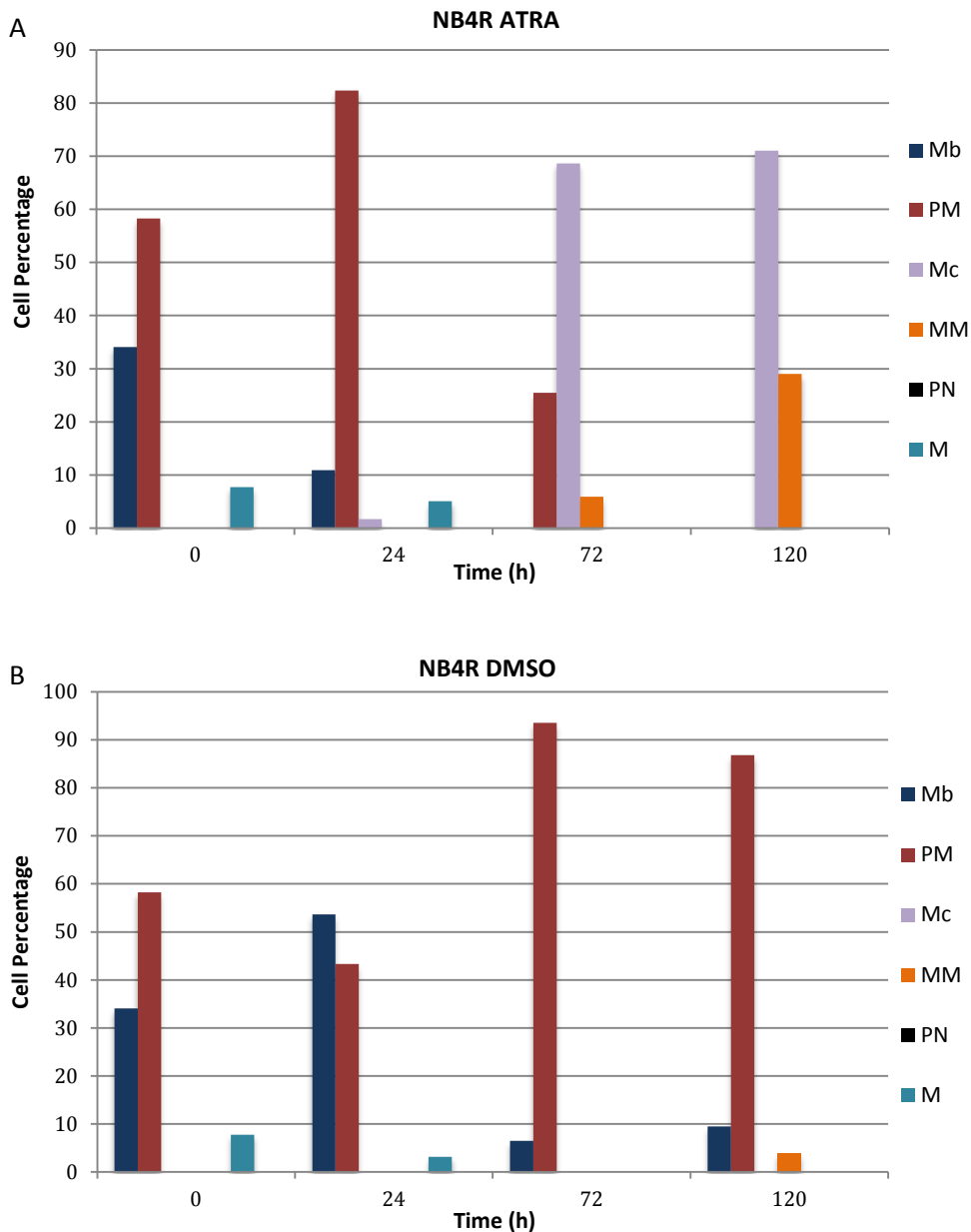


Figure 24. Differentiation of NB4R cells treated with. (A) ATRA and (B) DMSO. The graphs present the percentage of the different cell stages at different time points of treatment (0h (before treatment application) 24h, 72h and 120h). In dark blue the percentage of Myeloblast (Mb), in red the ProMyelocyte (PM), in light purple the Myelocyte (Mc), in orange the MetaMyelocyte (MM), in black the Polynuclear (PN) and in light blue the mitotic cells (M).

As for NB4 cells, I followed the effect of ATRA on NB4R cells. With ATRA (Figure 24A) or DMSO (Figure 24B), NB4R are mainly mitotic or early maturing cells. After 72 hours of ATRA treatment NB4R enter also in the maturation process since a high percentage of Mc (Myelocyte) and MM (MetaMyelocyte) are present. Therefore like in the case of NB4 cells, ATRA releases the differentiation block. Cells become adhesive and the differentiation process is maintained until 120 hours. However it is incomplete

since PN are never observed. Therefore NB4R are sensitive to ATRA but they cannot follow a complete differentiation process. In the presence of DMSO NB4R cells remain mainly in early maturation stages.

2. Effect of ATRA on NB4 and NB4R proliferation

The effect of ATRA on cell proliferation was monitored in parallel to cell differentiation in order to verify the impact of the drug treatments over time and especially if the progressive differentiation is accompanied by an expected decrease of cell proliferation. For this purpose, the number of cells collected from the flasks (adhesive and suspension cells) was counted in the presence of ATRA and DMSO for each time of treatment. The result is shown in Figure 25.

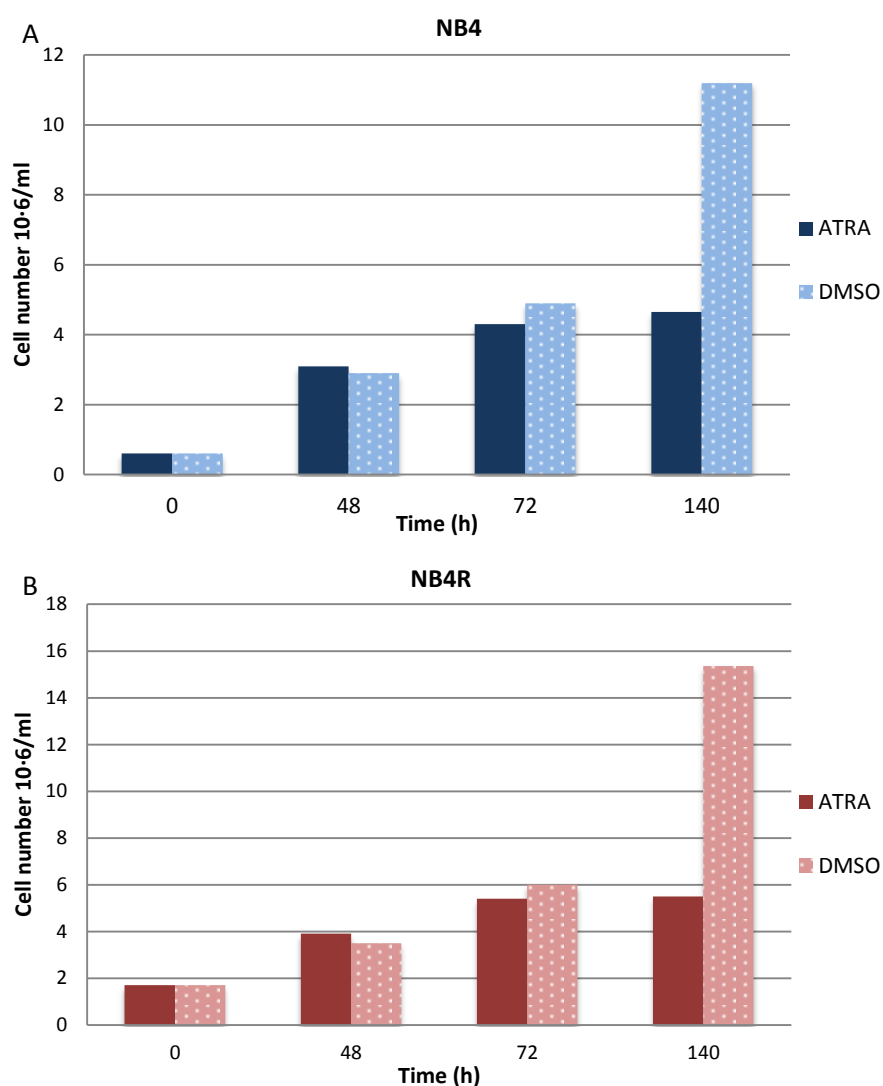


Figure 25. Proliferation of (A) NB4 and (B) NB4R cells in the presence of ATRA or DMSO at different time points of treatment.

In the presence of ATRA, The number of NB4 (Figure 25A) as well as NB4R (Figure 25B) cells increases until 72 hours of treatment then stabilizes. On the other hand, in the presence of DMSO both cell types keep proliferating constantly. Therefore, both cell lines are sensitive to ATRA, which induces a real proliferation block in NB4 and NB4R cells concomitant to the triggered differentiation.

Identification of RNA partners of RIG-I involved in the proliferation/cell differentiation balance in the case of Acute Promyelocytic leukemia (APL)

3. Expression of RIG-I in NB4 cells

We decided firstly to start the biochemical work on NB4 cells only. Before trying to unmask RIG-I partners, it was important to make sure that RIG-I is correctly expressed in the cells, during the differentiation of granulocytes induced by ATRA. Western blots on total cell extract were performed in the same experimental conditions as further experiments, after cell crosslinking at 254 nm to create or enhance the interaction between the protein and the possible RNA partner. Then RIG-I expression was estimated by ImageLab (BioRad) software allowing the optical density quantification for each band. Background was subtracted and the RIG-I presence was plotted relative to the level of RIG-I at time zero.

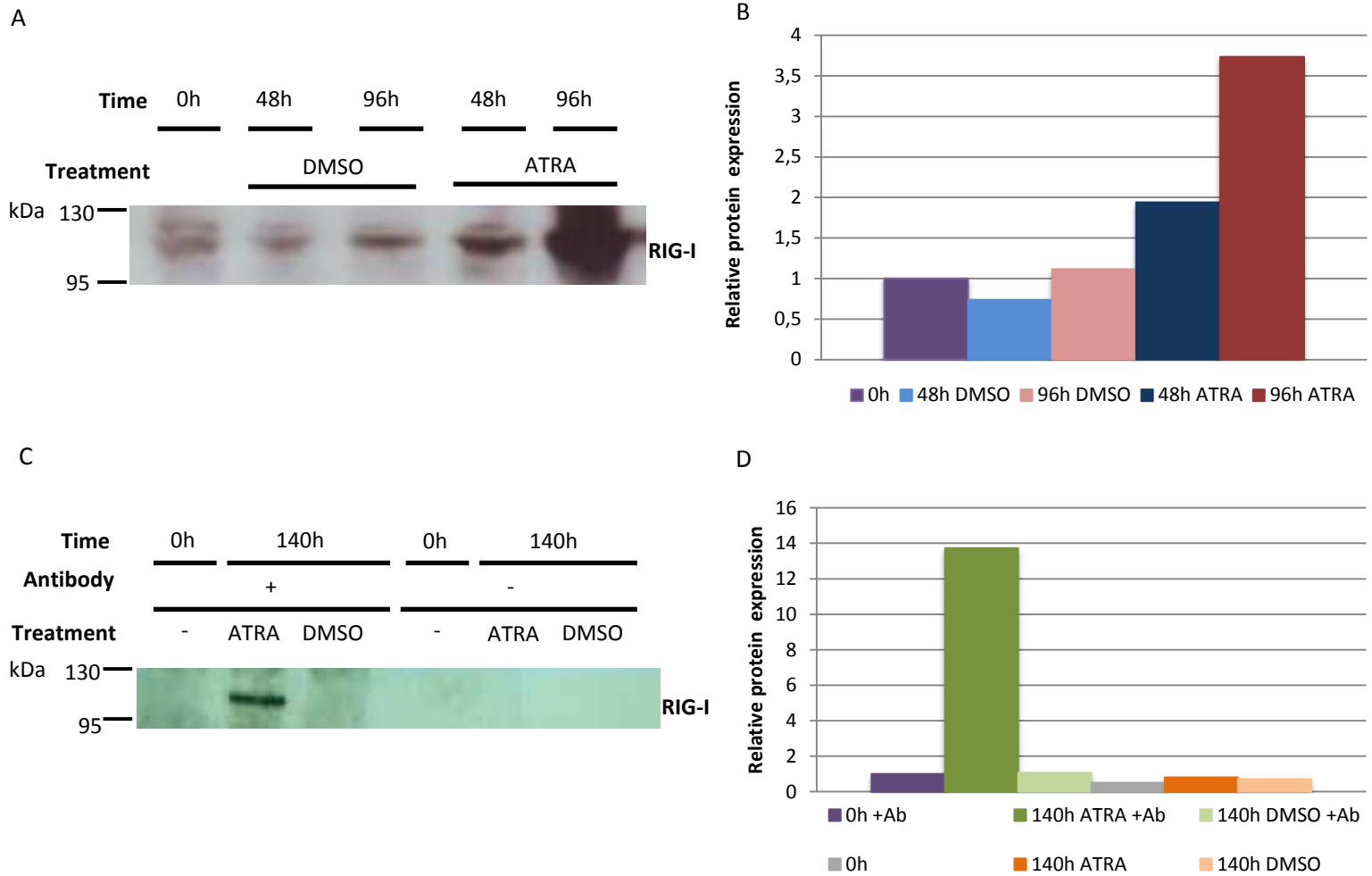


Figure 26. RIG-I in NB4 cells: western blot performed with: (A) 50 μ l of total cell extract and (C) 50 μ l of immunoprecipitated RIG-I complexes. (B) and (D) show respective quantification graph relative to 0h for each time point of treatment with 10 μ M ATRA or DMSO.

As shown by Figure 26A, a strong RIG-I signal was detected around 100-110 kDa after 48 hours of ATRA treatment (2 times higher than 0h) and a dramatic increase of the protein is observed after 96 hours (3,7 times higher than 0h). In a much lower amount as judged by the intensity of the signal, without any drug or after 48h of DMSO treatment a light signal is observed around 100-110 kDa, which can correspond to the basal and low expression level of RIG-I. Later after 96h in the presence of DMSO, a slight increase of RIG-I band is seen (1,1 times higher than 0h), but is in no way comparable to that of 96h treatment with ATRA (3,4 times higher than with DMSO). Therefore I could verify that RIG-I expression is upregulated during ATRA induced differentiation of our NB4 cells. This result allowed me to proceed with immunoprecipitation of RIG-I

and RIG-I complexes. As shown in Figure 26B by the 100-110 kDa band, RIG-I was efficiently immunoprecipitated from cell extracts treated with ATRA.

4. Detection of RIG-I/RNA complexes in NB4 cells

To detect RIG-I complexes, we firstly decided to start working with NB4 cells. Cells were grown for various periods of time with 10 μ M ATRA or DMSO, and the CLIP technique was performed. Cells were UV-crosslinked and 1 mg of total cell extracts was treated with proteases inhibitor cocktail 1X (Millipore), RNasin 1:100 (Promega) and RQ1 DNase 1:50 (Promega). The sample was then prepared for RIG-I immunoprecipitation which was followed by radiolabelling of potential RIG-I bound RNA partners. Radiolabelled immunocomplexes are visualized on autoradiographic films after migration of 8% polyacrylamide/urea firstly. The result is presented by Figure 27.

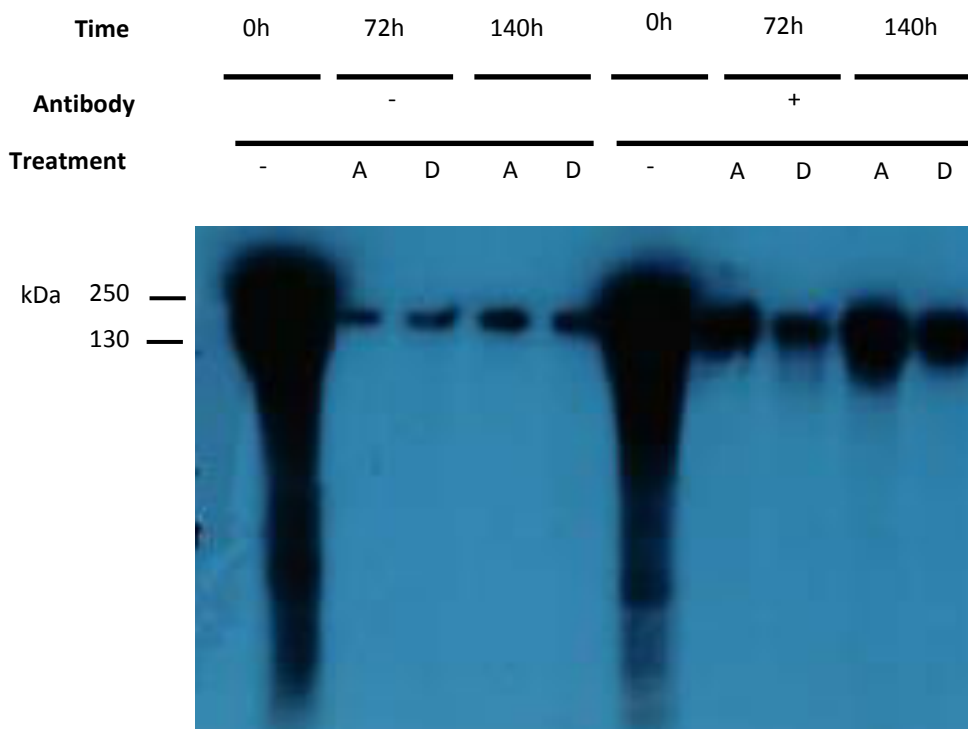


Figure 27. Detection of RIG-I complexes immunoprecipitated in NB4 cells treated with ATRA or DMSO during 72h and 140h. Migration of the samples was performed during 7 hours at 4°C in a 8% polyacrylamide (19:1) /urea gel.

When immunoprecipitation is performed thanks to RIG-I antibody after ATRA or DMSO treatment, a strong signal is obtained (Figure 27). Moreover a increase of intensity between 72 and 140h ATRA or 72 and 140h DMSO treatment is observed and

the signal is definitively more important in the case of ATRA treatment. In the case of control immunoprecipitations, without antibody, no such phenomenon is observed. The difference of signal intensity between 72 and 140h is less striking for both types of treatment. Moreover at the same time point (72h ATRA and DMSO or 140h ATRA and DMSO), the intensity of the obtained bands with ATRA and DMSO seem very similar. The molecular weight of the immunoprecipitated product is much higher than RIG-I molecular weight (100-110 kDa). All together, these results suggest that possible complexes containing RIG-I have been immunoprecipitated from NB4 cells treated with ATRA (and maybe also in a smaller proportion with DMSO). Moreover, since the extracts were prepared in the presence of DNase degrading DNA and RNasin, which protect RNAs, it is quite possible that the signal obtained corresponds to RIG-I/RNA complexes. In the absence of drug (0h), with or without antibody, we can also see a strong and totally different signal. In this case, the cells are in a proliferating state. This signal appears difficult to explain precisely at this point.

As a first step to verify that RNA(s) is/are present in immunoprecipitated complexes after 72h and 140h, samples were treated with RNase A after elution of the radiolabelled products just before the gel migration. The Figure 28 presents the effect of the treatment.

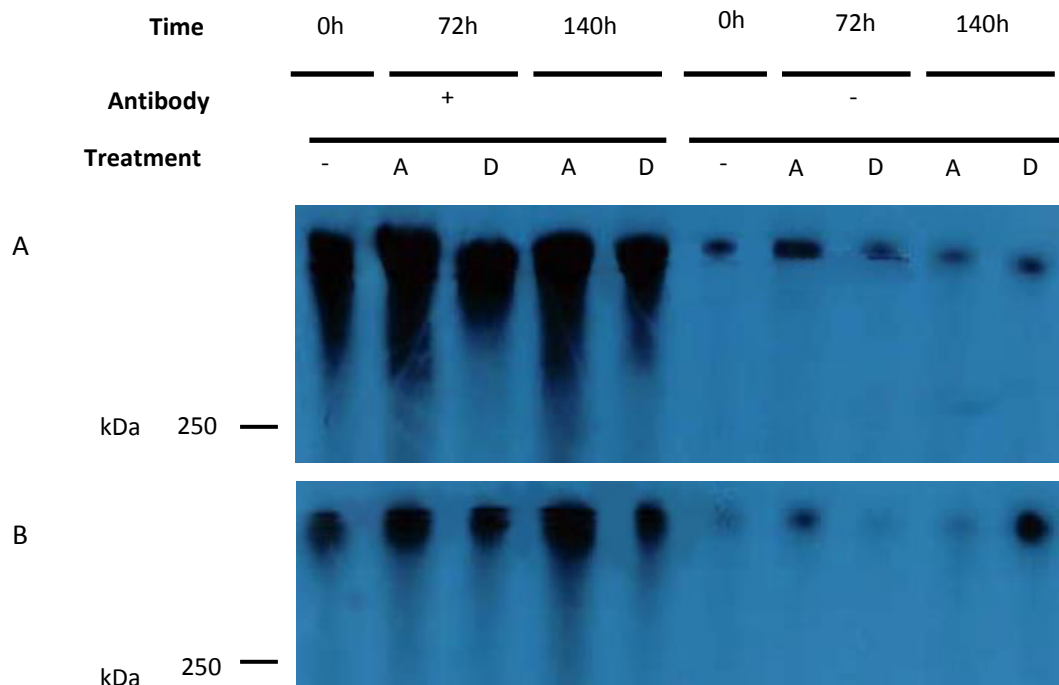


Figure 28. Detection of RIG-I-RNA complexes in NB4 cells treated with ATRA or DMSO: (A) without RNase A (B) with RNase A (0,01mg), after 4 hours of migration at 20°C in 8% polyacrylamide(37.5:1)/urea gel.

Without RNase A (Figure 28A), the signal obtained previously is confirmed being more intense with ATRA than with DMSO. On the other hand after treatment of the samples with the enzyme (Figure 28B), the signal is significantly reduced without disappearing completely. Therefore we can suppose that RNA is present in immunoprecipitated complexes in both types of treatment. In the case of samples without ATRA and DMSO, RNase A has also an effect. Because of this observation, it is legitimate to think that this signal at 0h can be artefacts due to sticky RNAs in the proliferative state and that the observed bands with ATRA and DMSO could result from different RNAs kinds.

In the same way, it was important to verify that the immunoprecipitated protein RIG-I was present in these complexes. Moreover in the Figures 27 and 28, the complexes are characterized by a slow migration in the gel, staying in the area underneath the wells. The immunoprecipitated proteins can form complexes with various partners of different sizes or aggregates with several RIG-I molecules slowing down the migration. Therefore, to break the complexes and facilitate the migration, but also to be sure they contain proteins, I treated the immunoprecipitated and radiolabelled samples with proteinase K (Figure 29). Two kinds of result were expected: 1) a more or less complete disappearance of the signal due to the protein degradation and fast migration of the RNA, which might exit the gel; 2) Several bands characterized by different molecular weights revealing fragments of immunoprecipitated RNAs. The result is shown by Figure 29.

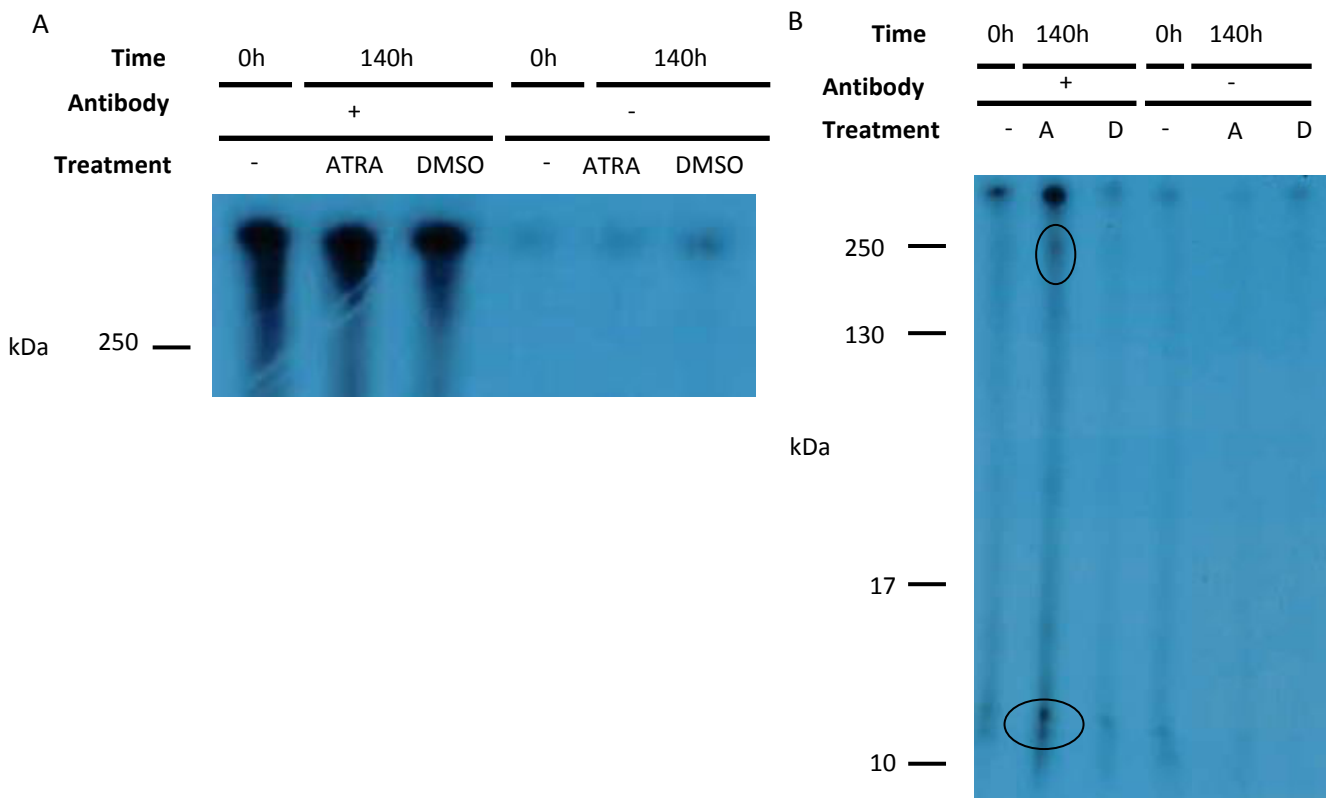


Figure 29. Effect of Proteinase K on RIG-I-RNA complexes in NB4 cells treated with ATRA or DMSO. (A) Treatment without Proteinase K, after 4,30 hours of migration at 20°C in a 8% polyacrylamide(37.5:1)/urea. (B) Treatment with Proteinase K (2mg/ml), after 2,30 hours of migration at 20°C in a 8% polyacrylamide(37.5:1)/urea.

In the Figure 29A, after immunoprecipitation with the antibody, radiolabelled RIG-RNA complexes are again visualized by a strong signal on the film after 140 hours of ATRA treatment. Like in the precedent experiment a signal is also observed with DMSO. After digestion by Proteinase K, in the Figure 29B, the result appears different. The treatment by the enzyme leads to a reduction of the intensity of the bands in the upper part of the gel. Moreover, two unclear bands can be detected in the ATRA treated samples, between 250 kDa and 10 kDa. This signal was never obtained before and at this point we cannot conclude anything about its nature. These observations suggest only that proteinase K has digested a major part of RIG-I in the immunoprecipitated RIG-I-RNA complexes in differentiated NB4 cells by ATRA.

To improve the migration resolution and to obtain a more significant signal after the co-immunoprecipitation, different types of gels migrations were performed. I worked with a lower percentage of acrylamide (8%) to facilitate the migration of potential big size complexes. I also performed SDSPage gels (8%) and finally NuPage gels (8%), which preserve RNAs by pH stabilization. But none of these approaches gave a clear result

despite several protocol adjustments. Therefore we decided to stop this search of RNAs RIG-I partners and to reorient my PhD project on the search of protein partners.

Identification of protein partners of RIG-I involved in the proliferation/cell differentiation balance in the case of Acute Promyelocytic leukemia (APL)

5. Isolation of RIG-I from NB4 cells

Unmasking Proteic RIG-I partners does not necessarily require cell cross-linking, and the cell lysis buffer is different from the buffer used in order to isolate co-immunoprecipitated RNAs. Therefore as a first step, it was cautious to check the detection of RIG-I in the lysis conditions allowing later on the protein-protein interaction detection, and without cross-linking. A western blot was performed in the proliferative state of the cells and after treatment with 10 μ M ATRA or DMSO during 96h. Then RIG-I expression was estimated by ImageLab (BioRad) software allowing the optical density quantification for each band. Background was subtracted and the RIG-I presence was plotted relative to the level of RIG-I at time zero.

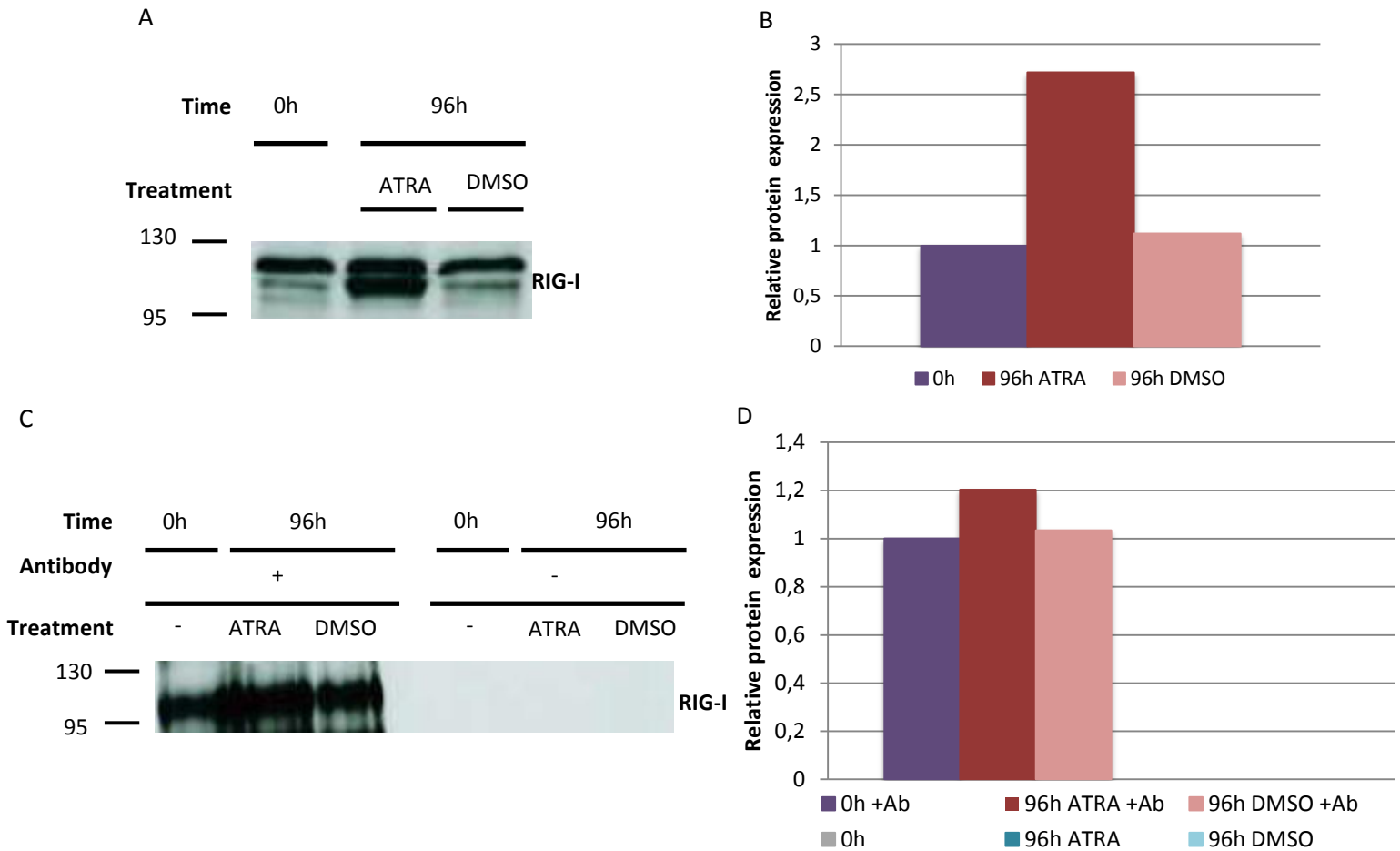


Figure 30. RIG-I in NB4 cells: western blot performed with: (A) 50 μ l of total cell extract and (C) 50 μ l of immunoprecipitated RIG-I complexes. (B) and (D) show respective quantification graph relative to 0h for each time point of treatment with 10 μ M ATRA or DMSO.

As shown by Figure 30A, a strong signal reflecting RIG-I expression is observed as presented by the lower band of a kind of doublet after 96 h of ATRA treatment (2,7 times higher than 0h). A much less intense band is obtained in control and DMSO treated cultures (1,1 times higher than 0h).

After immunoprecipitation with anti RIG-I antibody (Figure 30B), three elutions of potential complexes were performed, pooled and TCA precipitated. A classical western blot was then performed. As shown by Figure 30B, once again a stronger RIG-I signal was detected in the case of ATRA treatment (1,2 times higher than 0h) than with DMSO. No signal is observed as expected in the case of co-immunoprecipitation in the absence of RIG-I antibody.

To probe protein-protein interactions in the case of RIG-I in the framework of NB4 APL cells differentiation, we considered performing a proteomic approach. Before

performing 2D gel electrophoresis and mass spectrometry for protein profiling thanks to a proteomic facility, I realized SDS page migration followed by silver staining which is the most sensitive technique to detect proteins in gels.

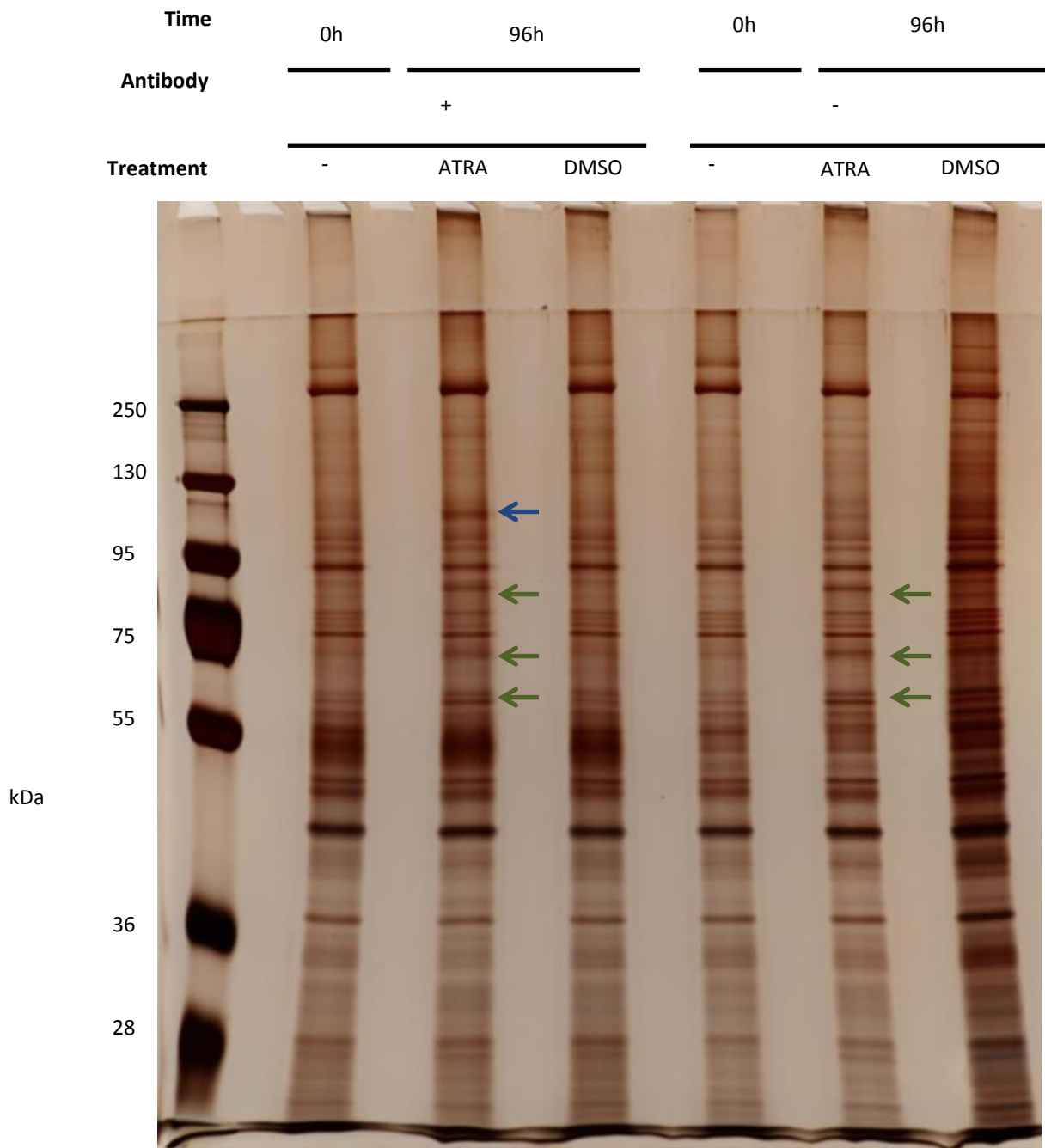


Figure 31. RIG-I in NB4 cells: silver stained SDS page gel after migration of 50 μ l of immunoprecipitated RIG-I complexes, for each time point of treatment with 10 μ M ATRA or DMSO.

Figure 31 presents the migration pattern of a single eluted fraction after co-immunoprecipitation, and the experiment was performed only once. On this silver

stained gel, the RIG-I signal (blue arrow) appears in the case of ATRA treatment and immunoprecipitation with anti RIG-I antibody. We can notice that RIG-I is not very abundant as judged by the band intensity. Moreover on this gel, it is very difficult to see differences of migration pattern and band intensities between the different treatment conditions. One can observe some bands (green arrow) which are present only in the case of ATRA treatment with and without IP, meaning probably that some compounds can stick to the beads. This experiment needed probably to be improved to get a cleaner migration. In addition, it is quite difficult to appreciate on a one dimension gel the presence of new bands which can migrate at the same level as others already present and characterized by the same size, particularly if they are poorly present in the prepared sample. This experiment of 1D gel followed by silver staining was tempting in case a striking signal could be observed. But obviously we did not consider the 1D gel as the way to answer the question we were asking. The next experimental step was to undertake 2D gels to separate more accurately the proteins.

Discussion-Conclusion

Helicases are involved in various infectious mechanisms and several cancers. They are therefore potentially interesting pharmacological targets but their function and the molecular and cellular interactions are still poorly understood. Mounting evidence has accumulated that RIG-I helicase contains the specialized domains that recognize foreign RNA ligands to wake up it to initiate antiviral innate immunity. Previous works have also shown that RIG-I expression is modulated by ATRA and related to granulocytic differentiation (Liu TX et al., 2000; Zhang NN et al. 2008). Although a number of studies were conducted to elucidate the mechanism of myeloid differentiation and improve therapeutic strategy against myeloproliferative syndromes such as Acute Promyelocytic Leukemia (APL), a number of questions remain. The purpose of this work was to contribute to better understand the role of the RIG-I helicase in the myeloid differentiation. The project aimed specifically to identify new partners of RIG-I during ATRA treatment inducing differentiation and proliferation block, in the NB4 cell line which is the cellular model derived from a patient with APL (Lanotte M et al., 1991).

It is generally accepted that RIG-I can bind and be activated by viral 5'triphosphate (5'ppp) single-stranded RNA (ssRNA) or dsRNA (Yoneyama M et al., 2004; Hornung V et al., 2006; Lu C et al., 2010; Pichlmair A et al., 2006; Wang Y et al., 2010; Baum A et al., 2010) and it prefers short size RNAs (10-25 nucleotides long) (Kato H et al., 2008). Therefore when I started my PhD work it was reasonable to look for RNA(s) partners first. Through the CLIP experiments, the stronger signal observed each time in the case of ATRA treatment than with DMSO can reveal as already mentioned the presence of RIG-I-partner complexes (Figures 27, 28A and 29A). The samples being beforehand treated with DNase, it can be considered that either endogenous RNA(s) or protein(s) in addition to RIG-I are present in the complexes. But the UV-CLIP technique is specific to cross-link nucleic acids to proteins (Greenberg JR, 1979). The IP signal obtained with DMSO treatment could be surprising. However, we have seen like already mentioned by others teams (Khanna-Gupta A et al., 1994; Qiu H et al., 2011) that in the presence of DMSO, the differentiation process is initiated. But it is incomplete since the cells never reach the polynuclear stage and keep proliferating. Additionnaly, in this condition, although expressed to a lesser degree than during ATRA treatment, a RIG-I signal is observed by western blot (Figure 26A). As reported

by Liu TX et al., and Zhang NN et al., RIG-I is upregulated as soon as 24h of myeloid differentiation in early maturing cells such as promyelocytes (Liu TX et al., 2000; Zhang NN et al., 2008). Therefore, these observations raise more the question of the nature of the RNA partner(s), which is particularly reinforced by the compact signal aspect at the level of high molecular weight. Several attempts were performed to obtain a better detection and an improved signal resolution by adjusting the preclearing step, the migration time and temperature, by using different acrylamide types (19:1, 37:5.1) and different gel types to facilitate the complexes migration. It can not be excluded that RIG-I oligomerizes (Patel JR et al., 2013), moreover it is possible that rRNAs or tRNAs known to be abundant and “sticky” are present, “contaminating” the samples. Detection of significant RNAs has to be improved by discarding undesired RNAs (centrifugation, molecular biology Kit such as Ribominus....). The control experiments strongly suggest this possibility. Indeed, in the absence of ATRA and DMSO at 0h, an unexpected and strong signal is obtained, not completely abolished by RNase A and only weakened when treated with proteinase K (probably because the concentration of enzymes were not enough) (Figures 27, 28B and 29B). Moreover, bands are also present in the case of control immunoprecipitations (without antibodies) of samples either treated with ATRA or DMSO and later on with RNase A (Figures 27 and 28A/B). In the absence of ATRA or DMSO, we also have to consider that the cells are in a proliferating state. We know that the capacity of cells to grow and proliferate is coupled to the rRNA transcription. During differentiation (e.g. myogenesis, osteogenesis, adipogenesis, granulopoiesis, and monocytic differentiation) the expression of the proto-oncogenic protein c-Myc is decreased in response to the transition from proliferating state to non-proliferating state. This downregulation of c-Myc decreases the expression of Pol I related transcription factors leading to the downregulation of rRNA transcription (Hayashi Y et al., 2014). Therefore this difference of rRNA level between proliferating and differentiating state can explain the strong signal obtained in the absence of any drug or solvent corresponding to the proliferating state.

As a result these non specific immunoprecipitated RNAs can mask the presence of other interesting RNAs candidates. In the litterature not only viral RNAs but several and different kinds of RNAs are known to bind to RIG-I. In the case of murine B lymphocytes, His-tagged RIG-I binds to multiple endogenous mRNAs such as NF- κ b1 3'UTR mRNA (Zhang HX et al., 2013). Also snRNA U1 and U2 in colorectal carcinoma cells can bind RIG-I leading to IFN pathway activation (Ranoa DR et al.,

2016). Among the possible RNA partners, miRNAs are also good clients. Several works have shown that miRNAs affect tumor progression and cell differentiation. In the case of hematopoietic differentiation, they can both have tumor suppressor or oncogenic activities (Schotte D et al., 2012). Considering that a RNA helicase can also have activities through impairing a suppressing miRNA as seen with DDX20, we can also consider that RIG-I could interact with a miRNA. Unfortunately at this stage of the performed work we can not conclude anything.

Despite the several tests, the results obtained with the CLIP technique were far to be clear-cut and the controls or signal intensities were not always reproducible. This lack of reliability has led us to reorient the project and to look for protein partners. As already mentioned earlier, previous works have shown that upon activation by foreign RNAs, RIG-I interacts with different proteins triggering signalisation cascades (such as apoptosis through activation of IPS-1 and caspases (Besch R et al. 2009). Moreover, Zhang HX et al., have observed that RIG-I can interact with both endogenous RNA and protein (Zhang HX et al., 2013). Also, Li XY et al., show that RIG-I interacts with the Src protein in an independent manner of RNA ligand (Li XY et al., 2014). These protein partners can interact with the CARDs domains, which are typically involved in direct interactions with a wide range of proteins, but they also can bind RIG-I through its helicase domain (Lyn, HSP90, PKC- α/β) or its CTD domain (HSP90, UPS15, ARL16, PACT). Therefore we did not restrict our search of partners. The silver stained gel (Figure 31) I obtained seems to show the presence of RIG-I between 95 and 130 kDa, in ATRA treated samples by comparison to the other conditions but it does not indicate anything about its abundance and the general migration pattern does not present striking differences. This one dimension gel was performed as a first approach to have a general view of what can be obtained after IP. We can not exclude that some proteins with molecular weight close to that of RIG-I can be coimmunoprecipitated. In the same way, specific and unspecific coimmunoprecipitated proteins are not discriminated. Only 2D-DIGE gels could have given a more resolutive picture of possible partners. In case high-molecular-weight protein complexes would have been obtained they could also have been separated by using agarose 2-DE (Oh-Ishi M and Maeda T, 2007; Chevalier F, 2010). Later on mass spectrometry was considered. At this point we can not conclude anything.

In the case of myeloid differentiation only the Src protein is currently known to interact with RIG-I (Li XY et al., 2014). It takes place in the CARD domains and the linker

between the CARD and the Helicase domains. First of all, this study takes place in the U937 cell line, a macrophage line. Although it is a myeloid line, it is different from our APL NB4 cell line corresponding to a real pathological situation. The authors asserts that this interaction occurs in a manner independent of RNA, since transfection of synthetic small RNAs such as PolyI:C or 5'-pppssRNA partially inhibits the interaction. But they do not take into account that these RNAs are not endogenous RNAs, which can behave differently. Moreover they propose a model of interaction between RIG-I and Src, which releases completely the helicase and ATPase domains. The conformation of RIG-I thus modified makes these two domains completely accessible either for RNAs or other proteins. This does not invalidate what Li XY et al. obtained. When they identified the interaction between Src and RIG-I, their work participated greatly to the understanding of RIG-I position in the signaling cascade of the proliferation control. Indeed they showed that the helicase interacts with the proliferation process by a death program via an apoptosis-independent AKT-mTOR inhibition and on autophagic activation (Li XY et al., 2014). But another group, already mentioned above, has observed this possibility of multiple interactions. Indeed, Zhang HX et al., have demonstrated by immunoprecipitation and iTRAQ-MS that RIG-I interacts both with 3'UTR of Nf-kb1/p105 mRNA and Rpl13, which is a component of the large 60S subunit of ribosome. In this study, it is also important to note that other proteins have also been identified by iTRAQ-MS. Only few of them presented a total ion score confidence interval higher than 95%. The group did not investigate further these candidates. Among them and except trivial candidates such as BSA or histone found very frequently with this technique, three of them (IGFBP5, Hip1-related protein, and VLA-4) could have deserved to be more investigated because of their interesting role in the proliferation, differentiation and cell adhesion (Zhang HX et al., 2013). It would have been interesting to pay attention in our search of protein partners if these candidates were also obtained in differentiated NB4 cells (granulocytes) since their work was performed in a different cellular model, a murine B cell line and later on to investigate the real effect of these interactions in the cells.

To conclude, searching either RNAs or protein partners of RIG-I in the context of the myeloid differentiation would not only clarify the role of RIG-I in the proliferation/differentiation balance. It could also help to understand how the RIG-I helicase behaves with these partners, if enzymatic activities in certain conditions could

be activated or not. Moreover, it would consolidate the versatility of this helicase (immunity and cell differentiation) as it has been observed for other proteins such as the catalytic telomerase reverse transcriptase (TERT) which in association with a noncoding RNA (TERC) has the ability to elongate telomeres. But in the mitochondria TERT associates with another type of RNA (RMRP) and regulates gene expression by generating specific siRNAs (Martínez P and Blasco MA, 2011). Finally, this type of study can be of high impact for diagnosis and therapeutic strategy in oncology based on cellular reprogramming.

Chapter II: Characterization of G-quadruplex resolving by the helicase Pif1 in Bacteroides

Objectif

As already explained earlier helicases are enzymes that travel through paired nucleic acids in double-stranded form to catalyse strand separation and allow replication or transcription of the DNA molecule. This translocation occurs initially thanks to the binding between the nucleic acids and the helicase allowing a conformational change of the helicase allowing its ATPase activity. The hydrolysis of ATP triggers an oscillation state between a maximum affinity state and low affinity state in the DNA binding site resulting in the translocation through the DNA. In the case of non-canonical DNA structures formed by the stacking of several G-quartets called G-quadruplexes (G4), the molecular mechanism underlying their unwinding is more complex because of the formation of several stacks of guanine. G-quadruplexes are present in telomeres, DNA replication origins, gene transcriptional regulatory regions, promoters of certain oncogenes and also immunoglobulin switch regions. Their formation can influence biological processes including DNA replication, translation and telomere integrity maintenance. To counteract the G4 formation certain specific helicases have the ability to resolve them, such as Pif-1, RecQ helicases, FANCI, but the molecular mechanism is not yet completely understood. Among the remaining questions, it is not clear if G4-resolving helicases possess a G4-specific binding site that is different from the classical ss/dsDNA binding site, secondly if G-quadruplex unwinding is ATP dependent and finally how G4-resolving helicase employs the energy derived from ATP hydrolysis to drive G-quadruplex unfolding. To contribute to answer these questions, during the second part of my thesis, I used a BsPif1 helicase, a *S cerevisiae* Pif1p homolog from *Bacteroides sp. 3_1_23* to quantitatively analyse and compare the DNA stimulation of ATPase activities between different G-quadruplexes dsDNA and ssDNA. Then the possibility of different binding sites of G-quadruplex and ssDNA with the helicase was investigated and I studied the relationship between ATP hydrolysis and G-quadruplex unfolding or ss/dsDNA. Finally the annealing activity of BsPif1 was also studied. In

conclusion these experiments will allow us to establish a possible model to explain how BsPif1 transform the energy derived from ATP hydrolysis into mechanical translocation activity to disrupt G4 structure.

Introduction

1. Pif1

1.1. Discovery and definition

Pif1 protein (Petite Integration Frequency protein 1) was identified the first time in 1983, in *S. cerevisiae*. It was discovered for its mitochondrial DNA repair role after induction of DNA damage by Ultraviolet (UV) light or Ethidium Bromide treatment (Foury F and Kolodynski J, 1983). In 1991, the same team purified Pif1 from the mitochondria and demonstrated that this 5'-3' helicase was specific for DNA and ATP-dependent (Lahaye A et al., 1991). Few years later, a genetic screen in yeast aiming to detect mutants losing their expression of subtelomeric genes led to identify Pif1 in the nucleus and to demonstrate its role in the inhibition of telomeres elongation and de novo formation (Schulz VP and Zakian VA, 1994). During this time, a second Pif1 family helicase in *S. cerevisiae*, Rrm3, was found and described as repressing ribosomal DNA (rDNA) recombination (Keil RL and McWilliams AD, 1993). Pif1 helicases are highly conserved from bacteria to humans and belong to the superfamily (SF1) as revealed by sequence alignments. It has been shown that several fungi, such as *Candida albicans* and *Cryptococcus neoformans*, possess two Pif1 helicases, *Arabidopsis thaliana* can have three Pifs and kinetoplastid parasites possess seven to eight Pif1 helicases. Different organisms contain variable numbers of homologue proteins but higher eukaryotes and metazoans contain only one (Bochman ML et al., 2010; Bochman ML et al., 2011). They share essentially equal sequence similarity to ScPif1 and ScRrm3 but little is known about these enzymes.

The different studies of Pif1 have established that this helicase plays multiple roles in the inhibition of telomere elongation and de novo telomere formation at the level of DNA double-strand breaks (Schulz VP and Zakian VA, 1994), the regulation of ribosomal DNA replication (Ivessa AS et al., 2000), a role in the resolution of particular structures of DNA such as G-quadruplexes (Ribeyre C et al., 2009; Lopes J et al., 2011; Paeschke K et al., 2011) and finally, in the maturation of the Okazaki fragments in cooperation with Dna2 helicase/nuclease (Budd ME et al., 2006; Stith CM et al 2008). Its physiological importance was further highlighted by the fact that mutations in human Pif1 are found in families with high risk of breast cancer affecting replication, transcription and elongation of telomeres (Chisholm KM et al., 2012).

The principal biochemical characteristics of Pif1 helicases have been described. They are ATP and Mg²⁺ dependent enzymes that unwind DNA with a 5'-3' polarity (Lahaye A et al., 1993, Gu Y et al., 2008, Liu NN et al., 2015). Although Pif1 helicases display only limited unwinding processivity *in vitro* (Barranco-Medina S and Galletto R, 2010; Ramanagoudr-Bhojappa R et al., 2013; Liu NN et al., 2015), they are capable of unwinding a variety of DNA structures resembling stalled DNA replication forks and other B-form duplexes such as forked duplexes, DNA/RNA duplexes (Boule JB and Zakian VA, 2007; Liu NN et al., 2015), R-loop, D-loop and G-quadruplex DNA (Sanders CM, 2010; Liu NN et al., 2015).

1.2. Pif1 isoforms and cell localization

As mentioned above ScPif1 was first discovered for its role in recombination between the mtDNA (Foury F and Kolodynski J, 1983) then for affecting telomeres (Schulz VP and Zakian VA, 1994) suggesting its presence in the nucleus. The mitochondrial and nuclear isoforms (respectively α and β isoforms) are expressed from the same gene ScPIF1 but they are translated from two different start sites separated by the mitochondrial targeting signal (MTS) (Zhou JQ et al., 2002). ScPif1 translated from the first start site is targeted to the mitochondria thanks to its MTS, which is cleaved upon import into the mitochondria. The nuclear isoform translated from the second start site is slightly larger than the mitochondrial isoform (Zhou J et al., 2000).

In Human like in *Saccharomyces*, Pif1 helicase has two isoforms (α mitochondrial and β nuclear), which are encoded by chromosome 15 and generated by alternative splicing (Figure 32). Their translations are shifted by one codon. A pre-mitochondrial hPif1 isoform, translated from the first one, is exported to the mitochondria by a C-terminal addressing signal, which is finally cleaved generating an 80kDa (707aa) protein. The translation of the nuclear isoform starting at the second codon generates a 74kDa (641 aa) hPif1 with an NLS, which is cleaved later on. Both isoforms share conserved helicase motifs but have differential C-terminal regions, which are responsible of the subcellular distribution of the protein. Moreover, it was found only in the C-terminus of the β isoform the lipocalin signature, which is a characteristic protein secretion signal (Futami K et al., 2007). In yeast, Pif1 expression of isoforms is regulated during the cell cycle with a maximal rate expression at the end of the S phase and the beginning of the G2 phase (Vega LR et al., 2007).

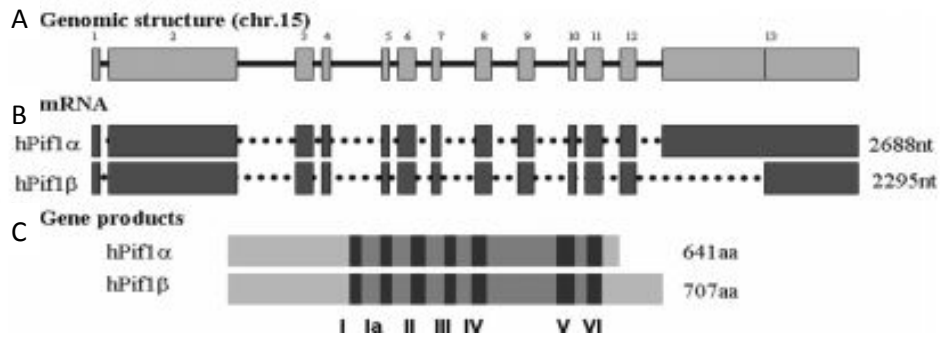


Figure 32. Structure of hPif1 genes and hPif1 proteins. (A) Genomic structure of the Pif1 gene. (B) Schematic representation of the two Pif1 isoforms mRNA. (C) Representation of Pif1 of the two isoforms of Pif1. Adapted from Futami K et al., 2007.

1.3. Pif1 structure

Pif1 helicases vary in size from 420 to more than 1000 amino acids per polypeptide chain. Pif1 belongs to the SF1 family (described above), which is characterized for the presence of two preserved RecA domains (1A and 2A), such as other helicases like *Deinococcus Radiodurans* RecD2 (Saikrishnan K et al., 2009) and bacteriophage T4 Dda (He X et al., 2012). Pif1 is functionally and structurally divided into three domains: the N-terminal domain, the helicase core domain and the C-terminal domain (Figure 33). The N-terminal domain is variable between the different species and not required for helicase activity in vitro (Ivessa AS et al., 2002). Actually the N-terminal function is unknown, but it has been proposed that some of its regions are involved in protein–protein interactions, oligomerization, and substrate recognition (Hall MC and Matson SW, 1999). In *Saccharomyces cerevisiae*, the Pif1 N-terminal domain allows the interaction with the chromatin assembly factor 1 subunit, Cac1 (Monson EK et al., 1997), and is required for double-stranded DNA (dsDNA) unwinding in the presence of the mitochondrial ssDNA-binding protein Rim1 (Ramanagoudr-Bhojappa R et al., 2013). In human this domain contributes to enhance the interaction with ssDNA through intrinsic binding activity and DNA strand annealing activity (Gu Y et al., 2008). The helicase core domain is highly conserved in various organisms. It is composed of two RecA domains (1A and 2A) and the seven classical conserved motifs (I, Ia, II, III, IV, V and VI) present in SF1. Three additional motifs (A, B and C) are found specifically in Pif1 and RecD family helicases (Bochman ML et al., 2011). In some bacteria, such as BsPif1 in *Bacteroides sp 3_1_23* and BaPif1 from *Bacteroides sp. 2_1_16* the motifs I, III, IV and VI interact with the ATP (Chen WF et al., 2016;

Zhou X et al., 2016). In BsPif1 Q145 in motif IV acts as a sensor to detect the presence or absence of γ -phosphate (Chen WF et al., 2016; Saikrishnan K et al., 2009). Pif1 helicases are also characterized by the unique Pif1-family specific sequence (PFSS, 21aa), which is located between motifs II and III (Bochman ML et al., 2010; Bochman ML et al., 2011). The PFSS motif may contribute to DNA unwinding and binding. The interactions between the 1B domain and the PFSS motif may allow the pin of domain 1B to form a more rigid structure and help the residues on the loop to adopt a precise spatial conformation (Chen WF et al., 2016). The DNA binding site is located between the domains 1A and 1B and between domains 2A and 2B (Figure 33) and for the ATP binding site it is localized between domains 1A and 2A.

Finally, the C-terminal domain (CTD), is a non conserved domain in terms of length and sequence going as far as being absent in certain species. Like the N-terminal domain, its role is not completely understood. It is probably involved in protein–protein interactions, oligomerization, and substrate recognition (Hall MC and Matson SW, 1999). Truncation of this domain in yeast leads to a lower processivity probably because of the dissociation of the Pif1 during the unwinding (Singh SP et al., 2016). Also its phosphorylation in ScPif1 in response to DSBs is required to prevent aberrant healing of broken DNA ends by telomerase (Makovets S and Blackburn EH, 2009).

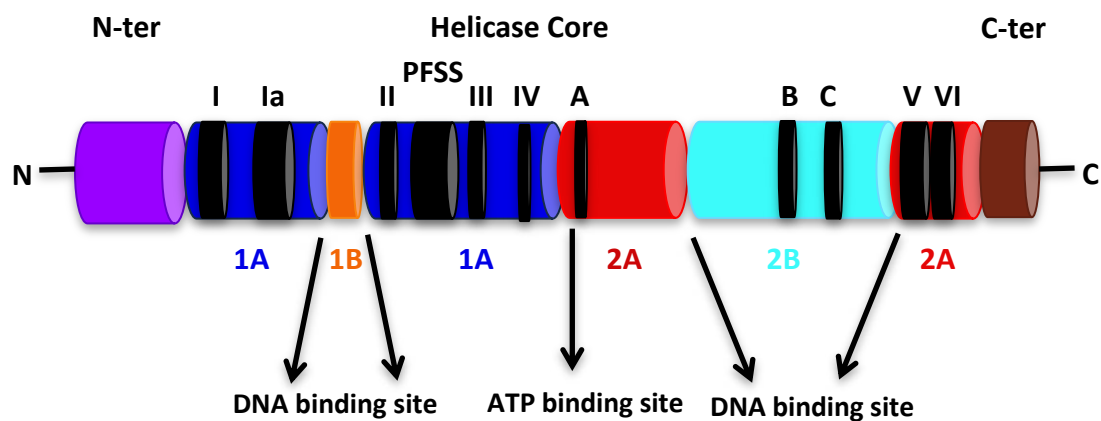


Figure 33. Schematic representation of the different Pif1 domains. N-terminal domain is shown in pink, helicase domains with the four subdomains represented in dark blue for 1A, orange 1B, red 2A and blue 2B, also the different characteristic motif represented in black. Finally C-terminal domain in brown.

Pif1 secondary structure has been determined by crystallization in different bacteroids (*Bacteroides sp 3_1_23* called BsPif1 by Chen WF et al., 2016 and *Bacteroides sp. 2-1-16* called BaPif1 by Zhou X et al., 2016) and in human (Zhou X et al., 2016) (Figure 34). The 2B domain of Pif1 forms an SH3 (SRC Homology 3) domain, which is characterized by a β -barrel fold consisting in a large beta-sheet that twists and coils to form a closed structure. The BsPif1 1B domain forms an ordered loop whereas in BaPif1 and hPif1 a loop and an α -helix have been observed. In all the cases, this 1B domain forms a pin or wedge that splits the incoming DNA duplex (Saikrishnan K et al., 2009; He X et al., 2012). The PFSS is composed of an α -helix and a turn in all three reported Pif1 structures. It is located at the entrance of the DNA-binding site, opposite the strand separation pin/wedge (Chen WF et al., 2016; Zhou X et al., 2016).

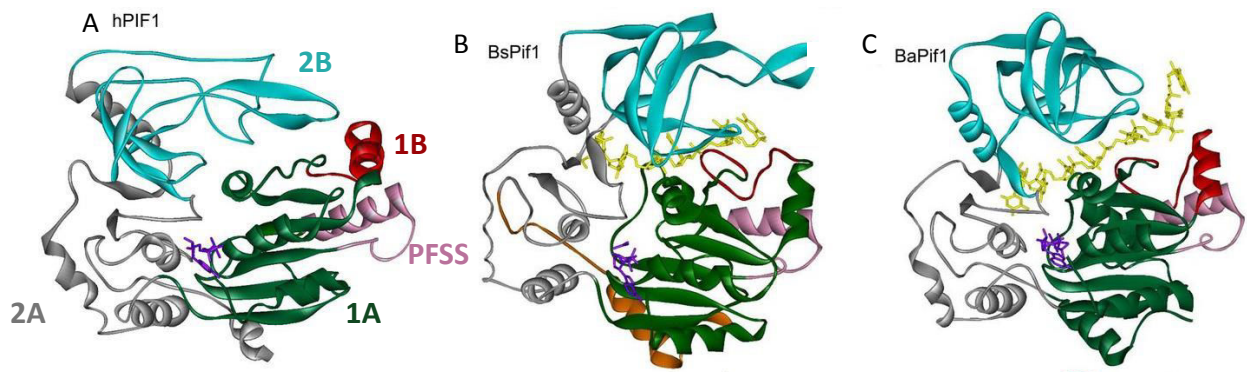


Figure 34. Crystal structures of Pif1. The domain 1A is shown in green, 1B in red, 2A in gray, 2B in cyan, and the Pif1 signature sequence in pink. (A) Structure of hPif1-HD (PDB: 5FHH), in purple is represented the ADP-AIF4 (Zhou X et al., 2016). (B) Structure of BsPif1 (PDB: 5FTE), the C-terminal domain is represented in orange, the AMPPNP in purple and DNA in yellow (Chen WF et al., 2016). (C) Structure of BaPif1 (PDB: 5FHD), the DNA is shown in yellow (Zhou X et al., 2016). Adapted from Byrd AK and Raney KD, 2017.

Investigation of ScPif1 quaternary structure has shown that ScPif1 works as a dimer (Barranco-Medina S and Galletto R, 2010). However, the monomeric form has also the capacity to translocate on a ssDNA (Galletto R and Tomko EJ, 2013) and to unwind dsDNA (Singh SP et al., 2016). Contradictory studies have suggested that the monomeric form of ScPif1 is unable to unwind DNA:DNA duplexes, but can unwind DNA:RNA duplexes (Zhou R et al., 2014).

1.4. Functions of Pif1

1.4.1. Synthesis of Okazaki fragments

During DNA replication, the leading strand (5' to 3') is the strand of the nascent DNA continuously synthesized in the same direction as the growing replication fork. The lagging strand (3' to 5') is the strand of the nascent DNA synthesized in the opposite direction of the growing replication fork. This synthesis occurs in a discontinuous manner, leading to short DNA fragments called Okazaki fragments (Sakabe K and Okazaki R, 1966; Okazaki R et al., 1968). These short DNA segments are initiated by the primase activity of the DNA polymerase α (Pol α) complex, which synthesizes an RNA primer of 10-12nt followed by a DNA sequence of 20-30nt (Rossi ML and Bambara RA, 2006; Burgers PM, 2009). This primer is recognized by the Replication Factor C (RFC), which recruits the Proliferating Cell Nuclear Antigen protein (PCNA) able to replace the Pol α by the DNA polymerase Pol δ . Pol δ raises the strand primer and synthesizes a new Okazaki fragment up to find the 5' end of the preceding one (Figure 35). Then the primer is cleaved by a Flap endonuclease, called FEN-1 and the two ends of DNA created are fused by DNA ligase I (Liu Y et al., 2004). But a single-stranded 5' DNA, which has not been cleaved immediately by FEN-1 is lengthened up to 30nt which allows the fixation of Replication Protein A (RPA). The presence of RPA would inhibit the cleavage activity of FEN-1. Finally the 30nt primer is resolved by Dna2, a 5' to 3' helicase and endonuclease, which cleaves the DNA into small fragments and finally allows the ligation of the two fragments by the ligase I (Bae SH et al., 2001). The role of Pif1 in the synthesis of Okazaki fragments has been described for the first time in 2006 in *S. cerevisiae*. Pif1 interacts with Pol δ during DNA replication. The formation of the outgoing 5' strand would recruit the Pif1 helicase in addition to Pol δ . The combined action of Pol δ and Pif1 would promote elongation of the outgoing 5' allowing the recruitment of Dna2 for its cleavage. The deletion of Pif1 wouldn't permit the extension of the outgoing 5' DNA that will be cleaved by FEN-1 without requiring the presence of Dna2 (Budd ME et al., 2006). The reconstitution of the Synthesis of Okazaki fragments in vitro confirmed this model (Pike JE et al., 2009).

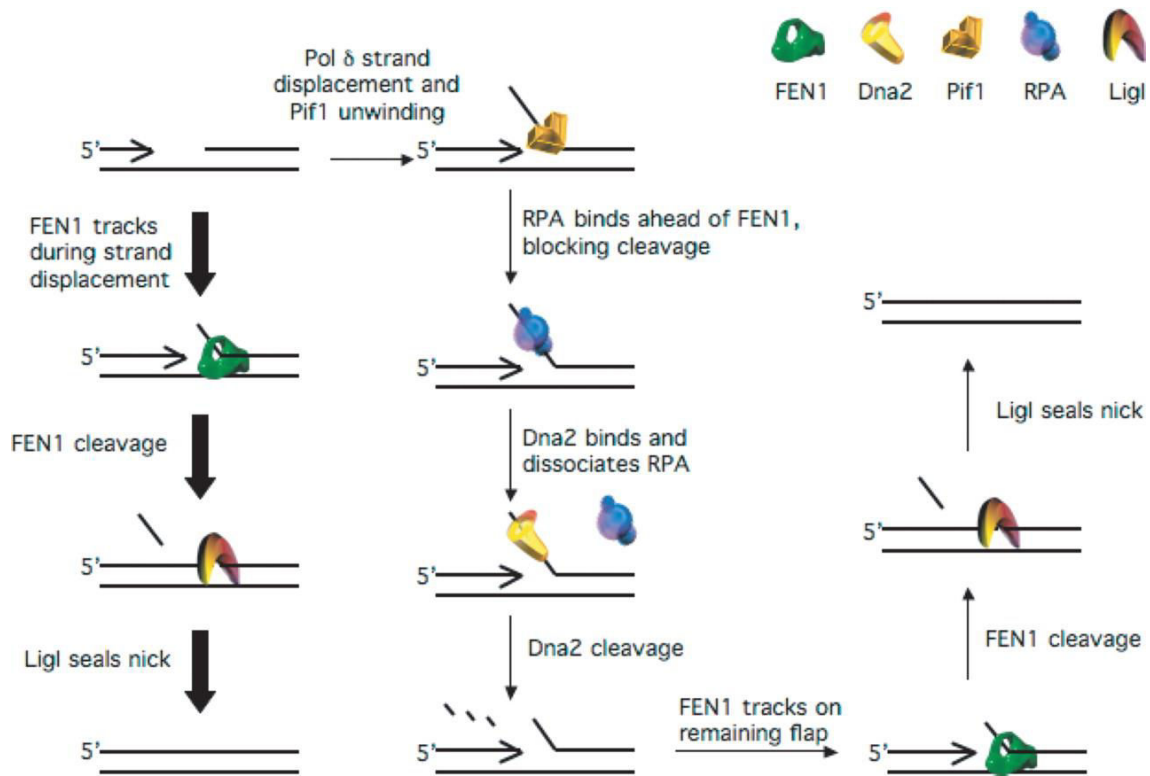


Figure 35. The two-nuclease pathway for flap processing. The synthesis of Okazaki fragments requires an RNA primer, Pol δ synthesizes the complementary strand until it encounters the upstream primer and generates an outgoing 5' DNA. A majority of flaps (denoted by the thick arrows) the endonuclease FEN-1, which has a 5' flap activity cleaves this outgoing 5' DNA. Finally LigI will ligate the two ends generated. On a minority of flaps (denoted by the thin arrows), Pif1 binds the short flap displaced by Pol δ prior to FEN-1 action. Pif1 activity lengthens the size of the flap generating a long single-strand, allowing binding of RPA and FEN-I inhibition. It is then Dna2, which thanks to its nuclease activity, will reduce the size of the outgoing 5' DNA until it is short enough to stop fixing RPA. As initially, FEN-1 will cleave the outgoing 5' DNA and the generated ends will be ligated by LigI. Adapted from Pike JE et al., 2009.

Otherwise during replication and transcription R-loops (RNA-DNA hybrids) appear and their persistent formation is a source of genome instability. Pif1 has the capacity to unwind them (Boule JB and Zakian VA, 2007; Aguilera A and Garcia-Muse T, 2012). Indeed, Pif1 can utilize its activity to remove the RNA strand from 31-bp RNA-DNA hybrids (Zhou R et al., 2014) (Figure 36).

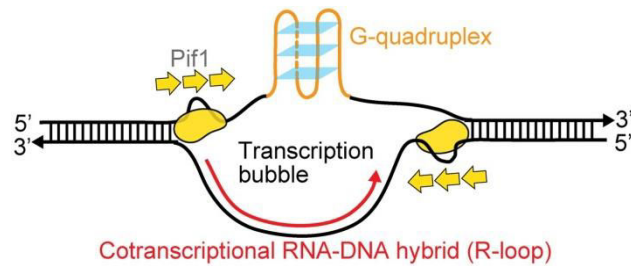


Figure 36. The patrolling activity of Pif1 in R-loops. Adapted from Zhou R et al., 2014.

1.4.2. Unfolding G-quadruplexes

In 2009, it has been shown that Pif1 is involved in the stability of G-quadruplexes. The allele of the human minisatellite of 1.8 kb, called CEB1-1.8 was inserted into the genome of yeast *S. cerevisiae*. This guanine rich allele is composed of 42 tandem repeats ranging in size from 36 to 43bp and is able to form in vitro G-quadruplexes (Lopes J et al., 2006). In vitro, Pif1 is able to unwind the G4 structures formed by CEB1. In vivo, the absence of Pif1 promotes genetic instability of the G-rich human minisatellite CEB1 alleles. On the other hand, helicases such as Sgs1, Dna2, Rrm3 or Mph1 have no effect on the stability of the minisatellite CEB1-1.8 (Ribeyre C et al., 2009). The ability of Pif1 to resolve these G4 structures suggests that Pif1 contributes to the stability of the genome by preventing rearrangements induced by structures formation in vivo (Figure 37). To better understand the role of Pif1, the same team measured the instability of the CEB1 minisatellite inserted beside the ARS305 (Autonomous Replication Sequence) on the leading orientation (orientation I) or on the lagging strand (orientation II) (Lopes J et al., 2011). In WT cells, CEB1 appears to be fairly stable with rates of 0.5% rearrangements for both orientations. In *pif1* Δ cells, the instability of the minisatellite in orientation II is quite similar to the WT with a rearrangement rate of 2%. In contrast, it is extremely unstable in orientation I, the instability reaches 56.3%. Similar results were obtained with the catalytic mutant of Pif1 (*pif1*-K264A) showing that the helicase activity of Pif1 plays a role in the stabilization of the minisatellite in orientation I. In order to confirm that the instability of CEB1 close to the ARS305 depends on the ability to form G-quadruplexes in vivo, the cells were treated with Phen-DC3, a G-quadruplexe ligand able to inhibit the unwinding of G4 by Pif1 in vitro. The results show a low rate of rearrangements (0.5%) without treatment whereas the addition of the Phen-DC3 ligand generates 11.2% of rearrangements in Orientation I versus only 4.1% in orientation II, suggesting that the

instability of CEB1 close to the ARS305 depends on the formation of G4 in vivo stabilized by Phen-DC3 (Lopes J et al., 2011). The Pif1-K264A protein binds to the DNA in a way similar to the wild-type protein but its absence of ATPase / helicase activity facilitates the detection of its binding sites. Pif1-K264A has been shown to be associated with 11% of the G4 sites at the end of S phase, after replication of the G4 sequence, suggesting that it has not a role in replication but in mitosis preparation. Absence of Pif1 leads replication fork slowing specifically near those G4 motifs to which Pif1 normally binds (Paeschke K et al. 2011). Finally it has been shown that Pif1 can unwind intramolecular G-quadruplexes at every patrolling cycle, by the capacity of G-quadruplexes to refold immediately (~0.2 s) (Zhou R et al., 2014). The capacity of Pif1 to unwind G-quadruplexes allows keeping this structures unfolded during transcription bubble, on DSBs, telomers and on the lagging and/or leading strand during replication.

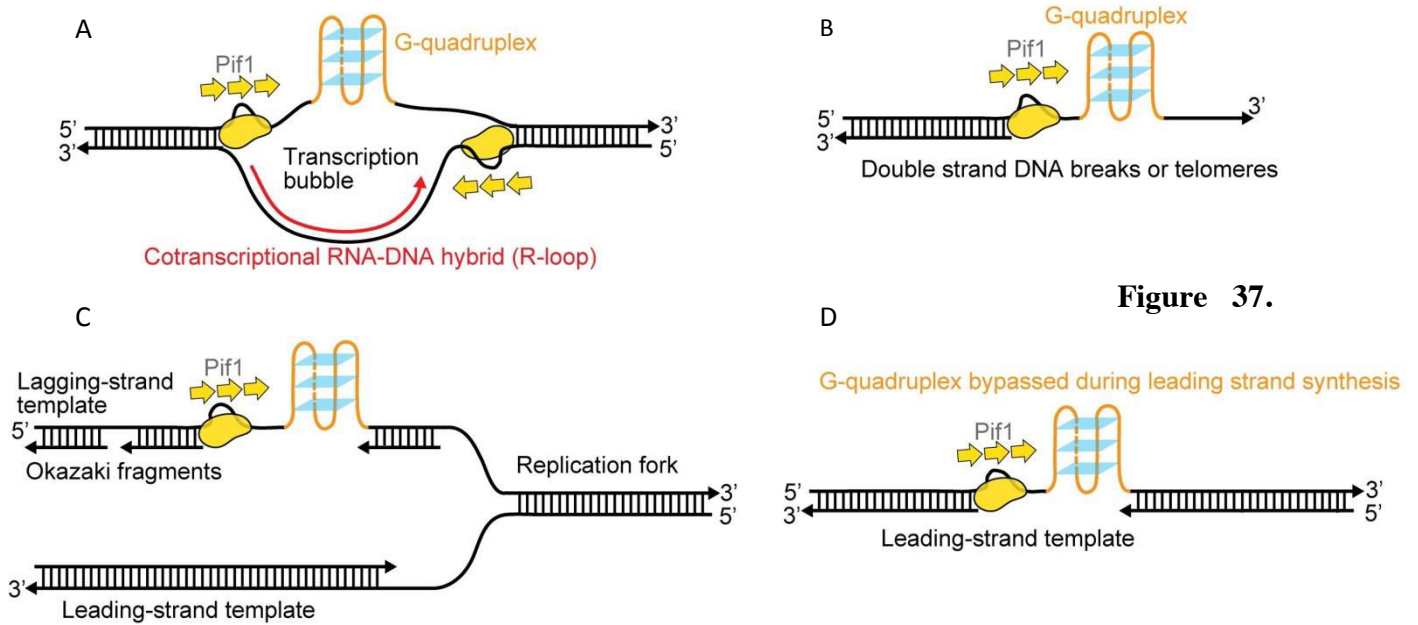


Figure 37.

The patrolling activity of Pif1 in G-quadruplexes. (A) Unwinding of G-quadruplexes during transcription (B) Pif1 allows G-quadruplexes unwinding on the 3' ssDNA tails at telomeres and DSBs (C and D) unwinding G4 structures on the lagging and/or leading strands during DNA replication. Adapted from Zhou R et al., 2014.

1.4.3. Telomerase regulation

The role of Pif1 as a negative regulator of the telomere length by telomerase processivity was first demonstrated in 1994, in a gene screen. Indeed, a mutant of the nuclear form of Pif1 called pif1-m2 resulted in telomere lengthening whereas a mutant

of the mitochondrial form of Pif1, *pif1-m1*, had no effect (Schulz VP and Zakian VA, 1994). Nuclear Pif1 limits therefore telomerase activity. Different mechanisms were supposed (Figure 38): the prevention of initiation of telomerase-mediated telomere lengthening or limitation of telomerase processivity or unwinding of telomere DNA from the telomerase RNA template (hybrid DNA telomeric and RNA telomerase) formed during telomere replication and dislodging telomerase from the chromosome terminus (Boule JB et al., 2005). Pif1 over-expression leads to less interactions of telomerase with telomeres producing telomere shortening. Conversely, Pif1 depletion results in telomere elongation. Also Pif1 promotes genome stability by ejecting telomerase from non-telomeric DNA (Schulz VP and Zakian VA, 1994).

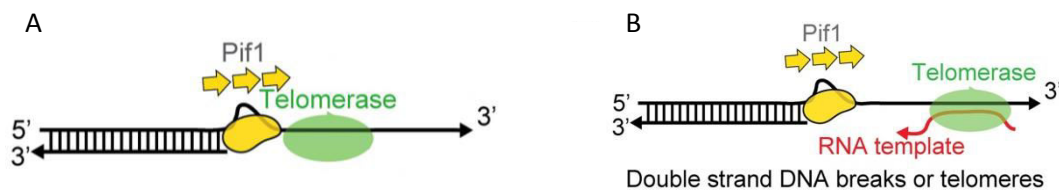


Figure 38. The patrolling activity of a Pif1 in the telomers. (A) Pif1 allows telomerase displacing from 3' ssDNA ends at telomeres. (B) Pif1 permits unwinding of telomere DNA from the telomerase RNA template. Adapted from Zhou R et al., 2014.

1.4.3.1. Processivity of telomerase limitation by Pif1

It has been suggested that telomerase processivity is a significant determinant of telomere length. Two types of processivity have been described for telomerase. The first is based on the ability of telomerase to fully copy the TLC1 (Templating telomerase RNA) substrate without being dissociated from the DNA. The second is based on its ability to translocate RNA in order to initiate a second replication without being dissociated from DNA (Lue NF, 2004). The preferential activity of Pif1 for DNA-RNA hybrids led to the hypothesis that Pif1 could take off telomerase of telomere. The telomerase processivity was measured *in vitro* in the presence and absence of Pif1. The obtained results showed that in the absence of Pif1, telomerase initiates elongation products of approximately 5 to 7nt against only 2nt in the presence of Pif1. Also, chromatin co-immunoprecipitation experiments showed that overexpression of Pif1 results in a decrease of telomerase association with telomeres, whereas depleting cells of Pif1 increases the levels of telomere-bound Est1p, a telomerase subunit that is

present on the telomere when telomerase is active. This study shows that Pif1 limits the processivity of telomerase in vitro and releases telomerase from telomere oligonucleotides in vitro and in vivo (Boule JB et al., 2005).

1.4.3.2. Pif1 inhibits the recruitment of telomerase to DNA double-strand breaks

In order to differentiate the telomere ends of double-strand breaks from DNA, the cell implements different strategies. One of them is linked to the presence of telomere specific proteins that form a telomere cap necessary for both telomere protection and for specific recruitment of telomerase. In the DNA double-strand breaks, there are telomerase inhibition pathways that prevent the de novo telomere addition and promoting double-strand breaks repair through various DNA repair pathways, either by Homolog Recombination (HR) or Non Homologous End Joining (NHEJ). The Pif1 helicase actively participates in this de novo telomere addition. The use of a pif1-m2 mutant (nuclear form) has shown a 600 higher presence of Gross Chromosome Rearrangement (GCR) levels, the majority corresponding to de novo telomere addition, whereas a pif1-m1 mutant which abolishes the mitochondrial form of Pif1 has not effect (Schulz VP and Zakian VA, 1994). Other proteins such as Est1, Est2, Cdc13 and the KU complex contribute to the novo telomere addition depending in the presence of telomerase. Also it has been proposed that specific phosphorylation of Pif1 inhibits the recruitment of telomerase at double-stranded DNA breaks (Makovets S and Blackburn EH, 2009).

1.5. Pif1 regulation

In 2009, Chang M et al. find that overexpression of *Saccharomyces cerevisiae* Pif1 is toxic, in a dose-dependent manner. This Pif1 toxicity is tied to the DNA damage accumulation in genes involved in DNA replication and the DNA damage response demonstrating that its activity must be regulated (Chang M et al., 2009). Also it has been reported that DNA damage activates a serie of kinases such as Rad53 in yeast, leading to cell cycle arrest and DNA repair (Branzei D and Foiani M, 2009). The same year Makovets and Blackburn hypothesized that Pif1 would be regulated in response to DNA damage (Makovets S and Blackburn EH, 2009). Different treatments, such as phleomycin (intercalating DNA causing breaks), hydroxyurea (causing stopping of

replication forks) or induction of a non-repairable breakage, cause phosphorylation of the ScPif1 protein on the threonine 763 and serine 766 residues (C-terminal domain) depending on the MEC1-RAD53 DNA damage signalling pathway. The Pif1 phosphorylation induces inhibition of telomerase specifically at DSBs (Makovets S and Blackburn EH, 2009). Recently it has been shown that Rad53 also phosphorylates both, ScPif1 and Rrm3 in response to replication fork stalling in the N-terminal domain. This phosphorylation causes ScPif1 and Rrm3 inhibition, prevents fork reversal and genome instability (Rossi SE et al., 2015).

2. Bacteroides spp

My work has consisted in studying molecular mechanisms of Pif1 in prokaryotes and particularly in *Bacteroides sp 3_1_23*. *Bacteroides sp 3_1_23* belongs to the bacteria family and more specifically to genus Bacteroides (Oliver WW and Wherry WB, 1921; Roy TE and Kelly CD, 1939) and fragilis family. Bacteroides are gram negative, presenting a cell envelope composed of a thin peptidoglycan cell wall sandwiched between an inner cytoplasmic cell membrane and a bacterial outer membrane. They are anaerobic bacteria, since they are killed by normal atmospheric concentration of oxygen (20,95% O₂). They use fermentation and anaerobic respiration to produce energy. Anaerobic respiration differs from aerobic respiration by electron transport chain; they use alternative electron acceptors as sulphate, nitrate, iron, manganese, mercury and carbon monoxide. Bacteroides do not present endospores, a dormant, tough and non-reproductive structure permitting the bacterium to resist in harsh conditions. Finally they present a bacilli form and may be motile or no motile depending on the species. Their DNA base composition is 40-48% GC (Johnson JL, 1978; Holdeman LV et al., 1986; Shaheduzzaman SM et al., 1997). Bacteroides are found in the gastrointestinal tract more precisely in the colon as members of the endogenous flora. They contribute to immunity and digestive metabolism leading to polysaccharide breakdown or nitrogen cycling. But Bacteroides also present disadvantageous roles by rapid deconjugation of bile acids or the production of mutagenic compounds (Macy JM, 1984; Salyers AA, 1984). The low presence of Bacteroides is linked with obesity (Ley RE et al., 2005; Ley RE et al., 2006; Turnbaugh PJ et al., 2006). They also permit the development of gut-associated lymphoid tissues (GALT) (Rhee KJ et al., 2004), they produce polysaccharides that activate the T-cell dependent immune response (Mazmanian SK and Kasper DL, 2006; Mazmanian SK et al., 2005) and they can affect positively the

expression of Paneth cell proteins that protect the stem cells of epithelium (Ganz T, 2000). But some *Bacteroides* species also are pathogens and resistant to several antibiotics like. The most studied *Bacteroides* pathogen is *Bacteroides fragilis*, being an important opportunistic pathogen causing anaerobic infections (intra-abdominal sepsis principally and perforated and gangrenous appendicitis) and the associated mortality is higher than 19% (Finegold M and George WL 1989; Goldstein EJ, 1996).

2.1. Biochemical characterization of BsPif1

In the literature Pif1 has been characterised in *Bacteroides sp 3_I_23*. BsPif1 can hydrolyse all types of nucleotides triphosphates (NTP) and deoxynucleotide triphosphates (dNTP) without significant preference except for GTP or dGTP, which led to 50–60% of helicase activity. The structural basis for this promiscuity is the missing selectivity filter for the adenine base, which is replaced by M10 in BsPif1. The biological advantage of non-selective nucleotide base binding over, a selective one should be that in the situation of ATP depletion in a cell, helicases can continue to use other types of nucleotides to ensure their function (Liu NN et al., 2015; Chen WF et al., 2016). In the case of its eukaryotic homolog, ScPif1 has a preference for adenosine nucleotides (ATP and dATP) as an energy source (Lahaye A et al., 1993). For unwinding, hPIF1 and BsPIF1 have a preference for partial duplexes in contrast to ScPIF1, which unwinds more efficiently forked than partial duplex (Ramanagoudr-Bhojappa R et al., 2013). This preference for a substrate could be determinate by the oligomerization state. It has been shown that the forked DNA substrate enforces dimerization of ScPif1 (Barranco-Medina S and Galletto R, 2010). BsPif1 has only a monomeric form, whereas ScPif1 is dimeric in the presence of DNA but not in solution (Liu NN et al., 2015; Barranco-Medina S and Galletto R, 2010). In the presence of hybrids, BsPif1 has a higher unwinding activity for DNA/DNA duplexes than RNA/DNA hybrids, especially on the resolution of the R-loops. This preference for DNA/DNA is expected because *Bacteroides sp. 3_I_23*, have circular genomes and thus no telomere. But this capacity of resolution of R-loops is necessary for maintaining genome integrity (Liu NN et al., 2015; Aguilera A and Garcia-Muse TR, 2012). On the contrary ScPIF1 prefers the RNA/DNA hybrids to DNA/DNA duplexes, this phenomenon was interpreted like the capacity of ScPif1 mediated telomerase disruption to form telomere (Boule JB and Zakian VA, 2007). BsPif1 has more difficulties to unwind G4 DNA than partial duplex DNA like hPif1 (Liu NN et al., 2015; Sanders CM,

2010). ScPIF1 resolves the G4 more effectively than the canonical double helix and other non-B form DNA secondary structures (Paeschke K et al., 2013; Duan XL et al., 2015). In conclusion BsPif1 resembles more to human Pif1 than to *Saccharomyces* Pif1 in the choice of substrate.

2.2. BsPif1 mechanism of unwinding

The crystallization of BsPif1 in complex with a partial duplex has to propose a mechanism for DNA unwinding (Chen WF et al., 2016) (Figure 39). After nucleotide binding, the loop3 of the 2B domain suffers a closing movement, which causes its interaction with the 1B domain forming a hole where only the ssDNA can pass through. Then ATP binds to the helicase in the hydrolysis site leading to the activation of the translocase activity by a relative movement of the two RecA domains 1A and 2A. The ssDNA is moved in the 5' to 3' direction and incoming duplex is blocked by the rigid structure formed by 2B and 1B domains. The translocation force is sufficient to destabilize the incoming duplex and to trigger its unwinding. After translocation, the 2B domain may move back in the initial position for another cycle of unwinding.

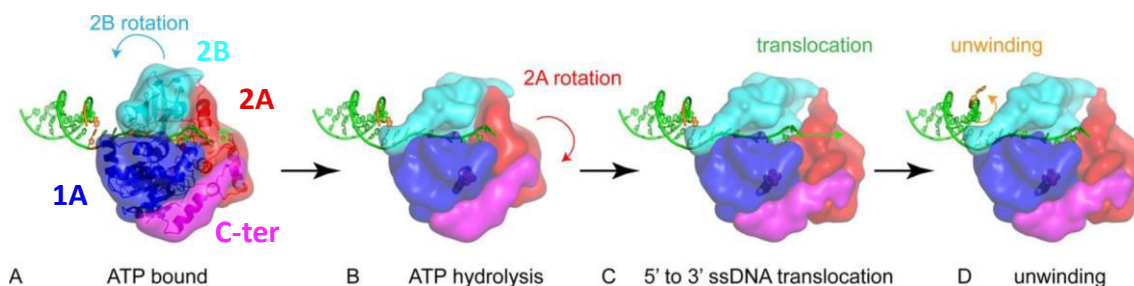


Figure 39. Unwinding mechanism of BsPif1. (A) The 2B domain is in the upper position. The ssDNA binding triggers the configuration change of the 2B domain forming a tunnel by 2B and 1B domains, where only ssDNA can pass through. (B) ATP binding and hydrolysis allows the two RecA domains 1A and 2A to act as a molecular motor to move ssDNA. But the 2B domain acts as a wedge, blocking the incoming duplex. (C and D) The translocation force is sufficient to open dsDNA on the 2B wedge. Finally the 2B domain rotates back for a new cycle. Adapted from Chen WF et al., 2016.

3. DNA structures

Deoxyribonucleic acid (DNA) carries the genetic instructions used in the growth, development, functioning and reproduction. The DNA can take different tridimensional structures depending on the sequences and experimental conditions (solvent, ionic strength, presence/absence of salt...). The most common structure of DNA is the B-helix or double helix, first described by Watson JD and Crick FH in 1953 (Watson JD and Crick FH, 1953) (Figure 40B). This structure is possible by the pairing of two anti-parallel polynucleotides strands held together by hydrogen bonds (named Watson-Crick) between bases A-T and G-C and base-stacking interactions among aromatic nucleobases by π -bonds. In some conditions the complementary nucleic acid sequences can adopt two other structures, A-helix and Z-helix. The A-helix (Figure 40A) presents slight increase in the number of base pairs (bp) per turn, resulting in a smaller twist angle and smaller rise per base pair compared with the B-helix. This A-form is preferentially adopted by RNA or DNA in a dehydrated medium (Franklin RE and Gosling RG, 1953). The Z-helix (Figure 40C) consists in a left-handed double helical structure in which the double helix winds to the left in a zig-zag pattern (Mitsui Y et al., 1970). Duplexes are not the only structure that DNA or RNA adopts. Other structures such as triplex, i-motif and G-quadruplex can be formed. A triple helix (Figure 40D) consists in the interaction of a third single strand inside the major groove of a double helix through Hoogsteen or reverse Hoogsteen bonding with the purine-rich strand (Broitman SL et al., 1987). The i-motif (Figure 40E) are characteristic of cytosine-rich sequences at acidic pH, they form four strands interacting together two by two via C⁺-C base pairs (two cytosines sharing a proton) (Gehring K et al., 1993). In 1910 the formation of a gel with a high concentration of G in aqueous solution was reported the first time by Bang. In 1962 Gellert and his colleagues elucidated the phenomenon of aggregation formed by guanylic acid using X-rays, due to stacking of four associated 5' monophosphate guanines through H bonds at their Watson-Crick and Hoogsteen sites, permitting the formation a quartet of guanines (Gellert M et al., 1962). The stacking of these G-quartets forms a non-canonical structure called G-quadruplex (G4-DNA or G4) (Figure 40F).

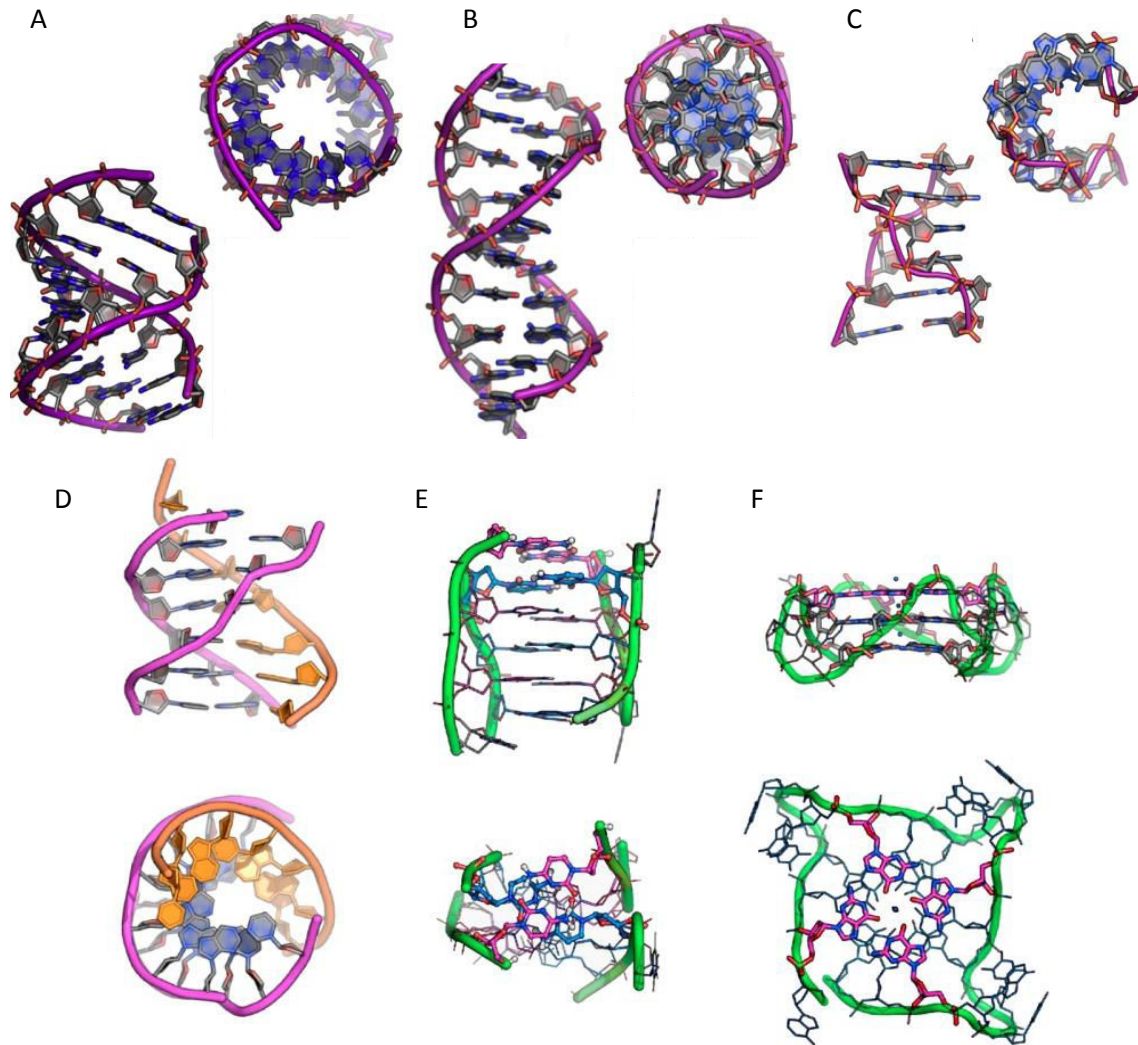


Figure 40. DNA structures. (A) A form. (B) B form. (C) Z form. (D) Triplex (E) i-motif (F) G-quadruplex. Adapted from Ho PS and Carter M, 2011.

4. G-quadruplexes

As it has been said before, the G-quadruplex (G4) consists in two or more stacked G-quartets, which are planar structures formed by the association of four guanines. The guanines are linked by two H-bonds: 1) internal: established between the oxygen of the carbonyl group in position 6 (O6) and the hydrogen of the nitrogen at position 1 (N1); 2) External: consisting in H bonds via nitrogen at position 7 (N7) and the hydrogen of the amino group at position 2. The G-quadruplex is stabilized by monovalent cations, which interact with the four oxygen atoms belonging to the carbonyl group (O6) of the four guanines during the stacking (Pinnavaia TJ et al., 1978). Also the presence of loops and the sequences between the G blocks will determine the G-quadruplex stability.

Finally, G-quadruplex present three key type interactions: H bonding, dipole interactions and π - π stacking that stabilize and determine the structural diversity of G4 between other parameters.

4.1. Structural polymorphism of G4

Different parameters have been described to explain the structural diversity of G4 mainly: the number of strands, their orientations, the loops conformation and the nature of cations.

4.1.1. Strands number

According to the number of DNA molecules involved in the formation of G4, two main categories of G4 can be described (Figure 41). They can be intermolecular including two subcategories: Tetramolecular G4 formed by the association of four strands and Bimolecular G4 formed by two strands. Intramolecular or monomolecular G4 made by one single strand containing several blocks of guanines are able to fold back and form a G4 structure.

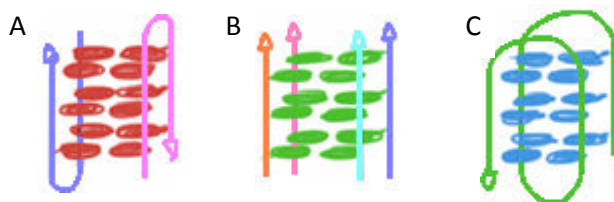


Figure 41. Schematic representation of different G4 conformations according to the DNA molecules involved. Intermolecular: (A) Bimolecular and (B) Tetramolecular. (C) Intramolecular or Monomolecular.

4.1.2. Glycosidic torsion angle

The sugar of the G (guanine) is usually in a C2'-endo/C3'-exo conformation. However, the glycosidic bond angle can adopt two different orientations: syn and anti (Figure 42). The syn conformation appears when the base and the sugar are on the same side of the glycosidic bond and the anti conformation when the base and the sugar are on opposite sides of the bond. The syn/anti conformations of guanines within a G-quartet define the groove dimension between two adjacent guanines, which can be wide, narrow or medium (Smith FW and Feigon J, 1992).

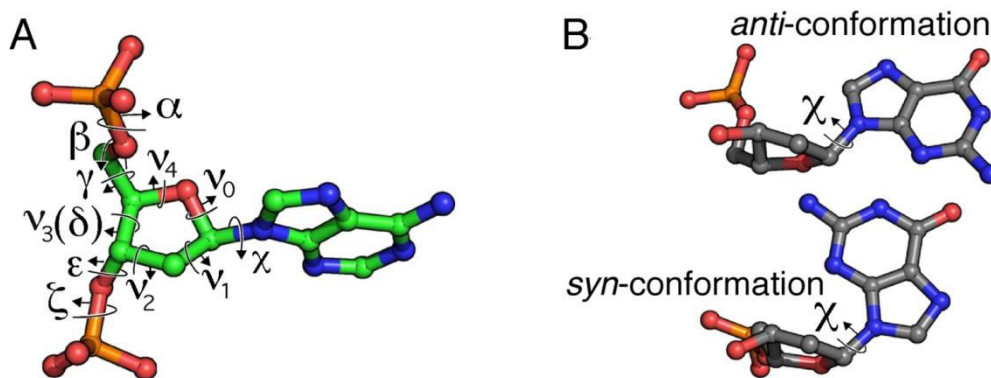


Figure 42. Torsion angles of nucleic acids. (A) Torsion angles along the backbone (α to ζ), within the sugar ring (ν_0 to ν_4), and the rotation of the nucleobase relative to the sugar (χ). (B) Rotation about the glycosidic bond defines χ -angles for the *anti*- and *syn*-conformations of the bases. Adapted from Ho PS and Carter M, 2011.

4.1.3. Strand orientation

The strand orientation is defined by the phosphate backbone directionality 5' - 3'. The G-quadruplexes are grouped in 3 categories (Figure 43): Parallel if it contains four strands oriented in the same direction. Hybrid (3+1) if three strands are oriented in the same direction and the fourth in the opposite one. Antiparallel if the strands have opposite direction two by two.

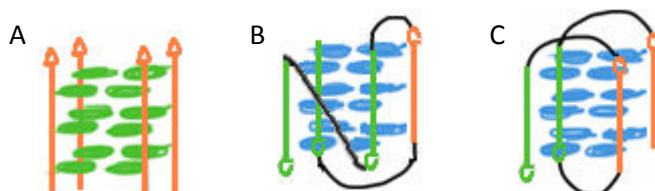


Figure 43. Schematic representation of different G4 conformations according to strand orientation. (A) Parallel (B) Hybrid (C) Antiparallel.

4.1.4. Loop conformation

The loops are the sequences located between the blocks of guanines. In the case of tetramolecular G-quadruplex, all G-tracts are independent and there are not interconnection loop. However, Bimolecular and Monomolecular G-quadruplexes present 2 or 3 loops respectively. There are four types of loop conformation (Figure 44): 1) Lateral loop or edgewise, which connects two antiparallel adjacent strands, 2) Propeller or chain reversal loop, connecting two parallel adjacent strands and 3) Diagonal loop connecting antiparallel opposite strands. V-shaped or snap-back loop connects the wedges of G-quartet (Yang Q et al., 2010). Moreover loop length will also

determine G-quadruplex conformation: short loops are usually external and favour a stable parallel conformation and longer loops give rise to anti-parallel conformation with a reduced stability of G-quadruplex (Rachwal PA et al., 2007; Guedin A et al., 2010). Finally the type of the nucleotide, which forms the loops determines also the G-quadruplex stability, the adenine presence reduces remarkably the stability comparing to pyrimidines (C and T) (Guedin A et al., 2008).

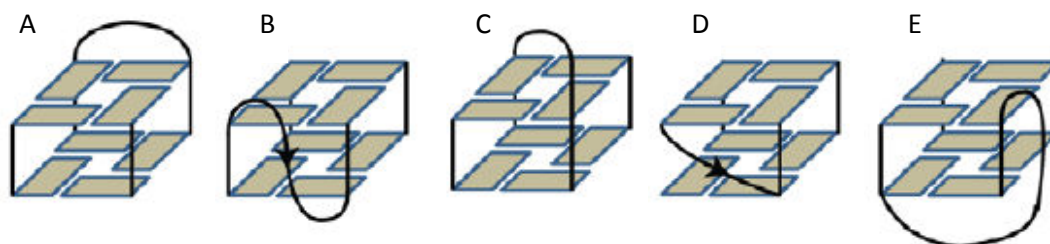


Figure 44. Schematic representation of different G4 conformations according to loop conformation. (A) Lateral loop or edgewise (B) Propeller or chain reversal loop (C) Diagonal loop (D) V-shaped (E) Snap-back loop.

4.1.5. Cation nature

G-quadruplexes are stabilized by monovalent cations, metallic cations such as K^+ principally and in a lesser extend by the presence of Na^+ (Mergny JL et al., 1998) and NH_4^+ (Wong A and Wu G, 2003). Other monovalent (Rb^+ , Cs^+ , Tl^+ , Li^+) and divalent (Sr^{2+} , Ca^{2+} and Pb^{2+}) cations can also be incorporated between G-quartets determining different G-quadruplex structures (Wong A and Wu G, 2003; Włodarczyk A et al., 2005). In the literature it has been reported that $d[AGGG(TTAGGG)]_3$ G-quadruplex exhibit conformational changes in the glycosidic bonds in the presence of K^+ and Na^+ . In the presence of Na^+ the G-quadruplex present three quartets with *syn-anti-anti-syn* conformations in each G-quartet, but in the presence of K^+ all the G residues adopt an anti conformation (Balagurumorthy P and Brahmachari SK, 1994; Gilbert DE and Feigon J, 1999; Parkinson GN et al., 2002). Also $[d(G_4T_4G_3)]_2$ has been observed in the presence of Na^+ , K^+ and NH_4^+ , and several structures were observed suggesting an influence of cation determining the G-quadruplex polymorphism (Črnugelj M et al., 2002).

4.1.6. Bulges in G-quadruplexes

Discontinuous arrangements of guanines in one column of the G-tetrad core have been observed in the sequence of Pu24 from the human c-myc promoter (Phan AT et al., 2005) and c-kit87up from the human c-kit promoter (Todd AK et al., 2007; Wei D et al., 2012), despite the presence of four G-tracts having each at least three continuous guanines (Phan AT et al., 2005; Todd AK et al., 2007; Wei D et al., 2012). These structures present the bulges, which are projections of bases from the G-quartet core connecting two non-adjacent guanines of the same strand within the G-quartet core. Phan and his collaborators have shown that many different bulges can exist in G4 structures, varying in sequence, size, position and number within the G-quadruplex (Mukundan VT and Phan AT, 2013) (Figure 45).

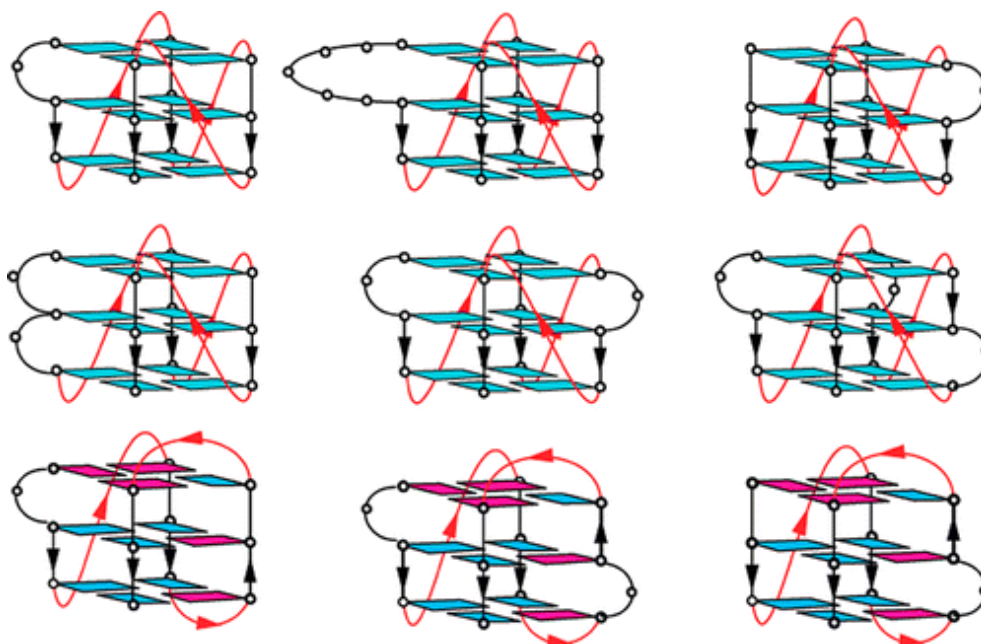


Figure 45. Schematic representation of different G4 conformations according to the presence of bulges. Different sequences have the ability to form different bulges. Adapted from Mukundan VT and Phan AT, 2013.

4.2. Regulation of G-quadruplex formation

The participation of G-quadruplexes in biology is determined by their folding and unfolding capacity. These two mechanisms are determined by chaperones and helicases, respectively. The folding kinetics of G-quadruplexes is sequence dependent and it can occur on a time scale ranging from a few milliseconds to minutes. For instances, sequences that fold fast are human telomere repeats in 60ms (Zhang AY and Balasubramanian S, 2012). But the G-quadruplex kinetics formation can be increased

by the presence of protein chaperones (Fang G and Cech TR, 1993). The most identified chaperones are in the telomeres, such as the *S. cerevisiae* telomere double strand binding protein Rap1 (Rhodes D and Giraldo R, 1995), the regulatory subunit of yeast telomerase Est1 (Li QJ et al., 2013) and the human telomere binding protein TRF2 implicated in DNA and RNA G-quadruplex binding (Biffi G et al., 2012). Other proteins have also the capacity to bind G-quadruplexes and to stabilize them like in human. One can cite the DNA mismatch recognizing factor MutS α promoting synapsis of transcriptionally activated immunoglobulin switch regions (Larson ED et al., 2005), and others as nucleophosmin (NPM1), which interacts with several G-quadruplex regions in ribosomal DNA implicated in ribosome maturation and export (Chiarella S et al., 2013), or nucleolin (NCL), which is an essential nucleolar phosphoprotein that binds DNA G-quadruplexes with high affinity (Dempsey LA et al., 1999).

To unfold the G-quadruplexes, some specific helicases are put into play, and their loss-of-function is linked to various cancers and genetic disorders. These specific G-quadruplex helicases play important roles in DNA replication and telomere maintenance (Brosh RM Jr, 2013). The human helicases WRN (Werner syndrome), BLM (Bloom syndrome) and *S. cerevisiae* Sgs1 are involved in telomere maintenance by their G-quadruplex unwinding capacity (Lipps HJ and Rhodes D, 2009). Mutations in WRN cause the Werner syndrome and mutations in BLM the Blooms syndrome, that gives rise to premature aging (adult progeria) and increased risk of cancer, respectively. Also the FANCD1 helicase, the orthologous of the *C. Elegans* DOG-1 helicase is essential for G-quadruplexes unwinding and its loss of function is associated with the Fanconi anaemia (London TB et al., 2008). As said before Pif1 presents a strong G-quadruplex unwinding activity and its loss of function gives a high DNA double strands breaks presence (Ribeyre C et al., 2009; Paeschke K et al., 2011; Paeschke K et al., 2013). But it has been reported that in the absence of G-quadruplex helicases, a number of nucleases act to process G-quadruplexes, leading to G-tract deletions, such as FEN1, EXO1 and DNA2 in human (Vallur AC and Maizels N, 2008). EXO1 and FEN1 play a role in DNA replication and are involved in telomere maintenance (Saharia A et al., 2008; León-Ortiz AM et al., 2014). In addition, the single-strand binding replication protein RPA that is also involved in telomere maintenance has been shown to facilitate G-quadruplex unfolding by shifting the equilibrium from a folded to an unfolded state (Safa L et al., 2014). RNA G-quadruplexes can also be unwound by the RHAU helicase (Lattmann S et al., 2010; Giri B et al., 2011). The knockdown of RHAU cause impaired

telomerase assembly and changes in telomere length (Booy EP et al., 2012). These examples provide evidence that there are proteins that directly regulate G-quadruplexes resolution or removal to prevent replication fork stalling and DNA breakage, and RNA folding.

4.3. G-quadruplexes in vivo

Since the first description of G-quadruplexes in vitro, the key question was if these structures occur in vivo and what is their function. Firstly by bioinformatic studies the G-quadruplexes were searched in the human genome (Huppert JL and Balasubramanian S, 2005; Todd AK et al., 2005). These identified regions are called Putative Quadruplex Sequences (PQS) (Huppert JL and Balasubramanian S, 2005; Huppert JL, 2008). The reference sequence is $G_3N_{1-7}G_3N_{1-7}G_3N_{1-7}G_3N_{1-7}$, where G represents the guanine tracts and N the loop regions that are made of any nucleotide. The G tracts were restricted in 3 and the loops to 1-7 nucleotides. This pattern gave 360 000 motifs in human (Huppert JL and Balasubramanian S, 2005), 27 motifs in *Saccharomyces cerevisiae* (Piazza A et al., 2015). In *Bacteroides sp 3_1_23* I could find 2 motifs determined by the reference sequence $G_3N_{1-7}G_3N_{1-7}G_3N_{1-7}G_3N_{1-7}$ research in the *Bacteroides sp 3_1_23* genome. But G-quadruplexes can show longer loops made of more than seven nucleotides (Dai J et al., 2006; Balkwill GD et al., 2009; Amrane S et al., 2012). Recently, it has been observed that G-quadruplexes can be formed by $4n-1$ guanines: one G tract can be shorter by one guanine, the G-quadruplex will contain two G-tetrads and one $n-1$ G-quartets a G-triad (Heddi B et al., 2015). This G-triad was observed in the structure of truncated thrombin aptamer (Cerofolini L et al., 2014) and in G-quadruplex formed by a human minisatellite sequence (Adrian M et al., 2014). Because G-quadruplex sequences are not archetypal as it seems, a new algorithm has been developed to determine G-richness and poorness of regions in the genome (Bedrat A et al., 2016) in agreement to high-resolution sequencing approach, which permitted the identification of more than 700 000 sequences forming G4 structures in human (Chambers VS et al., 2015).

The first direct evidence came from the development of a G-quadruplex structure-specific antibody to detect G-quadruplexes in *Styloynchia lemnae* macronuclei telomers (Schaffitzel C et al., 2001). Then other labs have tried to produce other antibodies to detect G-quadruplex, especially in mammalian cells. Biffi et al. have produced a specific antibody, BG4, to visualize DNA G-quadruplex structures, without any preference and any particular conformation, in human cells (Biffi G et al., 2013).

Finally, a murine monoclonal antibody, 1H6, which permits the visualization of G-quadruplexes in human and murine cells has also been developed (Henderson A et al., 2014). Moreover the DNA binding protein studies has contributed to detect G-quadruplex in vivo such as in bacteria, ciliates and human in which their unwinding and folding take place (Sundquist WI and Klug A, 1989; Paeschke K et al., 2005; Zaug AJ et al., 2005).

4.4. G-quadruplexes localization

These studies in human, yeast and bacterial genomes, have then allowed to determine the localization of such structures. Principally the G-quadruplexes are localised in non-coding regions, with a higher density in telomeres and promoters (Huppert JL et al., 2008) (Huppert JL and Balasubramanian S, 2005; Todd AK et al., 2005; Bedrat A et al., 2016; Rawal P et al., 2006; Maizels N and Gray LT, 2013) but also in coding strand determining gene transcription (Rankin S et al., 2005). G-quadruplexes localization is not random. Indeed they are present in functional regions and furthermore, are highly conserved between different species (König SL et al., 2010) by a selection pressure to retain such sequences at specific genomic regions. This high conservation is present in mammalian species and decreases in non-mammalian and lower organisms (Frees S et al., 2014). The highest abundance of G-quadruplexes is at telomeres, consisting of 5 to 10000 bp of 5'TTAGGG repeat in humans. Then in the gene promoters, at the border between introns and exons and target immunoglobulin switch regions (S regions) (Maizels N and Gray LT, 2013). Also the G-quadruplexes are present in 90% of human DNA replication origins (Cayrou C et al., 2011; Cayrou C et al., 2012; Besnard E et al., 2012). The genome instability is the hallmark in many cancers. Genome-wide analysis of DNA breakpoints in different cancer types show a significant enrichment in G-quadruplexes in the vicinity of somatic copy number alterations (SCNA) (De S and Michor F, 2011), as well as telomeres being favoured targets of persistent DNA damage response in aging (Hewitt G et al., 2012). Also G-quadruplexes have been found in the 5'-UTR regions of encoded mRNA (3000 G-quadruplex motifs in humans) having the role of translational repressors. (Bugaut A and Balasubramanian S, 2012). But they are also present in the 3'-UTR regions in mRNA, which impact in the polyadenylation (PA) process permitting mRNA maturation (Beaudoin JD and Perreault JP, 2013). TERRA (Telomere repeat-containing RNA) is a transcript of telomere DNA, which forms a G-quadruplex structure and participates in the regulation of telomerase and telomeres (Xu

Y et al., 2010). The presence of G-quadruplexes in important genomic regions suggests that they provide a regulatory role.

4.5. Fonctions of G-quadruplexes

4.5.1. Role of G-quadruplexes in promoter region

It has been possible by bioinformatic techniques to identify G-quadruplex motifs at 1kb upstream of TSS regions (Transcription Start Site) in more than 40% of human genes (Huppert JL and Balasubramanian S, 2007). These G-quadruplexes are more present in oncogene promoters and regulatory genes than in tumour suppressor promoters and housekeeping genes (Eddy J and Maizels N, 2006; Huppert JL and Balasubramanian S, 2007). This G-quadruplex enrichment in promoter regions is also found in yeast, bacteria, plants and mammals (Hershman SG et al., 2008; Capra JA et al., 2010; Rawal P et al., 2006; Mullen MA, et al., 2010; Yadav VK et al., 2008). Additionally, in humans, G-quadruplexes are less found in the template strand (particularly the 3'UTR) than in the non-template strand (Huppert JL et al., 2008). In yeast, they are present in the two strands indistinctly, but there is a correlation between nucleosome-free regions and G-quadruplexes in promoters (Capra JA et al., 2010). This observation suggests that G-quadruplexes play a role in gene expression regulation. In humans, these structures have been described in different genes including HIF1 α , BCL-2, c-MYC (De Armond R et al., 2005; Dai J et al., 2006; Simonsson T et al., 1998). G-quadruplexes have four roles in the promoters (Figure 46). 1) Their presence in the template strand causes the inhibition of the transcription, being a block factor (Figure 46A). In the case of NHEIII1 (Nuclease hypersensitive element III1), which is downstream of the MYC promoter, the presence of G-quadruplex causes transcription repression (Siddiqui-Jain A et al., 2002). 2) On the contrary the G-quadruplex presence in the non-template strand could prevent annealing to the template strand allowing accessibility of the transcription machinery (Figure 46B). In this case the G-quadruplex structures could be enhancers of the high transcription level of some genes. 3) Proteins bound to the G-quadruplex structures can have a dual role as transcriptional enhancers and repressors. Some proteins cause the unfolding of the G-quadruplexes allowing the final transcription of the template strand (Figure 46C), like some specific helicases: PIF1, WNR, BLM or 22 helicase that have this ability. 4) Other repressors work by stabilizing G-quadruplexes presents in the template strand (Figure 46D), such as TMPyP4 that binds to the G-quadruplex in

NHEIII1 reducing MYC transcription (Siddiqui-Jain A et al., 2002; Grand CL et al., 2002).

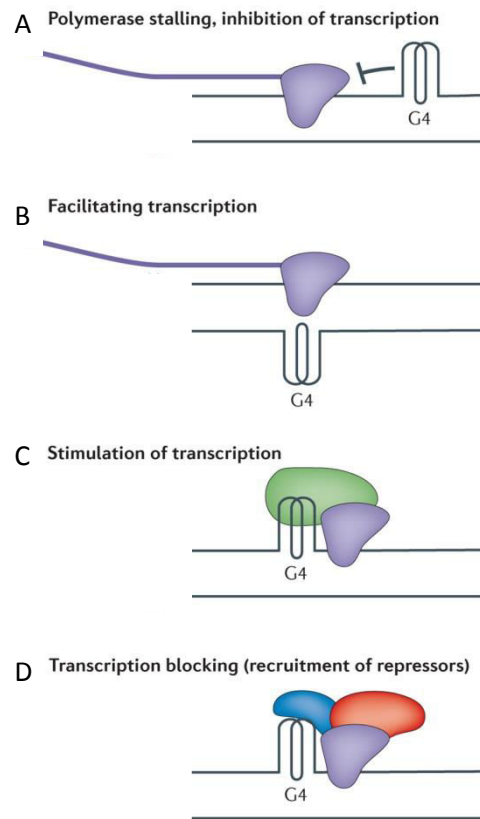


Figure 46. Functions of G4 structures during transcription in promoter regions. (A) G-quadruplexes block transcription by polymerase (purple) inhibition. (B) G-quadruplexes facilitate transcription by keeping the dsDNA unwound and allowing the transcription of the template strand. (C) G-quadruplexes stimulate transcription by recruiting proteins (green) such as helicases, which are able to unwind G-quadruplexes. (D) G-quadruplexes block transcription via the recruitment of G4 binding proteins (blue), which directly or indirectly (red) repress transcription. Adapted from Bochman ML et al., 2012.

4.5.2. Role of G-quadruplexes in DNA replication

In the replication the double stranded DNA is separated into two strands. Firstly the G-quadruplex can appear before the replication origin by slowing or stalling the replication fork machinery (Zeman MK and Cimprich KA, 2014) (Figure 47). It can also have an initiating role thanks to the recruitment of helicase specific for G-quadruplex, the strand localization of the G-quadruplex determines the precise position of the replication start site (Valton AL et al., 2014). Secondly during replication, the

leading strand is continuously duplicated but G-quadruplex structures can be formed before. Also the lagging strand's replication is opposite to the direction of the growing replication fork. For this reason the lagging strand is discontinuous and some portions are free to form secondary structures, such as G-quadruplexes, which could act as transcriptional regulators (Bochman ML et al., 2012). The absence or inactivity of these helicases prevents the unwinding of these G-quadruplexes, slowing down the DNA replication and the apparition of DSBs at many of the G-quadruplex, as in the case of Pif1 absence (Ribeyre C et al., 2009; Lopes J et al., 2011). Also the Pif1 deficient cells present a high level of G-quadruplexes mutations, which eliminate the ability of the motif to form a G-quadruplex structure. When these mutated motifs are reintroduced in the genome of a normal cell (in presence the Pif1), they do not bind Pif1, and slow down DNA replication or cause DSBs (Ribeyre C et al., 2009; Lopes J et al., 2011; Paeschke K et al., 2011).

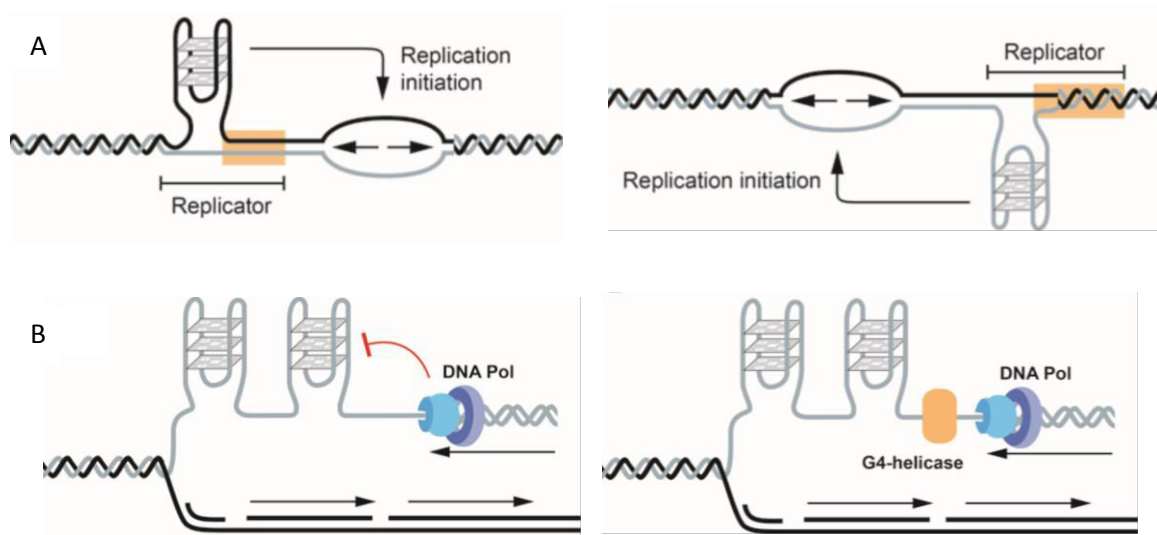


Figure 47. Functions of G4 structures during replication. (A) Origins of replication are GC-rich. G-quadruplex formation causes slowing or stalling or initiation of DNA replication, and its localization determines the site of initiation. (B) G-quadruplexes formed during replication in the leading or lagging strand when the DNA is single stranded impede replication but the presence of helicases specific for G-quadruplex unwinding allows the replication. Adapted from Rhodes D and Lipps HJ, 2015.

4.5.3. Role of G-quadruplexes in telomeres

The telomeres are constituted by DNA sequences protected by proteins at the ends of chromosomes and they are composed of a double stranded region and 3' single stranded overhang (Bochman ML et al., 2012). The principal role of telomeres is to protect the chromosome from degradation and end-to-end fusion. Usually this 3' single stranded overhang sequence consists in repetitions of G-rich motif, like (TTAGGG)_n in vertebrates (Dreesen O et al., 2005). Several studies using specific binding protein and antibodies binding have shown that this G-rich sequences are able to form G-quadruplexes in vivo (Paeschke K et al., 2005; Biffi, G et al., 2013; Chambers VS et al., 2015; Fang G and Cech TR, 1993; Giraldo R and Rhodes D, 1994; Zaug AJ et al., 2005; Wang H et al., 2011) suggesting that G-quadruplexes might act as a telomere capping structure (Figure 48). This telomere capping structure allows telomere protection from nucleases (Capra JA et al., 2010) (Figure 48A). In ciliates, they protect the telomeres by recruitment of telomere end binding protein TEBP α , which allows two telomeres fusion and attachment to a sub-nuclear structure (the nuclear matrix or scaffold) via recruitment of the telomere-end binding protein TEBP β (Paeschke K et al., 2005) (Figure 48B). The telomeres length is regulated by telomerase and influenced by G-quadruplexes structure. Intramolecular antiparallel G-quadruplexes structures block telomerase activity, whereas intermolecular parallel G-quadruplexes do not (Zahler AM et al., 1991; Oganessian L et al., 2006; Oganessian L et al., 2007). Also like in the case of transcription and replication, a variety of ligands stabilize the G-quadruplexes causing telomerase inhibition by preventing annealing of telomerase RNA to G-strand overhangs, as telomestatin (Kim MY et al., 2002; Rezler EM et al., 2005) (Figure 48C).

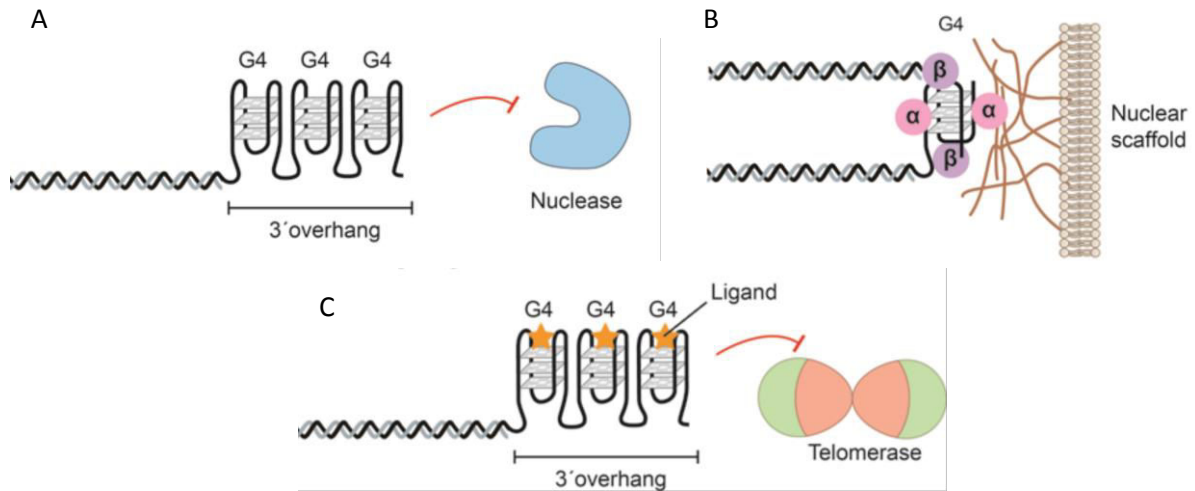


Figure 48. Functions of G4 structures at telomeres. (A) The G-rich 3' overhang can form folded G-quadruplexes that protects telomeres from nuclease degradation. (B) Ciliate telomeres form G-quadruplex structures involving two telomeres promoted by the telomere-end binding protein TEBP α and the attachment to sub-nuclear structure (the nuclear matrix or scaffold) with the recruitment of the telomere-end binding protein TEBP β . (C) Stabilizing of G-quadruplexes by G-quadruplex binding ligands blocks telomerase action. Adapted from Rhodes D and Lipps HJ, 2015.

4.6. Characterization of telomeric G-quadruplex motif and (GGGT)₄ motif

The GGGTTA motif is found in many phylogenetically distant organisms, such as vertebrates (Moyzis RK et al., 1988), several fungi (Schechtman MG, 1990) and slime mold (Forney J et al., 1987). Variants of this motif are found in many other organisms such parasites (Le Blancq et al., 1991), plants (Richards EJ and Ausubel FM, 1988), algae (Petracek ME et al., 1990), nematodes (Wicky C et al., 1996) and yeasts (Lue NF, 2010). Different studies determine that the sequence can fold into a parallel, hybrid or antiparallel G-quadruplexes depending on experimental conditions and the exact sequence (Phan AT, 2010).

In human this GGGTTA motif is present in the telomeres that comprises thousands of this tandem repeats with a 3'-end overhang of 100-200nt long (Makarov VL et al., 1997). This motif in different experimental conditions could adopt four different intramolecular G-quadruplexes forms involving three G-tetrad layers (Figure 49): 1) in Na⁺ d[A(GGGTTA)₃GGG] presents an antiparallel stranded basket form (Wang Y and Patel DJ, 1992), 2) in K⁺ d[A(GGGTTA)₃GGG] presents a parallel stranded propeller form (Parkinson GN et al., 2002), 3) in K⁺ d[TA(GGGTTA)₃GGG] presents a hybride form type 1 (Luu KN et al., 2006). 4) in K⁺ d[TA(GGGTTA)₃GGGTT] presents a hybride form type 2 (Phan AT et al., 2006). The presence of these structures in the

telomeres causes inhibition of the telomerase activity (Zahler AM et al., 1991), which is critical for the proliferation of most cancer cells (Kim NW et al., 1994).

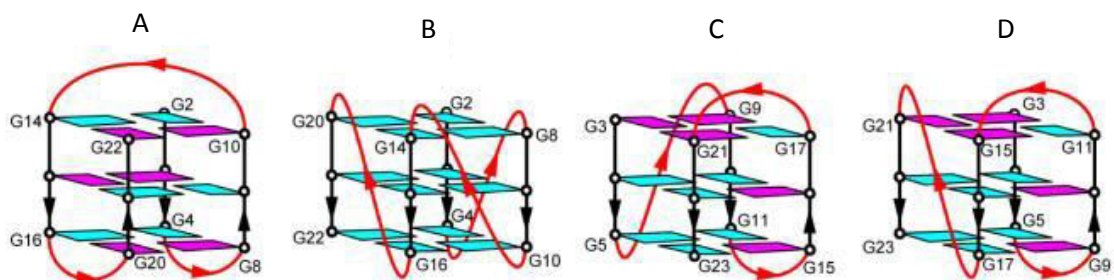


Figure 49. Schematic structures of intramolecular G-quadruplexes formed by the human telomeric sequences: (A) $d[A(GGGTTA)_3GGG]$ in Na^+ solution a basket-type form (B) $d[A(GGGTTA)_3GGG]$ in a K^+ a propeller-type form, (C) $d[TA(GGGTTA)_3GGG]$ in K^+ solution hybrid form type 1 and (D) $[TA(GGGTTA)_3GGGTT]$ in K^+ solution hybrid form type 2. The G-rich columns in are represented in black and connecting loops in red. The *anti* guanines are coloured cyan; *syn* guanines are coloured magenta. Adapted from Lim KW et al., 2009.

In the literature the structure of this human telomere $d[(GGGTTA)_3GGGT]$ sequence has been investigated and characterized (Figure 50). It is the most similar to the sequence we use in this thesis. This sequence was studied in presence of K^+ establishing a basket-type G-quadruplex fold. The G-quadruplex core consists of two tetrads, G1-G14-G20-G8 and G2-G7-G19-G15 with a glycosidic conformation of guanines of syn-syn-anti-anti in each tetrad. Each strand constituting the core has both a parallel and antiparallel adjacent strands. The loops are successively edgewise diagonal edgewise. This structure, with two G-tetrads in the core, is more stable than the intramolecular G-quadruplexes with three-G-tetrads. In terms of melting temperature the G-quadruplexes with two-G-tetrads presents a $57^\circ C$ melting temperature compared to G-quadruplexes with three-G-tetrads, which presents a lower melting temperature $47.2^\circ C$ and $53.6^\circ C$. This high stability is explained by the extensive base pairing and stacking of thymine bases (T4, T10, and T16) into the hydrophobic grooves in the loops capping both ends of the G-tetrad core (Lim KW et al., 2009).

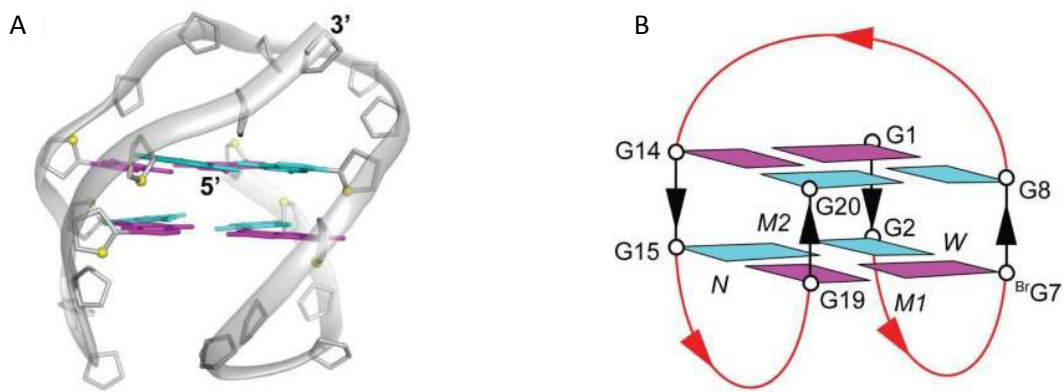


Figure 50. Structure of the human telomeric G-quadruplex d[(GGGTTA)₃GGGT]. (A) Ribbon view of a representative structure of natural d[(GGGTTA)₃GGGT]. The *anti* guanines are coloured cyan; *syn* guanines are coloured magenta. The backbone is represented in grey and the O4' atoms in yellow. (B) Schematic view of a representative structure of natural d[(GGGTTA)₃GGGT]. The G-rich columns are represented in black and connecting loops in red. The *anti* guanines are coloured cyan; *syn* guanines are coloured magenta. The letters W, M1, M2 and N represent wide, medium 1, medium 2 and narrow grooves, respectively. Adapted from Lim KW et al., 2009

The d[(GGGT)₄] motif is used as an HIV-1 integrase inhibitor, a viral enzyme responsible for the integration of viral DNA into the host-cell genome (Jing N et al., 1997; Jing NJ et al., 2000). Its variants are unusually high thermal stable. The d[(GGGT)₄] motif folds in presence of K⁺ and forms a dimeric G-quadruplex composed by the stacking of two-propeller type parallel stranded by their 5'-ends (Figure 51A). This dimeric characteristic, trained to investigate to obtain a monomeric form of this kind of G-quadruplex (Do NQ et al., 2011). It has been shown that the addition of terminal non-G residues reduces the stacking propensity of these G-quadruplexes (Wang Y and Patel DJ, 1992; Kato Y et al., 2005; Martadinata H and Phan AT, 2009). The addition of two thymine at the 5'-end of d[(GGGT)₄] motif give a monomeric form with a similar condition, a propeller-type G-quadruplex with three G-tetrad layers (Do NQ et al., 2011) (Figure 51B). The use of this monomeric form d[TT(GGGT)₄] showed the capacity of Rhau18 to bind to the 5'-end G-tetrad, projecting the first two thymine bases outward (Heddi B et al., 2015).

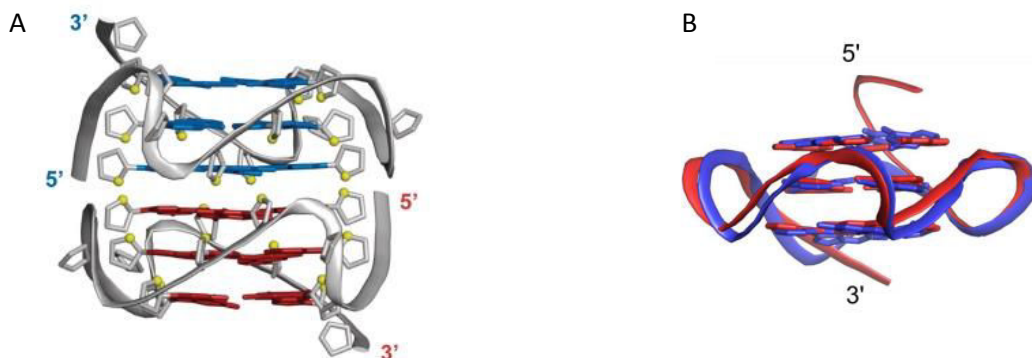


Figure 51. Structure of G-quadruplex d[(GGGT)₄] and d[TT(GGGT)₄]. (A) Ribbon view of a representative structure of the dimeric parallel-stranded G-quadruplex structure of d[(GGGT)₄] in K⁺ solution. Bases from the top monomer are colored blue while those from the bottom monomer are colored red. Backbone and sugar atoms are coloured gray, with O4' atoms in yellow. Adapted from Do NQ et al., 2011. (B) Ribbon view of d[TT(GGGT)₄]. Superposition of the free (red) and bound to Rhau18 (blue). Adapted from Heddi B et al., 2015.

Also a variant of HIV-1 integrase inhibitor named G3T d[(GGGT)₃GGG] has been investigated and was used for my thesis research. As d[(GGGT)₄] in presence of K⁺, it forms parallel G-tracts and chain-reversal single-loops and dimerise giving a melting temperature of 75°C (Rachwal PA et al., 2007; Kankia B et al., 2016). The stability of this HIV-1 integrase inhibitor variant G3T d[(GGGT)₃GGG] G-quadruplex has been tested also in presence of Sr²⁺. This ion leads to the highest thermal stability and stable dimers are formed through end-to-end stacking. But the increase in the cation concentration causes a hysteretic behaviour determined by the dimerization of the G3T through stacking and the dimerization occurs after G3T folding (Lomidze L et al., 2016).

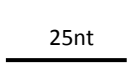
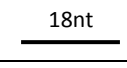
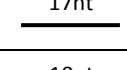




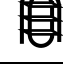

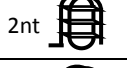
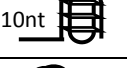
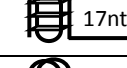
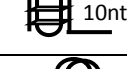
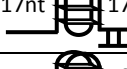
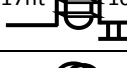
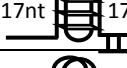
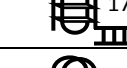

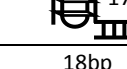
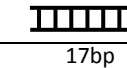
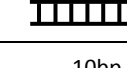
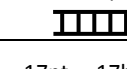
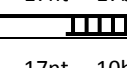
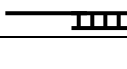
Materials and Methods

1. Protein expression and purification

BsPif1 was prepared in XG Xi laboratory in China with the following procedure. The gene encoding BsPif1 protein (Genebank number: WP_008647876.1) was amplified with genomic DNA prepared from *Bacteroides sp. 3_1_23* strain. The amplified polymerase chain reaction (PCR) products were cloned into pET15b-SUMO (Invitrogen) using ExTaq PCR (Takara) according to the manufacturer's protocol. In this system, BsPif1 was tagged with an N-terminal Sumo fusion domain preceded by a 6x-His tag. All constructs were verified using PCR screening and sequencing (Invitrogen, Shanghai). The BsPif1 expression vector was transformed into the *Escherichia coli* strain BL21(DE3) and cultures were performed at 37°C until an OD₆₀₀ of ~0.6 and then incubated overnight with 0.4 mM IPTG at 18°C. After centrifugation, the cell pellets were re-suspended in lysis buffer (20 mM Tris-HCl pH 8.0, 500 mM NaCl, 10 mM Imidazole and 10% glycerol (v/v)). The cells were sonicated and then centrifuged at 12 000 rpm for 40 min. Before loading on a Ni²⁺ charged IMAC column (GE Healthcare), the samples were filtered through a 0.45-µm filter. The protein was then eluted from the Ni²⁺ affinity column by running a 20–300 mM imidazole gradient in a 20 mM Tris-HCl buffer (pH 8.0), 500 mM NaCl and 10% glycerol (v/v). The eluted protein was incubated with Sumo protease (Invitrogen, Beijing) for 20h at 4°C and dialyzed against the lysis buffer at 4°C overnight. Then the Sumo-digested proteins were loaded on a Ni²⁺ affinity column (equilibrated in the lysis buffer) and flow through. The protein was dialyzed against buffer Q (20 mM Tris-HCl, pH 7.4, 200 mM NaCl, 1 mM EDTA, 1 mM Dithiothreitol (DTT) and 5% glycerol (v/v)), and loaded on a Source Q column (GE Healthcare). The protein was then eluted by a NaCl gradient (200–1000 mM in buffer Q). The eluted fraction containing BsPif1 was collected, concentrated and was further purified by gel filtration using a Superdex 200 10/300 GL column. The final purified protein was dialyzed against the storage buffer (20 mM Tris-HCl, pH 7.4, 350 mM NaCl, 1 mM DTT and 20% glycerol (v/v)) and was stored at –80°C.

2. DNA sequences

The following table (Table 4) presents the different DNA sequences, which were used in this work. The structures differ by the position of the G quadruplex in the sequences either preceded or followed by single/double strand DNAs. Moreover, the length as well as the nucleotide sequence are variable.

| Name | Structure | Sequence |
|-------------|---|---|
| ssDNA 25nt |  | 5'TTTTTCTTTTCTTTTCTTTTCTTT |
| ssDNA 18nt |  | 5'GCCTCGCTGCCGTCGCCA-F |
| ssDNA 17nt |  | 5'TTTTTTTTTTTTTTTTTT |
| ssDNA 10nt |  | 5'TTCCTCGGAC |
| G4TTA |  | 5'GGGTTAGGGTTAGGGTTAGGG |
| G4TTA 2 |  | 5'F-TGGGTTAGGGTTAGGGTTAGGG |
| G4T |  | 5'GGGTGGGTGGGTGGG |
| G4T 2 |  | 5'F-AGGGTGGGTGGGTGGGT |
| 17TG4T |  | 5'TTTTTTTTTTTTTTTTTTGGGTGGGTGGGTGGG |
| 2TG4T |  | 5'TTGGGTGGGTGGGTGGG |
| 10TG4TTA |  | 5'TTTTTTTTTTGGGTTAGGGTTAGGGTTAGGG-F |
| G4TD17b |  | 5'GGGTGGGTGGGTGGGATGTATGTCAAGGAAGG |
| G4TTA10T |  | 5'GGGTTAGGGTTAGGGTTAGGGTTTTTTTTT-F |
| 17TG4TD17 |  | 5'TTTTTTTTTTTTTTTTTTGGGTGGGTGGGTGGGATGTATGTCAAGGAAGG 3'TACATACAGTTCCTTCC |
| 17TG4TD10 |  | 5'TTTTTTTTTTTTTTTTTTGGGTGGGTGGGTGGGTTCCCTCGGAC 3'AAGGAGCCTG |
| 17TG4TTAD17 |  | 5'TTTTTTTTTTTTTTTTTTGGGTTAGGGTTAGGGTTAGGGATGTATGTCAAGGAAGG 3'TACATACAGTTCCTTCC |
| G4TD17 |  | 5'GGGTGGGTGGGTGGGATGTATGTCAAGGAAGG 3'TACATACAGTTCCTTCC |
| G4TD10 |  | 5'GGGTGGGTGGGTGGGTTCCCTCGGAC 3'AAGGAGCCTG |
| G4TTAD17 |  | 5'GGGTTAGGGTTAGGGTTAGGGATGTATGTCAAGGAAGG 3'TACATACAGTTCCTTCC |
| D18 |  | 5'GCCTCGCTGCCGTCGCCA-F 3'CGGAGCGACGGCAGCGGT |
| D17 |  | 5'ATGTATGTCAAGGAAGG 3'TACATACAGTTCCTTCC |
| D10 |  | 5'TTCCTCGGAC 3'AAGGAGCCTG |
| 17TD17 |  | 5' TTTTTTTTTTTTTTTTTTATGTATGTCAAGGAAGG 3'TACATACAGTTCCTTCC |
| 17TD10 |  | 5'TTTTTTTTTTTTTTTTTTCCCTCGGAC 3'AAGGAGCCTG |

3. DNA substrates preparation

The DNA oligonucleotides were synthesized by Eurogentec (Kaneka Eurogentec SA, Seraing, Belgium) on a 40 nmoles scale (see table 4 for sequences). Single Strands were dissolved in distilled water at 100 μ M. A 1mM working stock solution of G-quadruplex containing DNAs were folded by incubating at 90°C for 25 min in a buffer containing 20 mM K Phosphate and 100 mM KCl (pH 6.5), then cooled down to room temperature overnight. The various DNA substrates were then stored at -20°C.

4. ATPase activity assay

The ATPase activity of BsPif1 was measured at 37°C in a reaction mixture (40 μ l) containing 27 mM Tris-HCl (pH 7.5), 69 mM NaCl, 2.2 mM MgCl₂, 0.005 mg/ml BSA, and 2.2 mM DTT, 2 μ M DNA substrate and 150nM BsPIF1. In the presence of G-quadruplexes, K phosphate and KCl was added in a final concentration of 4mM K phosphate and 20mM KCl. The reaction was initiated by the addition of indicated amounts of [γ -³²P] ATP (Perkin Elmers, The Netherlands, 3000Ci/mmol) and stopped by transferring 35 μ l of the mixture every 20 s into 600 μ l of hydrochloric solution of ammonium molybdate (Ammonium molybdate (NH₄)₂MoO₄ 5g with HCl 10N 40ml in a final volume of 500ml saturated in water) with 6 μ l 20mM Phosphate acid. The enzymatic activity was monitored by quantification of released radioactive ³²P_i extracted, 1ml of the solution of 2-butanol–cyclohexane–acetone–hydrochloric solution of ammonium molybdate (250:250:50:0.1) saturated with water was added. The mix of the two solutions was vortexed and centrifuged at 14000 rpm for 1 min, permitting the separation of the organic phase and the aqueous phase. Finally 500 μ l of organic solution were taken-out and transferred in a new tube. The CPM value of radioactivity was counted with a Tri-Carb Counter (Perkin Elmers, Wellesley, MA, USA). The hydrolysis rate was determined by the following equation and plotted using KaleidaGraph software.

$$V/[enzyme] = \frac{(CPM \text{ sample} - CPM \text{ control}) \times 1000000}{CPM \text{ ATP} \times V \times T \times [enzyme]}$$

Where V/[enzyme] is the hydrolysis rate (μ M ATP/ min) in dependance of the enzyme concentration (μ M protein); CPM sample is the radioactive value of the sample; CPM control is the radioactive value of blank control without radioactivity; CPM ATP presents the radioactive value of 1 μ mol of ATP; V is the volume (μ l) of the reaction; T

is the reaction time (min) and [enzyme] is the concentration of enzyme (μM) used during the reaction.

5. DNA labelling

Oligonucleotides were 5'-end labelled using [γ - ^{32}P] ATP (Perkin Elmers, The Netherlands, 3000Ci/mmol) and T4 polynucleotide kinase (New England BioLabs) by incubation for 1h at 37°C. 5 μM Oligonucleotide was labelled in a 1x PNK buffer (New England BioLabs) with 2000U of T4 polynucleotide kinase (New England BioLabs) and 1.3 μM [γ - ^{32}P] ATP (Perkin Elmers, The Netherlands, 3000Ci/mmol). The 5'-end labelled oligonucleotides were purified by illustra MicroSpin G-25 columns (GE Healthcare). The columns were firstly washed once with 1xTE buffer and centrifuged at 3000 rpm for 3min at 4°C. The labelled-oligo was loaded onto the column, centrifuged at 3000 rpm for 3 min at 4°C and the flow-through solution were collected. The column was washed with 20 μL of H₂O four times and centrifuged to collect the flow-through. The CPM value of each fraction was counted and the highest CPM values fractions were pulled and stored at -20°C. The concentration of labelled-oligo was calculated with the following expression:

$$\text{C label} = \frac{C_0 \times V_0 \times (\text{CPM}_P / \text{CPM}_T)}{V_P}$$

The “C label” is the concentration of labeled oligo, C_0 is the original concentration of oligo, V_0 is the original volume of oligo before addition into reaction system; CPM_P is the total count of CPM of pooled fractions; CPM_T is the total count of CPM of all fractions; V_P is the volume of pooled oligo.

6. DNA strand annealing

Hybridization mix was composed of the labelled and unlabelled ssDNA at ratio of 1:1 (6pmol/ 6pmol) and 1X Hybridization buffer (20mM Tris HCl pH 7.4, 0.1M NaCl), incubated at 37°C for 1hour and finally stored at -20°C. In the presence of G-quadruplexes, K phosphate and KCl was added in a final concentration of 20 mM Kphosphate and 100 mM KCl.

7. Helicase assays

Helicase reactions were performed for 15 min at 30°C in 20 µl of a reaction mixture containing 30 mM Tris-HCl (pH 7.5), 100 mM NaCl, 2.4 mM MgCl₂, 2.4 mM DTT, 0.005 mg/ml BSA, 4 mM ATP and indicated amounts of BsPif1 enzyme. In the presence of G-quadruplexes K phosphate and KCl was added in a final concentration of 3 mM Kphosphate and 15 mM KCl. The reaction was initiated by adding ³²P-labeled DNA substrate at 1.5 nM final concentration into the mixture and stopped by the addition of 5 µl of the quench solution (150 mM EDTA, 2% SDS, 30% glycerol, and 0.1% bromphenol blue). Reaction products were resolved on 12% (19:1) native polyacrylamide gels run at 4°C for 2 h 30 min at 140-200V, visualized and analysed following exposure on an X-ray film at -80°C with ChemiDoc XRS (BioRad). Quantifications were performed with ImageLab (BioRad) software.

8. Annealing assays

The annealing activity reaction was performed by adding first the labelled ssDNA and then quickly the unlabelled ssDNA at ratio of 1:1 (1.5nM/ 1.5nM). ATP is not added for annealing activity and because sometimes it can inhibit the annealing activity by the helicase. The annealing reaction buffer contained 27 mM Tris-HCl (pH 7.5), 69 mM NaCl, 2.2 mM MgCl₂, 0.005 mg/ml BSA, and 2.2 mM DTT and indicated amounts of BsPif1 enzyme. Controls were performed with ATP, ATPγS (adenosine 5'-[γ-thio] triphosphate), added to a final concentration of 4 mM. The reaction system was incubated at 30°C for 30 min and then stopped by the addition of 5 µl of the quench solution (150 mM EDTA, 2% SDS, 30% glycerol, and 0.1% bromphenol blue). The helicase assays reaction products were resolved on 12% (19:1) native polyacrylamide. The gels were run at 4°C for 2h30 at 140-200V, visualized and analysed after exposure on an X-ray film at -80°C with ChemiDoc XRS (BioRad). Quantifications were performed with ImageLab (BioRad) software.

9. DNA-binding assay

DNA-binding assays were performed in XG Xi laboratory in China with the following procedure. The binding of BsPif1 to fluorescein-labeled DNA substrates was analyzed by fluorescence polarization assay using Ininite F200 instrument (TECAN). Varying amounts of protein were added to a 150 µl solution of buffer A (25 mM Tris HCl, pH7.5, 50 mM NaCl, 2mM MgCl₂ and 2mM DTT) containing 5nM fluorescein labeled

DNA. Each sample was allowed to equilibrate in solution for 5 min. After 5 min, the steady-state fluorescence anisotropy (r) was measured. A second reading was taken after 10min, in order to ensure that the mixture was well-equilibrated and stable. Less than 5% change was observed between the 5- and 10-min measurements.

Competition experiments were performed with complexes of BsPif1 (100nM) bound to fluorescein G4 or ssDNA labeled (5nM) and varying amount of non labeled indicated DNA (0-500nM).

10. Circular dichroism (CD)

The circular dichroism was used to probe G4 folding and conformation of the tested DNA oligonucleotides. Oligonucleotides previously folded were diluted to a final concentration of 5 μ M in 28.6 mM Tris-HCl (pH 7.5), 95.2 mM NaCl, 2.3 mM MgCl₂, 2.3 mM DTT, 0.47% glycerol and 3.8mM Kphosphate, 15.2mM KCl. The CD spectra were recorded on a Jobin-Yvon CD6 dichrograph using a quartz cell of 1mm path length. The temperature was set at 30°C and the spectra were recorded over a wavelength range of 230–320 nm after 15min of incubation. Acquired spectra were baseline corrected for signal contribution due to the buffer and the observed ellipticities in mdeg.

11. Electrostatic potential surface map

The electrostatic potential of solvent-accessible surface area (SASA) of BsPif1 (PDB code: 5FTE) was solved using the APBS (Adaptive Poisson-Boltzmann Solver) plugin (Baker NA et al., 2001) in PyMOL (Schrödinger LLC, 2015) software, with the ion charges of PARSE and ionic strength of 150 mM. The obtained results appear as color-coded electrostatic surfaces. The dielectric constants of the solvent and the solute were set to 80.0 and 2.0, respectively at pH= 7.

Results

1. Verification of G-quadruplex structure

Circular dichroism allows the secondary structure of proteins and DNA to be understood by the ability of a sample to absorb circularly polarized right light and circularly polarized left light. The dichroic spectrum corresponds to the difference in absorbance between these two types of light, for each wavelength. This technique can be applied to G-quadruplex to verify that the sequence is correctly folded as revealed by a typical spectrum. Principally CD spectra are empirically used to speculate on the relative orientation of the four strands constituting the G-tetrad core. Parallel-stranded are characterized by a positive peak at 260 nm and antiparallel-stranded are characterized by a positive peak at 290–295 nm. Therefore, not only informations about quadruplex structures of DNAs can be obtained but also the effects of sequence, cations, chemical modification and ligand binding on quadruplex structure can be observed and monitored. To make sure that the G-quadruplex used during my work was correctly folded and had the expected structure I performed the CD spectra of the three principal G-quadruplexes that were planned to be used (G4T, G4TTA and 17TG4T). The Figure 52 shows that G4T and 17TG4T had a parallel-stranded form with a high mDEG in the positive peak (~2mDEG) indicating their high stability. On the contrary the G4TTA presents antiparallel-stranded form with a low mDEG in the positive peak (~0.4mDEG) indicating its low stability.

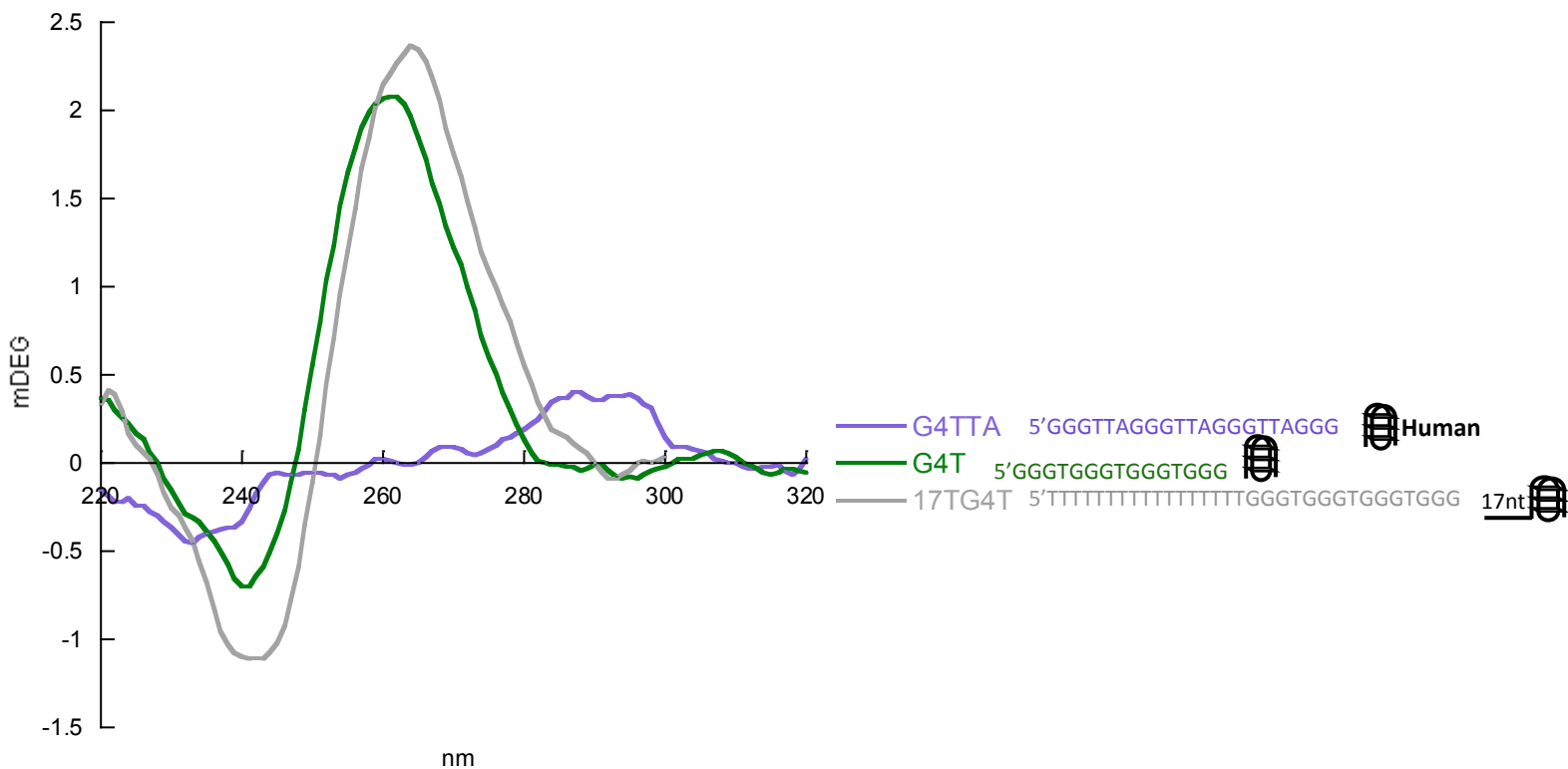


Figure 52. G-quadruplex structure by circular dichroism. CD Spectra were recorded by varying the wavelength between 220 and 320 nm with the DNA in final concentration of 5 μ M after 15min of incubation at 30 $^{\circ}$ C. In blue is represented the Human telomeric G-quadruplex (G4TTA), in red the variant HIV-1 integrase inhibitor G-quadruplex (G4T) and in green the variant HIV-1 integrase inhibitor G-quadruplex with an ssDNA tail in 5' of 17nt (17TG4T).

2. ATP hydrolysis stimulation

It has been shown that ATPase activity is required for double strand unwinding in *Saccharomyces cerevisiae* by Pif1 (Lahaye A et al., 1993; Galletto R and Tomko EJ, 2013). Previously other labs have tested G-quadruplexes ATP stimulation with a certain type of tetramolecular G-quadruplexes: these structures are all G-tracts which are constituted by four single stranded DNA being hybridized by intermolecular bonds and each strand is long enough to stimulate ATPase activity by loading into the classical SF1 ss/dsDNA binding channel (Sanders CM, 2010). Also it has been reported that ATP hydrolysis is stimulated by ScPif1 when the enzyme is bound to a parallel quadruplex linked with an ssDNA (15T) 5' tail. This ATP hydrolysis is reduced when is compared to a single-stranded DNA. However it occurs at a faster rate than G-quadruplex unfolding, indicating that some ATP hydrolysis events are non-productive (Byrd AK and Raney KD, 2015). Therefore it is not established whether the G4 structure is the only factor necessary to cooperatively stimulate ATPase activity or if it

can be in combination with ssDNA. To answer this question and investigate the substrate features necessary to stimulate ATPase activity in BsPif1. I tested 3 different types of structures: 1) 3 ssDNA, 2 dsDNA of different length and sequence and a partial duplex DNA with 5'-overhang ssDNA (ssDNA 25nt, ssDNA17nt and ssDNA10nt, D17 and D10, 17TD17 a 5's-3'ds), 2) A parallel G4-motif (G4T), a parallel G4-motif linked with 2 nucleotides at 5' end (2TG4T) and a telomere antiparallel G4-motif (G4TTA), 3) A parallel G4-motif (G4T) linked with a ssDNA at both 5' or 3' end (17TG4T a 5'sG4T and G4TD17b a G4T-3's), also with a ssDNA at 5' and duplex in 3' (17TG4TD10 a 5'sG4T-3'ds) and a dsDNA at 3' end (G4TD10 a G4T-3'ds). The ATPase activity was determined by measuring the inorganic phosphate Pi released during the hydrolysis of radioactive ATP then the velocity was calculated by using the Michaelis-Menten equation. To ensure the stability of the G-quadruplex structures, an appropriate potassium concentration was used.

The Figure 53 shows the comparison of the ATPase activities of BsPif1 in the presence of ssDNAs and the parallel G4-motif. Strikingly, 3 categories of ATPase activities are obtained in terms of amplitudes, depending on the DNA structures. 1) In the presence of ssDNA 25nt and 17nt, the ATPase activity is greatly stimulated, with Vmax values of 880.13 $\mu\text{M ATP/min}/\mu\text{M BsPif1}$; 2) In the presence of a shorter ssDNA (10nt) the ATPase activity is about half from that of ssDNA17nt and 25nt. 3) In the presence of G4T the ATPase activity is even weaker. These results taken together allow us to say that the structure and the length of the single strand of DNA (not the sequence of the ssDNA) determine the ATPase activity. Obviously 10 nucleotides are not sufficient for optimal ATPase activity.

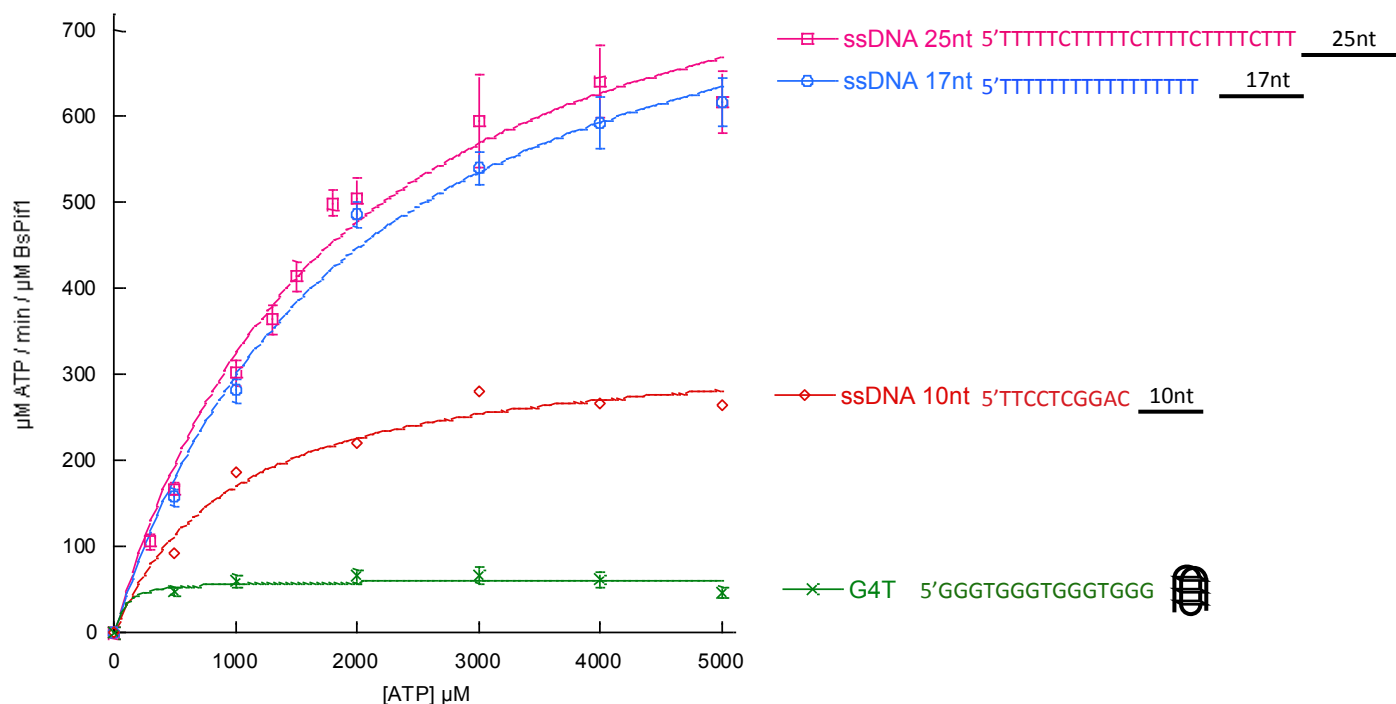


Figure 53. BsPif1 ATPase activity in the presence of ssDNA (ssDNA 25nt, ssDNA 17nt and ssDNA 10nt) and parallel G4-motif (G4T). The enzymatic assay was performed with 150nM of BsPif1, 2µM DNA, without any co-factor during 6min at 37°C. Data were obtained after subtracting the ATPase activity in the absence of DNA, and fitted to the Michaelis–Menten equation.

To test the effect of the DNA folding or strand hybridization on the BsPif1 ATPase activity, I compared the enzymatic activity with 3 different G4 (G4T, 2TG4T and G4TTA) and 2 double strand (D17 and D10) structures. Results are presented in Figure 54. Like in the precedent case three categories of ATPase activities were obtained: 1) In the presence of the ssDNA 17nt the ATPase activity was unchanged with a maximal amplitude like above. 2) In the presence of the two dsDNA and the human telomere G4-motif (G4TTA), the ATPase activity is greatly reduced. 3) In the presence of the parallel G4-motif (G4T) with or without 2nt at its 5' end (2TG4T) the ATPase activity is insignificant. These results allow us to conclude that a G-quadruplex structure affects the ATPase activity. The striking effect is observed with the parallel G4-motif (G4T). This G-quadruplex is the most stable structure because of its dimerization, which is prevented by the addition of 2nt at its 5' end (2TG4T) (Do NQ et al., 2011) without any changes of ATPase activity. In contrast the telomere antiparallel G-motif (G4TTA) is less stable and seems to stimulate the ATPase activity. More details shall be given in the discussion section.

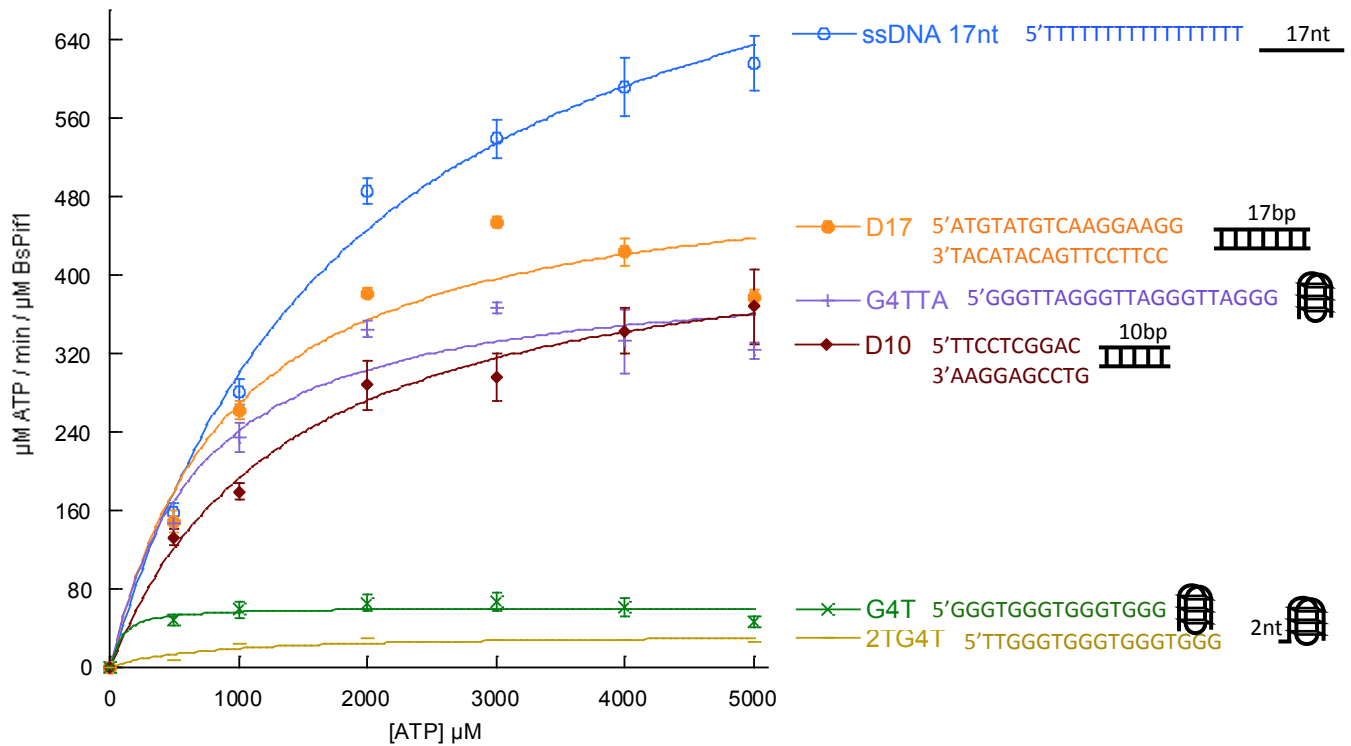


Figure 54. BsPif1 ATPase activity in the presence of ssDNA (ssDNA 17nt), dsDNA (D17 and D10) and G-quadruplexes (G4TTA, 2TG4T and G4T). The reaction was performed in 150nM of BsPif1, 2µM DNA during 6min at 37°C. Data were obtained after subtracting the ATPase activity in the absence of DNA, and fitted to the Michaelis–Menten equation.

Since only ssDNA seems to stimulate ATPase activity, we asked if the presence of a 5' or a 3' ss DNA sequence or a 3' ds DNA sequence in the parallel G-quadruplex (G4T) could affect its activity. The Figure 55 reveals that full BsPif1 ATPase activity is recovered when the parallel G4-motif and stable G4 (G4T) bears a ssDNA sequence at the 5' end (17TG4T a 5'sG4T) reaching equal amplitudes to those of ssDNA. Also the presence of a duplex in the 3' of the ssDNA and the G-quadruplex with 5' ssDNA tail didn't affect the amplitude, giving a high ATPase activity rate (17TD10 a 5's-3'ds and 17TG4TD10 a 5'sG4T-3'ds). On the other hand, the presence of either an ssDNA (G4TD17b a G4T-3's) or dsDNA (G4TD10 a 5'sG4T-3'ds) sequence at the 3' end of the G4 does not allow this full recovery of activity. However, ATPase activity of G4 motif bearing a dsDNA at it 3' end is higher than that of the G4 only motif (G4T) and reaches equal amplitude to that of a dsDNA of the same length.

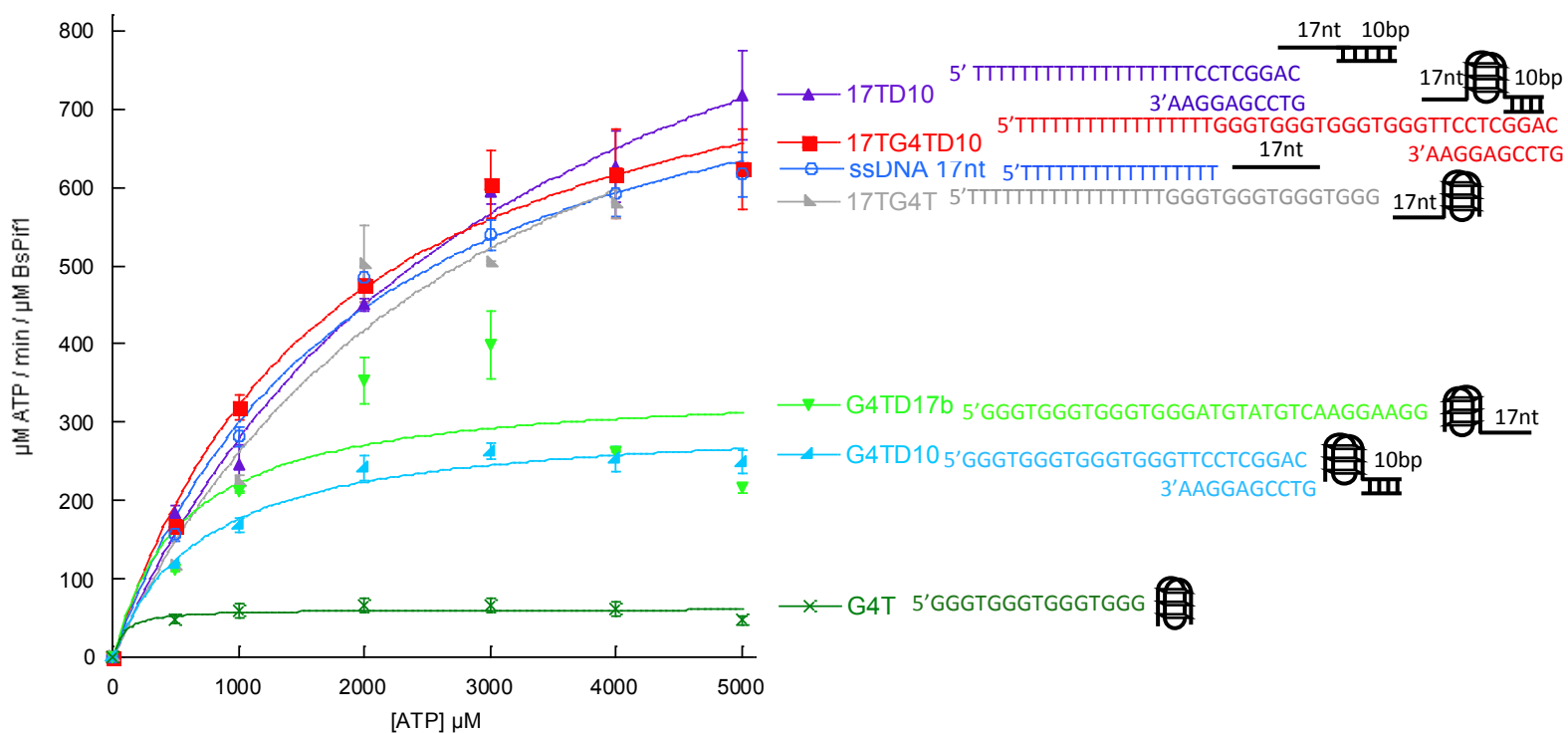


Figure 55. BsPif1 ATPase activity. In the presence of ssDNA (ssDNA 17nt), a partial duplex DNA with 5'-overhang ssDNA (17TD10 a 5's-3'ds), G-quadruplex linked with a ssDNA in 5' or 3' (17TG4T a 5'sG4T and G4TD17b a G4T-3's), G-quadruplex linked with a ssDNA in 5' and a duplex in 3' (17TG4TD10 a 5'sG4T-3'ds), G-quadruplex linked with a dsDNA in 3' (G4TD10 a G4T-3'ds) and G-quadruplex (G4T). The reaction was performed in 150nM of BsPif1, 2µM DNA during 6min at 37°C. Data were obtained after subtracting the ATPase activity in the absence of DNA, and fitted to the Michaelis–Menten equation.

Taken together, these results demonstrate that ssDNA is an essential factor to stimulate BsPif1 ATP hydrolysis. The stimulation of ATPase activity by an isolated and stable G4 motif is fairly weak.

3. Determination of distinct binding sites for ssDNA and G4 motif

The precedent observations that only ssDNA stimulate ATPase activity and not the G4-motif may suggest that BsPif1 possesses two kinds of DNA binding sites: one specific to ssDNA being the main stimulating ATPase activity and an other one which is G4-specific but fails to stimulate ATPase activity. To confirm this conjecture, two competition experiments were performed. Firstly after saturation of BsPif1 with the ssDNA (ssDNA 17nt) the parallel G4-motif lonely (G4T) was added up to three times

the concentration of ssDNA. If parallel G4-motif competitively binds the same site as ssDNA the ATPase activity will be affected causing a fall of ATPase activity. Secondly the reverse experiment was carried out: BsPif1 was bound with a high concentration of parallel G4-motif lonely (G4T), then ssDNA (ssDNA 17nt) was gradually increased to three times the concentration of G-quadruplex. In this experimental case if the G4-motif competes with the ssDNA, it is expected that ssDNA stimulation does not affect ATPase activity, which will be close to zero when G4 motif bind. The results are shown in Figure 56. Indeed, the G4-motif cannot counteract ssDNA stimulation ATPase activity whereas ATPase activity of BsPif1 was gradually increased with ssDNA concentration.

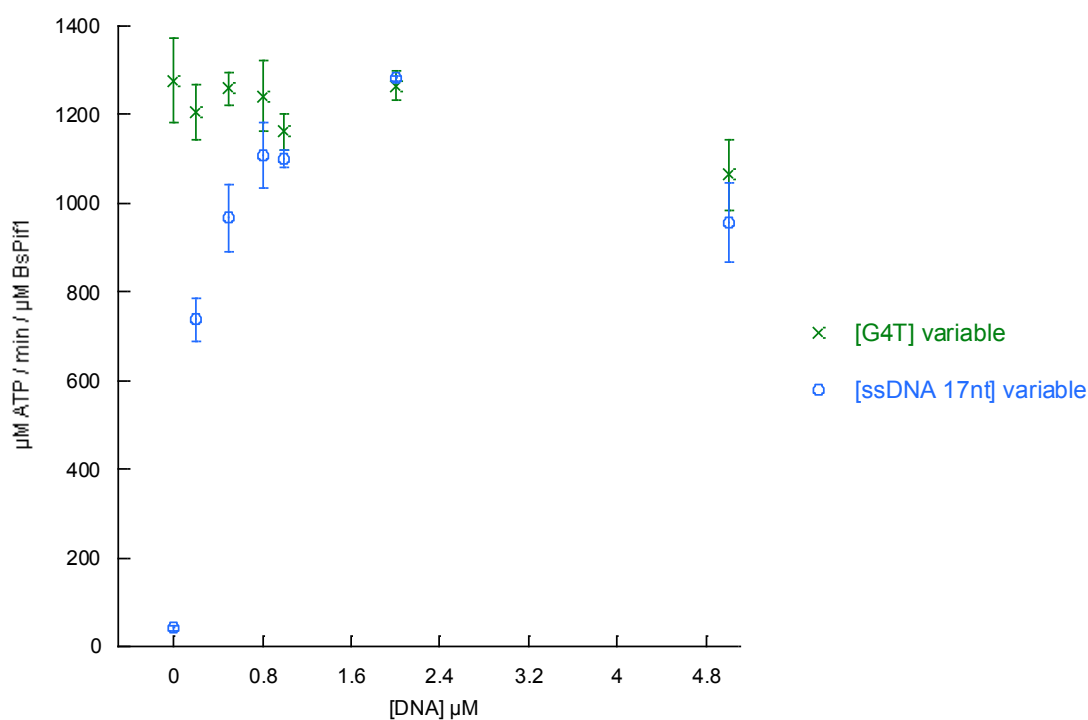


Figure 56. BsPif1 ATPase activity competition. The green crosses represent the ATPase activity when 2µM ssDNA (ssDNA 17nt) is saturated and parallel G4-motif (G4T) is progressively added. The blue empty circles present the ATPase activity when 2µM of parallel G4-motif (G4T) is saturated and ssDNA (ssDNA 17nt) is progressively added. The reaction was performed with 150nM of BsPif1 during 6min at 37°C.

These results clearly show that there is no competition between the two different types of DNA, which trigger two different ATPase activities. At this point, it is not clear whether this difference results from different affinities of DNAs towards BsPif1 or

these phenomena reflect BsPif1 intrinsic properties of ATPase activity stimulated by the different DNA structures. To answer the question, the Xuguang Xi's lab in China performed a DNA binding assay by fluorescence anisotropy. The experiments permitted to assess the equilibrium binding properties of the BsPif1 with six similar substrates used for ATPase assay (ssDNA 18nt, D18, G4T 2, G4TTA 2, 10TG4TTA and G4TTAT10). These DNA substrates were labelled with a fluorescein group at their 3' or 5' ends and BsPif1 concentration-dependent changes in fluorescence anisotropy were measured. Interestingly, BsPif1 binds the five substrates (ssDNA 18nt, G4T 2, G4TTA 2, 10TG4TTA and G4TTAT10) with a similar apparent dissociation constant $K_d \sim 25\text{nM}$ (Figure 57A). However, the binding affinity for dsDNA (D18) was reduced as revealed by $K_d \sim 200\text{nM}$ (Figure 57A). To finally confirm that BsPif1 possesses distinct binding sites for G-quadruplex and ssDNA respectively, they performed binding competitive experiments by fluorescence anisotropy. BsPif1 was firstly bound with a fluorescein-labelled G4-motif (G4TTA 2) (Figure 57B) or ssDNA (ssDNA 18nt) (Figure 57C), and then the binding fractions were determined with increasing concentration of no-labelled ssDNA (ssDNA 18nt) (Figure 57B) or G4-motif (G4TTA 2) (Figure 57C). Figure 57 B and C shows that the fluorescein-labelled G4-motif or ssDNA binding with BsPif1 were not influenced by the addition of non-labelled DNA, confirming the first hypothesis. Both ssDNA and G4 bind to BsPif1 with similar binding affinity, but at distinct sites.

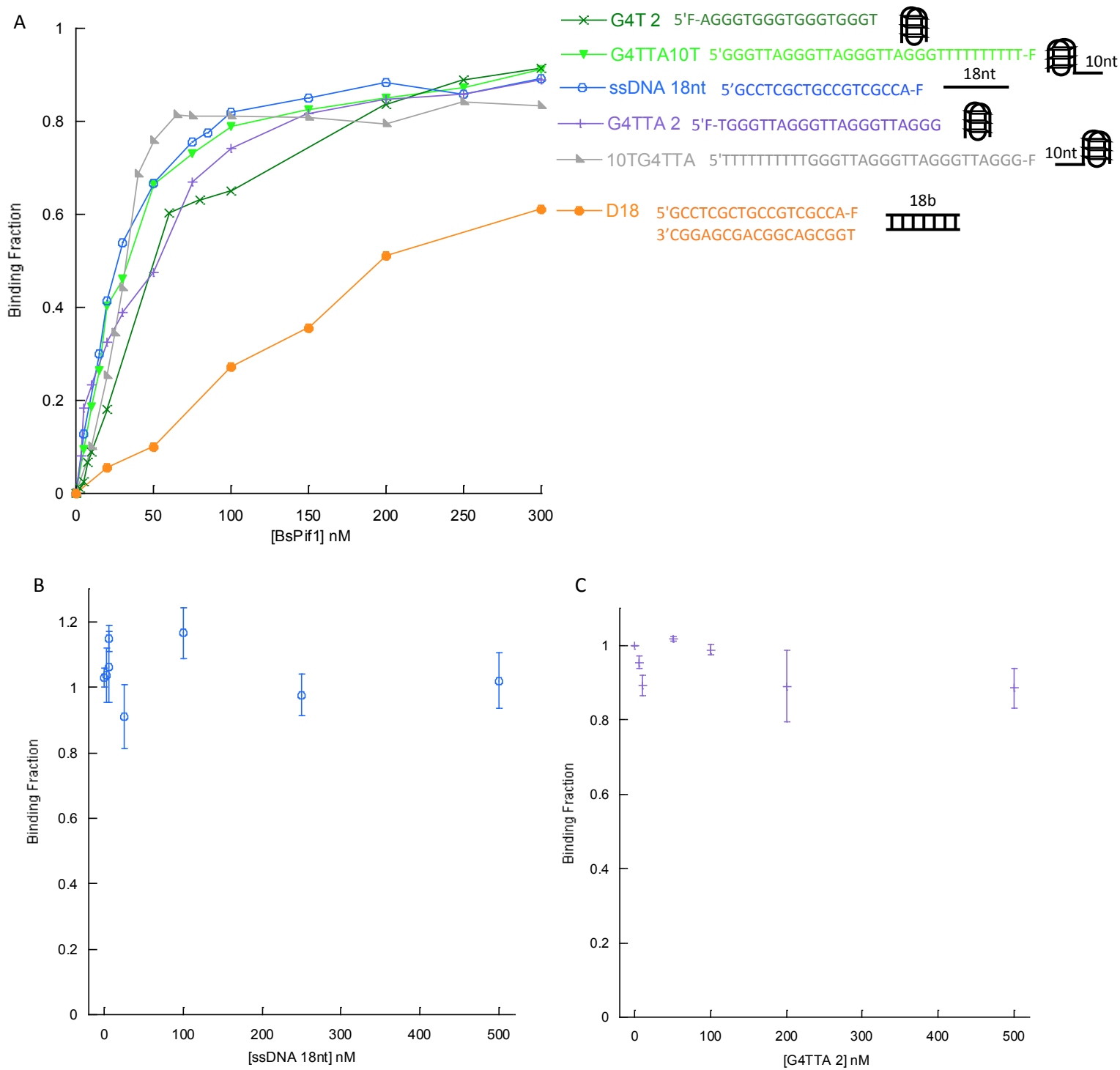


Figure 57. DNA binding assay of BsPif1 by fluorescence anisotropy. (A) Binding curves in presence of different DNA substrates: ssDNA 18nt, D18, G4T 2, G4TTA 2, 10TG4TTA and G4TTAT10. The reaction was performed 2 or 3 times in different BsPif1 concentrations and 5nM of DNA. (B) Binding competition with BsPif1 (100nM) bound with a fluorescein-labelled G4-motif (G4TTA 2) (5nM) and increasing concentration of no-labelled ssDNA (ssDNA 18nt) (0-500nM). (C) Binding competition with BsPif1 (100nM) bound with a fluorescein-labelled ssDNA (ssDNA 18nt) (5nM) and increasing concentration of no-labelled G4-motif (G4TTA 2) (0-500nM).

4. Potential G4 bindings sites

The verification that isolated G-quadruplexes (G4T and G4TTA) bind BsPif1 and the absence of competition with ssDNA led us to think that G-quadruplex and ssDNA have different binding sites on the protein. Their accurate determination requires more extensive investigations. But I have attempted rapid determination of this possible G4 binding site by electrostatic potential surface map. This was performed with the crystallized BsPif1 structure in complex with ssDNA and ADP-AIF3 (PDB code: 5FTE; Chen WF et al., 2016) by Adaptive Poisson-Boltzmann Solver (APBS) plugin in PyMOL. A similar study was also undertaken on ScPif1p in complex with an 8T3G4 (5'TTTTTTTTGGGTGGGTGGGTGGGT) by SAXS experiments, and determination of electrostatic potential surface (Lu KY et al., 2017). It appeared that the G4 DNA, which is principally an electronegative structure (Lane AN et al., 2008), potentially interacts into the positively charged pliers in its positive residues (Lu KY et al., 2017). Also a NMR study of RHAU18 helicase with G4 DNA (5'TTGGGTGGGTGGGTGGGT) determined the interaction between three positively charged amino acids and negatively charged phosphate groups of the G-quadruplex (Heddi B et al., 2015).

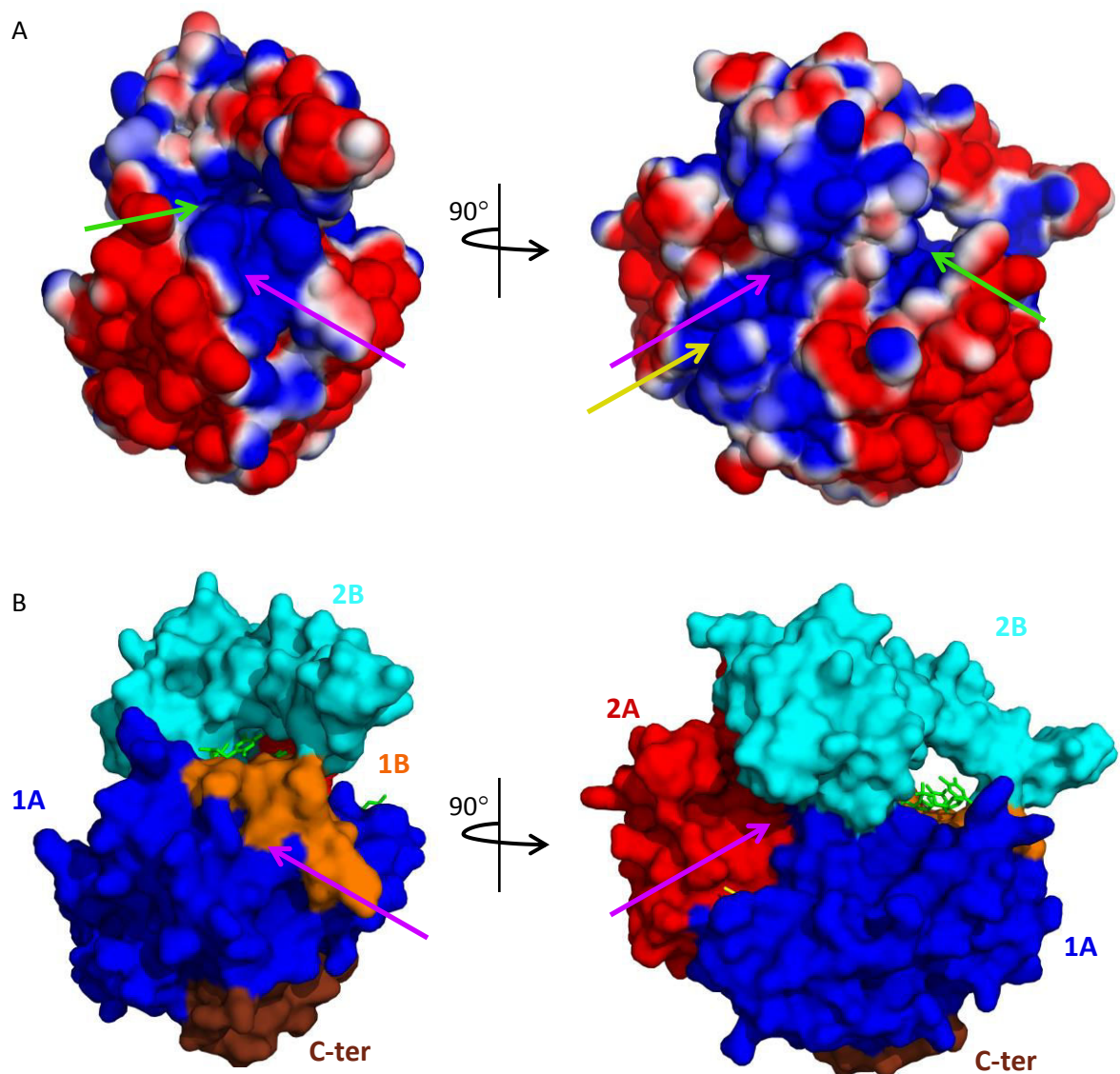


Figure 58. Potential G-quadruplex binding site of the crystal structure of BsPif1 (PDB code: 5FTE) in presence of ssDNA (6nt) and ADP-AIF3. (A) Molecular electrostatic potential distribution on solvent-accessible surface of BsPif1 generated in PyMOL with the positively charged regions in blue and negatively charged regions in red, $\pm 1\text{kT}/e$. The positively charged patch being the possible binding regions of G-quadruplex are indicated with a pink arrow. The binding site of ssDNA is indicated with a green arrow and the ADP-AIF3 binding site with a yellow arrow. (B) Van der Waals surface model of the different domains compositions of BsPif1. The domains of the helicase core: 1A in dark blue; 1B in orange; 2A in red and 2B in cyan and the domain C-terminal in brown. The co-crystallized ssDNA molecule is shown in green and the ADP-AIF3 in yellow. The possible binding regions of G-quadruplex are indicated with a pink arrow.

The electrostatic surface potential of BsPif1 has several positively polarized regions that could function as DNA-binding sites (Figure 58). One is a cluster of positively charged residues that surround the ssDNA between the domains 1A, 1B, 2A, 2B and the second is a positively charged pocket between the domains 1A and 2A where ADP-AIF3 is disposed. Two positive charged regions are preferentially adapted for host G-quadruplex. One between the domains 1A and 1B, but this region does not form a deep pocket where the G-quadruplex can be inserted and protected from external conditions. The second area is localized between the domains 1A, 2A and 2B. This latter seems to be the most possible one because it forms a clear pocket where the molecule could be inserted and trapped allowing possible interactions with different protein residues.

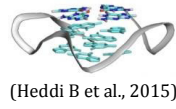
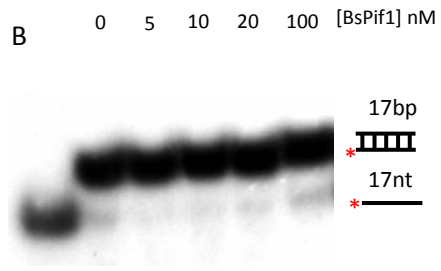
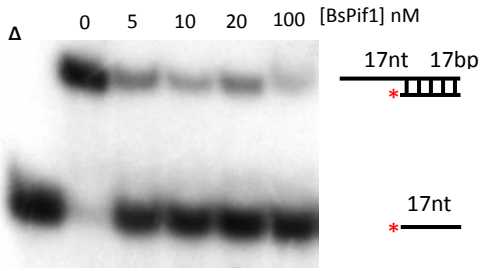
5. ATP hydrolysis is required for G4 unfolding

Different works have shown that G4 resolving helicases require ATP hydrolysis to unfold G-quadruplexes. Among these helicases, one can cite FANCD1 (Wu Y et al., 2008) and WRN (Fry M and Loeb LA, 1999). But the mechanism by which G4 resolving helicases unfold these structures appears more complicated. Indeed, other observations with apparent contradictory results question whether G4 unfolding is driven by ATP hydrolysis. By using single molecular assays Budhathoki JB et al, reported that BLM unfolds G-quadruplexes in an ATP-independent manner when high protein concentration are preincubated for a long period of time (Budhathoki JB et al., 2014). However Xi's lab observed that ATP hydrolysis is necessary for BLM to resolve G4 structures (Wu WQ et al., 2015). Other contradictory observations were obtained in the case of the RHAU helicase. Tippana R et al, show by smFRET that human RHAU unfold G4 in an ATP-independent manner (Tippana R et al., 2016). But You H et al, show with a different technique (magnetic tweezers) that ATP hydrolysis is necessary to the Drosophila RHAU which is homolog to the human enzyme (You H et al., 2017). Studies on hPif1 and ScPif1 have demonstrated that ATP binding and ATP hydrolysis is absolutely required for unfolding G4 structure (Sanders CM, 2010; Duan XL et al., 2015). To clarify whether ATP hydrolysis is necessary or not for G4-motif unfolding, a comparison of BsPif1 unwinding activity in the presence of four different DNAs structures was performed. They differ as observed above by their ability to stimulate BsPif1 ATPase activity: a partial duplex DNA with 5'-overhang ssDNA (17TD10 a 5's-3'ds), the parallel G4-motif linked with a ssDNA and a dsDNA at 5' and 3' ends respectively (17TG4TD10 a 5'sG4T-3'ds) and the parallel G4-motif linked with

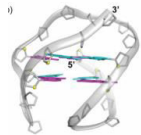
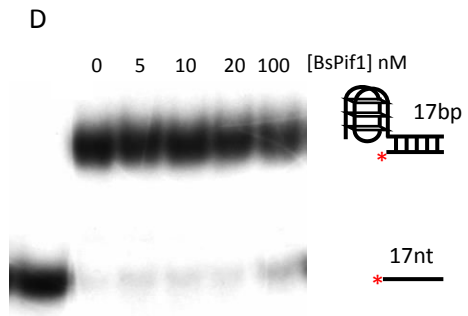
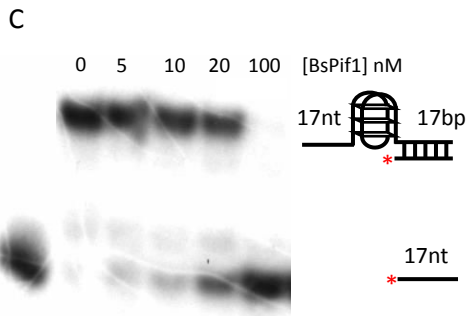
a ssDNA at 5' (17TG4T a 5'sG4T) which efficiently hydrolyse ATP; dsDNA (D17 and D10) and the parallel G4-motif linked with a dsDNA at its 3'-end (G4TD10 a G4-3'ds), which poorly hydrolyse ATP. In the case of the parallel G4-motif (G4T) ATPase activity is poorly stimulated whereas telomere antiparallel G4-motif (G4TTA) triggers a higher but not maximal ATPase activity. The capacity of BsPif1 for unwinding was monitored by the helicase test, which consists in labelling one of the two strands of the DNA duplex with radioactive ATP and observing the gel migration shift when the duplex is unwound by the helicase. Then the percentage of unwound DNA was estimated by ImageLab (BioRad) software allowing the optical density quantification of each bands observed on the gel. In the present case, background was subtracted and the unwound percentage was determined by the total signal obtained in the lane, considering the spontaneous unwinding.

The Figure 59 presents the unwinding efficiency of BsPif1 in the presence of the different aforesaid structures. When BsPif1 is as low as 10nM, it quickly drives the unwinding of duplex DNA with 5' overhang (17TD17 a 5's-3'ds) (Figure 59A) leading to about 75% of unwound DNA (Figure 59G). The parallel G4-motif with a 5' overhang and a 3'ds (17TG4TD17 a 5'sG4T-3'ds) was almost completely unwound by 100nM of the protein (Figure 59C and 59G). However, the duplex DNA (D17) and the parallel G4-motif with a duplex in 3' (G4TD17 a G4T-3'ds) cannot be efficiently unwound below 100nM protein (Figure 59B and 59D). At this concentration, only 6% and 11% of each DNA respectively is resolved (Figure 59G). Only a slight unwinding was observed by 800nM protein, suggesting that the ssDNA-stimulated ATPase activity is essential for the duplex DNA and G4-3'ds unwinding (G4TD17 a G4T-3'ds). But the G4-motif type seems to influence the BsPif1 concentration necessary for its unwinding. As mentioned above the parallel G4-motif with a 5' overhang and a 3'ds (17TG4TD17 a 5'sG4T-3'ds) which is stable needs 40nM of BsPif1 for a 50% G4-motif unwound (Figure 59G), on the other hand the telomere antiparallel G4 motif with a 5' overhang and a 3'ds (17TG4TTAD17 a 5'sG4TTA-3'ds) will need only 6nM of BsPif1 for a 50% G4-motif unwound (Figure 59G). But the parallel G4-motif linked at the 3' duplex without a 5' overhang (17TG4TD17 a 5'sG4T-3'ds) cannot be efficiently unwound below 100nM protein (as mentioned above) (Figure 59D). It is important to notice that telomere antiparallel G4-motif linked with a duplex in the 3' (G4TTAD17 a G4TTA-3'ds) was totally unwound in 100nM of BsPif1 (Figure 59F), suggesting that this difference of unwinding between the two G4-motifs is determined by its stability.

ATGTATGTCAAGGAAGG
TACATACAGTTCCTTCC



GGGTGGGTGGTGG



GGGTTAGGGTTAGGGTTAGG Human

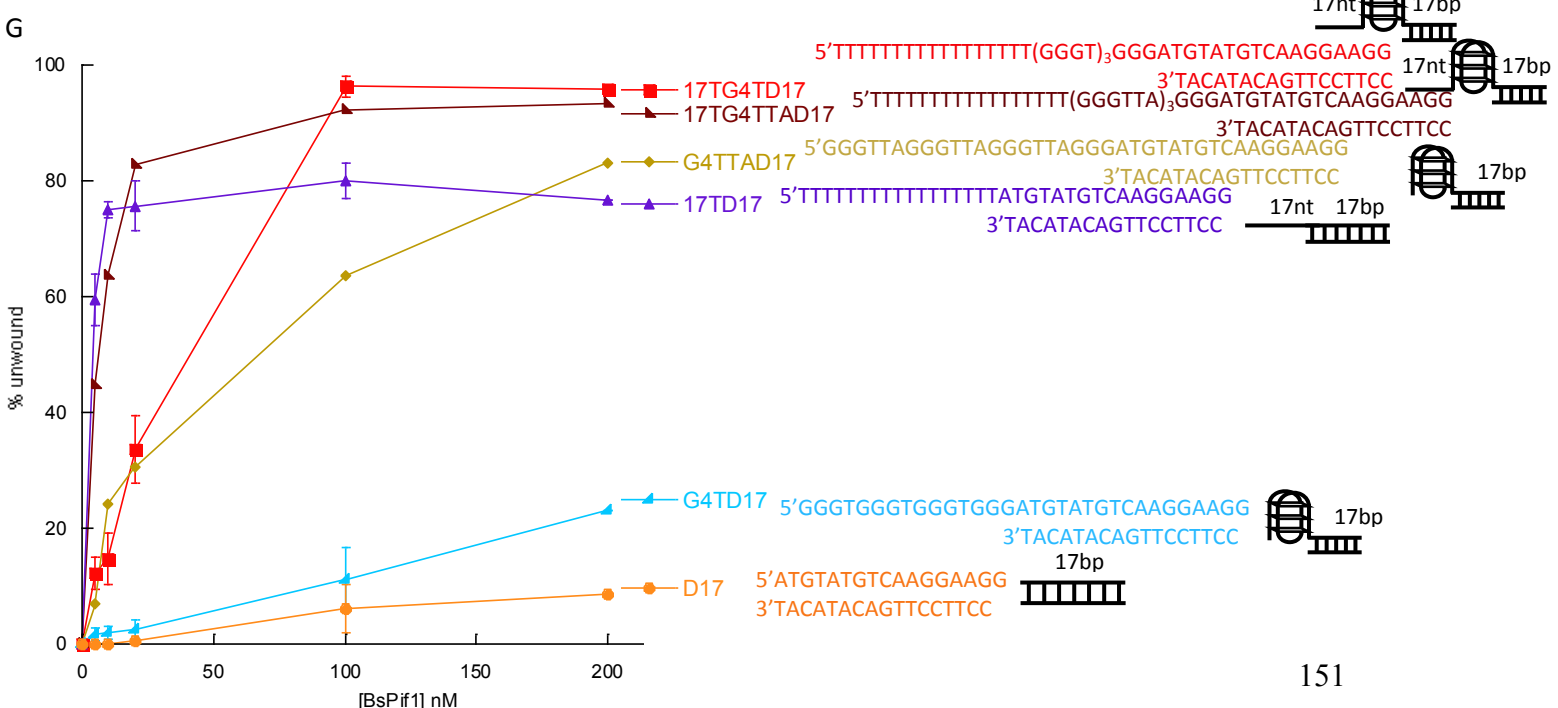
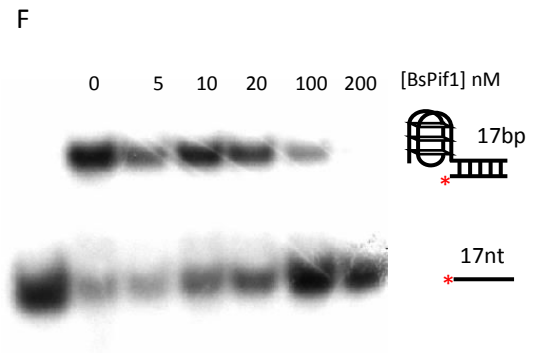
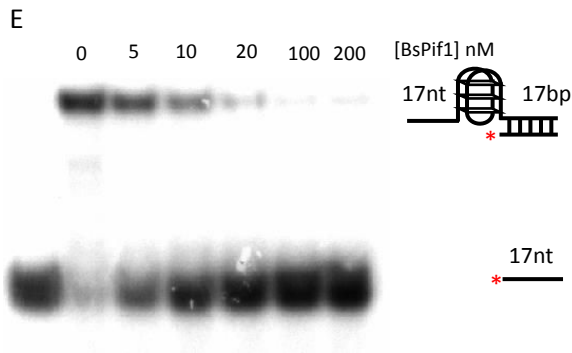


Figure 59. Unwinding characteristics of BsPif1 helicase using various DNA substrates. DNA unwinding assays were processed 2 or 3 times in the presence of 4mM ATP, 1.5nM of DNAs (with a 5'-32P-labelled (*) D17a) and different concentrations of BsPif1 after 15 min incubation at 30°C. (A) a duplex 5' overhang (17TD17 a 5's-3'ds), (B) duplex DNA substrate (D17), (C) parallel G4-motif with a duplex in 3' and a ssDNA in 5' (17TG4TD17 a 5'sG4T-3'ds), (D) a parallel G4-motif with a duplex in 3' (G4TD17 a G4T-3'ds), (E) telomere antiparallel G4-motif with a duplex in 3' and a ssDNA in 5' (17TG4TTAD17 a 5'sG4TTA-3'ds), (F) telomere antiparallel G4-motif with a duplex in 3' (G4TTAD17 a G4TTA-3'ds), (G) DNA unwinding kinetics graph.

6. BsPif1 does not catalyse dsDNA annealing

To better characterize the BsPif1 activities, and after showing that the protein doesn't have the capacity to unwind dsDNA and stable G4 structures, I investigated if BsPif1 has the ability to rewind DNA. Indeed, in the literature it has been reported that an increasing number of helicases have the capacity to anneal complementary strands of oligonucleotides in the presence of ATP such as HARP and AH2 (Yusufzai T and Kadonaga JT, 2008; Yusufzai T and Kadonaga JT, 2010) or in the absence of ATP such as RecQ family (Vindigni A and Hickson ID, 2009), Dna2 (Masuda-Sasa T et al., 2012) TWINKLE (Sen D et al., 2012) and UvsW (Nelson SW and Benkovic SJ, 2007). This annealing capacity is used to stabilize stalled replication forks, double-strand break (DSB) repair, to regulate telomere metabolism, chromatin remodelling and transcription (Wu Y, 2012). Human Pif1 and *Saccharomyces cerevisiae* Pif1 (Gu Y et al., 2008; George T et al., 2009) are some of them since they are involved in telomere metabolism by strand-annealing activity, as well as WRN, DNA2, RECQL4 (Opresko PL et al., 2004; Opresko PL et al., 2005; Masuda-Sasa T et al., 2006; Ghosh AK et al., 2012). This Pif1 annealing activity is supposed to be required to stabilize structure such as a T-loop in single-stranded telomere overhang (Ramanagoudr-Bhojappa R et al., 2014). To test whether BsPif1 has strand-annealing property, two complementary single stranded oligonucleotides (oligos D17a and D17b at 1,5nM / 1,5nM each and one of them is labelled with [γ - 32P] ATP) were incubated during 30 min at 30°C with a series of BsPif1 concentrations (Figure 60). The experiment could be performed only once but has to be reproduced with other conditions. The products were analysed on 12% (19:1) native polyacrylamide gels. If strand annealing occurred, a duplex strand would be

formed. In the absence of ATP one can observe that a spontaneous hybridization of the oligonucleotides occurs. Addition of BsPif1 in increasing concentration (0 to 200nM) to the oligonucleotide mix seems to prevent spontaneous hybridization as seen by the increasing signal of single strand on the gel. Addition of ATP to the reaction occurring in the presence of high BsPif1 concentration (200nM) does not induce annealing. In the presence of dsDNA previously hybridized and with ATP or ATP γ S, no unwinding occurs. Therefore we can verify that the presence of the single strands does not result in the unwinding activity of BsPif1 on spontaneously hybridized DNA duplex in the presence of ATP. Therefore BsPif1 does not have the ability to rewind DNA, further experiments have to be performed to establish a reliable result.

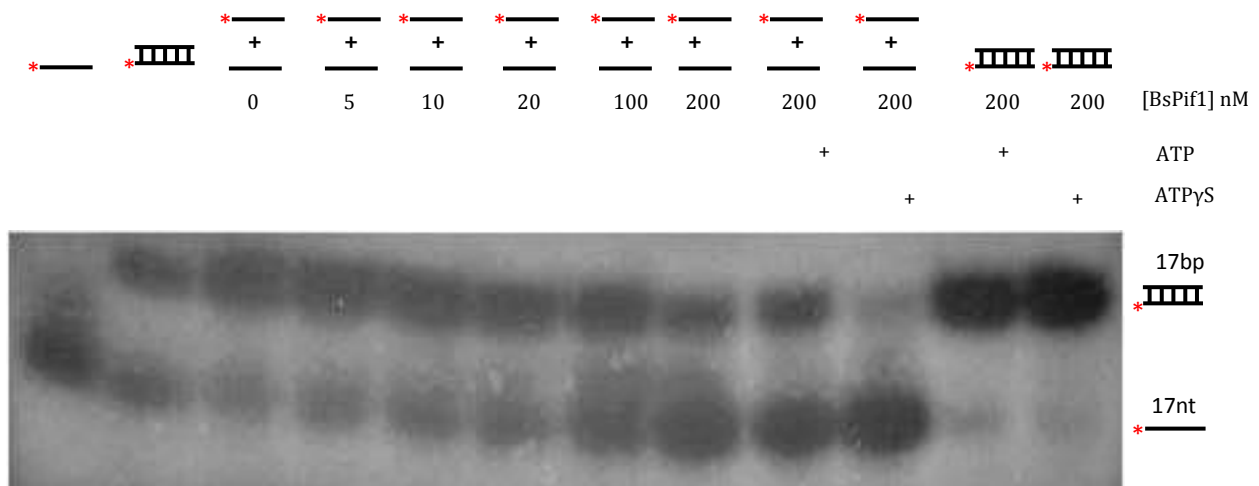


Figure 60. BsPif1 does not have annealing activity. Annealing of the 5'-32P-labelled (*) D17a (1,5nM) and D17b ssDNA (1,5nM) substrates by BsPif1 was performed once. Control annealing was performed with hybridized D17. Reactions were performed with the indicated protein concentrations for 30 min at 30°C and ATP or ATP γ S was added when cited in the Figure. The reaction products were separated by 12% (19:1) native polyacrylamide and visualized on X-ray film.

Discussion-Conclusion

Many works have been focused on the understanding of DNA duplex unwinding by different helicases such as Pif1 leading to establish that it occurs stepwise, 1 base pair per step movement coupled to the hydrolysis of one ATP molecule (Ramanagoudr-Bhojappa R et al., 2013; Zhou R et al., 2014; Duan XL et al., 2015; Zhou X et al., 2016; Chen WF et al., 2016). DNA G-quadruplexes are radically different from canonical DNA. The presence of several G quartets generates a specific conformation characterized by special electro-physical properties, maintained by Hoogsteen pairing and monovalent cations. These structures display particular roles in DNA replication, transcription and telomere maintenance (Brosh RM Jr, 2013). As a consequence, only few helicases can unfold these structures (Pif1 and DNA2 in the SF1 family, FANCI, DDX11, RTEL1, BLM, WRN and DHX9 in the SF2 family, SV40T-ag in the SF3 family, Twinkle in the SF4 family and RHAU for the SF5 family) (Mendoza O et al., 2016). This non-canonical structure makes very challenging to elucidate the molecular mechanisms underlying G4 unwinding. Recent papers have started investigations on G-quadruplex unfolding by ScPif1 giving different numbers of base step process of unwinding such as three steps (Zhou R et al., 2014) or two steps (Hou XM et al., 2015). But how this stepwise mechanism might contribute to G-quadruplex unfolding and how ATP hydrolysis drives G4 resolving remains to be clarified. The purpose of this study was to contribute to answer these questions and the prokaryotic Pif1 of *Bacteroides sp 3_1_23* has been chosen because its structure was previously well described (Chen W et al., 2016).

The first step of my work consisted in comparing BsPif1 ATPase activities stimulated by different DNA structures and particularly the effect of G-quadruplexes. The results showed that only ssDNA efficiently fires ATP hydrolysis but this activity is proportional to the ssDNA length. A similar result was observed with human Pif1, which requires a minimum of 10 bases for an efficient binding of the enzyme (Gu Y et al., 2013). When the DNA structure is more complex and especially in the case of strand/base pairing this activity is strongly decreased as shown by dsDNA. In the case of G-quadruplex, its structure and conformation determines the ATPase activity. Other groups have tested in the past two types of G-quadruplexes: a tetramolecular G-quadruplex (Sanders CM, 2010) and an intramolecular parallel G-quadruplex (Byrd AK

and Raney KD, 2015). In this work I tested two G-quadruplexes and by circular dichroism I could observe their difference of stability: 1) a monomeric G4 (G4T) with a parallel conformation appeared as a very stable structure and 2) an antiparallel G-quadruplex (G4TTA) more unstable since it was characterized by a low mDEG close to the value expected for a single strand DNA (0mDEG). The G4 stable (G4T) structure leads to negligible ATP hydrolysis. When the stability of the G-quadruplex structure is weaker (G4TTA), ATP hydrolysis is partially recovered (about 50%). On the other hand, when an ssDNA is present at 5' end of the G-quadruplexes (G4T) and does not affect the G4 folding as seen by Circular dichroism a high ATP hydrolysis rate is restored, comparable to the case of ssDNA. The need of a tail in 5' end of the G-quadruplex for ATPase activity was also reported by Sanders CM with human Pif1 (Sanders CM, 2010). Moreover, in the case of ScPif1 the unfolding of different G-quadruplexes is made possible by a periodic patrolling mechanism in the presence of a tail in 5' end (Zhou R et al., 2014; Hou XM et al., 2015). These results show clearly that G-quadruplex is a constraint in ATP hydrolysis. By combination of ATPase and DNA binding assays, and competitive experiments between ssDNA and G-quadruplex, it has demonstrated that ssDNA and G4 DNA bind at distinct separate sites with similar binding affinity (nM). G-quadruplex binding experiment rules out the possibility that inefficient stimulation of ATP hydrolysis by G-quadruplex motif is not due to inefficient G-quadruplex binding. The performance of an electrostatic potential surface map of the BsPif1 structure permitted to determine two positive charged regions preferentially adapted for host the G-quadruplex, but further investigation have to be done such SAXS to discriminate between the two possible binding sites.

After clarifying the relationship between the binding of the G-quadruplex to the enzyme and the ATPase activity, I tried to investigate the link between unwinding and ATP hydrolysis. In the presence of the parallel and stable G-quadruplex (G4T) neither of these two activities were observed whereas the G-quadruplex with a ssDNA tail at 5' end stimulates high ATPase activity and can be unwound from a certain and high BsPif1 concentration. Moreover the fact that 10 and 100nM proteins are respectively needed for the partial duplex DNA (17TD17 a 5's-3'ds) and G-quadruplex with a ssDNA tail at 5' and a duplex in 3' (17TG4TD17 a 5'sG4T-3'ds) to be unwound at comparable level indicates that the stable G4 motif is a physical obstacle and that more energy is required to resolve G4 structure. In addition, a middle ATPase activity of the less stable G-quadruplex (G4TTA) was present, giving also an unwinding activity

(G4TTAD17 a G4TTA-3'ds) but more efficient when a 5' ssDNA tail is added (17TG4TTAD17 a 5'sG4TTA-3'ds). However the presence of this 5' tail does not improve the unwinding activity, which is similar to the activity of the partial duplex DNA (17TD17 a 5's-3'ds). Taken together these results demonstrate that BsPif1 requires a 5' ssDNA tail for efficient G4 unfolding by covalent continuity of the ribose-phosphate backbone but its stability will determine the efficiency of unfolding. As tested with other G-quadruplex helicases the addition of G-quadruplex stabilization compounds gave unwinding inhibition by RecQ helicases (Wu X and Maizels N, 2001; Huber MD et al., 2002).

The annealing activity of Pif1 has been studied by other groups in order to understand the contribution of this activity to G-quadruplex unfolding and reduce genomic stability. It has been observed that Pif1 can form T-loops in the single-stranded telomere sequences or can melt G-quadruplex during replication by annealing of the complementary strand prior to refolding of the G-quadruplex structure (Gu Y et al., 2008; George T et al., 2009; Ramanagoudr-Bhojappa R et al., 2014). In our experiences BsPif1 didn't present any annealing activity in the presence of two complementary ssDNA wherever in absence and presence of ATP. One can even think that Pif1 prevents spontaneous duplex formation by binding to single strand. In some helicases the annealing activity has been linked to specific domains such as in the case of BRG1 (Brahma-related gene 1, a central catalytic ATPase of the SWI/SNF chromatin-remodelling complex) and the HELLS (Lymphoid-specific helicase). These proteins are devoid of the 2HP domain that is tandem HARP domain, which endows ATP driven annealing activity (Ghosal G et al., 2011). Further investigations have to be performed to strengthen the observation made with BsPif1 and if it is related to this protein domain.

Finally on the basis of previously determined crystallographic structures and the discoveries reported previously with BsPif1 (Chen W et al., 2016) and the present work, a tentative "molecular wire stripper" model is proposed to interpret how BsPif1 use the energy derived from ATP hydrolysis to drive G4 unfolding (Figure 54). Accordingly, ssDNA was loaded into the classical ssDNA binding channel and the highly negative charged G4 was locked at 5'-DNA entry gate where 2A and 1B domains constituted a physical tunnel which allow ssDNA, but impede native structured G4 enter into the ssDNA binding channel due to the steric hindrance of G4. Upon ATP binding and hydrolysis, ssDNA translocate from 5' to 3' and force G4 to be disrupted to pass

through the channel. Certainly, this speculative model needs to be further studied with other G4-resolving helicases to probe whether this is a common mechanism shared by other type of G4-unfolding helicases.

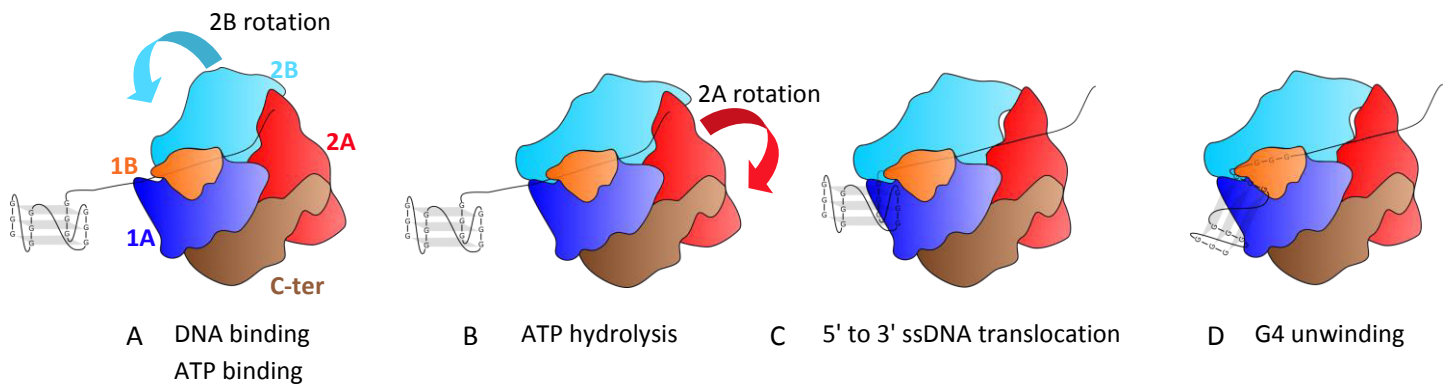


Figure 61. G-quadruplex unwinding mechanism of BsPif1. (A) The 2B domain is in the upper position. The ssDNA binding triggers the configuration change of the 2B domain forming a tunnel by 2B and 1B domains, where only ssDNA can pass through. (B) ATP hydrolysis allows the two RecA domains 1A and 2A to act as a molecular motor to move ssDNA. But the 2B domain acts as a wedge, blocking the incoming G-quadruplex. (C and D) The translocation force is sufficient to unwind the G-quadruplex.

References

- Abdel-Monem M and Hoffmann-Berling H. (1976) Enzymic unwinding of DNA. 1. Purification and characterization of a DNA-dependent ATPase from *Escherichia coli*. *Eur. J. Biochem.* 65, 431-40.
- Abdelhaleem M. (2005) RNA helicases: regulators of differentiation. *Clin. Biochem.* 38, 499-503.
- Ablasser A, Bauernfeind F, Hartmann G, Latz E, Fitzgerald KA and Hornung V. (2009) RIG-I-dependent sensing of poly(dA:dT) through the induction of an RNA polymerase III-transcribed RNA intermediate. *Nat. Immunol.* 10, 1065–1072.
- Ablasser A, Goldeck M, Cavlar T, Deimling T, Witte G, Rohl I, Hopfner KP, Ludwig J and Hornung V. (2013a) cGAS produces a 2'- 5'-linked cyclic dinucleotide second messenger that activates STING. *Nature.* 498, 380–384.
- Ablasser A, Schmid-Burgk JL, Hemmerling I, Horvath GL, Schmidt T, Latz E and Hornung V. (2013b) Cell intrinsic immunity spreads to bystander cells via the intercellular transfer of cGAMP. *Nature.* 503, 530–534.
- Adrian M, Ang DJ, Lech CJ, Heddi B, Nicolas A and Phan AT. (2014) Structure and conformational dynamics of a stacked dimeric G-quadruplex formed by the human CEB1 minisatellite. *J. Am. Chem. Soc.* 136, 6297-305.
- Aguilera A and Garcia-Muse T. (2012) R loops: from transcription byproducts to threats to genome stability. *Mol. Cell.* 46, 115–124.
- Ahnert P and Patel SS. (1997) Asymmetric interactions of hexameric bacteriophage T7 DNA helicase with the 5'- and 3'-tails of the forked DNA substrate. *J. Biol. Chem.* 272, 32267–32273.
- Alberts IL, Nadassy K and Wodak SJ. (1998) Analysis of zinc binding sites in protein crystal structures. *Protein Sci.* 7, 1700-1716.
- Altucci L, Rossin A, Raffelsberger W, Reitmair A, Chomienne C and Gronemeyer H. (2001) Retinoic acid-induced apoptosis in leukemia cells is mediated by paracrine action of tumor-selective death ligand TRAIL. *Nat. Med.* 7, 680-6.
- Alzu, A, Bermejo R, Begnis M, Lucca C, Piccini D, Carotenuto W, Saponaro M, Brambati A, Cocito A, Foiani M and Liberi, G. (2012) Senataxin Associates with Replication Forks to Protect Fork Integrity across RNA-Polymerase-II-Transcribed Genes. *Cell*, 151, 835–846.
- Amrane S, Adrian M, Heddi B, Serero A, Nicolas A, Mergny JL and Phan AT. (2012) Formation of Pearl-Necklace Monomorphic G-Quadruplexes in the Human CEB25 Minisatellite. *J. Am. Chem. Soc. USA.* 134, 5807–5816.

Andrews NW. (2005) Membrane repair and immunological danger. *EMBO Rep.* 6, 826–830.

Anchisi S, Guerra J and Garcin D. (2015) RIG-I ATPase Activity and Discrimination of Self-RNA versus Non-Self-RNA. *mBio.* 6, e02349–14.

Aratani S, Fujii R, Oishi T, Fujita H, Amano T, Ohshima T, Hagiwara M, Fukamizu A and Nakajima T. (2001) Dual roles of RNA helicase A in CREB-dependent transcription. *Mol. Cell. Biol.* 21, 4460 - 9.

Are AF, Galkin VE, Pospelova TV and Pinaev GP. (2000) The p65/RelA subunit of NF-kappaB interacts with actin-containing structures. *Exp. Cell. Res.* 256, 533-44.

Arenas JE and Abelson JN. (1997) Prp43: An RNA helicase-like factor involved in spliceosome disassembly. *Proc Natl Acad Sci U S A.* 94, 11798-11802.

Arimoto K, Takahashi H, Hishiki T, Konishi H, Fujita T and Shimotohno K. (2007) Negative regulation of the RIG-I signaling by the ubiquitin ligase RNF125. *Proc. Natl. Acad. Sci. USA.* 104, 7500-7505.

Bachrati CZ and Hickson ID. (2003) RecQ helicases: suppressors of tumorigenesis and premature aging. *Biochem. J.* 374, 577-606.

Bae SH, Bae KH, Kim JA and Seo YS. (2001) RPA governs endonuclease switching during processing of Okazaki fragments in eukaryotes. *Nature.* 412, 456-461.

Bae SH, Kim JA, Choi E, Lee KH, Kang HY, Kim HD, Kim JH, Bae KH, Cho Y, Park C and Seo YS. (2001) Tripartite structure of *Saccharomyces cerevisiae* Dna2 helicase/endonuclease. *Nucleic Acids Res.* 29, 3069-79.

Baker NA, Sept D, Joseph S, Holst MJ and McCammon, JA. (2001) Electrostatics of Nanosystems: Application to Microtubules and the Ribosome. *Proc. Natl. Acad. Sci. U. S. A.* 98, 10037–10041.

Baker TA, Funnell BE and Kornberg A. (1987) Helicase action of dnaB protein during replication from the *Escherichia coli* chromosomal origin in vitro. *J. Biol. Chem.* 262, 6877-85.

Balagurumoorthy P and Brahmachari SK. (1994) Structure and stability of human telomeric sequence. *J. Biol. Chem.* 269, 21858-69.

Balkwill GD, Garner TP, Williams HEL and Searle MS. (2009) Folding Topology of a Bimolecular DNA Quadruplex Containing a Stable Mini-hairpin Motif within the Diagonal Loop. *J. Mol. Biol.* 385, 1600–1615.

Bangert A, Andrassy M, Muller AM, Bockstahler M, Fischer A, Volz CH, Leib C, Goser S, Korkmaz-Icoz S, Zittrich S, Jungmann A, Lasitschka F, Pfitzer G, Müller OJ, Katus HA and Kaya Z. (2016) Critical role of RAGE and HMGB1 in inflammatory heart disease. *Proc. Natl. Acad. Sci. U S A.* 113, E155–E164.

- Baril M, Racine ME, Penin F and Lamarre D. (2009) MAVS dimer is a crucial signaling component of innate immunity and the target of hepatitis C virus NS3/4A protease. *J. Virol.* 83, 1299-311.
- Barranco-Medina S and Galletto R. (2010) DNA Binding Induces Dimerization of *Saccharomyces cerevisiae* Pif1. *Biochemistry.* 49, 8445–8454.
- Bartos JD, Wang W, Pike JE and Bambara RA. (2006) Mechanisms by which Bloom protein can disrupt recombination intermediates of Okazaki fragment maturation. *J. Biol. Chem.* 281, 32227-32239.
- Baum A, Sachidanandam R and Garcia-Sastre A. (2010) Preference of RIG-I for short viral RNA molecules in infected cells revealed by next-generation sequencing. *Proc. Natl. Acad. Sci. USA.* 107, 16303-8.
- Beachboard DC and Horner SM. (2016) Innate immune evasion strategies of DNA and RNA viruses. *Curr. Opin. Microbiol.* 32, 113–119.
- Beaudoin JD and Perreault JP. (2013) Exploring mRNA 3'-UTR G-quadruplexes: evidence of roles in both alternative polyadenylation and mRNA shortening. *Nucleic Acids Res.* 41, 5898–5911.
- Beckham SA, Brouwer J, Roth A, Wang D, Sadler AJ, John M, Jahn-Hofmann K, Williams BR, Wilce JA and Wilce MC. (2013) Conformational rearrangements of RIG-I receptor on formation of a multiprotein:dsRNA assembly. *Nucleic Acids Res.* 41, 3436-45.
- Bedrat A, Lacroix L and Mergny JL. (2016) Re-evaluation of G-quadruplex propensity with G4Hunter. *Nucleic Acids Res.* 44, 1746–1759.
- Bennett RJ and Keck JL. (2004) Structure and function of RecQ DNA helicases. *Crit. Rev. Biochem. Mol. Biol.* 39, 79–97.
- Bennett RJ, Keck JL and Wang JC. (1999) Binding specificity determines polarity of DNA unwinding by the Sgs1 protein of *S. cerevisiae*. *J. Mol. Biol.* 289, 235-248.
- Benoit G, Altucci L, Flexor M, Ruchaud S, Lillehaug J, Raffelsberger W, Gronemeyer H and Lanotte M. (1999) RAR-independent RXR signaling induces t(15;17) leukemia cell maturation. *EMBO J.* 18, 7011-8.
- Berke IC and Modis Y. (2012) MDA5 cooperatively forms dimers and ATP-sensitive filaments upon binding double-stranded RNA. *EMBO J.* 31, 1714–26.
- Bernard J, Weil M, Boiron M, Jacquillat C, Flandrin G and Gemon MF. (1973) Acute promyelocytic leukemia: results of treatment by daunorubicin. *Blood.* 41, 489–496.

- Bernardi R and Pandolfi PP. (2007) Structure, dynamics and functions of promyelocytic leukaemia nuclear bodies. *Nat. Rev. Mol. Cell Biol.* 8, 1006-16.
- Bernstein E, Caudy AA, Hammond SM and Hannon GJ. (2001) Role for a bidentate ribonuclease in the initiation step of RNA interference. *Nature.* 409, 363–366.
- Bernstein KA, Gangloff S and Rothstein R. (2010) The RecQ DNA helicases in DNA repair. *Annu. Rev. Genet.* 44, 393-417.
- Besch R, Poeck H, Hohenauer T, Senft D, Häcker G, Berking C, Hornung V, Endres S, Ruzicka T, Rothenfusser S and Hartmann G. (2009) Proapoptotic signaling induced by RIG-I and MDA-5 results in type I interferon-independent apoptosis in human melanoma cells. *J. Clin. Invest.* 119, 2399–2411.
- Besnard E, Babled A, Lapasset L, Milhavet O, Parrinello H, Dantec C, Marin JM and Lemaitre JM. (2012) Unraveling cell type-specific and reprogrammable human replication origin signatures associated with G-quadruplex consensus motifs. *Nat. Struct. Mol Biol.* 19, 837-44.
- Betterton MD and Julicher F. (2005) Opening of nucleic-acid double strands by helicases: active versus passive opening. *Phys. Rev. E. Stat. Nonlin. Soft Matter Phys.* 71, 011904.
- Bianco PR, Brewer LR, Corzett M, Balhorn R, Yeh Y, Kowalczykowski SC and Baskin RJ. (2001) Processive translocation and DNA unwinding by individual RecBCD enzyme molecules. *Nature.* 409, 374-8.
- Bicker S, Khudayberdiev S, Weiß K, Zocher K, Baumeister S, Schrott G. (2013) The DEAH-box helicase DHX36 mediates dendritic localization of the neuronal precursor-microRNA-134. *Genes Dev.* 27, 991–996.
- Biffi G, Tannahill D and Balasubramanian S. (2012) An intramolecular G-quadruplex structure is required for binding of telomeric repeat-containing RNA to the telomeric protein TRF2. *J. Am. Chem. Soc.* 134, 11974-6.
- Biffi G, Tannahill D, McCafferty J and Balasubramanian S. (2013) Quantitative visualization of dna g-quadruplex structures in human cells. *Nat. Chem.* 5, 182–186.
- Bizard AH and Hickson ID. (2014) The dissolution of double Holliday junctions. *Cold Spring Harb. Perspect. Biol.* 6, a016477.
- Blackwood JK, Rzechorzek NJ, Bray SM, Maman JD, Pellegrini L and Robinson NP. (2013) End-resection at DNA double-strand breaks in the three domains of life. *Biochemical Society Transactions.* 41, 314–320.
- Bleichert F and Baserga SJ. (2007) The long unwinding road of RNA helicases. *Mol Cell.* 27, 339-52.

- Bléoo S, Sun X, Hendzel MJ, Rowe JM, Packer M and Godbout R. (2001) Association of human DEAD box protein DDX1 with a cleavage stimulation factor involved in 3'-end processing of pre-mRNA. *Mol. Biol. Cell.* 12, 3046 - 59.
- Bochman ML, Judge CP and Zakian VA. (2011) The Pif1 family in prokaryotes: what are our helicases doing in your bacteria? *Mol. Biol. Cell.* 22, 1955-9.
- Bochman ML, Paeschke K and Zakian VA. (2012) DNA secondary structures: stability and function of G-quadruplex structures. *Nat. Rev. Genet.* 13, 770–780.
- Bochman ML, Sabouri N and Zakian VA. (2010) Unwinding the functions of the Pif1 family helicases. *DNA Repair (Amst).* 9, 237-49.
- Bochman ML. (2014) Roles of DNA helicases in the maintenance of genome integrity. *Mol. Cell.* 1, e963429.
- Bond AT, Mangus DA, He F and Jacobson A. (2001) Absence of Dbp2p alters both nonsense-mediated mRNA decay and rRNA processing. *Mol. Cell. Biol.* 21, 7366–7379.
- Booy EP, Meier M, Okun N, Novakowski SK, Xiong S, Stetefeld J and McKenna SA. (2012) The RNA helicase RHAU (DHX36) unwinds a G4-quadruplex in human telomerase RNA and promotes the formation of the P1 helix template boundary. *Nucleic Acids Res.* 40, 4110-24.
- Bouchier-Hayes L and Martin SJ. (2003) CARD games in apoptosis and immunity. *EMBO Rep.* 3, 616-21.
- Boukarabila H, Saurin AJ, Batsché E, Mossadegh N, van Lohuizen M, Otte AP, Pradel J, Muchardt C, Sieweke M and Duprez E. (2009) The PRC1 Polycomb group complex interacts with PLZF/RARA to mediate leukemic transformation. *Genes Dev.* 23, 1195-206.
- Boule J.B and Zakian VA. (2007) The yeast Pif1p DNA helicase preferentially unwinds RNA DNA substrates. *Nucleic Acids Res.* 35, 5809–5818.
- Boule JB, Vega LR and Zakian VA. (2005) The yeast Pif1p helicase removes telomerase from telomeric DNA. *Nature.* 438, 57–61.
- Bourgeois CF, Mortreux F and Auboeuf D. (2016) The multiple functions of RNA helicases as drivers and regulators of gene expression. *Nat. Rev. Mol. Cell Biol.* 17, 426-38.
- Bradley TR and Metcalf D. (1966) The growth of mouse bone marrow cells in vitro. *Aust. J. Exp. Biol. Med. Sci.* 44, 287-299.
- Branzei D and Foiani M. (2009) The checkpoint response to replication stress. *DNA Repair.* 8, 1038–1046.

Brightbill HD, Libraty DH, Krutzik SR, Yang RB, Belisle JT, Bleharski JR, Maitland M, Norgard MV, Plevy SE, Smale ST, Brennan PJ, Bloom BR, Godowski PJ and Modlin RL. (1999) Host defense mechanisms triggered by microbial lipoproteins through toll-like receptors. *Science*. 285, 732–736.

Brimacombe R, Stiege W, Kyriatsoulis A and Maly P. (1988) Intra-RNA and RNA-protein cross-linking techniques in *Escherichia coli* ribosomes. *Methods Enzymol.* 164, 287-30.

Broitman SL, Im DD and Fresco JR. (1987) Formation of the triple-stranded polynucleotide helix, poly(A.A.U). *Proc. Natl. Acad. Sci. USA*. 84, 5120-4.

Broquet AH, Hirata Y, McAllister CS and Kagnoff MF. (2011) RIG-I/MDA5/MAVS are required to signal a protective IFN response in rotavirus-infected intestinal epithelium. *J. Immunol.* 186, 1618-26.

Brosh RM Jr, Li JL, Kenny MK, Karow JK, Cooper MP, Kureekattil RP, Hickson ID and Bohr VA. (2000) Replication protein a physically interacts with the Bloom's syndrome protein and stimulates its helicase activity. *J. Biol. Chem.* 275, 23500–23508.

Brosh RM Jr, Opresko PL and Bohr VA. (2006) Enzymatic mechanism of the WRN helicase/nuclease. *Methods Enzymol.* 409, 52-85.

Brosh RM Jr, Orren DK, Nehlin JO, Ravn PH, Kenny MK, Machwe A and Bohr VA. (1999) Functional and physical interaction between WRN helicase and human replication protein A. *J. Biol. Chem.* 274, 18341–18350.

Brosh RM Jr. (2013) DNA helicases involved in DNA repair and their roles in cancer. *Nat. Rev. Cancer.* 13, 542-58.

Bruns AM and Horvath CM. (2011) Activation of RIG-I-like receptor signal transduction. *Crit. Rev. Biochem. Mol. Biol.* 47, 194-206.

Bruns AM and Horvath CM. (2015) LGP2 synergy with MDA5 in RLR-mediated RNA recognition and antiviral signaling. *Cytokine.* 74, 198-206.

Bruns AM, Pollpeter D, Hadizadeh N, Myong S, Marko JF, Horvath CM. (2013) ATP hydrolysis enhances RNA recognition and antiviral signal transduction by the innate immune sensor, laboratory of genetics and physiology 2 (LGP2). *J. Biol. Chem.* 288, 938-46.

Budd ME, Reis CC, Smith S, Myung K and Campbell JL. (2006) Evidence suggesting that Pif1 helicase functions in DNA replication with the Dna2 helicase/nuclease and DNA polymerase delta. *Mol. Cell. Biol.* 26, 2490-500.

Budhathoki JB, Ray S, Urban V, Janscak P, Yodh JG and Balci H. (2014) RecQ-core of BLM unfolds telomeric G-quadruplex in the absence of ATP. *Nucleic Acids Res.* 42, 11528-45.

- Bugaut A and Balasubramanian S. (2012) 5'-UTR RNA G-quadruplexes: translation regulation and targeting. *Nucleic Acids Res.* 40, 4727-41.
- Buijs A and Bruin M. (2007) Fusion of FIP1L1 and RARA as a result of a novel t(4;17)(q12; q21) in a case of juvenile myelomonocytic leukemia. *Leukemia.* 21, 1104-8.
- Burckin T, Nagel R, Mandel-Gutfreund Y, Shiue L, Clark TA, Chong JL, Chang TH, Squazzo S, Hartzog G and Ares M Jr. (2005) Exploring functional relationships between components of the gene expression machinery. *Nat. Struct. Mol. Biol.* 12, 175-182.
- Bürckstümmer T, Baumann C, Blüml S, Dixit E, Dürnberger G, Jahn H, Planyavsky M, Bilban M, Colinge J, Bennett KL and Superti-Furga G. (2009) An orthogonal proteomic-genomic screen identifies AIM2 as a cytoplasmic DNA sensor for the inflammasome. *Nat. Immunol.* 10, 266-272.
- Burdette DL and Vance RE. (2013) STING and the innate immune response to nucleic acids in the cytosol. *Nat. Immunol.* 14, 19-26.
- Burgers PM. (2009) Polymerase dynamics at the eukaryotic DNA replication fork. *J. Biol. Chem.* 284, 4041-5.
- Buxbaum AR, Haimovich G and Singer RH. (2015) In the right place at the right time: visualizing and understanding mRNA localization. *Nat. Rev. Mol. Cell Biol.* 16, 95-109.
- Byrd AK and Raney KD. (2007) Structure and function of Pif1 helicase. *Biochem. Soc. Trans.* 45, 1159-1171.
- Cannavo E and Cejka P. (2014) Sae2 promotes dsDNA endonuclease activity within Mre11-Rad50-Xrs2 to resect DNA breaks. *Nature.* 514, 122-25.
- Capra JA, Paeschke K, Singh M and Zakian VA. (2010) G-quadruplex DNA sequences are evolutionarily conserved and associated with distinct genomic features in *Saccharomyces cerevisiae*. *PLoS Comput. Biol.* 6, e1000861.
- Caruthers JM and McKay DB. (2002) Helicase structure and mechanism. *Curr. Opin. Struct. Biol.* 12, 123-33.
- Catalano A, Dawson MA, Somana K, Opat S, Schwarzer A, Campbell LJ and Iland H. (2007) The PRKAR1A gene is fused to RARA in a new variant acute promyelocytic leukemia. *Blood.* 110, 4073-6.
- Cayrou C, Coulombe P, Vigneron A, Stanojcic S, Ganier O, Peiffer I, Rivals E, Puy A, Laurent-Chabalier S, Desprat R and Méchali M. (2011) Genome-scale analysis of metazoan replication origins reveals their organization in specific but flexible sites defined by conserved features. *Genome Res.* 21, 1438-49.

- Cayrou C, Grégoire D, Coulombe P, Danis E and Méchali M. Genome-scale identification of active DNA replication origins. (2012) *Methods*. 57, 158-64.
- Cejka P and Kowalczykowski SC. (2010) The full-length *Saccharomyces cerevisiae* Sgs1 protein is a vigorous DNA helicase that preferentially unwinds Holliday junctions. *J. Biol. Chem.* 285, 8290–301.
- Cejka P, Cannavo E, Polaczek P, Masuda-Sasa T, Pokharel S, Campbell JL and Kowalczykowski SC. (2010) DNA end resection by Dna2– Sgs1–RPA and its stimulation by Top3–Rmi1 and Mre11–Rad50–Xrs2. *Nature*. 467, 112–16.
- Cerofolini L, Amato J, Giachetti A, Limongelli V, Novellino E, Parrinello M, Fragai M, Randazzo A and Luchinat C. (2014) G-triplex structure and formation propensity. *Nucleic Acids Res.* 42, 13393-404.
- Cerutti H and Casas-Mollano JA. (2006) On the origin and functions of RNA-mediated silencing: from protists to man. *Curr Genet.* 50, 81-99.
- Chaganti RS, Schonberg S and German J. (1974) A manyfold increase in sister chromatid exchanges in Bloom's syndrome lymphocytes. *Proc Natl Acad Sci U S A.* 71, 4508–12.
- Chambers VS, Marsico G, Boutell JM, Di Antonio M, Smith GP and Balasubramanian S. (2015) High-throughput sequencing of DNA G-quadruplex structures in the human genome. *Nat. Biotechnol.* 33, 877–881.
- Chambon P. (1996) A decade of molecular biology of retinoic acid receptors. *FASEB J.* 10, 940-54.
- Chamot D, Colvin KR, Kujat-Choy SL and Owttrim GW. (2005) RNA structural rearrangement via unwinding and annealing by the cyanobacterial RNA helicase, CrhR. *J. Biol. Chem.* 280, 2036-2044.
- Chan IT, Kutok JL, Williams IR, Cohen S, Moore S, Shigematsu H, Ley TJ, Akashi K, Le Beau MM and Gilliland DG. (2006) Oncogenic K-ras cooperates with PML-RAR alpha to induce an acute promyelocytic leukemia-like disease. *Blood.* 108, 1708-15.
- Chan YK and Gack MU. (2016) Viral evasion of intracellular DNA and RNA sensing. *Nat. Rev. Microbiol.* 14, 360–373.
- Chang M, Luke B, Kraft C, Li Z, Peter M, Lingner J and Rothstein R. (2009) Telomerase is essential to alleviate pif1-induced replication stress at telomeres. *Genetics.* 183, 779-91.
- Chauffaille MLLF, Figueiredo MS, Beltrani R, Antunes SV, Yamamoto M and Kerbauy J. (2001) Acute promyelocytic leukemia: the study of t(15;17) translocation by fluorescent *in situ* hybridization, reverse transcriptase-polymerase chain reaction and cytogenetic techniques. *Braz. J. Med. Biol. Res.* 34, 735-743.

Chen GQ, Shen ZX, Wu F, Han JY, Miao JM, Zhong HJ, Li XS, Zhao JQ, Zhu J, Fang ZW, Chen SJ, Chen Z and Wang ZY. (1996) Pharmacokinetics and efficacy of low-dose all-trans retinoic acid in the treatment of acute promyelocytic leukemia. *Leukemia*. 10, 825-8.

Chen GQ, Shi XG, Tang W, Xiong SM, Zhu J, Cai X, Han ZG, Ni JH, Shi GY, Jia PM, Liu MM, He KL, Niu C, Ma J, Zhang P, Zhang TD, Paul P, Naoe T, Kitamura K, Miller W, Waxman S, Wang ZY, de The H, Chen SJ and Chen Z. (1997) Use of arsenic trioxide (As₂O₃) in the treatment of acute promyelocytic leukemia (APL): I. As₂O₃ exerts dose-dependent dual effects on APL cells. *Blood*. 89, 3345-53.

Chen W, Han C, Xie B, Hu X, Yu Q, Shi L, Wang Q, Li D, Wang J, Zheng P, Liu Y and Cao X. (2013) Induction of Siglec-G by RNA viruses inhibits the innate immune response by promoting RIG-I degradation. *Cell*. 152, 467-78.

Chen WF, Dai YX, Duan XL, Liu NN, Shi W, Li N, Li M, Dou SX, Dong YH, Rety S and Xi XG. (2016) Crystal structures of the Bspif1 helicase reveal that a major movement of the 2B SH3 domain is required for DNA unwinding. *Nucleic Acids Res*. 44, 2949–2961.

Cheok CF, Wu L, Garcia PL, Janscak P and Hickson ID. (2005) The Bloom's syndrome helicase promotes the annealing of complementary single-stranded DNA. *Nucleic Acids Res*. 33, 3932-3941.

Chevalier F. (2010) Highlights on the capacities of "Gel-based" proteomics. *Proteome Sc*. 8, 23.

Chiarella S, De Cola A, Scaglione GL, Carletti E, Graziano V, Barcaroli D, Lo Sterzo C, Di Matteo A, Di Ilio C, Falini B, Arcovito A, De Laurenzi V and Federici L. (2013) Nucleophosmin mutations alter its nucleolar localization by impairing G-quadruplex binding at ribosomal DNA. *Nucleic Acids Res*. 41, 3228-39.

Chisholm KM, Aubert SD, Freese KP, Zakian VA, King MC and Welsh PL. A genomewide screen for suppressors of Alu-mediated rearrangements reveals a role for PIF1. *PLoS One*. 7, e30748.

Choe J, Ryu I, Park OH, Park J, Cho H, Yoo JS, Chi SW, Kim MK, Song HK, Kim YK. (2014) eIF4AIII enhances translation of nuclear cap-binding complex-bound mRNAs by promoting disruption of secondary structures in 5'UTR. *Proc. Natl Acad. Sci. USA*. 111, E4577–E4586.

Choi SJ, Lee HC, Kim JH, Park SY, Kim TH, Lee WK, Jang DJ, Yoon JE, Choi YI, Kim S, Ma J, Kim CJ, Yao TP, Jung JU, Lee JY and Lee JS. (2016) HDAC6 regulates cellular viral RNA sensing by deacetylation of RIG-I. *EMBO J*. 35, 429–442.

Chou WC, Jie C, Kenedy AA, Jones RJ, Trush MA and Dang CV. (2004) Role of NADPH oxidase in arsenic-induced reactive oxygen species formation and cytotoxicity in myeloid leukemia cells. *Proc. Natl. Acad. Sci. U S A*. 101, 4578-83.

Christian H, Hofele RV, Urlaub H and Ficner R. (2014) Insights into the activation of the helicase Prp43 by biochemical studies and structural mass spectrometry. *Nucleic Acids Res.* 42, 1162-1179.

Civril F, Bennett M, Moldt M, Deimling T, Witte G, Schiesser S, Carell T and Hopfner KP. (2011) The RIG-I ATPase domain structure reveals insights into ATP-dependent antiviral signalling. *EMBO Rep.* 12, 1127–1134.

Civril F, Deimling T, de Oliveira Mann CC, Ablasser A, Moldt M, Witte G, Hornung V and Hopfner KP. (2013) Structural mechanism of cytosolic DNA sensing by cGAS. *Nature.* 498, 332-7.

Coburn GA, Miao X, Briant DJ and Mackie GA. (1999) Reconstitution of a minimal RNA degradosome demonstrates functional coordination between a 3' exonuclease and a DEAD-box RNA helicase. *Genes Dev.* 13, 2594-603.

Coin F, Bergmann E, Tremeau-Bravard A and Egly JM. (1999) Mutations in XPB and XPD helicases found in xeroderma pigmentosum patients impair the transcription function of TFIIH. *EMBO J.* 18, 1357-66.

Coller JM, Tucker M, Sheth U, Valencia-Sanchez MA and Parker R. (2001) The DEAD box helicase, Dhh1p, functions in mRNA decapping and interacts with both the decapping and deadenylase complexes. *RNA.* 7, 1717–1727 (2001).

Collins SJ. (2002) The role of retinoids and retinoic acid receptors in normal hematopoiesis. *Leukemia.* 16, 1896-905.

Company M, Arenas J and Abelson J. (1991) Requirement of the RNA helicase-like protein PRP22 for release of messenger RNA from spliceosomes. *Nature.* 349, 487-493.

Coombs CC, Tavakkoli M and Tallman MS. (2015) Acute promyelocytic leukemia: where did we start, where are we now, and the future. *Blood Cancer J.* 5, e304.

Cooper MP, Machwe A, Orren DK, Brosh RM, Ramsden D and Bohr VA. (2000) Ku complex interacts with and stimulates the Werner protein. *Genes Dev.* 14, 907-12.

Cordin O, Banroques J, Tanner NK and Linder P. (2006) The DEAD-box protein family of RNA helicases. *Gene.* 367, 17–37.

Corey SJ, Locker J, Oliveri DR, Shekhter-Levin S, Redner RL, PENCHANSKY L and GOLLIN SM. (1994) A non-classical translocation involving 17q12 (retinoic acid receptor alpha) in acute promyelocytic leukemia (APML) with atypical features. *Leukemia.* 8, 1350-3.

Crnugelj M, Hud NV and Plavec J. (2002) The solution structure of d(G(4)T(4)G(3))(2): a bimolecular G-quadruplex with a novel fold. *J. Mol. Biol.* 320, 911-24.

Cui J, Song Y, Li Y, Zhu Q, Tan P, Qin Y, Wang HY and Wang RF. (2014) USP3 inhibits type I interferon signaling by deubiquitinating RIG-I-like receptors. *Cell Res.* 24, 400-416.

- Cui S, Arosio D, Doherty KM, Brosh RM Jr, Falaschi A and Vindigni A. (2004) Analysis of the unwinding activity of the dimeric RECQ1 helicase in the presence of human replication protein A. *Nucleic Acids Res.* 32, 2158-70.
- Cui S, Eisenächer K, Kirchhofer A, Brzózka K, Lammens A, Lammens K, Fujita T, Conzelmann KK, Krug A and Hopfner KP. (2008) The C-terminal regulatory domain is the RNA 5'-triphosphate sensor of RIG-I. *Mol. Cell.* 29, 169-79.
- Cunningham TJ and Duester G. (2015) Mechanisms of retinoic acid signalling and its roles in organ and limb development. *Nat. Rev. Mol. Cell Biol.* 16, 110-23.
- Dai J, Chen D, Jones RA, Hurley LH and Yang D. (2006) NMR solution structure of the major G-quadruplex structure formed in the human BCL2 promoter region. *Nucleic Acids Res.* 34, 5133-44.
- Dai J, Dexheimer TS, Chen D, Carver M, Ambrus A, Jones RA and Yang D (2006). intramolecular G-quadruplex structure with mixed parallel/antiparallel G-strands formed in the human BCL-2 promoter region in solution. *J. Am. Chem. Soc.* 128: 1096-1098.
- Dardenne E, Polay Espinoza M, Fattet L, Germann S, Lambert MP, Neil H, Zonta E, Mortada H, Gratadou L, Deygas M, Chakrama FZ, Samaan S, Desmet FO, Tranchevent LC, Dutertre M, Rimokh R, Bourgeois CF and Auboeuf D. (2014) RNA helicases DDX5 and DDX17 dynamically orchestrate transcription, miRNA, and splicing programs in cell differentiation. *Cell Rep.* 7, 1900-1913.
- Davis JL, Kunisawa R and Thomer J. (1992) A presumptive helicase (MOT1 gene product) affects gene expression and IS required for for viability in the yeast *Saccharomyces cerevisiae*. *Mol. Cell. Biol.* 12, 1879-92
- Davison K, Mann KK, Waxman S and Miller WH Jr. (2003) JNK activation is a mediator of arsenic trioxide-induced apoptosis in acute promyelocytic leukemia cells. *Blood.* 103, 3496-502.
- de Armond R, Wood S, Sun D, Hurley LH and Ebbinghaus SW. (2005) Evidence for the presence of a guanine quadruplex forming region within a polypurine tract of the hypoxia inducible factor 1alpha promoter. *Biochemistry.* 44, 16341-16350.
- de Botton S, Chevret S, Coiteux V, Dombret H, Sanz M, San Miguel J, Caillot D, Vekhoff A, Gardembas M, Stamatoulas A, Conde E, Guerci A, Gardin C, Fey M, Cony Makhoul D, Reman O, de la Serna J, Lefrere F, Chomienne C, Degos L and Fenaux P. (2003) Early onset of chemotherapy can reduce the incidence of ATRA syndrome in newly diagnosed acute promyelocytic leukemia (APL) with low white blood cell counts: results from APL 93 trial. *Leukemia.* 17, 339-42.
- de Braekeleer E, Douet-Guilbert N and De Braekeleer M. (2014) RARA fusion genes in acute promyelocytic leukemia: a review. *Expert. Rev. Hematol.* 7, 347-57.
- de la Cruz J, Kressler D and Linder P. (1999) Unwinding RNA in *Saccharomyces cerevisiae*: DEAD-box proteins and related families. *Trends Biochem. Sci.* 24, 192-8.

de S and Michor F. (2011) DNA secondary structures and epigenetic determinants of cancer genome evolution. *Nat. Struct. Mol Biol.* 18, 950-5.

de Thé H and Chen Z. (2010) Acute promyelocytic leukaemia: novel insights into the mechanisms of cure. *Nat. Rev. Cancer.* 10, 775-83.

de Thé H, Chomienne C, Lanotte M, Degos L and Dejean A. (1990) The t(15;17) translocation of acute promyelocytic leukaemia fuses the retinoic acid receptor alpha gene to a novel transcribed locus. *Nature.* 347, 558-61.

de Thé H, Le Bras M and Lallemand-Breitenbach V. (2012) The cell biology of disease: Acute promyelocytic leukemia, arsenic, and PML bodies. *J. Cell Biol.* 198, 11-21.

Dempsey LA, Sun H, Hanakahi LA, Maizels N. (1999) G4 DNA binding by LR1 and its subunits, nucleolin and hnRNP D, A role for G-G pairing in immunoglobulin switch recombination. *J. Biol. Chem.* 274, 1066-71.

Denhardt DT, Dressler DH and Hathaway A. (1967) The abortive replication of PhiX174 DNA in a recombination-deficient mutant of *Escherichia coli*. *Proc. Natl. Acad. Sci. U S A.* 57, 813-20.

Dhote V, Sweeney TR, Kim N, Hellen CU and Pestova TV. (2012) Roles of individual domains in the function of DHX29, an essential factor required for translation of structured mammalian mRNAs. *Proc. Natl Acad. Sci. USA* 109, E3150–E3159.

Di Croce L, Raker VA, Corsaro M, Fazi F, Fanelli M, Faretta M, Fuks F, Lo Coco F, Kouzarides T, Nervi C, Minucci S, Pelicci PG. (2002) Methyltransferase recruitment and DNA hypermethylation of target promoters by an oncogenic transcription factor. *Science.* 295, 1079-82.

Diges CM and Uhlenbeck OC. (2001) *Escherichia coli* DbpA is an RNA helicase that requires hairpin 92 of 23S rRNA. *EMBO J.* 20, 5503–12.

Dillingham MS and Kowalczykowski SC. (2008) RecBCD enzyme and the repair of double-stranded DNA breaks. *Microbiol. Mol. Biol. Rev.* 72, 642–71.

Dillingham MS, Spies M and Kowalczykowski SC. (2003) RecBCD enzyme is a bipolar DNA helicase. *Nature.* 423, 893-897.

Dixit E, Boulant S, Zhang Y, Lee AS, Odendall C, Shum B, Hacohen N, Chen ZJ, Whelan SP, Fransen M, Nibert ML, Superti-Furga G and Kagan JC. (2010) Peroxisomes are signaling platforms for antiviral innate immunity. *Cell.* 141, 668-681.

Do NQ, Lim KW, Teo MH, Heddi B and Phan AT. (2011) Stacking of G-quadruplexes: NMR structure of a G-rich oligonucleotide with potential anti-HIV and anticancer activity. *Nucleic Acids Res.* 39, 9448-57.

Douer D. (2003) The epidemiology of acute promyelocytic leukaemia. *Best Pract. Res. Clin. Haematol.* 16, 357-67.

- Dreesen O, Li B and Cross GAM. (2005) Telomere structure and shortening in telomerase-deficient *Trypanosoma brucei*. *Nucleic Acids Res.* 33, 4536–43.
- Drexler HG, Quentmeier H, MacLeod RA, Uphoff CC, Hu ZB. (1995) Leukemia cell lines: in vitro models for the study of acute promyelocytic leukemia. *Leuk. Res.* 19, 681-91.
- Duan XL, Liu NN, Yang YT, Li HH, Li M, Dou SX and Xi XG. (2015) G-quadruplexes significantly stimulate Pif1 helicase-catalyzed duplex DNA unwinding. *J. Biol. Chem.* 290, 7722–7735.
- Dubois C, Schlageter MH, de Gentile A, Balitrand N, Toubert ME, Krawice I, Fenaux P, Castaigne S, Najean Y and Degos L. (1994) Modulation of IL-8, IL-1 beta, and G-CSF secretion by all-trans retinoic acid in acute promyelocytic leukemia. *Leukemia.* 8, 1750-7.
- Duprez E, Benoit G, Flexor M, Lillehaug JR and Lanotte M. (2000) A mutated PML/RARA found in the retinoid maturation resistant NB4 subclone, NB4-R2, blocks RARA and wild-type PML/RARA transcriptional activities. *Leukemia.* 14, 255-61.
- Duprez E, Lillehaug JR, Naoe T and Lanotte M. cAMP signalling is decisive for recovery of nuclear bodies (PODs) during maturation of RA-resistant t(15;17) promyelocytic leukemia NB4 cells expressing PML-RAR alpha. *Oncogene.* 12, 2451-9.
- Durr H, Korner C, Muller M, Hickmann V and Hopfner KP. (2005) X-ray structures of the *Sulfolobus solfataricus* SWI2/SNF2 ATPase core and its complex with DNA. *Cell.* 121, 363–373.
- Eddy J and Maizels N. (2006) Gene function correlates with potential for G4 DNA formation in the human genome. *Nucleic Acids Res.* 34, 3887–3896.
- Edwards-Gilbert G, Kim DH, Silverman E and Lin RJ. (2004) Definition of a spliceosome interaction domain in yeast Prp2 ATPase. *RNA.* 10, 210-220.
- Eghtedar A, Rodriguez I, Kantarjian H, O'Brien S, Daver N, Garcia-Manero G, Ferrajoli A, Kadia T, Pierce S, Cortes J and Ravandi F. (2015) Incidence of secondary neoplasms in patients with acute promyelocytic leukemia treated with all-trans retinoic acid plus chemotherapy or with all-trans retinoic acid plus arsenic trioxide. *Leuk. Lymphoma.* 56, 1342-5
- Egly JM and Coin F. (2011) A history of TFIIH: two decades of molecular biology on a pivotal transcription/repair factor. *DNA Repair (Amst).* 10, 714-21.
- Eichler DC and Craig N. (1994) Processing of eukaryotic ribosomal RNA. *Prog. Nucleic Acid Res. Mol. Biol.* 49, 197-239.
- Eisen A and Lucchesi JC. (1998) Unraveling the role of helicases in transcription. *Bioessays.* 20, 634-41.

Ellermeier J, Wei J, Duewell P, Hoves S, Stieg MR, Adunka T, Noerenberg D, Anders HJ, Mayr D, Poeck H, Hartmann G, Endres S and Schnurr M. (2013) Therapeutic efficacy of bifunctional siRNA combining TGF-beta1 silencing with RIG-I activation in pancreatic cancer. *Cancer Res.* 73, 1709-20.

Eoff RL, Spurling TL and Raney KD. (2005) Chemically modified DNA substrates implicate the importance of electrostatic interactions for DNA unwinding by Dda helicase. *Biochemistry.* 44, 666–674.

Erzberger JP and Berger JM. (2006) Evolutionary relationships and structural mechanisms of AAA+ proteins. *Annu. Rev. Biophys. Biomol. Struct.* 35, 93-114.

Fairman-Williams ME, Guenther UP and Jankowsky E. (2010) SF1 and SF2 helicases: family matters. *Curr. Opin. Struct. Biol.* 20, 313-24.

Fan Y, Mao R, Yu Y, Liu S, Shi Z, Cheng J, Zhang H, An L, Zhao Y, Xu X, Chen Z, Kogiso M, Zhang D, Zhang H, Zhang P, Jung JU, Li X, Xu G and Yang J. (2014). USP21 negatively regulates antiviral response by acting as a RIG-I deubiquitinase. *J. Exp. Med.* 211, 313–328.

Fang G and Cech TR. (1993) The beta subunit of Oxytricha telomere-binding protein promotes G-quartet formation by telomeric DNA. *Cell.* 74, 875-85.

Fang J, Acheampong E, Dave R, Wang F, Mukhtar M and Pomerantz RJ. (2005) The RNA helicase DDX1 is involved in restricted HIV-1 Rev function in human astrocytes. *Virology.* 336, 299 - 307.

Fernandes-Alnemri T, Yu JW, Datta P, Wu J and Alnemri ES. (2009) AIM2 activates the inflammasome and cell death in response to cytoplasmic DNA. *Nature.* 458, 509–513.

Finegold SM and George WL. (1989) Anaerobic Infections in Humans. Academic Press. San Diego, CA.

Fiorini F, Bagchi D, Le Hir H and Croquette V. (2015) Human Upf1 is a highly processive RNA helicase and translocase with RNP remodelling activities. *Nat. Commun.* 6, 7581.

Fischer N and Weis K. (2002) The DEAD box protein Dhh1 stimulates the decapping enzyme Dcp1. *EMBO J.* 21, 2788–2797.

Flaus A and Owen-Hughes T. (2004) Mechanisms for ATP-dependent chromatin remodelling: farewell to the tuna-can octamer? *Curr. Opin. Genet. Dev.* 14, 165–73.

Flaus A, Martin DM, Barton GJ and Owen-Hughes T (2006) Identification of multiple distinct Snf2 subfamilies with conserved structural motifs. *Nucleic Acids Res.* 34, 2887–905.

- Fogel BL and Perlman S. (2006) An approach to the patient with late-onset cerebellar ataxia. *Nat. Clin. Pract. Neurol.* 2, 629-35.
- Forney J, Henderson ER and Blackburn EH. (1987) Identification of the telomeric sequence of the acellular slime molds *Didymium iridis* and *Physarum polycephalum*. *Nucleic Acids Res.* 15, 9143–9152.
- Foury F and Kolodynski J. (1983) Pif mutation blocks recombination between mitochondrial rho⁺ and rho⁻ genomes having tandemly arrayed repeat units in *Saccharomyces cerevisiae*. *Proc. Natl. Acad. Sci. USA.* 80, 5345-9.
- Franklin RE and Gosling RG. (1953) Molecular Configuration in Sodium Thymonucleate. *Nature.* 171, 740-741.
- Fredericksen BL, Keller BC, Fornek J, Katze MG and Gale M Jr. (2008) Establishment and maintenance of the innate antiviral response to West Nile Virus involves both RIG-I and MDA5 signaling through IPS-1. *J. Virol.* 82, 609–616.
- Frees S, Menendez C, Crum M and Bagga PS. (2014) QGRS-Conserve: a computational method for discovering evolutionarily conserved G-quadruplex motifs. *Hum. Genomics.* 8, 8.
- Friedman CS, O'Donnell MA, Legarda-Addison D, Ng A, Cárdenas WB, Yount JS, Moran TM, Basler CF, Komuro A, Horvath CM, Xavier R and Ting AT. (2008) The tumour suppressor CYLD is a negative regulator of RIG-I-mediated antiviral response. *EMBO Rep.* 9, 930-936.
- Frit P, Bergmann E and Egly JM. (1999) Transcription factor IIIH: a key player in the cellular response to DNA damage. *Biochimie.* 81, 27-38.
- Fry M and Loeb LA. (1999) Human werner syndrome DNA helicase unwinds tetrahelical structures of the fragile X syndrome repeat sequence d(CGG)_n. *J. Biol. Chem.* 274, 12797–12802.
- Fu XD and Ares M Jr. (2014) Context-dependent control of alternative splicing by RNA-binding proteins. *Nat. Rev. Genet.* 15, 689–701.
- Fujii R, Okamoto M, Aratani S, Oishi T, Ohshima T, Taira K, Baba M, Fukamizu A and Nakajima T. (2001) A Role of RNA Helicase A in cis-Acting Transactivation Response Element-mediated Transcriptional Regulation of Human Immunodeficiency Virus Type 1. *J. Biol. Chem.* 276, 5445 - 51.
- Fujita T, Onoguchi K, Onomoto K, Hirai R and Yoneyama M. (2007) Triggering antiviral response by RIG-I-related RNA helicases. *Biochimie.* 89, 754-760.
- Fuller-Pace FV. (2006) DExD/H box RNA helicases: multifunctional proteins with important roles in transcriptional regulation. *Nucleic Acids Res.* 34, 4206–4215.

- Fuss JO and Tainer JA. (2011) XPB and XPD helicases in TFIIH orchestrate DNA duplex opening and damage verification to coordinate repair with transcription and cell cycle via CAK kinase. *DNA Repair (Amst)*. 10, 697-713.
- Futami K, Shimamoto A, Furuichi Y. (2007) Mitochondrial and nuclear localization of human Pif1 helicase. *Biol. Pharm. Bull.* 30, 1685-92.
- Gack MU, Albrecht RA, Urano T, Inn KS, Huang IC, Carnero E, Farzan M, Inoue S, Jung JU and García-Sastre A. (2009) Influenza A virus NS1 targets the ubiquitin ligase TRIM25 to evade recognition by the host viral RNA sensor RIG-I. *Cell Host. Microbe*. 5, 439-49.
- Gack MU, Nistal-Villan E, Inn KS, García-Sastre A and Jung JU. (2010) Phosphorylation-mediated negative regulation of RIG-I antiviral activity. *J. Virol.* 84, 3220-3229.
- Galletto R and Tomko EJ. (2013) Translocation of *Saccharomyces cerevisiae* Pif1 helicase monomers on single-stranded DNA. *Nucleic Acids Res.* 41, 4613–4627.
- Ganz T. (2000) Paneth cells-guardians of the gut cell hatchery. *Nat. Immunol.* 1, 99-100.
- Gao D, Yang YK, Wang RP, Zhou X, Diao FC, Li MD, Zhai ZH, Jiang ZF and Chen DY. (2009) REUL is a novel E3 ubiquitin ligase and stimulator of retinoic-acid-inducible gene-1. *PLoS One.* 4, e5760.
- Garcia PL, Liu Y, Jiricny J, West SC, Janscak P. (2004) Human RECQ51 β , a protein with DNA helicase and strand-annealing activities in a single polypeptide. *EMBO J.* 23, 2882–2891.
- Gatfield D, Le Hir H, Schmitt C, Braun IC, Kocher T, Wilm M and Izaurralde E. (2001) The DExH/D box protein HEL/UAP56 is essential for mRNA nuclear export in *Drosophila*. *Curr. Biol.* 11, 1716-1721.
- Gay NJ, Symmons MF, Gangloff M and Bryant CE. (2014) Assembly and localization of Toll-like receptor signalling complexes. *Nat. Rev. Immunol.* 14, 546–558.
- Gehring K, Leroy JL and Guéron M. (1993) A tetrameric DNA structure with protonated cytosine-cytosine base pairs. *Nature.* 363, 561-5.
- Geissler V, Altmeyer S, Stein, B, Uhlmann-Schiffler H and Stahl H. (2013) The RNA helicase Ddx5/p68 binds to hUpf3 and enhances NMD of Ddx17/p72 and Smg5 mRNA. *Nucleic Acids Res.* 41, 7875–7888.
- Gellert M, Lipsett MN and Davies DR. (1962) Helix formation by guanylic acid. *Proc. Natl. Acad. Sci. USA.* 48, 2013-8.
- George T, Wen Q, Griffiths R, Ganesh A, Meuth M and Sanders CM. (2009) Human Pif1 helicase unwinds synthetic DNA structures resembling stalled DNA replication forks. *Nucleic Acids Res.* 37, 6491–6502.

- Ghosal G, Yuan J and Chen J. (2011) The HARP domain dictates the annealing helicase activity of HARP/SMARCAL1. *EMBO Rep.* 12, 574–580.
- Ghosh AK, Rossi ML, Singh DK, Dunn C, Ramamoorthy M, Croteau DL, Liu Y and Bohr VA. (2012) RECQL4, the protein mutated in Rothmund-Thomson syndrome, functions in telomere maintenance. *J. Biol. Chem.* 287, 196–209.
- Gilbert DE and Feigon J. (1999) Multistranded DNA structures. *Curr. Opin. Struct. Biol.* 9, 305–14.
- Gillespie RF and Gudas LJ. (2007) Retinoid regulated association of transcriptional co-regulators and the polycomb group protein SUZ12 with the retinoic acid response elements of *Hoxa1*, *RAR β 2*, and *Cyp26A1* in F9 embryonal carcinoma cells. *J. Mol. Biol.* 372, 298–316.
- Giraldo R and Rhodes D. (1994) The yeast telomere-binding protein RAP1 binds to and promotes the formation of DNA quadruplexes in telomeric DNA. *EMBO J.* 13, 2411–2420.
- Giri B, Smaldino PJ, Thys RG, Creacy SD, Routh ED, Hantgan RR, Lattmann S, Nagamine Y, Akman SA and Vaughn JP. (2011) G4 resolvase 1 tightly binds and unwinds unimolecular G4-DNA. *Nucleic Acids Res.* 39, 7161–78.
- Gitlin L, Barchet W, Gilfillan S, Cella M, Beutler B, Flavell RA, Diamond MS and Colonna M. (2006) Essential role of mda-5 in type I IFN responses to polyriboinosinic:polyribocytidylic acid and encephalomyocarditis picornavirus. *Proc. Natl. Acad. Sci. U S A.* 103, 8459–8464.
- Glas M, Coch C, Trageser D, Dassler J, Simon M, Koch P, Mertens J, Quandt T, Gorris R, Reinartz R, Wieland A, Von Lehe M, Pusch A, Roy K, Schlee M, Neumann H, Fimmers R, Herrlinger U, Brüstle O, Hartmann G, Besch R and Scheffler B. (2013) Targeting the cytosolic innate immune receptors RIG-I and MDA5 effectively counteracts cancer cell heterogeneity in glioblastoma. *Stem Cells.* 31, 1064–74.
- Goldstein EJ. (1996) Anaerobic bacteremia. *Clin. Infect. Dis.* 23, S97–S101.
- Gorbalenya AE and Koonin EV. (1993) Helicases: amino acid sequence comparisons and structure-function relationships. *Curr. Opin. Struct. Biol.* 3, 419.
- Gorbalenya AE, Koonin EV and Wolf YI. (1990) A new superfamily of putative NTP-binding domains encoded by genomes of small DNA and RNA viruses. *FEBS Lett.* 262, 145–48.
- Gorbalenya AE, Koonin EV, Donchenko AP and Blinov VM. (1988) A conserved NTP-motif in putative helicases. *Nature.* 333, 22.
- Gorbalenya AE, Koonin EV, Donchenko AP and Blinov VM. (1989) Two related superfamilies of putative helicases involved in replication, recombination, repair and expression of DNA and RNA genomes. *Nucleic Acids Res.* 17, 4713–4730.

Goubau D, Deddouche S and Sousa CRE. (2013) Cytosolic sensing of viruses. *Immunity*. 38, 855–869.

Grand CL, Han H, Muñoz RM, Weitman S, Von Hoff DD, Hurley LH and Bearss DJ. (2002) The cationic porphyrin TMPyP4 down-regulates c-MYC and human telomerase reverse transcriptase expression and inhibits tumor growth in vivo. *Mol. Cancer Ther.* 1, 565–573.

Greenberg JR. (1979) Ultraviolet light-induced crosslinking of mRNA to proteins. *Nucleic Acids Res.* 6, 715-32.

Gregersen LH, Schueler M, Munschauer M, Mastrobuoni G, Chen W, Kempa S, Dieterich C and Landthaler M. (2014) MOV10 is a 5' to 3' RNA helicase contributing to UPF1 mRNA target degradation by translocation along 3' UTRs. *Mol. Cell.* 54, 573–585.

Grégoire C, Welch H, Astarie-Dequeker C and Maridonneau-Parini I. (1998) Expression of azurophil and specific granule proteins during differentiation of NB4 cells in neutrophils. *J. Cell. Physiol.* 175, 203-10.

Gregory RI, Yan KP, Amuthan G, Chendrimada T, Doratotaj B, Cooch N, Shiekhattar R. (2004) The Microprocessor complex mediates the genesis of microRNAs. *Nature*. 432, 235–240.

Gu Y, Masuda Y and Kamiya K. (2008) Biochemical analysis of human PIF1 helicase and functions of its N-terminal domain. *Nucleic Acids Res.* 36, 6295–6308.

Gu Y, Wang J, Li S, Kamiya K, Chen X and Zhou P. (2013) Determination of the biochemical properties of full-length human PIF1 ATPase. *Prion*. 7, 341–347.

Guedin A, De Cian A, Gros J, Lacroix L and Mergny JL. (2008) Sequence effects in single-base loops for quadruplexes. *Biochimie*. 90, 686-696.

Guedin A, Gros J, Alberti P and Mergny JL. (2010) How long is too long? Effects of loop size on G-quadruplex stability. *Nucleic Acids Res.* 38, 7858-7868.

Guo RB, Rigolet P, Zargarian L, Fermandjian S and Xi XG. (2005) Structural and functional characterizations reveal the importance of a zinc binding domain in Bloom's syndrome helicase. *Nucleic Acids Res.* 33, 3109-3124.

Guo Z, Chen LM, Zeng H, Gomez JA, Plowden J, Fujita T, Katz JM, Donis RO and Sambhara S. (2007) NS1 protein of influenza A virus inhibits the function of intracytoplasmic pathogen sensor, RIG-I. *Am. J. Respir. Cell. Mol. Biol.* 36, 263-9.

Gupta R, Sharma S, Sommers JA, Kenny MK, Cantor SB and Brosh RM Jr. (2007) FANCD1 (BACH1) helicase forms DNA damage inducible foci with replication protein a and interacts physically and functionally with the single-stranded DNA-binding protein. *Blood*. 110, 2390–2398.

- Ha M and Kim VN. (2014) Regulation of microRNA biogenesis. *Nat. Rev. Mol. Cell Biol.* 15, 509–524.
- Habjan M, Andersson I, Klingström J, Schümann M, Martin A, Zimmermann P, Wagner V, Pichlmair A, Schneider U, Mühlberger E, Mirazimi A and Weber F. (2008) Processing of genome 5' termini as a strategy of negative-strand RNA viruses to avoid RIG-I-dependent interferon induction. *PLoS One.* 3, e2032.
- Halaby MJ, Harris BR, Miskimins WK, Cleary MP and Yang DQ. (2015) Deregulation of internal ribosome entry site-mediated p53 translation in cancer cells with defective p53 response to DNA damage. *Mol. Cell. Biol.* 35, 4006–4017.
- Hall MC and Matson SW. (1999) Helicase motifs: the engine that powers DNA unwinding. *Mol. Microbiol.* 34, 867–877.
- Hallenbeck PL, Marks MS, Lippoldt RE, Ozato K, Nikodem VM. (1992) Heterodimerization of thyroid hormone (TH) receptor with H-2RIIBP (RXR beta) enhances DNA binding and TH-dependent transcriptional activation. *Proc. Natl. Acad. Sci. U S A.* 89, 5572-6.
- Han C, Liu Y, Wan G, Choi HJ, Zhao L, Ivan C, He X, Sood AK, Zhang X, Lu X. (2014) The RNA-binding protein DDX1 promotes primary microRNA maturation and inhibits ovarian tumor progression. *Cell Rep.* 8, 1447-60.
- Hartman TR, Qian S, Bolinger C, Fernandez S, Schoenberg DR and Boris-Lawrie K. (2006) RNA helicase A is necessary for translation of selected messenger RNAs. *Nat. Struct. Mol. Biol.* 13, 509-16.
- Hayashi Y, Kuroda T, Kishimoto H, Wang C, Iwama A and Kimura K. (2014) Downregulation of rRNA transcription triggers cell differentiation. *PLoS One.* 9, e98586.
- He LZ, Tribioli C, Rivi R, Peruzzi D, Pelicci PG, Soares V, Cattoretti G and Pandolfi PP. (1997) Acute leukemia with promyelocytic features in PML/RARalpha transgenic mice. *Proc. Natl. Acad. Sci. U S A.* 94, 5302-7.
- He X, Byrd AK, Yun MK, Pemble CW, Harrison D, Yeruva L, Dahl C, Kreuzer KN, Raney KD and White SW. (2012) The T4 phage SF1B helicase Dda is structurally optimized to perform DNA strand separation. *Structure.* 20, 1189–1200.
- Heddi B, Martín-Pintado N, Serimbetov Z, Kari TMA and Phan AT. (2015) G-quadruplexes with (4n-1) guanines in the G-tetrad core: formation of a G-triad·water complex and implication for small-molecule binding. *Nucleic Acids Res.* 44, 910–916.
- Hemmi H, Takeuchi O, Kawai T, Kaisho T, Sato S, Sanjo H, Matsumoto M, Hoshino K, Wagner H, Takeda K and Akira S. (2000) A Toll-like receptor recognizes bacterial DNA. *Nature.* 408, 740- 745.

- Henderson A, Wu Y, Huang YC, Chavez EA, Platt J, Johnson FB, Brosh RM Jr, Sen D, Lansdorp PM. (2014) Detection of G-quadruplex DNA in mammalian cells. *Nucleic Acids Res.* 42, 860–869.
- Hershman SG, Chen Q, Lee JY, Kozak ML, Yue P, Wang LS, Johnson FB. (2008) Genomic distribution and functional analyses of potential G-quadruplex forming sequences in *Saccharomyces cerevisiae*. *Nucleic Acids Res.* 36, 144–156.
- Hewitt G, Jurk D, Marques FDM, Correia-Melo C, Hardy T, Gackowska A, Anderson R, Taschuk M, Mann J and Passos JF. (2012) Telomeres are favoured targets of a persistent DNA damage response in ageing and stress-induced senescence. *Nat Commun.* 3, 708.
- Heyman RA, Mangelsdorf DJ, Dyck JA, Stein RB, Eichele G, Evans RM and Thaller C. (1992) 9-cis retinoic acid is a high affinity ligand for the retinoid X receptor. *Cell.* 68, 397-406.
- Hickson ID. (2003) RecQ helicases: caretakers of the genome. *Nat. Rev. Cancer.* 3, 169-178.
- Hillestad LK. (1957) Acute Promyelocytic Leukemia. *J. Intern. Med.* 159, 189-194.
- Hilliker A. (2012) Analysis of RNA helicases in P-bodies and stress granules. *Methods Enzymol.* 511, 323–346.
- Ho PS and Carter M. (2011) DNA Structure: Alphabet Soup for the Cellular Soul, DNA Replication-Current Advances. Dr Herve Seligmann (Ed.). InTech.
- Hockensmith JW, Kubasek WL, Vorachek WR and von Hippel PH. (1986) Laser cross-linking of nucleic acids to proteins. Methodology and first applications to the phage T4 DNA replication system. *J. Biol. Chem.* 261, 3512-8.
- Hodgman TC. (1988) A new superfamily of replicative proteins. *Nature.* 333, 578.
- Hoffmann JA, Kafatos FC, Janeway CA and Ezekowitz RA. (1999) Phylogenetic perspectives in innate immunity. *Science.* 284, 1313- 1318.
- Holdeman LV, Kelley RW and Moore WEC. (1986) Family I Bacteroidaceae and genus I Bacteroides. In: Krieg NR and Holt JG (Eds.) *Bergey's Manual of Systematic Bacteriology*. 1st ed. Williams and Wilkins. Baltimore, MD.
- Hooper C and Hilliker A. (2013) Packing them up and dusting them off: RNA helicases and mRNA storage. *Biochim. Biophys. Acta.* 1829, 824–834.
- Hörlein AJ, Näär AM, Heinzl T, Torchia J, Gloss B, Kurokawa R, Ryan A, Kamei Y, Söderström M, Glass CK and Rosenfeld MG. (1995) Ligand-independent repression by the thyroid hormone receptor mediated by a nuclear receptor co-repressor. *Nature.* 377, 397-404.

Horner SM, Liu HM, Park HS, Briley J and Gale M Jr. (2011) Mitochondrial-associated endoplasmic reticulum membranes (MAM) form innate immune synapses and are targeted by hepatitis C virus. *Proc. Natl. Acad. Sci. U S A.* 108, 14590-14595.

Hornung V, Ablasser A, Charrel-Dennis M, Bauernfeind F, Horvath G, Caffrey DR, Latz E and Fitzgerald KA. (2009) AIM2 recognizes cytosolic dsDNA and forms a caspase-1-activating inflammasome with ASC. *Nature.* 458, 514-8.

Hornung V, Ellegast J, Kim S, Brzózka K, Jung A, Kato H, Poeck H, Akira S, Conzelmann KK, Schlee M, Endres S and Hartmann G. (2006) 5'-Triphosphate RNA is the ligand for RIG-I. *Science.* 314, 994-997.

Hou J, Zhou Y, Zheng Y, Fan J, Zhou W, Ng IO, Sun H, Qin L, Qiu S, Lee JM, Lo CM, Man K, Yang Y, Yang Y, Yang Y, Zhang Q, Zhu X, Li N, Wang Z, Ding G, Zhuang SM, Zheng L, Luo X, Xie Y, Liang A, Wang Z, Zhang M, Xia Q, Liang T, Yu Y and Cao X. (2014) Hepatic RIG-I Predicts Survival and Interferon- α Therapeutic Response in Hepatocellular Carcinoma. *Cancer Cell.* 25, 49-63.

Hou XM, Wu WQ, Duan XL, Liu NN, Li HH, Fu J, Dou SX, Li M and Xi XG. (2015) Molecular mechanism of G-quadruplex unwinding helicase: sequential and repetitive unfolding of G-quadruplex by Pif1 helicase. *Biochem J.* 466, 189-99.

Hu G, McQuiston T, Bernard A, Park YD, Qiu J, Vural A, Zhang N, Waterman SR, Blewett NH, Myers TG, Maraia RJ, Kehrl JH, Uzel G, Klionsky DJ and Williamson PR. (2015) A conserved mechanism of TOR-dependent RCK-mediated mRNA degradation regulates autophagy. *Nat. Cell Biol.* 17, 930-942.

Hu J, He Y, Yan M, Zhu C, Ye W, Zhu H, Chen W, Zhang C and Zhang Z. (2013) Dose dependent activation of retinoic acid-inducible gene-I promotes both proliferation and apoptosis signals in human head and neck squamous cell carcinoma. *PLoS One.* 8, e58273.

Huang F, Zhang J, Zhang Y, Geng G, Liang J, Li Y, Chen J, Liu C and Zhang H. (2015) RNA helicase MOV10 functions as a co-factor of HIV-1 Rev to facilitate Rev/RRE-dependent nuclear export of viral mRNAs. *Virology.* 486, 15-26.

Huber MD, Lee DC and Maizels N. (2002) G4 DNA unwinding by BLM and Sgs1p: substrate specificity and substrate-specific inhibition. *Nucleic Acids Res.* 30, 3954-3961.

Hug N and Caceres JF. (2014) The RNA helicase DHX34 activates NMD by promoting a transition from the surveillance to the decay-inducing complex. *Cell Rep.* 8, 1845-1856.

Huppert JL and Balasubramanian S. (2005) Prevalence of quadruplexes in the human genome. *Nucleic Acids Res.* 33, 2908-2916.

Huppert JL, Bugaut A, Kumari S, Balasubramanian S. (2008) G-quadruplexes: the beginning and end of UTRs. *Nucleic Acids Res.* 36, 6260-6268.

Huppert JL. (2008) Four-stranded nucleic acids: structure, function and targeting of G-quadruplexes. *Chem. Soc. Rev.* 37, 1375-1384.

Hurt JA and Silver PA. (2008) mRNA nuclear export and human disease. *Dis. Model Mech.* 1, 103 - 8.

Idres N, Benoît G, Flexor MA, Lanotte M, Chabot GG. (2001) Granulocytic differentiation of human NB4 promyelocytic leukemia cells induced by all-trans retinoic acid metabolites. *Cancer Res.* 61, 700-5.

Ilgan JO, Chalkley RJ, Burlingame AL and Jurica MS. (2013) Rearrangements within human spliceosomes captured after exon ligation. *RNA.* 19, 400–412.

Ilyina TV, Gorbalenya AE and Koonin EV. (1992) Organization and evolution of bacterial and bacteriophage primase-helicase systems. *J. Mol. Evol.* 34, 351–57.

Inn KS, Gack MU, Tokunaga F, Shi M, Wong LY, Iwai K and Jung JU. (2011) Linear ubiquitin assembly complex negatively regulates RIG-I- and TRIM25- mediated type I interferon induction. *Mol. Cell.* 41, 354-365.

Irimia M and Blencowe BJ. (2012) Alternative splicing: decoding an expansive regulatory layer. *Curr. Opin. Cell Biol.* 24, 323–332.

Isakson P, Bjørås M, Bøe SO and Simonsen A. (2010) Autophagy contributes to therapy-induced degradation of the PML/RARA oncoprotein. *Blood.* 116, 2324-31.

Ishaq M, Ma L, Wu X, Mu Y, Pan J, Hu J, Hu T, Fu Q and Guo D. (2009) The DEAD-box RNA helicase DDX1 interacts with RelA and enhances nuclear factor kappaB-mediated transcription. *J. Cell Biochem.* 106, 296 - 305.

Ishikawa H and Barber GN. (2008) STING is an endoplasmic reticulum adaptor that facilitates innate immune signalling. *Nature.* 455, 674-678.

Ishov AM, Sotnikov AG, Negorev D, Vladimirova OV, Neff N, Kamitani T, Yeh ET, Strauss JF 3rd and Maul GG. (1999) PML is critical for ND10 formation and recruits the PML-interacting protein daxx to this nuclear structure when modified by SUMO-1. *J. Cell Biol.* 147, 221-34.

Ivessa AS, Zhou JQ and Zakian VA. (2000) The *Saccharomyces* Pif1p DNA helicase and the highly related Rrm3p have opposite effects on replication fork progression in ribosomal DNA. *Cell.* 100, 479-89.

Ivessa AS, Zhou JQ, Schulz VP, Monson EK and Zakian VA. (2002) *Saccharomyces* Rrm3p, a 5' to 3' DNA helicase that promotes replication fork progression through telomeric and subtelomeric DNA. *Genes Dev.* 16, 1383–1396.

Jackson RN, Lavin M, Carter J and Wiedenheft B. (2014) Fitting CRISPR-associated Cas3 into the Helicase Family Tree. *Curr. Opin. Struct. Biol.* 0, 106–114.

- Jeang KT and Yedavalli V. (2006) Role of RNA helicases in HIV-1 replication. *Nucleic Acids Res.* 34, 4198–4205.
- Jensen TH, Boulay J, Rosbash M and Libri D. (2001) The DECD box putative ATPase Sub2p is an early mRNA export factor. *Curr. Biol.* 11, 1711-1715.
- Jezewska MJ, Rajendran S and Bujalowski W. (1998) Complex of Escherichia coli primary replicative helicase DnaB protein with a replication fork: recognition and structure. *Biochemistry.* 37, 3116–3136.
- Jiang F, Ramanathan A, Miller MT, Tang GQ, Gale M Jr, Patel SS and Marcotrigiano J. (2011) Structural basis of RNA recognition and activation by innate immune receptor RIG-I. *Nature* 479, 423-427.
- Jiang LJ, Zhang NN, Ding F, Li XY, Chen L, Zhang HX, Zhang W, Chen SJ, Wang ZG, Li JM, Chen Z and Zhu J. (2011) RA-inducible gene-I induction augments STAT1 activation to inhibit leukemia cell proliferation. *Proc. Natl. Acad. Sci. USA.* 108, 1897–1902.
- Jiang X, Kinch LN, Brautigam CA, Chen X, Du F, Grishin NV and Chen ZJ. (2012) Ubiquitin-induced oligomerization of the RNA sensors RIG-I and MDA5 activates antiviral innate immune response. *Immunity.* 36, 959-73.
- Jiang Y, Zhu Y, Liu ZJ and Ouyang S. (2017) The emerging roles of the DDX41 protein in immunity and diseases. *Protein Cell.* 8, 83.
- Jin L, Waterman PM, Jonscher KR, Short CM, Reisdorph NA and Cambier JC. (2008) MPYS, a novel membrane tetraspanner, is associated with major histocompatibility complex class II and mediates transduction of apoptotic signals. *Mol. Cell Biol.* 28, 5014-5026.
- Jing N, Gao X, Rando RF and Hogan ME. (1997) Potassium-induced loop conformational transition of a potent anti-HIV oligonucleotide. *J. Biomol. Struct. Dyn.* 15, 573-585.
- Jing NJ, Marchand C, Liu J, Mitra R, Hogan ME and Pommier Y. (2000) Mechanism of inhibition of HIV-1 integrase by G-tetrad-forming oligonucleotides in vitro. *J. Biol. Chem.* 275, 21460-21467.
- Johnson JL. (1978) Taxonomy of the bacteroides. I: Deoxyribonucleic acid homologies among Bacteroides fragilis and other saccharolytic Bacteroides species. *Int. J. Syst. Bacteriol.* 28, 245–256.
- Johnson SJ and Jackson RN. (2013) Ski2-like RNA helicase structures: common themes and complex assemblies. *RNA Biol.* 10, 33–43.
- Jonas S and Izaurralde E. (2015) Towards a molecular understanding of microRNA-mediated gene silencing. *Nat. Rev. Genet.* 16, 421-33.

- Jonveaux P, Le Coniat M, Derre J, Flexor MA, Daniel MT and Berger R. (1996) Chromosome microdissection in leukemia: a powerful tool for the analysis of complex chromosomal rearrangements. *Genes Chromosomes Cancer*.15, 26-33.
- Jounai N, Takeshita F, Kobiyama K, Sawano, A, Miyawaki A, Xin KQ, Ishii KJ, Kawai T, Akira S, Suzuki K and Okuda K. (2007) The Atg5 Atg12 conjugate associates with innate antiviral immune responses. *Proc. Natl. Acad. Sci. USA*. 104, 14050–14055.
- Jude CD, Gaudet JJ, Speck NA and Ernst P. (2008). Leukemia and hematopoietic stem cells: balancing proliferation and quiescence. *Cell Cycle*. 7, 586-591.
- Kanai Y, Dohmae N and Hirokawa N. (2004) Kinesin transports RNA: isolation and characterization of an RNA-transporting granule. *Neuron*. 43, 513 - 25.
- Kaneda Y. (2013) The RIG-I/MAVS signaling pathway in cancer cell-selective apoptosis. *Oncoimmunology*. 2, e23566.
- Kankia B, Gvarjaladze D, Rabe A, Lomidze L, Metreveli N and Musier-Forsyth K. (2016) Stable Domain Assembly of a Monomolecular DNA Quadruplex: Implications for DNA-Based Nanoswitches. *Biophys. J.* 110, 2169–2175.
- Kaplan DL, Davey MJ and O'Donnell M. (2003) Mcm4,6,7 uses a "pump in ring" mechanism to unwind DNA by steric exclusion and actively translocate along a duplex. *J. Biol. Chem.* 278, 49171–49182.
- Kaplan DL. (2000) The 3'-tail of a forked-duplex sterically determines whether one or two DNA strands pass through the central channel of a replication-fork helicase. *J. Mol. Biol.* 301, 285–299.
- Karlsen TA and Brinchmann JE. (2013) Liposome delivery of microRNA- 145 to mesenchymal stem cells leads to immunological off-target effects mediated by RIG-I. *Mol. Ther.* 21, 1169–1181.
- Karow AR and Klostermeier D. (2009) A conformational change in the helicase core is necessary but not sufficient for RNA unwinding by the DEAD box helicase YxiN. *Nucleic Acids Res.* 37, 4464-71.
- Kashyap V and Gudas LJ. (2010) Epigenetic regulatory mechanisms distinguish retinoic acid-mediated transcriptional responses in stem cells and fibroblasts. *J. Biol. Chem.* 285, 14534-48.
- Kato H, Sato S, Yoneyama M, Yamamoto M, Uematsu S, Matsui K, Tsujimura T, Takeda K, Fujita T, Takeuchi O and Akira S. (2005) Cell type-specific involvement of RIG-I in antiviral response. *Immunity*. 23, 19-28.
- Kato H, Takahashi K and Fujita T. (2011) RIG-I-like receptors: Cytoplasmic sensors for non-self RNA. *Immunol. Rev.* 243, 91-98.

- Kato H, Takeuchi O, Mikamo-Satoh E, Hirai R, Kawai T, Matsushita K, Hiiragi A, Dermody TS, Fujita T and Akira S. (2008) Length-dependent recognition of double-stranded ribonucleic acids by retinoic acid-inducible gene-I and melanoma differentiation-associated gene 5. *J. Exp. Med.* 205, 1601–1610.
- Kato H, Takeuchi O, Sato S, Yoneyama M, Yamamoto M, Matsui K, Uematsu S, Jung A, Kawai T, Ishii KJ, Yamaguchi O, Otsu K, Tsujimura T, Koh CS, Reis e Sousa C, Matsuura Y, Fujita T and Akira S. (2006) Differential roles of MDA5 and RIG-I helicases in the recognition of RNA viruses. *Nature.* 441, 101-105.
- Kato Y, Ohyama T, Mita H, Yamamoto Y. (2005) Dynamics and thermodynamics of dimerization of parallel G-quadruplexed DNA formed from d(TTAGn) (n=3-5). *J. Am. Chem. Soc.* 127, 9980–9981.
- Kawai S and Amano A. (2012) BRCA1 regulates microRNA biogenesis via the DROSHA microprocessor complex. *J. Cell Biol.* 197, 201–208.
- Kawai T and Akira S. (2011) Toll-like receptors and their crosstalk with other innate receptors in infection and immunity. *Immunity.* 34, 637-650.
- Kawai T, Takahashi K, Sato S, Coban C, Kumar H, Kato H, Ishii KJ, Takeuchi O and Akira S. (2005) IPS-1, an adaptor triggering RIG-I- and Mda5- mediated type I interferon induction. *Nat. Immunol.* 6, 981-988.
- Kawaoka J, Jankowsky E and Pyle AM. (2004) Backbone tracking by the SF2 helicase NPH-II. *Nat. Struct. Mol. Biol.* 11, 526–530.
- Keil RL and McWilliams AD. (1993) A gene with specific and global effects on recombination of sequences from tandemly repeated genes in *Saccharomyces cerevisiae*. *Genetics.* 135, 711-8.
- Kelley S, Boroda S, Musier-Forsyth K and Kankia BI. (2011) HIV-integrase aptamer folds into a parallel quadruplex: a thermodynamic study. *Biophys. Chem.* 155, 82–88.
- Khanna-Gupta A, Kolibaba K, Zibello TA and Berliner N. (1994) NB4 cells show bilineage potential and an aberrant pattern of neutrophil secondary granule protein gene expression. *Blood.* 84, 294-302.
- Kim H and D'Andrea AD. (2012) Regulation of DNA cross-link repair by the Fanconi anemia/BRCA pathway. *Genes Dev.* 26, 1393-408.
- Kim JL, Morgenstern KA, Griffith JP, Dwyer MD, Thomson JA, Murcko MA, Lin C and Caron PR (1998) Hepatitis C virus NS3 RNA helicase domain with a bound oligonucleotide: the crystal structure provides insights into the mode of unwinding. *Structure.* 6, 89-100.
- Kim MY, Vankayalapati H, Shin-Ya K, Wierzba K and Hurley LH. (2002) Telomestatin, a potent telomerase inhibitor that interacts quite specifically with the human telomeric intramolecular G-quadruplex. *J. Am. Chem. Soc.* 124, 2098–2099.

Kim NW, Piatyszek MA, Prowse KR, Harley CB, West MD, Ho PL, Coviello GM, Wright WE, Weinrich SL and Shay JW. (1994) Specific association of human telomerase activity with immortal cells and cancer. *Science*. 266, 2011–2015.

Kim T, Pazhoor S, Bao M, Zhang Z, Hanabuchi S, Facchinetti V, Bover L, Plumas J, Chaperot L, Qin J and Liu YJ. (2010) Aspartateglutamate-alanine-histidine box motif (DEAH)/RNA helicase A helicases sense microbial DNA in human plasmacytoid dendritic cells. *Proc. Natl. Acad. Sci. U S A*. 107, 15181–15186.

Kirschning CJ, Wesche H, Merrill Ayres T and Rothe M. (1998) Human toll-like receptor 2 confers responsiveness to bacterial lipopolysaccharide. *J. Exp. Med.* 188, 2091–2097.

Klostermeier D and Rudolph MG (2009) A novel dimerization motif in the C-terminal domain of the *Thermus thermophilus* DEAD box helicase Hera confers substantial flexibility. *Nucleic Acids Res.* 37, 421–430.

Kok KH, Lui PY, Ng MH, Siu KL, Au SW, Jin DY. (2011) The double-stranded RNA-binding protein PACT functions as a cellular activator of RIG-I to facilitate innate antiviral response. *Cell Host. Microbe*. 9, 299–309.

Koken MH, Puvion-Dutilleul F, Guillemain MC, Viron A, Linares-Cruz G, Stuurman N, de Jong L, Szosteki C, Calvo F and Chomienne C. (1994) The t(15;17) translocation alters a nuclear body in a retinoic acid-reversible fashion. *EMBO J.* 13, 1073–83.

Komuro A and Horvath CM. (2006) RNA- and virus-independent inhibition of antiviral signaling by RNA helicase LGP2. *J. Virol.* 80, 12332–42.

Kondo T, Mori A, Darmanin S, Hashino S, Tanaka J and Asaka M. (2008) The seventh pathogenic fusion gene FIP1L1-RARA was isolated from a t(4;17)-positive acute promyelocytic leukemia. *Haematologica*. 93, 1414–16.

König SL, Evans AC and Huppert JL. (2010) Seven essential questions on G-quadruplexes. *Biomol. Concepts*. 1, 197–213.

Konno H, Yamamoto T, Yamazaki K, Gohda J, Akiyama T, Semba K, Goto H, Kato A, Yujiri T, Imai T, Kawaguchi Y, Su B, Takeuchi O, Akira S, Tsunetsugu-Yokota Y and Inoue J. (2009) TRAF6 establishes innate immune responses by activating NF- κ B and IRF7 upon sensing cytosolic viral RNA and DNA. *PLoS One*. 4, e5674.

Koodathingal P and Staley JP. (2013) Splicing fidelity: DEAD/H-box ATPases as molecular clocks. *RNA Biol.* 10, 1073–1079.

Korolev S, Hsieh J, Gauss GH, Lohman TM and Waksman G. (1997) Major domain swiveling revealed by the crystal structures of complexes of *E. coli* Rep helicase bound to single-stranded DNA and ADP. *Cell*. 90, 635–47.

Kouzaki H, Iijima K, Kobayashi T, O'Grady SM and Kita H. (2011) The danger signal, extracellular ATP, is a sensor for an airborne allergen and triggers IL-33 release and innate Th2-type responses. *J. Immunol.* 186, 4375–4387.

- Kowalinski E, Lunardi T, McCarthy AA, Louber J, Brunel J, Grigorov B, Gerlier D and Cusack S. (2011) Structural basis for the activation of innate immune pattern-recognition receptor RIG-I by viral RNA. *Cell*. 147, 423-435.
- Krause DS, Lazarides K, Lewis JB, von Andrian UH and Van Etten RA. (2014) Selectins and their ligands are required for homing and engraftment of BCR-ABL1+ leukemic stem cells in the bone marrow niche. *Blood*. 123, 1361-71.
- Kressler D, Linder P and de La Cruz J. (1999) Protein trans-acting factors involved in ribosome biogenesis in *Saccharomyces cerevisiae*. *Mol. Cell Biol*. 19, 7897-912.
- Krol J, Krol I, Alvarez CP, Fiscella M, Hierlemann A, Roska B and Filipowicz W. (2015) A network comprising short and long noncoding RNAs and RNA helicase controls mouse retina architecture. *Nat. Commun*. 4, 7305.
- Kubler K, Gehrke N, Riemann S, Böhnert V, Zillinger T, Hartmann E, Pölcher M, Rudlowski C, Kuhn W, Hartmann G and Barchet W. (2010) Targeted activation of RNA helicase retinoic acid-inducible gene-I induces proimmunogenic apoptosis of human ovarian cancer cells. *Cancer Res*. 70, 5293-304.
- Kusumoto R, Dawut L, Marchetti C, Wan Lee J, Vindigni A, Ramsden D and Bohr VA. (2008) Werner protein cooperates with the XRCC4-DNA ligase IV complex in end-processing. *Biochemistry*. 47, 7548-56.
- Lahaye A, Leterme S, Foury F. (1993) Pif1 DNA helicase from *Saccharomyces Cerevisiae*. Biochemical characterization of the enzyme. *J. Biol. Chem*. 268, 26155–26161.
- Lahaye A, Stahl H, Thines-Sempoux D and Foury F. (1991) PIF1: a DNA helicase in yeast mitochondria. *EMBO J*. 10, 997-1007.
- Lai MC, Chang WC, Shieh SY and Tarn WY. (2010) DDX3 regulates cell growth through translational control of cyclin E1. *Mol. Cell. Biol*. 30, 5444–5453.
- Lai MC, Lee YH and Tarn WY. (2008) The DEAD-box RNA helicase DDX3 associates with export messenger ribonucleoproteins as well as tip-associated protein and participates in translational control. *Mol. Biol. Cell*. 19, 3847–3858.
- Lallemand-Breitenbach V, Jeanne M, Benhenda S, Nasr R, Lei M, Peres L, Zhou J, Zhu J, Raught B and de Thé H. (2008) Arsenic degrades PML or PML-RARalpha through a SUMO-triggered RNF4/ubiquitin-mediated pathway. *Nat. Cell Biol*. 10, 547-55.
- Lane AN, Chaires JB, Gray RD and Trent, JO. (2008) Stability and kinetics of G-quadruplex structures. *Nucleic Acids Res*. 36, 5482–5515.
- Lanotte M, Martin-Thouvenin V, Najman S, Balerini P, Valensi F and Berger R. (1991) NB4, a maturation inducible cell line with t(15;17) marker isolated from a human acute promyelocytic leukemia (M3). *Blood*. 77, 1080-6.

- Larson ED, Duquette ML, Cummings WJ, Streiff RJ and Maizels N. (2005) MutSalpha binds to and promotes synapsis of transcriptionally activated immunoglobulin switch regions. *Curr Biol.* 15, 470-4.
- Larson RS, Brown DC and Sklar LA. (1997) Retinoic acid induces aggregation of the acute promyelocytic leukemia cell line NB-4 by utilization of LFA-1 and ICAM-2. *Blood.* 90, 2747-56.
- Lässig C, Matheisl S, Sparrer KM, de Oliveira Mann CC, Moldt M, Patel JR, Goldeck M, Hartmann G, García-Sastre A, Hornung V, Conzelmann KK, Beckmann R and Hopfner KP. (2015) ATP hydrolysis by the viral RNA sensor RIG-I prevents unintentional recognition of self-RNA. *eLife.* 4, e10859.
- Lattmann S, Giri B, Vaughn JP, Akman SA and Nagamine Y. (2010) Role of the amino terminal RHAU-specific motif in the recognition and resolution of guanine quadruplex-RNA by the DEAH-box RNA helicase RHAU. *Nucleic Acids Res.* 38, 6219-33.
- Laurent BC1, Treich I and Carlson M. (1993) The yeast SNF2/SWI2 protein has DNA-stimulated ATPase activity required for transcriptional activation. *Genes Dev.* 7, 583-91.
- Le Blancq SM, Kase RS and Van der Ploeg LH. (1991) Analysis of a *Giardia lamblia* rRNA encoding telomere with [TAGGG]_n as the telomere repeat. *Nucleic Acids Res.* 19, 5790.
- Le Guen T, Jullien L, Touzot F, Schertzer M, Gaillard L, Perderiset M, Carpentier W, Nitschke P, Picard C, Couillault G, Soulier J, Fischer A, Callebaut I, Jabado N, Londono-Vallejo A, de Villartay JP and Revy P. (2013) Human RTEL1 deficiency causes Hoyeraal-Hreidarsson syndrome with short telomeres and genome instability. *Hum. Mol. Genet.* 22, 3239-49.
- Lebel M, Lavoie J, Gaudreault I, Bronsard M and Drouin R. (2003) Genetic cooperation between the Werner syndrome protein and poly(ADP-ribose) polymerase-1 in preventing chromatid breaks, complex chromosomal rearrangements, and cancer in mice. *Am. J. Pathol.* 162, 1559-69.
- Lech CJ, Heddi B and Phan AT. (2013) Guanine base stacking in G-quadruplex nucleic acids. *Nucleic Acids Res.* 41, 2034–2046 .
- Lee CG, Zamore PD, Green MR and Hurwitz J. (1993) RNA annealing activity is intrinsically associated with U2AF. *J.Biol. Chem.* 268, 13472–13478.
- Lee JY and Yang W. (2006) UvrD helicase unwinds DNA one base pair at a time by a two-part power stroke. *Cell.* 127, 1349-60.
- Legrand-Poels S, Kustermans G, Bex F, Kremmer E, Kufer TA and Piette J. (2007) Modulation of Nod2-dependent NF-kappaB signaling by the actin cytoskeleton. *J. Cell. Sci.* 120, 1299-310.

- Legües ME, Franco G and Bertin P. (2002) Pilot study of PML/RAR alpha fusion by fluorescence in situ hybridization (FISH) method in acute promyelocyte leukemia. *Rev. Med. Chil.* 130, 737-44.
- Leid M, Kastner P, Lyons R, Nakshatri H, Saunders M, Zacharewski T, Chen JY, Staub A, Garnier JM, Mader S and Chambon P (1992) Purification, cloning, and RXR identity of the HeLa cell factor with which RAR or TR heterodimerizes to bind target sequences efficiently. *Cell.* 68, 377-95.
- León-Ortiz AM, Svendsen J and Boulton SJ. (2014) Metabolism of DNA secondary structures at the eukaryotic replication fork. *DNA Repair (Amst).* 19, 152-62.
- Leung DW and Amarasinghe GK. (2016) When your cap matters: structural insights into self vs non-self recognition of 5' RNA by immunomodulatory host proteins. *Curr. Opin. Struct. Biol.* 36, 133–141.
- Leung DW, Basler CF and Amarasinghe GK. (2012) Molecular mechanisms of viral inhibitors of RIG-I-like receptors. *Trends Microbiol.* 20, 139-146.
- Levin MK, Gurjar M and Patel SS. (2005) A Brownian motor mechanism of translocation and strand separation by hepatitis C virus helicase. *Nat. Struct. Mol. Biol.* 12, 429-35.
- Levy DE and Darnell JE Jr. (2002) Stats: transcriptional control and biological impact. *Nat. Rev. Mol. Cell. Biol.* 3, 651-62
- Ley RE, Backhed F, Turnbaugh PJ, Lozupone CA, Knight RD and Gordon JI. (2005) Obesity alters gut microbial ecology. *Proc. Natl. Acad. Sci. USA.* 102, 11070-11075.
- Ley RE, Turnbaugh PJ, Klein S and Gordon JI. 2006. Microbial ecology: human gut microbes associated with obesity. *Nature.* 444, 1022-1023.
- Li J, Briehner WM, Scimone ML, Kang SJ, Zhu H, Yin H, von Andrian UH, Mitchison T and Yuan J. (2007) Caspase-11 regulates cell migration by promoting Aip1-Cofilin-mediated actin depolymerization. *Nat Cell Biol.* 9, 276-86.
- Li QJ, Tong XJ, Duan YM and Zhou JQ. (2013) Characterization of the intramolecular G-quadruplex promoting activity of Est1. *FEBS Lett.* 587, 659-65.
- Li W, Chen H, Sutton T, Obadan A and Perez DR. (2014) Interactions between the influenza A virus RNA polymerase components and retinoic acid-inducible gene I. *J. Virol.* 88, 10432-47.
- Li X, Ranjith-Kumar CT, Brooks MT, Dharmiah S, Herr AB, Kao C and Li P. (2009) The RIG-I-like receptor LGP2 recognizes the termini of double-stranded RNA. *J. Biol. Chem.* 284, 13881-91.
- Li XD, Wu J, Gao D, Wang H, Sun L and Chen ZJ. (2013) Pivotal roles of cGAS-cGAMP signaling in antiviral defense and immune adjuvant effects. *Science.* 341, 1390–1394.

- Li XY, Jiang LJ, Chen L, Ding ML, Guo HZ, Zhang W, Zhang HX, Ma XD, Liu XZ, Xi XD, Chen SJ, Chen Z and Zhu J. (2014) RIG-I modulates Src-mediated AKT activation to restrain leukemic stemness. *Mol. Cell.* 53, 407-19.
- Li Y, Chen R, Zhou Q, Xu Z, Li C, Wang S, Mao A, Zhang X, He W and Shu HB. (2012) LSm14A is a processing body-associated sensor of viral nucleic acids that initiates cellular antiviral response in the early phase of viral infection. *Proc. Natl. Acad. Sci. U S A.* 109, 11770–11775.
- Lia G, Praly E, Ferreira H, Stockdale C, Tse-Dinh YC, Dunlap D, Croquette V, Bensimon D and Owen-Hughes T. (2006) Direct observation of DNA distortion by the RSC complex. *Mol. Cell.* 21, 417–425.
- Licht JD. (2006) Reconstructing a disease: What essential features of the retinoic acid receptor fusion oncoproteins generate acute promyelocytic leukemia? *Cancer Cell.* 9, 73-4.
- Lim KW, Alberti P, Guédin A, Lacroix L, Riou JF, Royle NJ, Mergny JL and Phan AT. (2009) Sequence variant (CTAGGG)_n in the human telomere favors a G-quadruplex structure containing a G·C·G·C tetrad. *Nucleic Acids Res.* 37, 6239–6248.
- Lim YJ, Koo JE, Hong EH, Park ZY, Lim KM, Bae ON and Lee JY. (2015) A Src-family-tyrosine kinase, Lyn, is required for efficient IFN-β expression in pattern recognition receptor, RIG-I, signal pathway by interacting with IPS-1. *Cytokine.* 72, 63-70.
- Lin RJ and Evans RM. (2000) Acquisition of oncogenic potential by RAR chimeras in acute promyelocytic leukemia through formation of homodimers. *Mol. Cell.* 5, 821-30.
- Lipps HJ and Rhodes D. (2009) G-quadruplex structures: in vivo evidence and function. *Trends Cell Biol.* 19, 414-22.
- Liu B, Baskin RJ, Kowalczykowski SC. (2013) DNA unwinding heterogeneity by RecBCD results from static molecules able to equilibrate. *Nature.* 500, 482–85.
- Liu HM, Jiang F, Loo YM, Hsu S, Hsiang TY, Marcotrigiano J and Gale MJ (2016) Regulation of retinoic acid inducible gene-I (RIG-I) activation by the histone deacetylase 6. *EBioMedicine.* 9, 195–206.
- Liu HM, Loo YM, Horner SM, Zornetzer GA, Katze MG, Gale M Jr. (2012) The mitochondrial targeting chaperone 14-3-3ε regulates a RIG-I translocon that mediates membrane association and innate antiviral immunity. *Cell Host. Microbe.* 11, 528-37.
- Liu NN, Duan XL, Ai X, Yang YT, Li M, Dou SX, Rety S, Deprez E and Xi XG. The Bacteroides sp. 3_1_23 Pif1 protein is a multifunctional helicase. *Nucleic Acids Res.* 43, 8942-54.
- Liu TX, Zhang JW, Tao J, Zhang RB, Zhang QH, Zhao CJ, Tong JH, Lanotte M, Waxman S, Chen SJ, Mao M, Hu GX, Zhu L and Chen Z. (2000) Gene expression networks underlying retinoic acid-induced differentiation of acute promyelocytic leukemia cells. *Blood.* 96, 1496-504.

- Liu Y, Kao HI, Bambara RA. (2004) Flap endonuclease 1: a central component of DNA metabolism. *Annu. Rev. Biochem.* 73, 589-615.
- Liu Y. (2010) Rothmund-Thomson syndrome helicase, RECQ4: On the crossroad between DNA replication and repair. *DNA Repair (Amst)*. 9, 325-30.
- Liu Z, Dou C, Yao B, Xu M, Ding L, Wang Y, Jia Y, Li Q, Zhang H, Tu K, Song T and Liu Q. (2016) Ftx non coding RNA-derived miR-545 promotes cell proliferation by targeting RIG-I in hepatocellular carcinoma. *Oncotarget*. 7, 25350–25365.
- Lohman TM and Bjornson KP. (1996) Mechanisms of helicase-catalyzed DNA unwinding. *Annu Rev Biochem.* 65, 169-214.
- Lohman TM. (1992) Escherichia coli DNA helicases: mechanisms of DNA unwinding. *Mol. Microbiol.* 6, 5–14.
- Lomidze L, Kelley S, Gogichaishvili S, Metreveli N, Musier-Forsyth K and Kankia B. (2016) Sr(2+) induces unusually stable d(GGGTGGGTGGGTGGG) quadruplex dimers. *Biopolymers*. 105, 811-8.
- London TB, Barber LJ, Mosedale G, Kelly GP, Balasubramanian S, Hickson ID, Boulton SJ and Hiom K. (2008) FANCD1 is a structure-specific DNA helicase associated with the maintenance of genomic G/C tracts. *J. Biol. Chem.* 283, 36132-9.
- Loo YM and Gale M Jr. (2011) Immune signaling by RIG-I-like receptors. *Immunity*. 34, 680-692.
- Loo YM, Fornek J, Crochet N, Bajwa G, Perwitasari O, Martinez-Sobrido L, Akira S, Gill MA, García-Sastre A, Katze MG and Gale M Jr. (2008) Distinct RIG-I and MDA5 signaling by RNA viruses in innate immunity. *J. Virol.* 82, 335–345.
- Lopes J, Piazza A, Bermejo R, Kriegsman B, Colosio A, Teulade-Fichou MP, Foiani M and Nicolas A. (2011) G-quadruplex-induced instability during leading-strand replication. *EMBO J.* 30, 4033–4046.
- Lopes J, Ribeyre C, Nicolas A. (2006) Complex minisatellite rearrangements generated in the total or partial absence of Rad27/hFEN1 activity occur in a single generation and are Rad51 and Rad52 dependent. *Mol. Cell Biol.* 26, 6675-89.
- Louber J and Gerlier D. (2010) Motifs d'ARN viraux et récepteurs de type RIG-I déclencheurs de l'interféron. *Virologie*. 14, 203-16.
- Lu C, Xu H, Ranjith-Kumar CT, Brooks MT, Hou TY, Hu F, Herr AB, Strong RK, Kao CC and Li P. (2010) The Structural Basis of 5' Triphosphate Double-Stranded RNA Recognition by RIG-I C-Terminal Domain. *Structure*. 18, 1032-43.
- Lu KY, Chen WF, Rety S, Liu NN, Wu WQ, Dai YX, Li D, Ma HY, Dou SX, Xi XG. (2017) Insights into the structural and mechanistic basis of multifunctional *S. cerevisiae* Pif1p helicase, *Nucleic Acids Res.* gkx1217.

- Lucic B, Zhang Y, King O, Mendoza-Maldonado R, Berti M, Niesen FH, Burgess-Brown NA, Pike ACW, Cooper CDO, Gileadi O and Vindigni A. (2011) A prominent β -hairpin structure in the winged-helix domain of RECQ1 is required for DNA unwinding and oligomer formation. *Nucleic Acids Res.* 39, 1703–1717.
- Lue NF. (2004) Adding to the ends: what makes telomerase processive and how important is it? *BioEssays.* 26, 955-962.
- Lue NF. (2010) Plasticity of telomere maintenance mechanisms in yeast. *Trends. Biochem. Sci.* 35, 8–17.
- Lüking A, Stahl U and Schmidt U. (1998) The protein family of RNA helicases. *Crit. Rev. Biochem. Mol. Biol.* 33, 259-96.
- Lund MK and Guthrie C. (2005) The DEAD-box protein Dbp5p is required to dissociate Mex67p from exported mRNPs at the nuclear rim. *Mol. Cell.* 20, 645-51.
- Luo D, Ding SC, Vela A, Kohlway A, Lindenbach BD and Pyle AM. (2011) Structural insights into RNA recognition by RIG-I. *Cell.* 147, 409-22.
- Luo ML, Zhou Z, Magni K, Christoforides C, Rappsilber J, Mann M and Reed R. (2001) Pre-mRNA splicing and mRNA export linked by direct interactions between UAP56 and Aly. *Nature.* 413, 644-647.
- Luu KN, Phan AT, Kuryavyi V, Lacroix L, Patel DJ. (2006) Structure of the human telomere in K⁺ solution: an intramolecular (3 + 1) G-quadruplex scaffold. *J. Am. Chem. Soc.* 128, 9963–9970.
- Lykke-Andersen S and Jensen TH. (2015) Nonsense-mediated mRNA decay: an intricate machinery that shapes transcriptomes. *Nat. Rev. Mol. Cell Biol.* 16, 665–677.
- Machwe A, Lozada EM, Xiao L and Orren DK. (2006) Competition between the DNA unwinding and strand pairing activities of the Werner and Bloom syndrome proteins. *BMC. Mol. Biol.* 7, 1.
- Macris MA, Krejci L, Bussen W, Shimamoto A and Sung P. (2006) Biochemical characterization of the RECQ4 protein, mutated in Rothmund-Thomson syndrome. *DNA Repair (Amst).* 5, 172-180.
- Macy JM. (1984) The biology of gastrointestinal Bacteroides. *Ann. Rev. Microbiol.* 33, 561–594.
- Maelfait J and Beyaert R. (2012) Emerging role of ubiquitination in antiviral RIG-I signaling. *Microbiol. Mol. Biol. Rev.* 76, 33-45.
- Maharaj NP, Wies E, Stoll A and Gack MU. (2012) Conventional protein kinase C-alpha (PKCalpha) and PKC-beta negatively regulate RIG-I antiviral signal transduction. *J. Virol.* 86, 1358-137.
- Maizels N and Gray LT. (2013) The G4 Genome. *PLoS Genet.* 9, e1003468.

- Makarov VL, Hirose Y and Langmore JP. (1997) Long G tails at both ends of human chromosomes suggest a C strand degradation mechanism for telomere shortening. *Cell*. 88, 657–666.
- Makovets S and Blackburn EH. (2009) DNA damage signalling prevents deleterious telomere addition at DNA breaks. *Nat. Cell Biol.* 11, 1383–1386.
- Malathi K, Dong B, Gale M and Silverman RH. (2007) Small self-RNA generated by RNase L amplifies antiviral innate immunity. *Nature*. 448, 816–819.
- Mangelsdorf DJ, Evans RM. (1995) The RXR heterodimers and orphan receptors. *Cell*. 83, 841-50.
- Mark M, Ghyselinck NB, Wendling O, Dupé V, Mascrez B, Kastner P and Chambon P. (1999) A genetic dissection of the retinoid signalling pathway in the mouse. *Proc. Nutr. Soc.* 58, 609-13.
- Marq JB, Hausmann S, Veillard N, Kolakofsky D and Garcin D. (2011) Short double-stranded RNAs with an overhanging 5' pppnucleotide, as found in arenavirus genomes, act as RIG-I decoys. *J. Biol. Chem.* 286, 6108–6116.
- Marq JB, Kolakofsky D and Garcin D. (2010) Unpaired 5' ppp-nucleotides, as found in arenavirus double-stranded RNA panhandles, are not recognized by RIG-I. *J. Biol. Chem.* 285, 18208–18216.
- Martadinata H and Phan AT. (2009) Structure of propeller-type parallel-stranded RNA G-quadruplexes, formed by human telomeric RNA sequences in K⁺ solution. *J. Am. Chem. Soc.* 131, 2570–2578.
- Martens JH and Stunnenberg HG. (2010) The molecular signature of oncofusion proteins in acute myeloid leukemia. *FEBS Lett.* 584, 2662-9.
- Martínez P and Blasco MA. (2011) Telomeric and extra-telomeric roles for telomerase and the telomere-binding proteins. *Nat. Rev. Cancer.* 11, 161-76.
- Martinon F and Tschopp J. (2004) Inflammatory caspases: linking an intracellular innate immune system to autoinflammatory diseases. *Cell*. 117, 561-74.
- Masuda-Sasa T, Polaczek P and Campbell JL. (2006) Single strand annealing and ATP-independent strand exchange activities of yeast and human DNA2: Possible role in Okazaki fragment maturation. *J. Biol. Chem.* 281, 38555–38564.
- Mathieu J and Besançon F. (2006) Arsenic trioxide represses NF-kappaB activation and increases apoptosis in ATRA-treated APL cells. *Ann. N. Y. Acad. Sci.* 1090, 203-8.
- Matson SW, Bean DW and George JW. (1994) DNA helicases: enzymes with essential roles in all aspects of DNA metabolism. *Bioessays*. 16, 13-22.

Matsumiya T, Imaizumi T, Yoshida H, Satoh K, Topham MK and Stafforini DM. (2009) The levels of retinoic acid-inducible gene I are regulated by heat shock protein 90-alpha. *J. Innunol.* 182, 2717-25.

Mazmanian SK and Kasper DL. (2006) The love-hate relationship between bacterial polysaccharides and the host immune system. *Nat. Rev. Immunol.* 6, 849-858.

Mazmanian SK, Liu CH, Tzianabos AO and Kasper DL. (2005) An immunomodulatory molecule of symbiotic bacteria directs maturation of the host immune system. *Cell.* 122, 107-118.

McCartney SA, Thackray LB, Gitlin L, Gilfillan S, Virgin HW and Colonna M. (2008). MDA-5 recognition of a murine norovirus. *PLoS Pathog.* 4, e1000108.

McGeoch AT, Trakselis MA, Laskey RA and Bell SD. (2005) Asymmetric interactions of hexameric bacteriophage T7 DNA helicase with the 5'- and 3'-tails of the forked DNA substrate. *Nat. Struct.Mol. Biol.* 12, 756-762.

McInerney EM, Rose DW, Flynn SE, Westin S, Mullen TM, Kronen A, Inostroza J, Torchia J, Nolte RT, Assa-Munt N, Milburn MV, Glass CK and Rosenfeld MG. (1998) Determinants of coactivator LXXLL motif specificity in nuclear receptor transcriptional activation. *Genes Dev.* 12, 3357-68.

Medzhitov R, Preston- Hurlburt P and Janeway CA Jr. (1997) A human homologue of the Drosophila Toll protein signals activation of adaptive immunity. *Nature.* 388, 394-397.

Meetei AR, de Winter JP, Medhurst AL, Wallisch M, Waisfisz Q, van de Vrugt HJ, Oostra AB, Yan Z, Ling C, Bishop CE, Hoatlin ME, Joenje H and Wang W. (2003) A novel ubiquitin ligase is deficient in Fanconi anemia. *Nat. Genet.* 35, 165-70.

Mehta K, McQueen T, Neamati N, Collins S and Andreeff M. (1996) Activation of retinoid receptors RAR alpha and RXR alpha induces differentiation and apoptosis, respectively, in HL-60 cells. *Cell Growth Differ.* 7, 179-86.

Melnick A, Fruchtman S, Zelent A, Liu M, Huang Q, Boczkowska B, Calasanz M, Fernandez A, Licht JD and Najfeld V. (1999) Identification of novel chromosomal rearrangements in acute myelogenous leukemia involving loci on chromosome 2p23, 15q22 and 17q21. *Leukemia.* 13, 1534-8.

Mendoza O, Bourdoncle A, Boulé JB, Brosh RM Jr and Mergny JL. (2016) G-quadruplexes and helicases. *Nucleic Acids Res.* 44, 1989-2006.

Mergny JL, Phan AT and Lacroix L. (1998) Following G-quartet formation by UV-spectroscopy. *FEBS Lett.* 435, 74-78.

Meylan E, Curran J, Hofmann K, Moradpour D, Binder M, Bartenschlager R and Tschopp J. (2005) Cardif is an adaptor protein in the RIG-I antiviral pathway and is targeted by hepatitis C virus. *Nature.* 437, 1167-1172.

Mi Z, Fu J, Xiong Y and Tang H. (2010) SUMOylation of RIG-I positively regulates the type I interferon signaling. *Prot. Cell.* 1, 275-283.

Minucci S, Maccarana M, Cioce M, De Luca P, Gelmetti V, Segalla S, Di Croce L, Giavara S, Matteucci C, Gobbi A, Bianchini A, Colombo E, Schiavoni I, Badaracco G, Hu X, Lazar MA, Landsberger N, Nervi C and Pelicci PG. (2000) Oligomerization of RAR and AML1 transcription factors as a novel mechanism of oncogenic activation. *Mol. Cell.* 5, 811-20.

Mitsui Y, Langridge R, Shortle BE, Cantor CR, Grant RC, Kodama M and Wells RD. (1970) Physical and enzymatic studies on poly d(I-C)-poly d(I-C), an unusual double-helical DNA. *Nature.* 228, 1166-9.

Mizel SB, West AP and Hantgan RR. (2003) Identification of a sequence in human toll-like receptor 5 required for the binding of Gramnegative flagellin. *J. Biol. Chem.* 278, 23624–23629.

Modelska A, Turro E, Russell R, Beaton J, Sbarrato T, Spriggs K, Miller J, Gräf S, Provenzano E, Blows F, Pharoah P, Caldas C and Le Quesne J. (2015) The malignant phenotype in breast cancer is driven by eIF4A1-mediated changes in the translational landscape. *Cell Death Dis.* 6, e1603.

Mohr G, Del Campo M, Mohr S, Yang Q, Jia H, Jankowsky E and Lambowitz AM (2008) Function of the C-terminal domain of the DEAD-box protein Mss116p analyzed in vivo and in vitro. *J Mol Biol.* 375, 1344-1364

Monie TP, Moncrieffe MC and Gay NJ. (2009) Structure and regulation of cytoplasmic adapter proteins involved in innate immune signaling. *Immunol. Rev.* 227, 161-75.

Monson EK, de Bruin D and Zakian VA (1997) The yeast Cac1 protein is required for the stable inheritance of transcriptionally repressed chromatin at telomeres. *Proc. Natl Acad. Sci. U.S.A.* 94, 13081–13086.

Morosky SA, Zhu J, Mukherjee A, Sarkar SN and Coyne CB. (2011) Retinoic acid-induced gene-I (RIG-I) associates with nucleotide-binding oligomerization domain-2 (NOD2) to negatively regulate inflammatory signaling. *J. Biol. Chem.* 286, 28574-83.

Motiño O, Francés DE, Mayoral R, Castro-Sánchez L, Fernández-Velasco M, Boscá L, García-Monzón C, Brea R, Casado M, Agra N, Martín-Sanz P. (2015) Regulation of microRNA 183 by cyclooxygenase 2 in liver is DEAD-box helicase p68 (DDX5) dependent: role in insulin signaling. *Mol. Cell. Biol.* 35, 2554–2567.

Moy RH, Cole BS, Yasunaga A, Gold B, Shankarling G, Varble A, Molleston JM, tenOever BR, Lynch KW and Cherry S. (2014) Stem-loop recognition by DDX17 facilitates miRNA processing and antiviral defense. *Cell.* 158, 764–777.

- Moyzis RK, Buckingham JM, Cram LS, Dani M, Deaven LL, Jones MD, Meyne J, Ratliff RL, and Wu JR. (1988) A highly conserved repetitive DNA sequence, (TTAGGG)_n, present at the telomeres of human chromosomes. *Proc Natl Acad Sci U S A*. 85, 6622–6626.
- Mu X, Ahmad S and Hur S. (2016) Endogenous retroelements and the host innate immune sensors. *Adv. Immunol.* 132, 47–69.
- Muchardt C and Yaniv M. (1993) A human homologue of *Saccharomyces cerevisiae* SNF2/SWI2 and *Drosophila* brm genes potentiates transcriptional activation by the glucocorticoid receptor. *EMBO J.* 12, 4279-90.
- Muftuoglu M, Kulikowicz T, Beck G, Lee JW, Piotrowski J and Bohr VA. (2008) Intrinsic ssDNA annealing activity in the C-terminal region of WRN. *Biochemistry.* 47, 10247-10254.
- Muftuoglu M, Sharma S, Thorslund T, Stevnsner T, Soerensen MM, Brosh RM Jr and Bohr VA. (2006) Cockayne syndrome group B protein has novel strand annealing and exchange activities. *Nucleic Acids Res.* 34, 295–304.
- Muindi J, Frankel SR, Miller WH Jr, Jakubowski A, Scheinberg DA, Young CW, Dmitrovsky E and Warrell RP Jr. (1992) Continuous treatment with all-trans retinoic acid causes a progressive reduction in plasma drug concentrations: implications for relapse and retinoid "resistance" in patients with acute promyelocytic leukemia. *Blood.* 79, 299-303.
- Mukherjee A, Morosky SA, Shen L, Weber CR, Turner JR, Kim KS, Wang T, Coyne CB. (2009) Retinoic Acid-induced Gene-1 (RIG-I) associates with the actin cytoskeleton via caspase activation and recruitment domain-dependent interactions. *J. Biol. Chem.* 284, 6486–6494.
- Mukundan VT and Phan AT. (2013) Bulges in G-quadruplexes: broadening the definition of G-quadruplex-forming sequences. *J. Am. Chem. Soc.* 135, 5017-28.
- Mullen MA, Olson KJ, Dallaire P, Major F, Assmann SM and Bevilacqua PC. (2010) RNA G-quadruplexes in the model plant species *Arabidopsis thaliana*: prevalence and possible functional roles. *Nucleic Acids Res.* 38, 8149–8163.
- Muller UF, Lambert L and Goringe HU. (2001) Annealing of RNA editing substrates facilitated by guide RNA-binding protein gBP21. *EMBO J.* 20, 1394-1404.
- Muzzolini L, Beuron F, Patwardhan A, Popuri V, Cui S, Niccolini B, Rappas M, Freemont PS and Vindigni A. (2007) Different quaternary structures of human RECQ1 are associated with its dual enzymatic activity. *PLoS Biology.* 5, e20.
- Myong S, Cui S, Cornish PV, Kirchhofer A, Gack MU, Jung JU, Hopfner KP and Ha T. (2009) Cytosolic viral sensor RIG-I is a 5'-triphosphate dependent translocase on double stranded RNA. *Science.* 323, 1070–1074.

- Nadanaciva S, Weber J, Wilke-Mounts S and Senior AE. (1999) Importance of F1-ATPase residue alpha-Arg-376 for catalytic transition state stabilization. *Biochemistry*. 38, 15493-9.
- Nagpal S, Friant S, Nakshatri H, Chambon P. (1993) RARs and RXRs: evidence for two autonomous transactivation functions (AF-1 and AF-2) and heterodimerization in vivo. *EMBO J*. 12, 2349-60.
- Nagy L, Thomázy VA, Shipley GL, Fésüs L, Lamph W, Heyman RA, Chandraratna RA, Davies PJ. Activation of retinoid X receptors induces apoptosis in HL-60 cell lines. *Mol. Cell Biol*. 15, 3540-51.
- Najfeld V, Scalise A and Troy K. (1989) A new variant translocation 11;17 in a patient with acute promyelocytic leukemia together with t(7;12). *Cancer Genet. Cytogenet*. 43, 103-8.
- Naji S, Ambrus G, Cimermančič P, Reyes JR, Johnson JR, Filbrandt R, Huber MD, Vesely P, Krogan NJ, Yates JR 3rd, Saphire AC and Gerace L. (2011) Host cell interactome of HIV-1 Rev includes RNA helicases involved in multiple facets of virus production. *Mol. Cell. Proteomics*. 11, M111.015313.
- Nakajima T, Uchida C, Anderson SF, Lee CG, Hurwitz J, Parvin JD and Montminy M. (1997) RNA helicase A mediates association of CBP with RNA polymerase II. *Cell*. 90, 1107-12
- Nakamaki T, Hino K, Yokoyama A, Hisatake J, Tomoyasu S, Honma Y, Hozumi M and Tsuruoka N. (1994) Effect of cytokines on the proliferation and differentiation of acute promyelocytic leukemia cells: possible relationship to the development of "retinoic acid syndrome". *Anticancer. Res*. 14, 817-23.
- Naqvi A, Tinsley E and Khan SA. (2003) Purification and characterization of the PcrA helicase of *Bacillus anthracis*. *J. Bacteriol*. 185, 6633-6639.
- Nasr R, Guillemain MC, Ferhi O, Soilihi H, Peres L, Berthier C, Rousselot P, Robledo-Sarmiento M, Lallemand-Breitenbach V, Gournel B, Vitoux D, Pandolfi PP, Rochette-Egly C, Zhu J and de Thé H. (2008) Eradication of acute promyelocytic leukemia-initiating cells through PML-RARA degradation. *Nat. Med*. 14, 1333-42.
- Nelson SW and Benkovic SJ. (2007) The T4 phage UvsW protein contains both DNA unwinding and strand annealing activities. *J. Biol. Chem*. 282, 407-416.
- Nimonkar AV, Genschel J, Kinoshita E, Polaczek P, Campbell JL, Wyman C, Modrich P and Kowalczykowski SC. (2011) BLM-DNA2-RPA-MRN and EXO1-BLM-RPA-MRN constitute two DNA end resection machineries for human DNA break repair. *Genes Dev*. 25, 350-62.
- Nistal-Villán E, Gack MU, Martínez-Delgado G, Maharaj NP, Inn KS, Yang H, Wang R, Aggarwal AK, Jung JU and García-Sastre, A. (2010) Negative role of RIG-I serine 8 phosphorylation in the regulation of interferon-beta production. *J. Biol. Chem*. 285, 20252-20261.

Niu C, Yan H, Yu T, Sun HP, Liu JX, Li XS, Wu W, Zhang FQ, Chen Y, Zhou L, Li JM, Zeng XY, Yang RR, Yuan MM, Ren MY, Gu FY, Cao Q, Gu BW, Su XY, Chen GQ, Xiong SM, Zhang TD, Waxman S, Wang ZY, Chen Z, Hu J, Shen ZX and Chen SJ. (1999) Studies on treatment of acute promyelocytic leukemia with arsenic trioxide: remission induction, follow-up, and molecular monitoring in 11 newly diagnosed and 47 relapsed acute promyelocytic leukemia patients. *Blood*. 94, 3315-24.

Niu H, Chung WH, Zhu Z, Kwon Y, Zhao W, Chi P, Prakash R, Seong C, Liu D, Lu L, Ira G and Sung P. (2010) Mechanism of the ATP-dependent DNA end-resection machinery from *Saccharomyces cerevisiae*. *Nature*. 467, 108–11.

Oganesian L, Graham ME, Robinson PJ and Bryan TM. (2007) Telomerase recognizes G-quadruplex and linear DNA as distinct substrates. *Biochemistry*. 46, 11279–11290.

Oganesian L, Moon IK, Bryan TM and Jarstfer MB. (2006) Extension of G-quadruplex DNA by ciliate telomerase. *EMBO J*. 25, 1148–1159.

Oganesyan G, Saha SK, Guo B, He JQ, Shahangian A, Zarnegar B, Perry A and Cheng G. (2006) Critical role of TRAF3 in the Toll-like receptor-dependent and -independent antiviral response. *Nature*. 439, 208-211.

Oh-Ishi M and Maeda T. (2007) Disease proteomics of high-molecular-mass proteins by two-dimensional gel electrophoresis with agarose gels in the first dimension (Agarose 2-DE). *J. Chromatogr. A*. 849, 211-222.

Okazaki R, Okazaki T, Sakabe K, Sugimoto K, Sugino A. (1968) Mechanism of DNA chain growth. I. Possible discontinuity and unusual secondary structure of newly synthesized chains. *Proc. Natl. Acad. Sci. U S A*. 59, 598-605.

Oliver WW and Wherry WB. (1921) Notes on some bacterial parasites of the human mucous membranes. *J. Infect. Dis*. 28, 341–345.

Opresko PL, Mason PA, Podell ER, Lei M, Hickson ID, Cech TR and Bohr VA. (2005) POT1 stimulates RecQ helicases WRN and BLM to unwind telomeric DNA substrates. *J. Biol. Chem*. 280, 32069–32080.

Opresko PL, Otterlei M, Graakjaer J, Bruheim P, Dawut L, Kolvraa S, May A, Seidman MM and Bohr VA. (2004) The Werner syndrome helicase and exonuclease cooperate to resolve telomeric D loops in a manner regulated by TRF1 and TRF2. *Mol. Cell*. 14, 763–774.

Orkin SH, Zon LI. (2008) Hematopoiesis: an evolving paradigm for stem cell biology. *Cell*. 132, 631-44.

Orzalli MH, Broekema NM, Diner BA, Hancks DC, Elde NC, Cristea IM and Knipe DM. (2015) cGAS-mediated stabilization of IFI16 promotes innate signaling during herpes simplex virus infection. *Proc. Natl. Acad. Sci. U S A*. 112, E1773–E1781.

Oshiumi H, Matsumoto M, Hatakeyama S and Seya T. (2009) Riplet/RNF135, a RING finger protein, ubiquitinates RIG-I to promote interferon-beta induction during the early phase of viral infection. *J. Biol. Chem.* 284, 807-817.

Oshiumi H, Miyashita M, Matsumoto M and Seya T. (2013) A distinct role of Riplet-mediated K63- Linked polyubiquitination of the RIG-I repressor domain in human antiviral innate immune responses. *PLoS Pathog.* 9, e1003533.

Paeschke K, Bochman ML, Garcia PD, Cejka P, Friedman KL, Kowalczykowski SC and Zakian VA. (2013) Pif1 family helicases suppress genome instability at G-quadruplex motifs. *Nature.* 497, 458–462.

Paeschke K, Capra JA and Zakian VA. (2011) DNA replication through G-quadruplex motifs is promoted by the *Saccharomyces cerevisiae* Pif1 DNA helicase. *Cell.* 145, 678–691.

Paeschke K, McDonald KR and Zakian VA. (2010) Telomeres: structures in need of unwinding. *FEBS Lett.* 584, 3760–72.

Paeschke K, Simonsson T, Postberg J, Rhodes D and Lipps HJ. (2005) Telomere end-binding proteins control the formation of G-quadruplex DNA structures in vivo. *Nat. Struct. Mol. Biol.* 12, 847–854.

Paludan SR, Bowie AG, Horan KA and Fitzgerald KA. (2011) Recognition of herpesviruses by the innate immune system. *Nat. Rev. Immunol.* 11, 143-154.

Pandolfi PP, Alcalay M, Fagioli M, Zangrilli D, Mencarelli A, Diverio D, Biondi A, Lo Coco F, Rambaldi A and Grignani F. (1992) Genomic variability and alternative splicing generate multiple PML/RAR alpha transcripts that encode aberrant PML proteins and PML/RAR alpha isoforms in acute promyelocytic leukaemia. *EMBO J.* 11, 1397-407.

Parkinson GN, Lee MP and Neidle S. (2002) Crystal structure of parallel quadruplexes from human telomeric DNA. *Nature.* 417, 876-80.

Parvatiyar K, Zhang Z, Teles RM, Ouyang S, Jiang Y, Iyer SS, Zaver SA, Schenk M, Zeng S, Zhong W, Liu Z, Modlin RL, Liu YJ and Cheng G. (2012) The helicase DDX41 recognizes the bacterial secondary messenger cyclic di-GMP and cyclic di-AMP to activate a type I interferon immune response. *Nat. Immunol.* 13, 1155–1161.

Patel JR, Jain A, Chou YY, Baum A, Ha T, Garcia-Sastre A. (2013) ATPase-driven oligomerization of RIG-I on RNA allows optimal activation of type-I interferon. *EMBO Rep.* 14, 780-7.

Patel SS and Donmez I. (2006) Mechanisms of helicases. *J. Biol. Chem.* 281, 18265-8.

Patel SS and Picha KM. (2000) Structure and function of hexameric helicases. *Annu. Rev. Biochem.* 69, 651-97.

- Pazin MJ and Kadonaga JT. (1997) What's up and down with histone deacetylation and transcription? *Cell*. 189, 325-8.
- Peng M, Litman R, Xie J, Sharma S, Brosh RM Jr and Cantor SB. (2007) The FANCI/MutL α interaction is required for correction of the cross-link response in FA-J cells. *EMBO J*. 26, 3238-49.
- Peng S, Chen LL, Lei XX, Yang L, Lin H, Carmichael GG and Huang Y. (2011) Genome-wide studies reveal that Lin28 enhances the translation of genes important for growth and survival of human embryonic stem cells. *Stem Cells*. 29, 496–504.
- Perez A, Kastner P, Sethi S, Lutz Y, Reibel C and Chambon P. (1993) PMLRAR homodimers: distinct DNA binding properties and heteromeric interactions with RXR. *EMBO J*. 12, 3171-82.
- Pestova TV and Kolupaeva VG. (2002) The roles of individual eukaryotic translation initiation factors in ribosomal scanning and initiation codon selection. *Genes Dev*. 16, 2906–2922.
- Petracek ME, Lefebvre PA, Silflow CD and Berman J. (1990) Chlamydomonas telomere sequences are A+T-rich but contain three consecutive G-C base pairs. *Proc. Natl. Acad. Sci. U S A*. 87, 8222–8226.
- Petrocca F and Lieberman J. (2008) RIG-ing an antitumor response. *Nat. Med*. 14,1152-3.
- Phan AT, Kuryavyi V, Gaw HY and Patel DJ. (2005) Small-molecule interaction with a five-guanine-tract G-quadruplex structure from the human MYC promoter. *Nat. Chem. Biol*. 1, 167-73.
- Phan AT, Luu KN and Patel DJ. (2006) Different loop arrangements of intramolecular human telomeric (3+1) G-quadruplexes in K⁺ solution. *Nucleic Acids Res*. 34, 5715–5719.
- Phan AT. (2010) Human telomeric G-quadruplex: structures of DNA and RNA sequences. *FEBS J*. 277, 1107–1117.
- Piazza A, Adrian M, Samazan F, Heddi B, Hamon F, Serero A, Lopes J, Teulade-Fichou MP, Phan AT and Nicolas A. (2015) Short loop length and high thermal stability determine genomic instability induced by G-quadruplex-forming minisatellites. *EMBO J*. 34, 1718–1734.
- Pichlmair A, Schulz O, Tan CP, Näslund TI, Liljeström P, Weber F and Reis e Sousa C. (2006) RIG-I-mediated antiviral responses to single-stranded RNA bearing 5'-phosphates. *Science*. 314, 997-1001.
- Pichlmair A, Schulz O, Tan CP, Rehwinkel J, Kato H, Takeuchi O, Akira S, Way M, Schiavo G and Reis e Sousa C. (2009) Activation of MDA5 requires higher-order RNA structures generated during virus infection. *J. Virol*. 83, 10761-9.

Pike JE, Burgers PM, Campbell JL and Bambara RA. (2009) Pif1 helicase lengthens some Okazaki fragment flaps necessitating Dna2 nuclease/helicase action in the two-nuclease processing pathway. *J. Biol. Chem.* 284, 25170-80.

Pimentel, J. & Boccaccio, G. L. (2014) Translation and silencing in RNA granules: a tale of sand grains. *Front. Mol. Neurosci.* 7, 68.

Pinnavaia TJ, Marshall, CL, Mettler, CM, Fisk CL, Miles HT and Becker ED. (1978) Alkali metal ion specificity in the solution ordering of a nucleotide, 5'- guanosine monophosphate. *J. Am. Chem. Soc.* 100, 3625- 3627.

Pisareva, V. P., Pisarev, A. V., Komar, A. A., Hellen, C. U. & Pestova, T. V. Translation initiation on mammalian mRNAs with structured 5'UTRs requires DExH-box protein DHX29. *Cell* 135, 1237–1250 (2008).

Plumet S, Herschke F, Bourhis JM, Valentin H, Longhi S and Gerlier D. (2007) Cytosolic 5'-triphosphate ended viral leader transcript of measles virus as activator of the RIG I-mediated interferon response. *PLoS One.* 2, e279.

Poock H, Besch R, Maihoefer C, Renn M, Tormo D, Morskaya SS, Kirschnek S, Gaffal E, Landsberg J, Hellmuth J, Schmidt A, Anz D, Bscheider M, Schwerd T, Berking C, Bourquin C, Kalinke U, Kremmer E, Kato H, Akira S, Meyers R, Häcker G, Neuenhahn M, Busch D, Ruland J, Rothenfusser S, Prinz M, Hornung V, Endres S, Tüting T and Hartmann G. (2008) 5'-Triphosphate-siRNA: turning gene silencing and Rig-I activation against melanoma. *Nat. Med.* 14, 1256-63.

Polprasert C, Schulze I, Sekeres MA, Makishima H, Przychodzen B, Hosono N, Singh J, Padgett RA, Gu X, Phillips JG, Clemente M, Parker Y, Lindner D, Dienes B, Jankowsky E, Sauntharajah Y, Du Y, Oakley K, Nguyen N, Mukherjee S, Pabst C, Godley LA, Churpek JE, Pollyea DA, Krug U, Berdel WE, Klein HU, Dugas M, Shiraishi Y, Chiba K, Tanaka H, Miyano S, Yoshida K, Ogawa S, Müller-Tidow C and Maciejewski JP (2015) Inherited and somatic defects in DDX41 in myeloid neoplasms. *Cancer Cell.* 27, 658–670.

Poltorak A, He X, Smirnova I, Liu MY, Van Huffel C, Du X, Birdwell D, Alejos E, Silva M, Galanos C, Freudenberg M, Ricciardi- Castagnoli P, Layton B and Beutler B. (1998) Defective LPS signaling in C3H/HeJ and C57BL/10ScCr mice: mutations in Tlr4 gene. *Science.* 282, 2085- 2088.

Potter JA, Randall RE and Taylor GL. (2008) Crystal structure of human IPS-1/MAVS/VISA/Cardif caspase activation recruitment domain. *BMC Struct. Biol.* 8, 11.

Prud'homme-Généreux A, Beran RK, Iost I, Ramey CS, Mackie GA and Simons RW. (2004) Physical and functional interactions among RNase E, polynucleotide phosphorylase and the cold-shock protein, CsdA: evidence for a 'cold shock degradosome'. *Mol. Microbiol.* 54, 1409-21.

Putnam AA and Jankowsky E. (2013) DEAD-box helicases as integrators of RNA, nucleotide and protein binding. *Biochim. Biophys. Acta.* 1829, 884-93.

- Py B, Higgins CF, Krisch HM and Carpousis AJ. (1996) A DEAD-box RNA helicase in the Escherichia coli RNA degradosome. *Nature*. 381, 169-72.
- Qiu H, Wu SL, Guo XH, Shen HJ, Zhang HP and Chen HL. (2011) Expression of β 1,3-N-acetylglucosaminyltransferases during differentiation of human acute myeloid leukemia cells. *Mol. Cell Biochem*. 358, 131-9.
- Qu J, Hou Z, Han Q, Zhang C, Tian Z and Zhang J. (2013) Poly(I: C) exhibits an anti-cancer effect in human gastric adenocarcinoma cells which is dependent on RLRs. *Int. Immunopharmacol*. 17, 814-20.
- Rachwal PA, Findlow IS, Werner JM, Brown T and Fox KR. (2007) Intramolecular DNA quadruplexes with different arrangements of short and long loops. *Nucleic Acids Res*. 35, 4214-4222.
- Ramanagoudr-Bhojappa R, Byrd AK, Dahl C and Raney KD. (2014) Yeast Pif1 accelerates annealing of complementary DNA strands. *Biochemistry*. 53, 7659-69.
- Ramanagoudr-Bhojappa R, Chib S, Byrd AK, Aarattuthodiyil S, Pandey M, Patel SS and Raney KD. (2013) Yeast Pif1 helicase exhibits a one-base-pair stepping mechanism for unwinding duplex DNA. *J. Biol. Chem*. 288, 16185–16195.
- Ranjith-Kumar CT, Murali A, Dong W, Srisathiyarayanan D, Vaughan R, Ortiz-Alacantara J, Bhardwaj K, Li X, Li P and Kao CC. (2009) Agonist and Antagonist Recognition by RIG-I, a Cytoplasmic Innate Immunity Receptor. *J. Biol. Chem*. 284, 1155–1165.
- Rankin S, Reszka AP, Huppert J, Zloh M, Parkinson GN, Todd AK, Ladame S, Balasubramanian S and Neidle S. (2005) Putative DNA quadruplex formation within the human c-kit oncogene. *J. Am. Chem. Soc*. 127, 10584-10589.
- Ranoa DR, Parekh AD, Pitroda SP, Huang X, Darga T, Wong AC, Huang L, Andrade J, Staley JP, Satoh T, Akira S, Weichselbaum RR and Khodarev NN. (2016) Cancer therapies activate RIG-I-like receptor pathway through endogenous non-coding RNAs. *Oncotarget*. 7, 26496–26515.
- Rawal P, Kummarasetti VBR, Ravindran J, Kumar N, Halder K, Sharma R, Mukerji M, Das SK and Chowdhury S. (2006) Genome-wide prediction of G4 DNA as regulatory motifs: role in Escherichia coli global regulation. *Genome Res*. 16, 644–655.
- Rawling DC, Fitzgerald ME and Pyle AM. (2015) Establishing the role of ATP for the function of the RIG-I innate immune sensor. *eLife*. 4, e09391.
- Reddy TR, Tang H, Xu W and Wong-Staal F. (2000) Sam68, RNA helicase A and Tap cooperate in the post-transcriptional regulation of human immunodeficiency virus and type D retroviral mRNA. *Oncogene*. 19, 3570–3575.

- Rehwinkel J and Reis e Sousa C. (2013) Targeting the viral Achilles' heel: recognition of 5'-triphosphate RNA in innate anti-viral defence. *Curr. Opin. Microbiol.* 16, 485-92.
- Ren H, Dou SX, Rigolet P, Yang Y, Wang PY, mor-Gueret M and Xi XG. (2007) The arginine finger of the Bloom syndrome protein: its structural organization and its role in energy coupling. *Nucleic Acids Res.* 35, 6029-6041.
- Ren H, Dou SX, Zhang XD, Wang PY, Kanagaraj R, Liu JL, Janscak P, Hu JS and Xi XG. (2008) The zinc-binding motif of human RECQ5beta suppresses the intrinsic strand-annealing activity of its DExH helicase domain and is essential for the helicase activity of the enzyme. *Biochem. J.* 412, 425-433.
- Rezler EM, Seenisamy J, Bashyam S, Kim MY, White E, Wilson WD and Hurley LH. (2005) Telomestatin and diseleno saphyrin bind selectively to two different forms of the human telomeric G-quadruplex structure. *J. Am. Chem. Soc.* 127, 9439-9447.
- Rhee KJ, Sethupathi P, Driks A, Lanning DK and Knight KL. (2004) Role of commensal bacteria in development of gut-associated lymphoid tissues and preimmune antibody repertoire. *J. Immunol.* 172, 1118-1124.
- Rhodes D and Giraldo R. (1995) Telomere structure and function. *Curr. Opin. Struct. Biol.* 5, 311-22.
- Rhodes D and Lipps HJ. (2015) G-quadruplexes and their regulatory roles in biology. *Nucleic Acids Res.* 43, 8627-37.
- Richardson JP. (2002) Rho-dependent termination and ATPases in transcript termination. *Biochim. Biophys. Acta.* 1577, 251-260.
- Ribeyre C, Lopes J, Boulé JB, Piazza A, Guédin A, Zakian VA, Mergny JL and Nicolas A. (2009) The yeast Pif1 helicase prevents genomic instability caused by G-quadruplex-forming CEB1 sequences in vivo. *PLoS Genet.* 5, e1000475.
- Richards EJ and Ausubel FM. (1988) Isolation of a higher eukaryotic telomere from *Arabidopsis thaliana*. *Cell.* 53, 127-136.
- Ricote M, Snyder CS, Leung HY, Chen J, Chien KR and Glass CK. (2006) Normal hematopoiesis after conditional targeting of RXRalpha in murine hematopoietic stem/progenitor cells. *J. Leukoc. Biol.* 80, 850-61.
- Ripmaster TL, Vaughn GP and Woolford JL Jr. (1992) A putative ATP-dependent RNA helicase involved in *Saccharomyces cerevisiae* ribosome assembly. *Proc. Natl. Acad. Sci. U S A.* 89, 11131-5.
- Ristic D, Wyman C, Paulusma C and Kanaar R. (2001) The architecture of the human Rad54-DNA complex provides evidence for protein translocation along DNA. *Proc. Natl Acad. Sci. USA.* 98, 8454-8460.
- Rittinger K, Walker PA, Eccleston JF, Nurmahomed K, Owen D, Laue E, Gamblin SJ and Smerdon SJ. (1997) Crystal structure of a small G protein in complex with the GTPase-activating protein rhoGAP. *Nature.* 388, 693-7.

- Robertson-Anderson RM, Wang J, Edgcomb SP, Carmel AB, Williamson JR and Millar DP. (2011) Single-molecule studies reveal that DEAD box protein DDX1 promotes oligomerization of HIV-1 Rev on the Rev response element. *J. Mol. Biol.* 410, 959 - 71.
- Rocak S and Linder P. (2004) DEAD-box proteins: the driving forces behind RNA metabolism. *Nat. Rev. Mol. Cell Biol.* 5, 232-41.
- Ross SA, McCaffery PJ, Drager UC and De Luca LM. (2000) Retinoids in embryonal development. *Physiol. Rev.* 80, 1021-54.
- Rossi ML and Bambara RA. (2006) Reconstituted Okazaki fragment processing indicates two pathways of primer removal. *J. Biol. Chem.* 281, 26051-61.
- Rossi ML, Ghosh AK and Bohr VA. (2010) Roles of Werner syndrome protein in protection of genome integrity. *DNA Repair (Amst).* 9, 331-44.
- Rossi SE, Ajazi A, Carotenuto W, Foiani M and Giannattasio M. (2015) Rad53-mediated regulation of Rrm3 and Pif1 DNA helicases contributes to prevention of aberrant fork transitions under replication stress. *Cell Rep.* 13, 80–92.
- Rothenfusser S, Goutagny N, DiPerna G, Gong M, Monks BG, Schoenemeyer A, Yamamoto M, Akira S and Fitzgerald KA. (2005) The RNA helicase Lgp2 inhibits TLR-independent sensing of viral replication by retinoic acid-inducible gene-I. *J. Immunol.* 175, 5260-8.
- Rowley JD, Golomb HM, Dougherty C. (1977) 15/17 translocation, a consistent chromosomal change in acute promyelocytic leukaemia. *Lancet.* 1, 549-50.
- Roy BB, Hu J, Guo X, Russell RS, Guo F, Kleiman L and Liang C. (2006) Association of RNA helicase a with human immunodeficiency virus type 1 particles. *J. Biol. Chem.* 281, 12625 - 35.
- Roy TE and Kelley CD. (1939) Genus VIII. *Bacteroides* Castellani and Chalmers, p. 556–569. In: Bergey DH, Breed RS, Murray EGD, and Hitchens AP (ed.), *Bergey's manual of determinative bacteriology*, 5th ed. Williams Wilkins Co., Baltimore.
- Roychowdhury A, Szymanski MR, Jezewska MJ and Bujalowski W. (2009) Mechanism of NTP Hydrolysis by the Escherichia coli Primary Replicative Helicase DnaB Protein. II. Nucleotide and Nucleic Acid Specificities. *Biochemistry.* 48, 6730-46.
- Ruberte E, Friederich V, Chambon P and Morriss-Kay G. (1993) Retinoic acid receptors and cellular retinoid binding proteins. III. Their differential transcript distribution during mouse nervous system development. *Development.* 118, 267-82.
- Ruchaud S, Duprez E, Gendron MC, Houge G, Genieser HG, Jastorff B, Doskeland SO and Lanotte M. (1994) Two distinctly regulated events, priming and triggering, during retinoid-induced maturation and resistance of NB4 promyelocytic leukemia cell line. *Proc. Natl. Acad. Sci. U S A.* 91, 8428-32.

- Ruggero D, Wang ZG and Pandolfi PP. (2000) The puzzling multiple lives of PML and its role in the genesis of cancer. *Bioessays*. 22, 827-35.
- Sachs L. (1985) Leukemogenesis and differentiation. *Annu. Rev. Med.* 36, 177-84.
- Safa L, Delagoutte E, Petruseva I, Alberti P, Lavrik O, Riou JF and Saintomé C. (2014) Binding polarity of RPA to telomeric sequences and influence of G-quadruplex stability. *Biochimie*. 103, 80-8.
- Saha A, Wittmeyer J and Cairns BR. (2002) Chromatin remodeling by RSC involves ATP-dependent DNA translocation. *Genes Dev*. 16, 2120–2134.
- Saha SK, Pietras EM, He JQ, Kang JR, Liu SY, Oganessian G, Shahangian A, Zarnegar B, Shiba TL, Wang Y and Cheng G. (2006) Regulation of antiviral responses by a direct and specific interaction between TRAF3 and Cardif. *EMBO J*. 25, 3257-3263.
- Saharia A, Guittat L, Crocker S, Lim A, Steffen M, Kulkarni S, Stewart SA. (2008) Flap endonuclease 1 contributes to telomere stability. *Curr. Biol*. 18, 496-500.
- Saikrishnan K, Griffiths SP, Cook N, Court R and Wigley DB. (2008) DNA binding to RecD: role of the 1B domain in SF1B helicase activity. *EMBO J*. 27, 2222-2229.
- Saikrishnan K, Powell B, Cook NJ, Webb, MR and Wigley DB. (2009) Mechanistic basis of 5'-3' translocation in SF1B helicases. *Cell*. 137, 849–859.
- Sainty D, Liso V, Cantù-Rajnoldi A, Head D, Mozziconacci MJ, Arnoulet C, Benattar L, Fenu S, Mancini M, Duchayne E, Mahon FX, Gutierrez N, Birg F, Biondi A, Grimwade D, Lafage-Pochitaloff M, Hagemeijer A and Flandrin G (2000) A new morphologic classification system for acute promyelocytic leukemia distinguishes cases with underlying PLZF/RARA gene rearrangements. *Blood*. 96, 1287-96.
- Saito T, Hirai R, Loo YM, Owen D, Johnson CL, Sinha SC, Akira S, Fujita T and Gale M Jr. (2007) Regulation of innate antiviral defenses through a shared repressor domain in RIG-I and LGP2. *Proc. Natl. Acad. Sci. USA*. 104, 582–587.
- Sakabe K and Okazaki R. (1966) A unique property of the replicating region of chromosomal DNA. *Biochim. Biophys. Acta*. 129, 651-4.
- Salyers AA. (1984) Bacteroides of the human lower intestinal tract. *Ann. Rev. Microbiol*. 38, 293–313.
- Salzman DW, Shubert-Coleman J and Furneaux H. (2007) P68 RNA helicase unwinds the human let-7 microRNA precursor duplex and is required for let-7-directed silencing of gene expression. *J. Biol. Chem*. 282, 32773–32779.
- Sanders CM. (2010) Human Pif1 helicase is a G-quadruplex DNA-binding protein with G-quadruplex DNA-unwinding activity. *Biochem. J*. 430, 119–128.

Satoh T, Kato H, Kumagai Y, Yoneyama M, Sato S, Matsushita K, Tsujimura T, Fujita T, Akira S and Takeuchi O. (2010) LGP2 is a positive regulator of RIG-I- and MDA5-mediated antiviral responses. *Proc. Natl. Acad. Sci. USA*. 107, 1512-7.

Sawaya MR, Guo S, Tabor S, Richardson CC and Ellenberger T. (1999) Crystal structure of the helicase domain from the replicative helicase-primase of bacteriophage T7. *Cell*. 99, 167–177.

Schaffitzel C, Berger I, Postberg J, Hanes J, Lipps HJ and Plückthun A. (2001) In vitro generated antibodies specific for telomeric guanine-quadruplex DNA react with *Stylonychia lemnae* macronuclei. *Proc. Natl. Acad. Sci. U S A*. 98, 8572-7.

Schechtman MG. (1990) Characterization of telomere DNA from *Neurospora crassa*. *Gene*. 88, 159–165.

Scheffzek K, Ahmadian MR, Kabsch W, Wiesmuller L, Lautwein A, Schmitz F and Wittinghofer A. (1997) The Ras-RasGAP complex: structural basis for GTPase activation and its loss in oncogenic Ras mutants. *Science*. 277, 333-8.

Schlee M, Roth A, Hornung V, Hagmann CA, Wimmenauer V, Barchet W, Coch C, Janke M, Mihailovic A, Wardle G, Juranek S, Kato H, Kawai T, Poeck H, Fitzgerald KA, Takeuchi O, Akira S, Tuschl T, Latz E, Ludwig J and Hartmann G. (2009) Recognition of 5' triphosphate by RIG-I helicase requires short blunt doublestranded RNA as contained in panhandle of negative-strand virus. *Immunity*. 31, 25-34.

Schmid SR and Linder P. (1992) D-E-A-D protein family of putative RNA helicases. *Mol. Microbiol*. 6, 283 - 91.

Schmidt A, Schwerd T, Hamm W, Hellmuth JC, Cui S, Wenzel M, Hoffmann FS, Michallet MC, Besch R, Hopfner KP, Endres S and Rothenfusser S. (2009) 5'-triphosphate RNA requires base paired structures to activate antiviral signaling via RIG-I. *Proc. Natl. Acad. Sci. U S A*. 106, 12067-72.

Schnurr M and Duewell P. (2013) Breaking tumor-induced immunosuppression with 5'-triphosphate siRNA silencing TGFbeta and activating RIG-I. *Oncoimmunology*. 2, e24170.

Schotte D, Pieters R and Den Boer ML. (2012) MicroRNAs in acute leukemia: from biological players to clinical contributors. *Leukemia*. 26, 1-12.

Schrödinger LLC. (2015) The PyMOL Molecular Graphics System, Version 1.8.

Schulz VP and Zakian VA. (1994) The *Saccharomyces* PIF1 DNA helicase inhibits telomere elongation and de novo telomere formation. *Cell*. 76, 145–55.

Schwandner R, Dziarski R, Wesche H, Rothe M and Kirschning CJ. (1999) Peptidoglycan- and lipoteichoic acid-induced cell activation is mediated by toll-like receptor 2. *J. Biol. Chem*. 274, 17406–17409.

- Seale J, Delva L, Renesto P, Balitrand N, Dombret H, Scrobohaci ML, Degos L, Paul P and Chomienne C. (1996) All-trans retinoic acid rapidly decreases cathepsin G synthesis and mRNA expression in acute promyelocytic leukemia. *Leukemia*. 10, 95-101.
- Semlow DR, Blanco MR, Walter NG and Staley JP. (2016) Spliceosomal DEAH-Box ATPases remodel pre-mRNA to activate alternative splice sites. *Cell*. 164, 985–998.
- Sen D, Nandakumar D, Tang GQ and Patel SS. (2012) Human mitochondrial DNA helicase TWINKLE is both an unwinding and annealing helicase. *J. Biol. Chem.* 287, 14545–14556.
- Sen ND, Zhou F, Ingolia NT and Hinnebusch AG. (2015) Genome-wide analysis of translational efficiency reveals distinct but overlapping functions of yeast DEAD-box RNA helicases Ded1 and eIF4A. *Genome Res.* 25, 1196–1205.
- Seth RB, Sun L and Chen ZJ. (2006) Antiviral innate immunity pathways. *Cell Res.* 16, 141-7.
- Seth RB, Sun L, Ea CK and Chen ZJ. (2005) Identification and characterization of MAVS, a mitochondrial antiviral signaling protein that activates NF-kappaB and IRF 3. *Cell*. 122, 669-682.
- Sexton AN and Collins K. (2011) The 5' guanosine tracts of human telomerase RNA are recognized by the G-quadruplex binding domain of the RNA helicase DHX36 and function to increase RNA accumulation. *Mol. Cell. Biol.* 31, 736 - 43.
- Shaheduzzaman SM, Akimoto S, Kuwahara T, Kinouchi T and Ohnishi Y. (1997) Genome analysis of Bacteroides by pulsed-field gel electrophoresis: Chromosome sizes and restriction patterns. *DNA Res.* 4, 19–25.
- Sharma S, Sommers JA, Choudhary S, Faulkner JK, Cui S, Andreoli L, Muzzolini L, Vindigni A and Brosh RM Jr. (2005) Biochemical analysis of the DNA unwinding and strand annealing activities catalyzed by human RECQ1. *J.Biol.Chem.* 280, 28072–28084.
- Shen JC, Gray MD, Oshima J and Loeb LA. (1998) Characterization of Werner syndrome protein DNA helicase activity: directionality, substrate dependence and stimulation by replication protein A. *Nucleic Acids Res.* 26, 2879–2885.
- Shen ZX, Shi ZZ, Fang J, Gu BW, Li JM, Zhu YM, Shi JY, Zheng PZ, Yan H, Liu YF, Chen Y, Shen Y, Wu W, Tang W, Waxman S, De Thé H, Wang ZY, Chen SJ and Chen Z. (2004) All-trans retinoic acid/As2O3 combination yields a high quality remission and survival in newly diagnosed acute promyelocytic leukemia. *Proc. Natl. Acad. Sci. U S A*. 101, 5328-35.
- Sheng Y, Tsai-Morris CH, Gutti R, Maeda Y and Dufau ML. (2006) Gonadotropin-regulated testicular RNA helicase (GRTH/Ddx25) is a transport protein involved in gene-specific mRNA export and protein translation during spermatogenesis. *J. Biol. Chem.* 281, 35048–35056.

- Shetlar MD, Taylor JA, Hom K. (1984) Photochemical exchange reactions of thymine, uracil and their nucleosides with selected amino acids. *Photochem. Photobiol.* 40, 299-308.
- Shi J, Zhao Y, Wang Y, Gao W, Ding J, Li P, Hu L and Shao F. (2014) Inflammatory caspases are innate immune receptors for intracellular LPS. *Nature.* 514, 187–192.
- Shiohara M, Dawson MI, Hobbs PD, Sawai N, Higuchi T, Koike K, Komiyama A and Koeffler HP. (1999) Effects of novel RAR- and RXR-selective retinoids on myeloid leukemic proliferation and differentiation in vitro. *Blood.* 93, 2057-66.
- Siddiqui-Jain A, Grand CL, Bearss DJ and Hurley LH. (2002) Direct evidence for a G-quadruplex in a promoter region and its targeting with a small molecule to repress c-MYC transcription. *Proc Natl Acad Sci USA.* 99, 11593–11598.
- Silverman EJ, Maeda A, Wei J, Smith P, Beggs JD and Lin RJ. (2004) Interaction between a G-patch protein and a spliceosomal DEXD/Hbox ATPase that is critical for splicing. *Mol. Cell. Biol.* 24, 10101-10110.
- Simonsson T, Pecinka P and Kubista M. (1998) DNA tetraplex formation in the control region of c-myc. *Nucleic acids Res.* 26, 1167-1172.
- Singh SP, Koc KN, Stodola JL and Galletto R. (2016) A monomer of Pif1 unwinds double-stranded DNA and it is regulated by the nature of the non-translocating strand at the 3'-end. *J. Mol. Biol.* 428, 1053–1067.
- Singleton MR, Dillingham MS and Wigley DB. (2007) Structure and mechanism of helicases and nucleic acid translocases. *Annu. Rev. Biochem.* 76, 23-50.
- Singleton MR, Dillingham MS, Gaudier M, Kowalczykowski SC and Wigley DB. (2004) Crystal structure of RecBCD enzyme reveals a machine for processing DNA breaks. *Nature.* 432, 187–93.
- Singleton MR, Sawaya MR, Ellenberger T and Wigley DB. (2000) Crystal structure of T7 gene 4 ring helicase indicates a mechanism for sequential hydrolysis of nucleotides. *Cell.* 101, 589–600.
- Siwaszek A, Ukleja M and Dziembowski A. (2014) Proteins involved in the degradation of cytoplasmic mRNA in the major eukaryotic model systems. *RNA Biol.* 11, 1122–1136.
- Smillie DA. and Sommerville J. (2002) RNA helicase p54 (DDX6) is a shuttling protein involved in nuclear assembly of stored mRNP particles. *J. Cell Sci.* 115, 395–407.
- Smith FW and Feigon J. (1992) Quadruplex structure of *Oxytricha* telomeric DNA oligonucleotides. *Nature.* 356, 164-168.

- Sohal J, Phan VT, Chan PV, Davis EM, Patel B, Kelly LM, Abrams TJ, O'Farrell AM, Gilliland DG, Le Beau MM and Kogan SC. (2003) A model of APL with FLT3 mutation is responsive to retinoic acid and a receptor tyrosine kinase inhibitor, SU11657. *Blood*. 101, 3188-97.
- Song B, Ji W, Guo S, Liu A, Jing W, Shao C, Li G and Jin G. (2014) miR- 545 inhibited pancreatic ductal adenocarcinoma growth by targeting RIG-I. *FEBS Lett*. 588, 4375–4381.
- Soultanas P, Dillingham MS, Wiley P, Webb MR and Wigley DB. (2000) Uncoupling DNA translocation and helicase activity in PcrA: direct evidence for an active mechanism. *EMBO J*. 19, 3799-810.
- Soultanas P and Wigley DB. (2001) Unwinding the 'Gordian knot' of helicase action. *Trends Biochem. Sci*. 26, 47-54.
- Steimer L and Klostermeier D. (2012) RNA helicases in infection and disease. *RNA Biol*. 9, 751-71.
- Stith CM, Sterling J, Resnick MA, Gordenin DA and Burgers PM. (2008) Flexibility of eukaryotic Okazaki fragment maturation through regulated strand displacement synthesis. *J. Biol. Chem*. 283, 34129-40.
- Story RM and Steitz TA. (1992) Structure of the recA protein-ADP complex. *Nature*. 355, 374-6.
- Strasser K and Hurt E. (2001) Splicing factor Sub2p is required for nuclear mRNA export through its interaction with Yra1p. *Nature*. 413, 648-652.
- Strudwick S and Borden KL. (2002) Finding a role for PML in APL pathogenesis: a critical assessment of potential PML activities. *Leukemia*. 16, 1906-17.
- Subramanya HS, Bird LE, Brannigan JA and Wigley DB. (1996) Crystal structure of a DExx box DNA helicase. *Nature*. 384, 379-83.
- Suhasini AN and Brosh RM Jr. (2013) Disease-causing missense mutations in human DNA helicase disorders. *Mutat. Res*. 752, 138-52.
- Sumpter R Jr, Loo YM, Foy E, Li K, Yoneyama M, Fujita T, Lemon SM and Gale M Jr. (2005) Regulating intracellular antiviral defense and permissiveness to hepatitis C virus RNA replication through a cellular RNA helicase, RIG-I. *J. Virol*. 79, 2689–2699.
- Sun Z, Ren H, Liu Y, Teeling JL and Gu J. (2011) Phosphorylation of RIG-I by casein kinase II inhibits its antiviral response. *J. Virol*. 85, 1036-1047.
- Sundquist WI and Klug A. (1989) Telomeric DNA dimerizes by formation of guanine tetrads between hairpin loops. *Nature*. 342, 825–829.

Svitkin YV, Pause A, Haghghat A, Pyronnet S, Witherell G, Belsham GJ and Sonenberg N. (2001) The requirement for eukaryotic initiation factor 4A (eIF4A) in translation is in direct proportion to the degree of mRNA 5' secondary structure. *RNA*. 7, 382–394.

Symington LS. (2014) End resection at double-strand breaks: mechanism and regulation. *Cold Spring Harb. Perspect. Biol.* 6, a016436.

Tackett AJ, Morris PD, Dennis R, Goodwin TE, and Raney KD. (2001) Unwinding of unnatural substrates by a DNA helicase. *Biochemistry*. 40, 543–548 .

Takahashi S, Hours C, Chu A and Denhardt DT. (1979) The rep mutation. VI. Purification and properties of the Escherichia coli rep protein, DNA helicaseIII. *Can. J. Biochem.* 57, 855-66.

Takahasi K, Kumeta H, Tsuduki N, Narita R, Shigemoto T, Hirai R, Yoneyama M, Horiuchi M, Ogura K, Fujita T and Inagaki F. (2009) Solution structures of cytosolic RNA sensor MDA5 and LGP2 C-terminal domains: identification of the RNA recognition loop in RIG-I-like receptors. *J Biol Chem*. 284, 17465-74.

Takaoka A, Wang Z, Choi MK, Yanai H, Negishi H, Ban T, Lu Y, Miyagishi M, Kodama T, Honda K, Ohba Y and Taniguchi T. (2007) DAI (DLM-1/ZBP1) is a cytosolic DNA sensor and an activator of innate immune response. *Nature*. 448, 501-5.

Tallman MS, Nabhan C, Feusner JH and Rowe JM. (2002) Acute promyelocytic leukemia: evolving therapeutic strategies. *Blood*. 99, 759–767.

Tamkun JW, Deuring R, Scott MP, Kissinger M, Pattatucci AM, Kaufman TC and Kennison JA. (1992) Brahma: a regulator of Drosophila homeotic genes structurally related to the yeast transcriptional activator SNF2/SWI2. *Cell*. 68, 561-72.

Tanaka K, Okamoto S, Ishikawa Y, Tamura H and Hara T. (2009) DDX1 is required for testicular tumorigenesis, partially through the transcriptional activation of 12p stem cell genes. *Oncogene*. 28, 2142 - 51.

Tanaka Y and Chen ZJ. (2012) STING specifies IRF3 phosphorylation by TBK1 in the cytosolic DNA signaling pathway. *Sci. Signal*. 5, ra20.

Tanner NK and Linder P. (2001) DExD/H box RNA helicases: from generic motors to specific dissociation functions. *Mol. Cell*. 8, 251-62.

Taschner S, Koesters C, Platzer B, Jörgl A, Ellmeier W, Benesch T and Strobl H. (2007) Down-regulation of RXRalpha expression is essential for neutrophil development from granulocyte/monocyte progenitors. *Blood*. 109, 971-9.

Tieg B and Krebber H. (2013) Dbp5 - from nuclear export to translation. *Biochim. Biophys. Acta*. 1829, 791–798.

- Tippana R, Hwang H, Opresko PL, Bohr VA and Myong S. (2016) Single-molecule imaging reveals a common mechanism shared by G-quadruplex-resolving helicases. *Proc. Natl. Acad. Sci. USA.* 113, 8448-53.
- Thomsen ND and Berger JM. (2009) Running in Reverse: The Structural Basis for Translocation Polarity in Hexameric Helicases. *Cell.* 139, 523–534.
- Todd AK, Haider SM, Parkinson GN and Neidle S. (2007) Sequence occurrence and structural uniqueness of a G-quadruplex in the human c-kit promoter. *Nucleic Acids Res.* 35, 5799-808.
- Todd AK, Johnston M and Neidle S. (2005) Highly prevalent putative quadruplex sequence motifs in human DNA. *Nucleic Acids Res.* 33, 2901–7.
- Tomko EJ, Fischer CJ, Niedziela-Majka A and Lohman TM. (2007) A nonuniform stepping mechanism for E. coli UvrD monomer translocation along single-stranded DNA. *Mol. Cell.* 26, 335–347.
- Tran EJ, Zhou Y, Corbett AH and Wentz SR. (2007) The DEAD-box protein Dbp5 controls mRNA export by triggering specific RNA:protein remodeling events. *Mol. Cell.* 28, 850-9.
- Tran H, Schilling M, Wirbelauer C, Hess D and Nagamine Y. (2004) Facilitation of mRNA deadenylation and decay by the exosome-bound, DExH protein RHAU. *Mol. Cell.* 13, 101 - 11.
- Trego KS, Chernikova SB, Davalos AR, Perry JJP, Finger LD, Ng C, Tsai MS, Yannone SM, Tainer JA, Campisi J, Cooper PK. (2011) The DNA repair endonuclease XPG interacts directly and functionally with the WRN helicase defective in Werner syndrome. *Cell Cycle.* 10, 1998–2007.
- Trotman LC, Alimonti A, Scaglioni PP, Koutcher JA, Cordon-Cardo C and Pandolfi PP. (2006) Identification of a tumour suppressor network opposing nuclear Akt function. *Nature.* 441, 523-7.
- Tsai-Morris CH, Sheng Y, Gutti RK, Tang PZ and Dufau ML. (2010) Gonadotropin-regulated testicular RNA helicase (GRTH/DDX25): a multifunctional protein essential for spermatogenesis. *J. Androl.* 31, 45–52.
- Tsunekawa N, Higashi N, Kogane Y, Waki M, Shida H, Nishimura Y, Adachi H, Nakajima M and Irimura T (2016) Heparanase augments inflammatory chemokine production from colorectal carcinoma cell lines. *Biochem. Biophys. Res. Commun.* 469, 878–883.
- Turnbaugh PJ, Ley RE, Mahowald MA, Magrini V, Mardis ER and Gordon JI. (2006) An obesity-associated gut microbiome with increased capacity for energy harvest. *Nature.* 444, 1027-1131.

- Uhlmann-Schiffler H, Jalal C and Stahl H. (2006) Ddx42p—a human DEAD box protein with RNA chaperone activities. *Nucleic Acids Research*. 34, 10–22.
- Ule J, Jensen KB, Ruggiu M, Mele A, Ule A and Darnell RB. (2003) CLIP identifies Nova-regulated RNA networks in the brain. *Science*. 302, 1212-5.
- Unterholzner L, Keating SE, Baran M, Horan KA, Jensen SB, Sharma S, Sirois CM, Jin T, Latz E, Xiao TS, Fitzgerald KA, Paludan SR and Bowie AG. (2010) IFI16 is an innate immune sensor for intracellular DNA. *Nat. Immunol*. 11, 997–1004.
- Uringa EJ, Lisaingo K, Pickett HA, Brind'Amour J, Rohde JH, Zelensky A, Essers J and Lansdorp PM. (2012) RTEL1 contributes to DNA replication and repair and telomere maintenance. *Mol. Biol. Cell*. 23, 2782-92.
- Vallur AC and Maizels N. (2008) Activities of human exonuclease 1 that promote cleavage of transcribed immunoglobulin switch regions. *Proc. Natl. Acad. Sci. USA*. 105, 16508-12.
- Valton AL, Hassan-Zadeh V, Lema I, Boggetto N, Alberti P, Saintomé C, Riou JF and Prioleau MN. (2014) G4 motifs affect origin positioning and efficiency in two vertebrate replicators. *EMBO J*. 33, 732-46.
- van Brabant AJ, Stan R and Ellis NA. (2000) DNA helicases, genomic instability, and human genetic disease. *Annu. Rev. Genomics Hum. Genet*. 1, 409-59.
- van den Boorn JG and Hartmann G. (2013) Turning tumors into vaccines: co-opting the innate immune system. *Immunity*. 39, 27-37.
- Vannier JB, Pavicic-Kaltenbrunner V, Petalcorin MI, Ding H and Boulton SJ. (2012) RTEL1 dismantles T loops and counteracts telomeric G4-DNA to maintain telomere integrity. *Cell*. 149, 795-806.
- Vasa-Nicotera M, Brouillette S, Mangino M, Thompson JR, Braund P, Clemitson JR, Mason A, Bodycote CL, Raleigh SM, Louis E and Samani NJ. (2005) Mapping of a major locus that determines telomere length in humans. *Am. J. Hum. Genet*. 76, 147-51.
- Vega LR, Phillips JA, Thornton BR, Benanti JA, Onigbanjo MT, Toczyski DP and Zakian VA. (2007) Sensitivity of yeast strains with long G-tails to levels of telomere-bound telomerase. *PLoS Genet*. 3, 1065–1075.
- Velankar SS, Soultanas P, Dillingham MS, Subramanya HS and Wigley DB. (1999) Crystal structures of complexes of PcrA DNA helicase with a DNA substrate indicate an inchworm mechanism. *Cell*. 97, 75–84.
- Villa R, Pasini D, Gutierrez A, Morey L, Occhionorelli M, Viré E, Nomdedeu JF, Jenuwein T, Pelicci PG, Minucci S, Fuks F, Helin K and Di Croce L. (2007) Role of the polycomb repressive complex 2 in acute promyelocytic leukemia. *Cancer Cell*. 11, 513-25.
- Vindigni A and Hickson ID. (2009) RecQ helicases: Multiple structures for multiple functions?. *HFSP J*. 3, 153–164.

Visani G, Tosi P, Ottaviani E, Zaccaria A, Baccini C, Manfroi S, Pastano R, Remiddi C, Morelli A, Molinari AL, Zanchini R and Tura S. (1996) All-trans retinoic acid and in vitro cytokine production by acute promyelocytic leukemia cells. *Eur. J. Haematol.* 57, 301-6.

von Hippel PH and Delagoutte E. (2001) A general model for nucleic acid helicases and their "coupling" within macromolecular machines. *Cell.* 104, 177-90.

Walker JE, Saraste M, Runswick MJ and Gay NJ. (1982) Distantly related sequences in the alpha- and beta-subunits of ATP synthase, myosin, kinases and other ATP-requiring enzymes and a common nucleotide binding fold. *EMBO J.* 1, 945.

Walne AJ, Vulliamy T, Kirwan M, Plagnol V and Dokal I. (2013) Constitutional mutations in RTEL1 cause severe dyskeratosis congenita. *Am. J. Hum. Genet.* 92, 448-53.

Wang H, Nora GJ, Ghodke H and Opresko PL. (2011) Single molecule studies of physiologically relevant telomeric tails reveal POT1 mechanism for promoting G-quadruplex unfolding. *J. Biol. Chem.* 286, 7479–7489.

Wang LD and Wagers AJ. (2011) Dynamic niches in the origination and differentiation of haematopoietic stem cells. *Nat. Rev. Mol. Cell. Biol.* 12, 643-55.

Wang Y and Patel DJ. (1992) Guanine residues in d(T2AG3) and d(T2G4) form parallel-stranded potassium cation stabilized G-quadruplexes with anti glycosidic torsion angles in solution. *Biochemistry.* 31, 8112–8119.

Wang Y, Arribas-Layton M, Chen Y, Lykke-Andersen J and Sen GL. (2015) DDX6 orchestrates mammalian progenitor function through the mRNA degradation and translation pathways. *Mol. Cell.* 60, 118–130.

Wang Y, Ludwig J, Schuberth C, Goldeck M, Schlee M, Li H, Juranek S, Sheng G, Micura R, Tuschl T, Hartmann G and Patel DJ. (2010) Structural and functional insights into 5'-ppp RNA pattern recognition by the innate immune receptor RIG-I. *Nat. Struct. Mol. Biol.* 17, 781-7.

Wang Y, Swiecki M, McCartney SA and Colonna M. (2011) dsRNA sensors and plasmacytoid dendritic cells in host defense and autoimmunity *Immunol. Rev.* 243, 74-90.

Watson JD and Crick FH. (1953) Molecular structure of nucleic acids; a structure for deoxyribose nucleic acid. *Nature.* 171, 737-8.

Weber M, Gawanbacht A, Habjan M, Rang A, Borner C, Schmidt AM, Veitinger S, Jacob R, Devignot S, Kochs G, García-Sastre A and Weber F. (2013) Incoming RNA virus nucleocapsids containing a 5'-triphosphorylated genome activate RIG-I and antiviral signaling. *Cell Host. Microbe.* 13, 336-46.

- Wei D, Parkinson GN, Reszka AP and Neidle S. (2012) Crystal structure of a c-kit promoter quadruplex reveals the structural role of metal ions and water molecules in maintaining loop conformation. *Nucleic Acids Res.* 40, 4691-700.
- Wells RA, Hummel JL, De Koven A, Zipursky A, Kirby M, Dubé I and Kamel-Reid S. (1996) A new variant translocation in acute promyelocytic leukaemia: molecular characterization and clinical correlation. *Leukemia.* 10, 735-40.
- Whitehouse I, Stockdale C, Flaus A, Szczelkun MD and Owen-Hughes T. (2003) Evidence for DNA translocation by the ISWI chromatin-remodeling enzyme. *Mol. Cell. Biol.* 23, 1935–1945.
- Wick G, Jakic B, Buszko M, Wick MC and Grundtman C. (2014) The role of heat shock proteins in atherosclerosis. *Nat. Rev. Cardiol.* 11, 516–529.
- Wickramasinghe VO and Laskey RA. (2015) Control of mammalian gene expression by selective mRNA export. *Nat. Rev. Mol. Cell Biol.* 16, 431-42.
- Wicky C, Villeneuve AM, Lauper N, Codourey L, Tobler H and Müller F. (1996) Telomeric repeats (TTAGGC)_n are sufficient for chromosome capping function in *Caenorhabditis elegans*. *Proc. Natl. Acad. Sci. U S A.* 93, 8983–8988.
- Wies E, Wang MK, Maharaj NP, Chen K, Zhou S, Finberg RW and Gack MU. (2013) Dephosphorylation of the RNA sensors RIG-I and MDA5 by the phosphatase PP1 is essential for innate immune signaling. *Immunity.* 38, 437-49.
- Wigley DB. (2000) DNA helicases: one small step for PcrA, one giant leap for RecBC? *Curr. Biol.* 10, R444.
- Will CL, Urlaub H, Achsel T, Gentzel M, Wilm M and Lührmann R. (2002) Characterization of novel SF3b and 17S U2 snRNP proteins, including a human Prp5p homologue and an SF3b DEAD-box protein. *EMBO J.* 21, 4978–4988.
- Witten JT and Ule J. (2011) Understanding splicing regulation through RNA splicing maps. *Trends Genet.* 27, 89–97.
- Wlodarczyk A, Grzybowski P, Patkowski A and Dobek A. (2005) Effect of ions on the polymorphism, effective charge, and stability of human telomeric DNA. Photon correlation spectroscopy and circular dichroism studies. *J. Phys. Chem. B.* 109, 3594-3605.
- Wolf D, Heine A and Brossart P. (2014) Implementing combinatorial immunotherapeutic regimens against cancer: the concept of immunological conditioning. *Oncoimmunology.* 3, e27588.
- Wolfe AL, Singh K, Zhong Y, Drewe P, Rajasekhar VK, Sanghvi VR, Mavrakis KJ, Jiang M, Roderick JE, Van der Meulen J, Schatz JH, Rodrigo CM, Zhao C, Rondou P, de Stanchina E, Teruya-Feldstein J, Kelliher MA, Speleman F, Porco JA Jr, Pelletier J, Räsch G and Wendel HG. (2014) RNA G-quadruplexes cause eIF4A-dependent oncogene translation in cancer. *Nature.* 513, 65–70.

- Won D, Shin SY, Park CJ, Jang S, Chi HS, Lee KH, Lee JO and Seo EJ. (2013) OBFC2A/RARA: a novel fusion gene in variant acute promyelocytic leukemia. *Blood*. 121, 1432-5.
- Wong A and Wu G. (2003) Selective binding of monovalent cations to the stacking G-quartet structure formed by guanosine 5'-monophosphate: a solid-state NMR study. *J. Am. Chem. Soc.* 125, 13895-13905.
- Wong I and Lohman TM. (1992) ATPase activity of Escherichia coli Rep helicase is dramatically dependent on DNA ligation and protein oligomeric states. *Science* 256, 350–355.
- Wu J and Chen ZJ. (2014) Innate immune sensing and signaling of cytosolic nucleic acids. *Annu Rev Immunol.* 32, 461–488.
- Wu J, Sun L, Chen X, Du F, Shi H, Chen C and Chen ZJ (2013) Cyclic GMP-AMP is an endogenous second messenger in innate immune signaling by cytosolic DNA. *Science*. 339, 826–830.
- Wu WQ, Hou XM, Li M, Dou SX and Xi XG. (2015) BLM unfolds G-quadruplexes in different structural environments through different mechanisms. *Nucleic Acids Res.* 43, 4614-26.
- Wu X and Maizels N. (2001) Substrate-specific inhibition of RecQ helicase. *Nucleic Acids Res.* 29, 1765–1771.
- Wu Y and Brosh RM Jr. (2010) G-quadruplex nucleic acids and human disease. *FEBS J.* 277, 3470–3488.
- Wu Y, Shin-ya K and Brosh RM Jr. (2008) FANCD1 Helicase Defective in Fanconi Anemia and Breast Cancer Unwinds G-Quadruplex DNA To Defend Genomic Stability. *Mol. Cell. Biol.* 28, 4116–4128.
- Wu Y, Shin-ya K and Brosh RM Jr. (2008) FANCD1 helicase defective in Fanconi anemia and breast cancer unwinds G-quadruplex DNA to defend genomic stability. *Mol. Cell. Biol.* 28, 4116-28.
- Wu Y. (2012) Unwinding and rewinding: Double faces of helicase?. *J. Nucleic Acids.* 2012, 140601.
- Wyatt HD and West SC. (2014) Holliday junction resolvases. *Cold Spring Harb. Perspect. Biol.* 6, a023192.
- Xia P, Wang S, Gao P, Gao G and Fan Z. (2016) DNA sensor cGAS-mediated immune recognition. *Protein Cell.* 7, 777-791.
- Xing J, Wang S, Lin R, Mossman KL and Zheng C. (2012) Herpes simplex virus 1 tegument protein US11 downmodulates the RLR signaling pathway via direct interaction with RIG-I and MDA-5. *J. Virol.* 86, 3528-40.

Xu LG, Wang YY, Han KJ, Li LY, Zhai Z and Shu HB. (2005) VISA is an adapter protein required for virus-triggered IFN-beta signaling. *Mol. Cell.* 19, 727-740.

Xu Y, Suzuki Y, Ito K and Komiyama M. (2010) Telomeric repeat-containing RNA structure in living cells. *Proc. Natl. Acad. Sci. USA.* 107, 14579-84.

Yadav VK, Abraham JK, Mani P, Kulshrestha R, Chowdhury S. (2008) QuadBase: genome-wide database of G4 DNA—occurrence and conservation in human, chimpanzee, mouse and rat promoters and 146 microbes. *Nucleic Acids Res.* 36, 381–385.

Yamamoto Y, Tsuzuki S, Tsuzuki M, Handa K, Inaguma Y and Emi N. (2010) BCOR as a novel fusion partner of retinoic acid receptor alpha in a t(X;17)(p11;q12) variant of acute promyelocytic leukemia. *Blood.* 116, 4274-83.

Yamazaki T, Fujiwara N, Yukinaga H, Ebisuya M, Shiki T, Kurihara T, Kioka N, Kambe T, Nagao M, Nishida E, Masuda S. (2010) The closely related RNA helicases, UAP56 and URH49, preferentially form distinct mRNA export machineries and coordinately regulate mitotic progression. *Mol. Biol. Cell.* 21, 2953–2965.

Yang P, An H, Liu X, Wen M, Zheng Y, Rui Y and Cao X. (2010) The cytosolic nucleic acid sensor LRRFIP1 mediates the production of type I interferon via a beta-catenin-dependent pathway. *Nat. Immunol.* 11, 487–494.

Yang Q, Xiang J, Yang S, Li Q, Zhou Q, Guan A, Zhang X, Zhang H, Tang Y and Xu G. (2010) Verification of specific G-quadruplex structure by using a novel cyanine dye supramolecular assembly: II. The binding characterization with specific 142 intramolecular G-quadruplex and the recognizing mechanism. *Nucleic Acids Res.* 38, 1022-1033.

Yang YK, Qu H, Gao D, Di W, Chen HW, Guo X, Zhai ZH, Chen DY. (2011) ARF-like protein 16 (ARL16) inhibits RIG-I by binding with its C-terminal domain in a GTP-dependent manner. *J. Biol. Chem.* 286, 10568-80.

Yarranton GT and Gefter ML. (1979) Enzyme-catalyzed DNA unwinding: studies on Escherichia coli rep protein. *Proc. Natl. Acad. Sci. U. S. A.* 76,1658–1662.

Yasuda-Inoue M, Kuroki M and Ariumi Y. (2013) Distinct DDX DEAD-box RNA helicases cooperate to modulate the HIV-1 Rev function. *Biochem. Biophys. Res. Commun.* 434, 803–808.

Yedavalli VS, Neuveut C, Chi YH, Kleiman L and Jeang KT. (2004) Requirement of DDX3 DEAD box RNA helicase for HIV-1 Rev-RRE export function. *Cell.* 119, 381–392.

Yin J, Park G, Lee JE, Choi EY, Park JY, Kim TH, Park N, Jin X, Jung JE, Shin D, Hong JH, Kim H, Yoo H, Lee SH, Kim YJ, Park JB and Kim JH. (2015) DEAD-box RNA helicase DDX23 modulates glioma malignancy via elevating miR-21 biogenesis. *Brain.* 138, 2553–2570.

Yin Q, Fu TM, Li J and Wu H. (2015) Structural biology of innate immunity. *Annu. Rev. Immunol.* 33, 393–416.

Yoneyama M and Fujita T. (2009) RNA recognition and signal transduction by RIG-I-like receptors. *Immunol. Rev.* 227, 54–65.

Yoneyama M, Kikuchi M, Matsumoto K, Imaizumi T, Miyagishi M, Taira K, Foy E, Loo YM, Gale M Jr, Akira S, Yonehara S, Kato A and Fujita T. (2005) Shared and unique functions of the DExD/H-box helicases RIG-I, MDA5, and LGP2 in antiviral innate immunity. *J. Immunol.* 175, 2851–2858.

Yoneyama M, Kikuchi M, Natsukawa T, Shinobu N, Imaizumi T, Miyagishi M, Taira K, Akira S and Fujita T. (2004) The RNA helicase RIG-I has an essential function in double-stranded RNA-induced innate antiviral responses. *Nat. Immunol.* 5, 730-7.

Yoo HH and Chung IK. (2011) Requirement of DDX39 DEAD box RNA helicase for genome integrity and telomere protection. *Aging Cell.*10, 557 - 71.

Yoshida R, Takaesu G, Yoshida H, Okamoto F, Yoshioka T, Choi Y, Akira S, Kawai T, Yoshimura A and Kobayashi T. (2008) TRAF6 and MEKK1 play a pivotal role in the RIG-I-like helicase antiviral pathway. *J. Biol. Chem.* 283, 36211-36220.

You H, Lattmann S, Rhodes D, Yan J. (2017) RHAU helicase stabilizes G4 in its nucleotide-free state and destabilizes G4 upon ATP hydrolysis. *Nucleic Acids Res.* 45, 206–214.

Yu M, Tong JH, Mao M, Kan LX, Liu MM, Sun YW, Fu G, Jing YK, Yu L, Lepaslier D, Lanotte M, Wang ZY, Chen Z, Waxman S, Wang YX, Tan JZ and Chen SJ. (1997) Cloning of a gene (RIG-G) associated with retinoic acid-induced differentiation of acute promyelocytic leukemia cells and representing a new member of a family of interferon-stimulated genes. *Proc. Natl. Acad. Sci. USA.* 94, 7406-11.

Yu VC, Delsert C, Andersen B, Holloway JM, Devary OV, Näär AM, Kim SY, Boutin JM, Glass CK, Rosenfeld MG. (1991) RXR beta: a coregulator that enhances binding of retinoic acid, thyroid hormone, and vitamin D receptors to their cognate response elements. *Cell.* 67, 1251-66.

Yusufzai T and Kadonaga JT. (2008) HARP is an ATP-driven annealing helicase. *Science.* 322, 748–750.

Yusufzai T and Kadonaga JT. (2010) Annealing helicase 2 (AH2), a DNA-rewinding motor with an HNH motif. *Proc. Natl. Acad. Sci. U.S.A.* 107, 20970–20973.

Zahler AM, Williamson JR, Cech TR and Prescott DM. (1991) Inhibition of telomerase by G-quartet DNA structures. *Nature.* 350, 718–720.

Zaug AJ, Podell ER and Cech TR. (2005) Human POT1 disrupts telomeric G-quadruplexes allowing telomerase extension in vitro. *Proc. Natl. Acad. Sci. USA.* 102, 10864–10869.

Zeman MK and Cimprich KA. (2014) Causes and Consequences of Replication Stress. *Nat. Cell Biol.* 16, 2-9.

Zhang AY and Balasubramanian S. (2012) The kinetics and folding pathways of intramolecular G-quadruplex nucleic acids. *J. Am. Chem. Soc.* 134, 19297-308.

Zhang DH, Zhou B, Huang Y, Xu LX and Zhou JQ. (2006) The human Pif1 helicase, a potential Escherichia coli RecD homologue, inhibits telomerase activity. *Nucleic Acids Res.* 34, 1393-1404.

Zhang FX, Kirschning CJ, Mancinelli R, Xu XP, Jin Y, Faure E, Mantovani A, Rothe M, Muzio M and Arditi M. (1999) Bacterial lipopolysaccharide activates nuclear factor-kappaB through interleukin-1 signaling mediators in cultured human dermal endothelial cells and mononuclear phagocytes. *J. Biol. Chem.* 274, 7611– 7614.

Zhang H, Wang D, Zhong H, Luo R, Shang M, Liu D, Chen H, Fang L and Xiao S. (2015) Ubiquitin-specific Protease 15 Negatively Regulates Virus-induced Type I Interferon Signaling via Catalytically-dependent and -independent Mechanisms. *Sci. Rep.* 5, 11220.

Zhang HX, Liu ZX, Sun YP, Zhu J, Lu SY, Liu XS, Huang QH, Xie YY, Zhu HB, Dang SY, Chen HF, Zheng GY, Li YX, Kuang Y, Fei J, Chen SJ, Chen Z and Wang ZG. (2013) RIG-I regulates NF-kappaB activity through binding to Nfkappab1 3'-UTR mRNA. *Proc. Natl. Acad. Sci. U S A.* 110, 6459-64.

Zhang NN, Shen SH, Jiang LJ, Zhang W, Zhang HX, Sun YP, Li XY, Huang QH, Ge BX, Chen SJ, Wang ZG, Chen Z and Zhu J. (2008) RIG-I plays a critical role in negatively regulating granulocytic proliferation. *Proc. Natl. Acad. Sci. U S A.* 105, 10553-8.

Zhang X, Brann TW, Zhou M, Yang J, Oguariri RM, Lidie KB, Imamichi H, Huang DW, Lempicki RA, Baseler MW, Veenstra TD, Young HA, Lane HC and Imamichi T. (2011) Cutting edge: Ku70 is a novel cytosolic DNA sensor that induces type III rather than type I IFN. *J. Immunol.* 186, 4541–4545.

Zhang X, Wang C, Schook LB, Hawken RJ and Rutherford MS. (2000) An RNA helicase, RHIV -1, induced by porcine reproductive and respiratory 188 syndrome virus (PRRSV) is mapped on porcine chromosome 10q13. *Microb. Pathog.* 28, 267-278.

Zhang Y, You J, Wang X and Weber J. (2015) The DHX33 RNA helicase promotes mRNA translation initiation. *Mol. Cell. Biol.* 35, 2918–2931.

Zhang Z, Yuan B, Bao M, Lu N, Kim T and Liu YJ. (2011) The helicase DDX41 senses intracellular DNA mediated by the adaptor STING in dendritic cells. *Nat. Immunol.* 12, 959–965.

Zhao C, Denison C, Huibregtse JM, Gygi S and Krug RM. (2005) Human ISG15 conjugation targets both IFN-induced and constitutively expressed proteins functioning in diverse cellular pathways. *Proc. Natl. Acad. Sci. USA.* 102, 10200-10205.

- Zhao L, Zhu J, Zhou H, Zhao Z, Zou Z, Liu X, Lin X, Zhang X, Deng X, Wang R, Chen H and Jin M. (2015) Identification of cellular microRNA-136 as a dual regulator of RIG-I-mediated innate immunity that antagonizes H5N1 IAV replication in A549 cells. *Sci. Rep.* 5, 14991.
- Zhao Q, Tao J, Zhu Q, Jia PM, Dou AX, Li X, Cheng F, Waxman S, Chen GQ, Chen SJ, Lanotte M, Chen Z and Tong JH. (2004) Rapid induction of cAMP/PKA pathway during retinoic acid-induced acute promyelocytic leukemia cell differentiation. *Leukemia.* 18, 285-92.
- Zheng Y, Shi Y, Tian C, Jiang C, Jin H, Chen J, Almasan A, Tang H and Chen Q. (2004) Essential role of the voltage-dependent anion channel (VDAC) in mitochondrial permeability transition pore opening and cytochrome c release induced by arsenic trioxide. *Oncogene.* 23, 1239-47.
- Zhong S, Salomoni P and Pandolfi PP. (2000) The transcriptional role of PML and the nuclear body. *Nat. Cell Biol.* 2, E85-90.
- Zhou J, Monson EK, Teng SC, Schulz VP and Zakian VA. (2000) Pif1p helicase, a catalytic inhibitor of telomerase in yeast. *Science.* 289, 771-4.
- Zhou JQ, Qi H, Schulz VP, Mateyak MK, Monson EK and Zakian VA. (2002) *Schizosaccharomyces pombe* pfh1⁺ encodes an essential 5' to 3' DNA helicase that is a member of the PIF1 subfamily of DNA helicases. *Mol. Biol. Cell.* 13, 2180-91.
- Zhou R, Zhang J, Bochman ML, Zakian VA and Ha T. (2014) Periodic DNA patrolling underlies diverse functions of Pif1 on R-loops and G-rich DNA. *eLife.* 3, e02190.
- Zhou W and Bao S. (2014) PML-mediated signaling and its role in cancer stem cells. *Oncogene.* 33, 1475-84.
- Zhou X, Ren W, Bharath SR, Tang X, He Y, Chen C, Liu Z, Li D and Song H. (2016) Structural and functional insights into the unwinding mechanism of *Bacteroides* sp. Pif1. *Cell Rep.* 14, 2030–2039.
- Zhu J, Gianni M, Kopf E, Honoré N, Chelbi-Alix M, Koken M, Quignon F, Rochette-Egly C and de Thé H. (1999) Retinoic acid induces proteasome-dependent degradation of retinoic acid receptor alpha (RARalpha) and oncogenic RARalpha fusion proteins. *Proc. Natl. Acad. Sci. U S A.* 96,

Titre : Identification et caractérisation des interactants de l'hélicase RIG-I impliquée dans la balance prolifération/différentiation cellulaire. Caractérisation du déroulement du G-quadruplex par l'hélicase Pif1 dans *Bacteroides* sp 3_1_23.

Mots clés : Hélicase, RIG-I, Leucémie, Cancer, Pif1, Translocation

Résumé : Les hélicases sont des protéines qui utilisent l'énergie fournie par l'hydrolyse de l'ATP ou du GTP pour catalyser la disjonction des doubles hélices d'ADN ou d'ARN. Cette activité de déroulement de double brin leur confère un rôle essentiel dans le métabolisme des acides nucléiques, le maintien de la stabilité du génome et les processus de signalisation cellulaire. En conséquence, ils sont impliqués dans des processus aussi divers que le vieillissement, l'apparition de cancers, l'immunité innée. Cette thèse est axée sur la compréhension de la fonction et des mécanismes moléculaires de deux hélicases différentes et le manuscrit est donc divisé en deux parties. Le premier est dédié à l'hélicase RIG-I, une hélicase à ARN, exprimée lorsque les cellules leucémiques cessent de proliférer et sont induites à se différencier en granulocytes, indispensables à la reconnaissance de l'ARN double brin des virus, initiant la protection des cellules contre la réplication des génomes viraux. Le mécanisme d'action de RIG-I est bien décrit dans le contexte d'une infection virale.

Mais dans le cas de la différenciation des cellules myéloïdes, l'intervention de RIG-I et son rôle dans la balance la prolifération / différenciation restent incomplets. En effet, les interactions RIG-I en particulier avec les ligands cellulaires ne sont pas totalement comprises. La première partie de mon travail consistait à tenter d'isoler et de caractériser les partenaires de RIG-I lors de la différenciation des cellules leucémiques NB4. La seconde est consacrée à l'étude des mécanismes sous-jacents aux G-quadruplexes résolus par les hélicases. Plusieurs questions subsistent quant aux interactions entre la structure particulière des G-quadruplexes et ces enzymes. Une hélicase de *Bacteroides* sp 3_1_23, BsPif1, a été choisie pour comparer et caractériser l'interaction entre les G-quadruplexes et l'ADN canonique de Watson-Crick. Dans les deux parties du travail, les interactions ont été étudiées par des techniques biochimiques utilisant soit une lignée cellulaire ou une protéine purifiée et des acides nucléiques synthétiques.

Titre : Identification and characterization of the RIG-I helicase partners involved in the balance proliferation / cell differentiation. Characterization of G-quadruplex resolving by the helicase Pif1 in *Bacteroides* sp 3_1_23.

Mots clés : Helicase, RIG-I, Leukaemia, Cancer, Pif1, Translocation

Résumé : Helicases are proteins that utilize the energy provided by the hydrolysis of ATP or GTP to catalyse the disjunction of double DNA or RNA helices. This double strand unwinding activity gives them an essential role in the metabolism of nucleic acids, the maintenance of the genome stability and cell signalling processes. As a result, they are involved in processes as diverse as aging, the appearance of cancers, innate immunity. This thesis is focused on the understanding of the function and the molecular mechanisms of two different helicases and the manuscript is therefore divided in two parts. The first one is dedicated to the RIG-I helicase, an RNA helicase, expressed when leukemic cells stop proliferate and are induced to differentiate in granulocytes, which are essential in the recognition of double-stranded RNA of viruses, initiating the protection of the cells against the replication of the viral genomes. The mechanism of action of RIG-I is well described in the context of viral infection.

But in the case of the differentiation of myeloid cells, the intervention of RIG-I and its influence on the equilibrium proliferation / differentiation remains incomplete. Indeed, RIG-I interactions in particular with cellular ligands are not fully understood. The first part of my work consisted in an attempt to isolate and characterize RIG-I partners during differentiation of NB4 leukemic cells. The second one is devoted to the study of mechanisms underlying G-quadruplexes resolving by helicases. Several questions remain about the interactions between the particular structure of G-quadruplexes and these enzymes. A *Bacteroides* sp 3_1_23 helicase, BsPif1, was chosen to compare and characterize the interaction between G-quadruplexes and canonical Watson-Crick DNA. In the two parts of the work, the interactions were investigated by biochemical techniques using either a cell line or purified protein and synthetic nucleic acids.